TECHNICAL REPORT STANDARD TITLE PAGE

1. Report No.	2. Government Accession No.	3. Recipient's Catalog No.

4. Title and Subtitle	5. Report Date
"Computer Analysis of Segmentally Erected Precast Prestressed Box Girder Bridges"	November 1974
	6. Performing Organization Code
7. Author(s)	8. Performing Organization Report No.
R. C. Brown, Jr., N. H. Burns, and J. E. Breen	Research Report 121-4
9. Performing Organization Name and Address	10. Work Unit No.
Center for Highway Research The University of Texas at Austin Austin, Texas 78712	11. Contract or Grant No. Research Study 3-5-69-121
	13. Type of Report and Period Covered
12. Sponsoring Agency Name and Address Texas Highway Department Planning & Research Division P. O. Box 5051 Austin, Texas 78763	Interim
	14. Sponsoring Agency Code

15. Supplementary Notes

Work done in cooperation with the Federal Highway Administration, Department of Transportation. Research Study Title: "Design Procedures for Long Span Prestressed Concrete Bridges of Segmental Construction"

16. Abstract

The economic advantages of precasting can be combined with the structural efficiency of prestressed concrete box girders for long span bridge structures when erected by segmental construction. The complete superstructure is precast in box segments of convenient size for transportation and erection. These precast segments are erected in cantilever and post-tensioned together to form the complete superstructure.

This report details the development of an analysis technique with an associated computer program to permit efficient analysis of constant depth segmental prestressed concrete box girders at all stages of erection. An existing box girder analysis program developed for analysis of completed structures was substantially altered to make it applicable to the multistage construction problem.

The computer program has been written to simulate the complete construction sequence after a reasonable amount of user-generated data. The program provides a complete analysis for stresses and deflections at each stage of construction and will, at the user's option, compute revised tendon stresses for all tendons stressed earlier in the sequence and bonded by grouting.

The use of the computer program is demonstrated by means of several practical examples, including an analysis of the first bridge of this type in the United States, erected at Corpus Christi, Texas. The general applicability of the program was verified in a related study by Kashima wherein measurements were made in a realistic model study of the Corpus Christi bridge and good correlation was obtained.

17. Key Words	18. Distribution Statement
bridges, box girder, prestressed, precast, segmentally erected, analysis, computer	

19. Security Classif. (of this report)	20. Security Classif. (of this page)	21. No. of Pages	22. Price
Unclassified	Unclassified	240	

Form DOT F 1700.7 (8-69)

COMPUTER ANALYSIS OF SEGMENTALLY ERECTED PRECAST PRESTRESSED BOX GIRDER BRIDGES

by

R. C. Brown, Jr., N. H. Burns, and J. E. Breen

RESEARCH REPORT NO. 121-4

Research Project Number 3-5-69-121
Design Procedures for Long Span Prestressed Concrete
Bridges of Segmental Construction

Conducted for

The Texas Highway Department
In Cooperation with the
U. S. Department of Transportation
Federal Highway Administration

by

CENTER FOR HIGHWAY RESEARCH
THE UNIVERSITY OF TEXAS AT AUSTIN

November 1974

The contents of this report reflect the views of the authors, who are responsible for the facts and the accuracy of the data presented herein. The contents do not necessarily reflect the official views or policies of the Federal Highway Administration. This report does not constitute a standard, specification, or regulation.

PREFACE

This report is the fourth in a series which summarizes a detailed investigation of the various problems associated with design and construction of long span prestressed concrete bridges of precast segmental construction. The initial report in the series summarized the general state of the art for design and construction of this type bridge as of May 1969. The second report outlined requirements for, and reported test results of, epoxy resin materials for jointing the large precast segments. The third report summarized design criteria and procedures for bridges of this type and included two design examples. One of these examples was the three-span segmental bridge constructed in Corpus Christi, Texas, during 1972-73. This report summarizes the development of an incremental analysis procedure and computer program which can be used to analyze segmentally erected box girder bridges and which realistically considers prestressing layouts and sequence of construction. Structural performance data for a realistic one-sixth scale model of the structure and comparisons with analytic results using the computer model outlined herein will be presented in a subsequent report.

Although the authors have personally tested the program as listed in this report and believe it to be correct, no warranty, expressed or implied, is made by the authors as to the accuracy of functioning of the program. No responsibility is assumed by the authors for incorrect results or damages resulting from the use of this program.

This work is a part of Research Project 3-5-69-121, entitled "Design Procedures for Long Span Prestressed Concrete Bridges of Segmental Construction." The studies described were conducted as a part of the overall research program at The University of Texas at Austin, Center for Highway Research. The work was sponsored jointly by the Texas Highway Department and the Federal Highway Administration under an agreement with The University of Texas at Austin and the Texas Highway Department.

Liaison with the Texas Highway Department was maintained through the contact representative, Mr. Robert L. Reed, and the State Bridge Engineer, Mr. Wayne Henneberger; Mr. D. E. Harley and Mr. Robert E. Stanford were the contact representatives for the Federal Highway Administration. The authors were particularly appreciative of the deep interest and assistance of Professor A. C. Scordelis of the University of California at Berkeley. Professor Scordelis made available copies of computer programs with documentation and answered many inquiries which were invaluable in development of the computer program SIMPLA2.

The overall study was directed by Dr. John E. Breen, Professor of Civil Engineering. Dr. Ned H. Burns, Professor of Civil Engineering, directed this analysis phase. The incremental analysis was developed by Robert C. Brown, Jr., Research Engineer, Center for Highway Research.

S U M M A R Y

The economic advantages of precasting can be combined with the structural efficiency of prestressed concrete box girders for long span bridge structures when erected by segmental construction. The complete superstructure is precast in box segments of convenient size for transportation and erection. These precast segments are erected in cantilever and post-tensioned together to form the complete superstructure.

This report details the development of an analysis technique with an associated computer program to permit efficient analysis of constant depth segmental prestressed concrete box girders at all stages of erection. An existing box girder analysis program developed for analysis of completed structures was substantially altered to make it applicable to the multistage construction problem.

The basic analytical element is rectangular, with uniform thickness formed by longitudinally dividing the prismatic box girder into finite segments. The finite segments are then subdivided transversely into finite elements. The analysis proceeds by obtaining transverse equilibrium and compatibility using the direct stiffness method and then ensuring longitudinal equilibrium and compatibility using a transfer matrix method. General effects of prestressing are accounted for by use of the equivalent load concept. Procedures to account for construction stage erection and detailed effects of prestressing, such as friction, have been developed and included in the program.

The computer program has been written to simulate the complete construction sequence after a reasonable amount of user-generated data. The program provides a complete analysis for stresses and deflections at each stage of construction and will, at the user's option, compute revised tendon stresses for all tendons stressed earlier in the sequence and bonded by grouting.

The use of the computer program is demonstrated by means of several practical examples, including an analysis of the first bridge of this type in the United States, erected at Corpus Christi, Texas. The general applicability of the program was verified in a related study by Kashima[33] wherein measurements were made in a realistic model study of the Corpus Christi bridge and good correlation was obtained.

I M P L E M E N T A T I O N

This report presents the background and details of a computer program developed specifically to permit efficient analysis of constant depth segmental prestressed concrete box girders at varied stages of erection. This type of construction is becoming increasingly popular in the United States and the use of such a program can reduce the burden of calculations required for checking the structure at various stages of development during the cantilever erection procedure.

The computer program provides a complete analysis for stresses and deflections at each stage of construction as well as a check on tendon stresses for all tendons stressed at any stage of the construction. The report includes a brief summary of the derivation of the analytical procedures, a detailed input guide to assist the user in preparing a data deck for use with the program, and provides several example problems with samples of both input data and output, so that a user can check his ability to develop a data deck on a sample problem. One of the example problems is based on the box girder bridge erected over the Intracoastal Waterway at Corpus Christi, Texas, where the program was used in a check of the structure.

While the program is limited to consideration of box girders of constant depth, it should be very useful in analysis of proposed structures in the 100 to 300 ft. span range and can deal with a wide variety of cross sections. Further development of such programs should extend the capabilities for handling variable depth and skew crossings. The program as written can consider a wide range of restraint conditions and thus can answer important questions concerning the need for provision of diaphragms, auxiliary supports, or special support devices required at various stages of erection. The program is based on elastic analysis and could also be used in connection with checking erection stresses in steel

box girders if careful extra attention was paid to local stability requirements.

C O N T E N T S

Chapter Page

Chapter Page

L I S T O F T A B L E S

LIST OF FIGURES

CHAPTER 1

INTRODUCTION

1.1 General

Bridge engineers continually face requirements for safer, more economical bridge structures. In response to many requirements imposed by traffic considerations, natural obstacles, more efficient use of land in urban areas, safety, and aesthetics, the trend is to longer span structures. At present, the most commonly used structural system for highway bridge structures in Texas consists of prestressed concrete I girders combined with a cast-in-place deck slab. This system has practical limitations for spans beyond the 120 ft. range. With the high costs and maintenance requirements of steel bridges, there exists a need to develop an economical approach to achieve precast, prestressed concrete spans in the 120-300 ft. range.

In the United States, spans in the 160 ft. range have been achieved by the use of post-tensioned, cast-in-place girders.[19*] The box, or cellular, cross section shown in Fig. 1.1 is ideal for bridge superstructures since its high torsional stiffness provides excellent transverse load distributing properties. Construction experience along the West Coast has indicated that this type bridge is a very economical solution to many long span challenges.

In Europe, Japan, and Australia, during the late 1960's and early 1970's, the advantages of the cellular cross section were combined with the substantial advantages obtained by maximum use of prefabricated

---

*Numbers refer to references listed at the end of this report.

Fig. 1.1. Typical cellular cross section.

components. By precasting the complete box girder cross section in short segments of a convenient size for transportation and erection, the entire bridge superstructure may be precast. These precast units are subsequently assembled on the site by post-tensioning them longitudinally. A number of extremely long span precast and cast-in-place box girder bridges have been segmentally constructed in Europe[7] and interest in this construction concept is rapidly growing in the United States. A three-span precast segmentally constructed box girder bridge with a 200 ft. maximum span was completed in Corpus Christi, Texas, in 1973.

1.2 Cantilever Segmental Construction

Figure 1.2 illustrates some of the wide range of cross-sectional shapes which can be used. Various techniques have been used for jointing between the precast segments, with thin epoxy resin joints being the widest used. The most significant variation in construction technique is the method employed to assemble the precast segments. The most widely used methods may be categorized as construction on falsework and cantilever construction. This report deals only with those structures constructed by the latter approach. The outstanding advantage of the cantilever approach to segmental construction lies in the fact that the complete construction may be accomplished without the use of falsework and hence minimizes traffic interruption.

(a) Single cell girder

(b) Single cells joined by deck

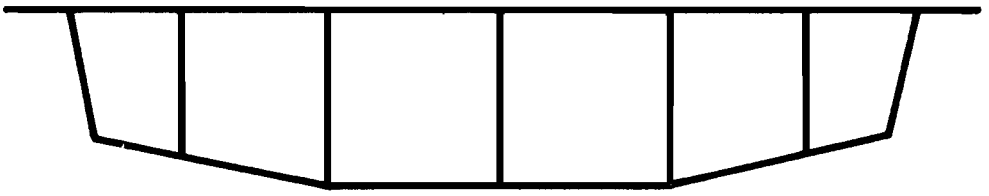

(c) Multicell girder

Fig. 1.2. Girder cross-sectional configurations.

Assembly of the segments is accomplished by sequential balanced cantilevering outward from the piers toward the span centerlines. Initially the "hammerhead" is formed by erecting the pier segment and attaching it to the pier to provide unbalanced moment capacity. The two adjoining segments are then erected and post-tensioned through the pier segment, as shown in Fig. 1.3(a). Auxiliary supports may be employed for added stability during cantilevering or to reduce the required moment capacity of the pier. Each stage of cantilevering is accomplished by applying the epoxy resin jointing material to the ends of the segments, lifting a pair of segments into place, and post-tensioning them to the standing portion of the structure [see Fig. 1.3(b)]. Techniques for positioning the segments vary. They may be lifted into position by means of a truck or floating crane, by a traveling lifting device attached to (or riding on) the completed portion of the superstructure, or by using a traveling gantry. In the latter case the segments are transported over the completed portion of the superstructure to the gantry and then lowered into position.

The stage-by-stage erection and prestressing of precast segments is continued until the cantilever arms extend nearly to the span centerline. In this configuration the span is ready for closure. The term closure refers to the steps taken to make the two independent cantilever arms between a pair of piers one continuous span. In earlier segmentally constructed bridges there was no attempt to ensure such longitudinal continuity. At the center of the span, where the two cantilever arms meet, a hinge or an expansion joint was provided. This practice has been largely abandoned in precast structures, since the lack of continuity allows unsightly creep deflections to occur.[2,14] Ensuring continuity is advised[2,14] and usually involves

(1) Ensuring that the vertical displacements of the two cantilever ends are essentially equal and no sharp break in end slope exists.

(2) Casting in place a full width closure strip, which is generally from 1 to 3 ft. in length.

(3) Post-tensioning through the closure strip to ensure structural continuity.

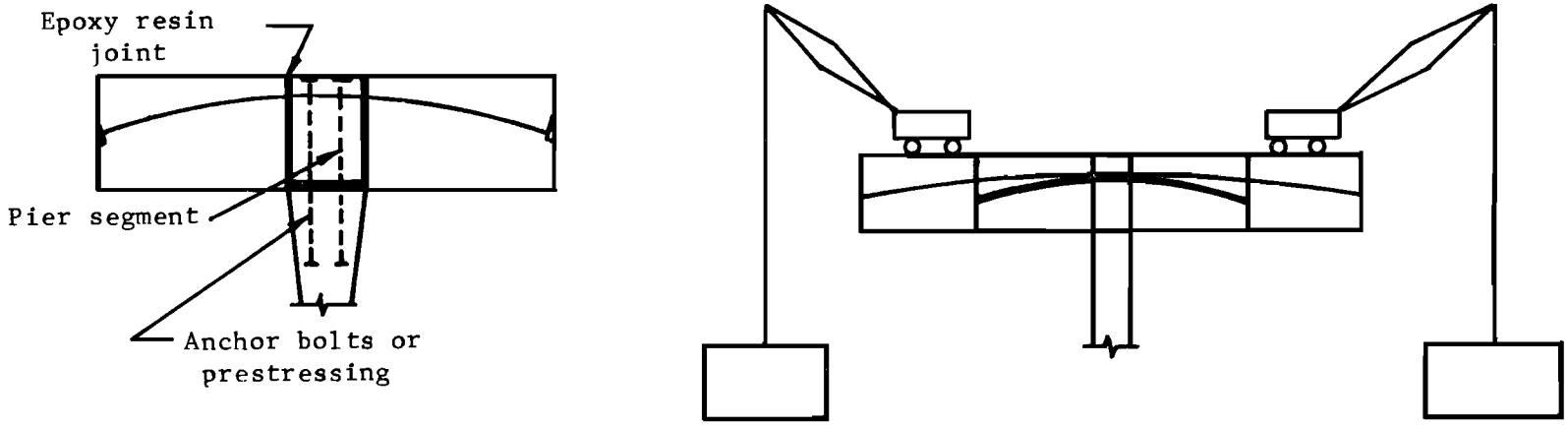

(a) Construction of hammerhead

(b) Segmental cantilevering

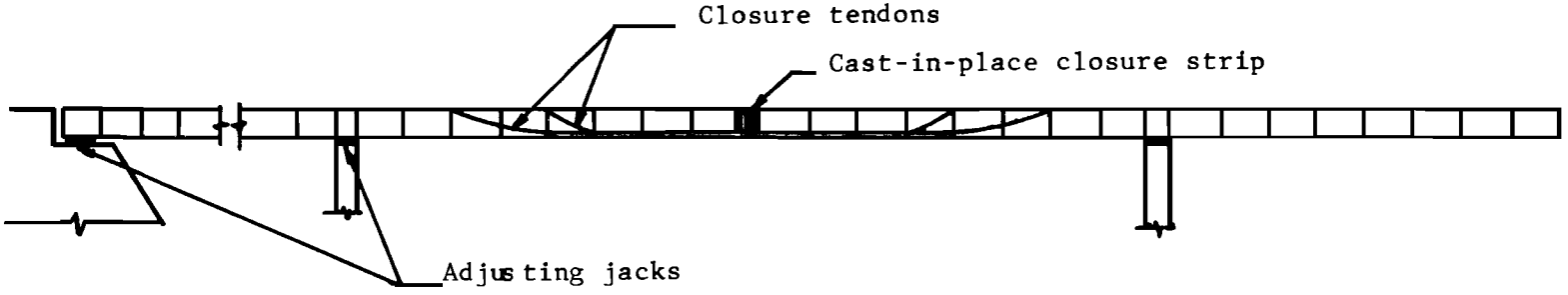

(c) Closure of span

Fig. 1.3. Construction of complete span.

The exact procedures required for closure of a given structure must be carefully specified in the construction sequence. The final step in closure is to adjust the distribution of stress throughout the girder to ensure maximum efficiency of prestress. Adjustment is usually necessary to offset undesirable secondary moments induced by continuity prestressing. The final adjustments may involve[14]

(1) Adjusting the elevation of the girder soffit, at the piers, to induce supplementary moments. The adjustment may be accomplished by means of jacks inserted between the pier and the soffit of the girder with subsequent shimming to hold the girder in position.

(2) Insertion of a hinge in the gap between the two cantilever arms to reduce the stiffness of the deck while the continuity tendons are partially stressed. The hinge is subsequently concreted before the continuity tendons are fully stressed.

(3) A combination of hinges and jacks inserted in the gap to control the moment at the center of the span while the continuity tendons are stressed. The final adjustment is made by further incrementing the jack force and finally concreting the joint in.

The first of these possibilities is the widest used. After final adjustments are complete, the operation is moved forward to the next pier and the erection sequence begins again.

The intent of this outline is to convey the general construction procedures which have been successfully employed. There are a number of variations of these procedures by which the construction could be successfully accomplished. The above discussion shows that from the onset of construction of a particular span until its completion, the structural configuration is continually changing, and at one stage changes from a determinate system to a continuous system. It is also evident that the structure is subject to a wide variety of loading and boundary conditions during erection. The girder must be designed to withstand the conditions existing at every stage; consequently, the girder must be analyzed under the conditions existing at every stage. The efficient analysis of the girder at each stage of erection is the goal of this research.

In spans of great length, erection considerations may dictate that segments be cast in place. The procedures outlined above can still be followed, except that allowances must be made for form weights and the entire process is more demanding of proper consideration of the time frame, particularly as it effects concrete strength development and creep.

1.3 Recent Research in Segmentally Constructed Bridges

In 1969, a comprehensive research effort dealing with segmental construction of precast concrete bridges was initiated at The University of Texas at Austin. This report summarizes one part of this multiphase project which had the following objectives:

(1) To investigate the state-of-the-art of segmental bridge construction.

(2) To establish design procedures and design criteria in general conformance with provisions of existing design codes and standards.

(3) To develop optimization procedures whereby the box girder cross section dimensions could be optimized with respect to cost to assist preliminary design.

(4) To develop a mathematical model of a prestressed box girder, and an associated computer program for the analysis of segmentally constructed girders during all stages of erection.

(5) To verify design and analysis procedures using a highly developed structural model of a segmental box girder bridge.

(6) To verify model techniques by observance of construction and service load testing of a prototype structure.

The first three phases of this work were reported in previous reports in this series and in the dissertation of Lacey.[6,30,31] Lacey and Breen used adaptations of methods recommended in the 1969 AASHO Specifications for the design of normal bridge cross sections under the action of wheel loads. This AASHO method was simplified somewhat and utilized in the development of a computerized optimization scheme by which the box girder cross section dimensions are optimized with respect to cost. The formulation is such that if the cross-sectional type, the spans, the overall deck width, and the web thicknesses are known, the remaining

cross-sectional dimensions are established to minimize the superstructure cost based on reasonable estimates of unit costs of major constituents.

Working within the philosophies of existing U.S. standards, Lacey and Breen established the necessary design criteria, and developed design procedures for the design of segmentally constructed, precast, prestressed box girders. The box girder is initially designed in the transverse direction for the action of wheel loads, ignoring any warping effects. For the preliminary design in the longitudinal direction, the box girder is treated by conventional beam theory. The effects of prestressing are accounted for by a simplified equivalent load scheme where the effective prestress force is estimated.

In order that the design procedures developed be useful in a typical design office, these simplifying assumptions are necessary. It is known,[18,24] however, that the longitudinal and the transverse response of a box girder depend on an interaction of both the transverse and longitudinal properties. In general, the response of a box girder is more complex than that assumed in developing the design procedure. Lacey and Breen recommended an analysis of the completed structure using established box girder analysis programs such as MUPDI.[31] The preliminary design can then be revised if significant warping stresses are indicated.

As suggested by Fig. 1.3(b), tendon profiles utilized in segmentally constructed box girders are characterized by large curvatures and slopes. Moreover, prestress forces applied to the negative moment tendons are typically quite large. The combination of these two factors suggests the requirement for a more rigorous approach to the calculation of equivalent prestress forces than traditionally used.

It became clear that while "beam" theory sufficed for initial design, a more rigorous check analysis was desirable at each stage of construction for verification of the design considering possible warping and with detailed consideration of prestressing.

As outlined in Ref. 31, the results of the overall project have been combined to provide a reasonable, accurate design-analysis package for segmentally constructed box girders, involving the following:

(1) Preliminary design based on conceptual considerations, span depth ratios, construction site limitations, and practical construction considerations.

(2) Revisions to initial designs are indicated by optimization studies.

(3) Detailed transverse and longitudinal design is carried out by "beam" analysis techniques.

(4) Behavior of the completed structure under unsymmetrical loading and warping effects is examined by use of existing box girder analysis programs such as MUPDI. Any needed revisions in design are made to accommodate these effects.

(5) The final design is thoroughly scrutinized at each proposed stage of erection by the computer program discussed herein.

(6) Changes in important details such as post-tensioning cable layouts, proposed by the constructor at the working drawing stage, can be quickly evaluated using the program included herein.

The design procedure suggested above was successfully followed in the design of the model of and the prototype structure built at Corpus Christi.

1.4 Objectives and Scope of this Research

Segmentally cantilevered box girders should be designed for and analyzed at each stage of erection. Analysis at each stage can represent a monumental task unless the problem is simplified considerably. Effects of simplification for purposes of design are often difficult to evaluate, since the degree to which a box girder behaves as a beam depends upon many variables and is difficult to determine.[23] The objective of this research is to develop a composite mathematical model and an associated computer program for the automatic analysis of cantilever-erected segmental prestressed box girders. The present program is limited to longitudinally prismatic (and hence constant depth) elastic structures, the cross section of which may be idealized by prismatic plates. A wide range of cross-sectional shapes, as shown in Fig. 1.2, have been employed in the past;

consequently, the capability to treat arbitrary cross-sectional shapes is desirable.

The discussion of Sec. 1.2 indicates that a stage of erection may involve a number of modifications to the structure, the loading or boundary conditions, or the support conditions. Moreover, the complete erection is accomplished in a large number of stages. Consequently, in addition to the basic analysis capability, it is the objective of this research to provide a computer program with the capability to accept, as input, a complete erection schedule, and to automatically update the structural system according to the input schedule to provide a complete analysis at each stage of erection. In addition, the computer model must be capable of accurately accounting for the effects of prestressing forces which generally constitute a significant portion of the total load during erection. This requires a careful evaluation of the effective prestress force at all locations along a tendon, requiring calculation of force loss due to friction and due to the stage prestressing. Prestress force loss due to friction and the transverse forces applied to the structure by the tendon (equivalent loads) are functions of the tendon profile; therefore, accurate force evaluation demands an accurate representation of the tendon profile. In keeping with the requirement for the analysis to apply to a large class of problems, the model should be capable of approximating general tendon profiles.

In summary, the objectives of this research may be separated into two basic parts. First, to develop an automatic analysis capability applicable to post-tensioned box girders under given conditions of load and restraint, and second, to extend this capability such that the structural analysis problem may be automatically altered according to an input sequence of erection events. The end result of this research will be an accurate, automatic analysis tool, with which a designer may rigorously check a box girder design at every stage of erection, which is based upon a simplified design approach.

The computer program developed during this research was used by the Texas Highway Department to check the final design of the Corpus Christi

Intracoastal Canal Bridge and to review the effects of tendon design changes suggested by a bidder and rapidly assess the feasibility of such changes.

There are various box girder computer analyses available. However, the treatment of the effects of prestressing developed herein and the application of a box girder analysis to a continuously changing structural system seems unique to this research.

1.5 Box Girder Behavior and Available Analytical Models

In order to provide a realistic analysis it is necessary that the mathematical model be sufficiently rigorous to model all significant behavior of the structure. However, the most rigorous approach may make the analysis of a practical problem so unwieldy as to be impractical even on a large computer. The degree of sophistication of the mathematical model necessary to accomplish the stated objectives of this research was established only after studying the characteristic behavior of box girders. A summary of the most important characteristics of box girders and of a review of previous analytical models is presented in the next section. A more detailed review is given in Ref. 32.

1.5.1 Box Girder Behavior. A general box girder load may be thought of as being composed of three components: a flexural component, a torsional component, and a component tending to distort the cross section, termed a distortional component. The flexural component produces longitudinal membrane stresses and flexural shears in the various plates of the cross section which may be determined by flexural theory. The torsional component, as shown in Fig. 1.4, produces St. Venant membrane shears and longitudinal membrane stresses, arising from restrained warping, which may be determined by the Prandtl-Bredt torsion theory. Generally, the stresses associated with restrained warping are small and highly localized. The distortional component produces longitudinal membrane stresses resulting from in-plane plate strains and transverse bending moments. Determination of these stresses requires considerations which are not as familiar to

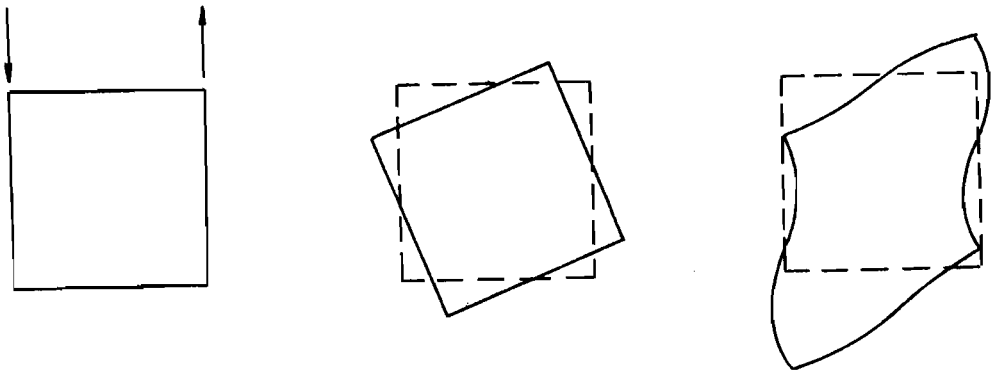

(a) Torsional (b) St. Venant torsion (c) Distortional

Fig. 1.4. Resolution of torsional component.

engineers as the flexural and torsion theories. Resolution of a given load into flexural and torsional components is a simple matter; however, the further resolution of the torsional component into a St. Venant torsional component and a distortional component is a complex problem for the general cellular cross section. Generally, it can be said that the amount of cross section deformation to be expected at a given section is a function of the relative stiffnesses in the longitudinal and transverse directions.[19] Previous investigators have determined that the cross-sectional deformation significantly alters the "beam analysis" stresses for many structures of interest in this study.[5,19]

A further characteristic of thin-walled box beams causing stresses to vary from values determined from flexural and torsional theory is the in-plane shear deformation of the flange plates. This phenomenon, known as shear lag, is an extremely complex problem and its significance in civil engineering structures has been the subject of only limited investigations.[10,15] The primary manifestation of shear lag in box girders is a nonuniformity of longitudinal membrane flexural stress across the flange plates, as shown in Fig. 1.5. The relative importance of shear lag in a given girder is a function of many variables with a short, wide cantilevered box girder most susceptible to shear lag.[15,17] In several such stubby box girders analyzed by the folded plate method, peak flange stresses were

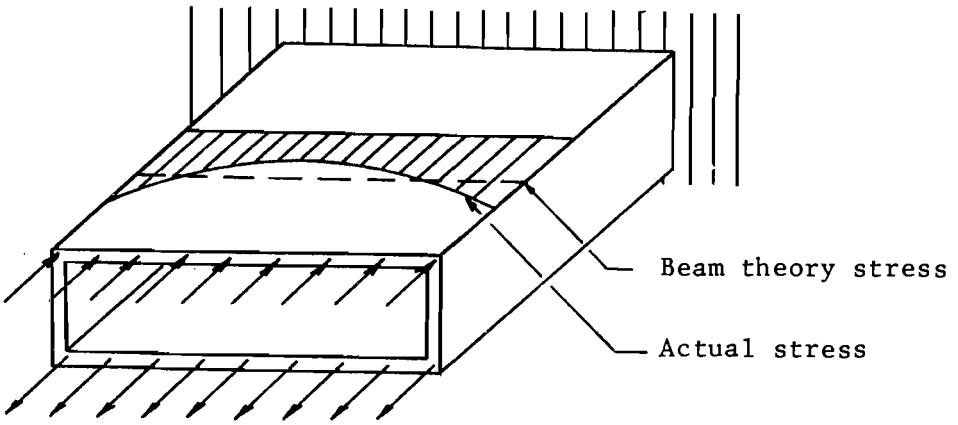

Fig. 1.5. Shear lag phenomenon.

determined as 30 percent greater than the value given by a flexural analysis. This finding is compatible with results reported by Reissner and Hildebrand,[17] and those reported from a field test of a box girder bridge under construction.[15]

Thus, under some circumstances cross section distortion combined with shear lag effects may cause stresses to vary significantly from values given by flexural and torsion theories alone. Therefore, an approach which considers a total elastic analysis of the structure was adopted.

1.5.2 Available Analytical Models. The past decade has seen a proliferation of publications dealing with the analysis of plate assemblages; i.e., folded plates and box girders, as seen from the bibliography accompanying Ref. 24. The most generally applicable analytical methods recently employed may be placed into one of three broad categories: (1) folded plate analysis, (2) thin-walled beam theory, and (3) finite element techniques. Detailed evaluation of the characteristics of each as they apply to the present problem are given in Ref. 32.

The folded plate analysis represents the most accurate of the three approaches noted above. The behavior of the plate element in its plane is governed by the plane stress equations of elasticity; and that normal to the plane is governed by the equations of biaxial plate bending. This

approach was utilized by Scordelis[18,19] to develop a general purpose computer program for the analysis of continuous, prismatic box girders of arbitrary cross section. Intermediate shear-rigid diaphragms and diaphragms over supports are treated by using a flexibility technique to solve for the indeterminate interaction forces. Because of experimental verification[11] and its sound theoretical basis, the folded plate method has been used[11,18,19] as a standard for other, less rigorous, techniques. The harmonic representation of loads and displacements limits the applicability of the technique to structures which are simply supported at the extreme ends. A further disadvantage is the inability to account for anisotropic plate elements.

A number of the analytical techniques presented recently[3] fall into a category of thin-walled beam theory. This approach takes advantage of the fact that, for the type of structures under consideration, the longitudinal slab moments and associated slab shears are quite small and can, therefore, be neglected. Most formulations are limited to either fixed or simply supported boundaries.

Lo and Scordelis[9] have adopted the assumption that longitudinal and torsional moments are negligible to arrive at still another formulation falling into the thin-walled beam category. The technique, termed "the finite segment method," requires division of the structure both transversely and longitudinally into rectangular subregions. Each subregion behaves as a beam in the longitudinal direction and a one-way slab in the transverse direction. Therefore, derivation of the stiffness matrix requires only the use of the differential equation of flexure. Longitudinal equilibrium and compatibility are ensured by a transfer matrix approach, while simultaneously ensuring transverse equilibrium and compatibility by the direct stiffness method. This results in a system of linear algebraic equations relating the boundary forces and displacements. This approach is closely akin to the finite element method and has many advantages associated with that method. The primary advantage realized is the generality of boundary and loading conditions which may be treated. Restraint from boundary and interior supports is specified

independently for each element of the cross section; therefore, the structure may be completely free, fixed, or something in between at the boundaries and supports. Both intermediate shear-rigid diaphragms and diaphragms over supports may be handled. The assumptions result in a minimum number of degrees of freedom necessary to model the main behavior of a box girder structure; however, they also impose limitations upon the method which can produce inaccuracies in the results under certain circumstances. Scordelis[19] reports that correlation between the approximate finite segment method and "exact" folded plate method is good.

Wright et al.,[23] and Tung[21] have used a technique for analysis of single cell, rectangular, or trapezoidal box girders which is suitable for hand calculation, termed the BEF analogy. The analysis falls into the thin-walled beam theory category and is reasonably accurate. It could be computerized for stage erection checks, but has the disadvantage of being strictly applicable to single cell sections. Wright compares the results from the BEF (beam on elastic foundation) analogy with results from a more rigorous analysis and concludes that this method predicts the longitudinal and transverse stresses resulting from torsional load components adequately for design purposes.

The finite element method is the most general analytical technique. The structure is divided into subregions, the deformation patterns of which are assumed. When displacement compatibility is explicitly enforced at two element nodal points, the displacements along the element interface connecting the two points will be compatible. Once the displacement assumptions are made, the element stiffness matrix may be derived and the analysis is carried out by the direct stiffness method.

Scordelis,[19] and Meyer and Scordelis[13] have employed the finite element method for the analysis of box girder structures. The size, thickness, and material properties of the elements may be varied arbitrarily throughout the structure, and arbitrary loading may be considered. Numerous boundary conditions and both intermediate shear-rigid diaphragms and diaphragms over supports may be treated. The primary disadvantage associated with the finite element method is the number of equilibrium

equations which must be solved. Vast computer storage and execution times are required for moderate size problems.

1.5.3 Mathematical Model for this Research. Two of the available analysis methods are sufficiently general with respect to cross-sectional configuration, loading conditions, and boundary conditions for purposes of this research--the finite element method, and the finite segment method. Both of these methods are finite element approaches in that the structure is divided into elementary subregions, of which the stiffness properties can be derived.

There are two basic differences between the conventional finite element method and the finite segment method. The finite segment method assumes that longitudinal slab moments and torsional moments may be neglected and enforces transverse displacement compatibility at only one point along the element edge. Investigations employing the finite element method[13,29] have considered longitudinal and torsional slab moments and have placed strict displacement compatibility requirements upon the elements. As a result of the rigorous requirements placed upon the element in the latter technique, the element was allowed up to 24 degrees of freedom. Use of these elements, even for moderate size problems, demands vast amounts of computer time and storage.

The simplifying assumptions made in the finite segment technique have been shown to be justified,[19] and as a consequence of these assumptions the basic structural element is allowed only 14 degrees of freedom. This approach offers a substantial saving in computational effort while retaining the required generality with respect to loading and boundary conditions and approximating all significant behavior of the structure. Moreover, use of the finite segment facilitates the representation of prestressing. Therefore, the finite segment analysis technique was adapted for this research.

In the following chapters the finite segment method and the techniques used to adapt it to segmentally constructed box girders are briefly presented. Full details and derivations are included in Ref. 32.

Chapter 2 outlines the basic finite segment method. In Chapter 3 necessary additions and modifications to the finite segment method to account for prestressing, stage erection, and closure are discussed. Several example problems are solved and results presented in Chapter 4. Chapter 5 is a summary with conclusions and recommendations.

CHAPTER 2

THE FINITE SEGMENT FORMULATION

2.1 Introduction

Reasons for the selection of the finite segment method of analysis have been reviewed in the previous chapter. A brief summary of the basic assumptions and the development of the segment progression computational technique are given in this chapter. Both the derivation of the element stiffness properties and the general computational technique utilized have been previously reported.[8,9,19] These procedures are reviewed and expanded in Ref. 32, which contains all of the detailed mathematical derivations and expansions required for a complete understanding of the procedure. Inclusion of the capability to treat elastic support restraints is unique to this investigation.

The basic structural element is formed by subdividing the structure transversely into a number of plate elements and longitudinally into a number of finite segments, as shown in Fig. 2.1. A typical element is bound by two longitudinal joints (transverse subdivisions) and by two stations (longitudinal subdivision). The solution is accomplished by first establishing transverse equilibrium and compatibility of all the elements between stations K and K+1 (the K^{th} finite segment). The influence at station K+1 of the actions (forces and displacements) at station K and the loads applied to segment K is determined from a segment progression method. This procedure is applied to each segment along the span, resulting in a set of linear equations relating the boundary actions. Specification of boundary conditions provides sufficient equations for solution of all unknowns.

2.2 Basis for the Mathematical Model

The assumptions upon which the analytical behavior of the basic structural element is formulated are essentially the same as those

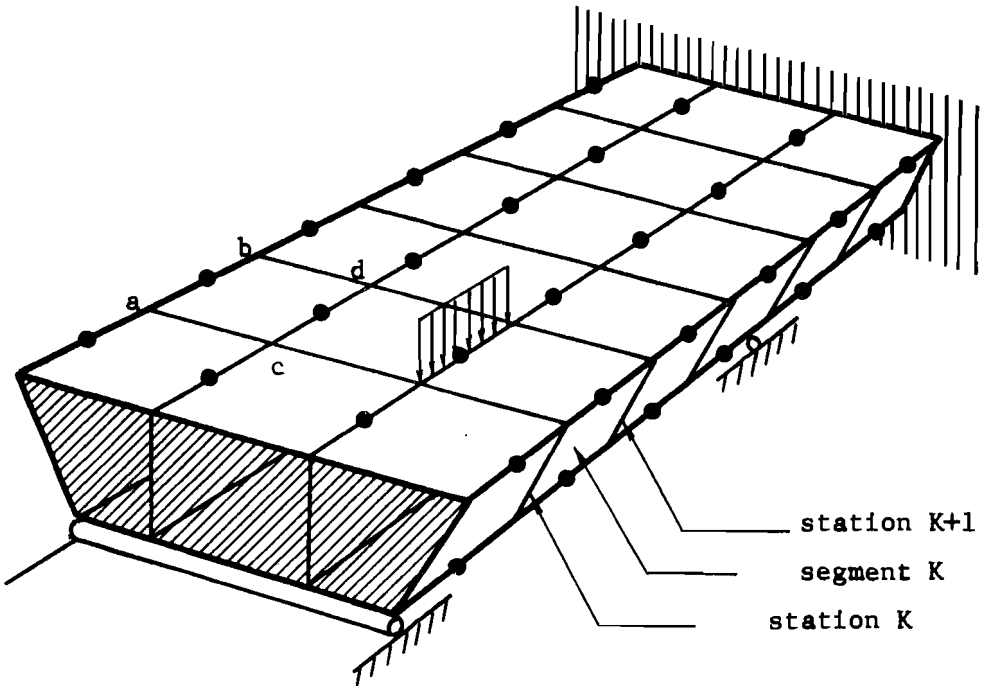

(a) Mathematical model - total structure

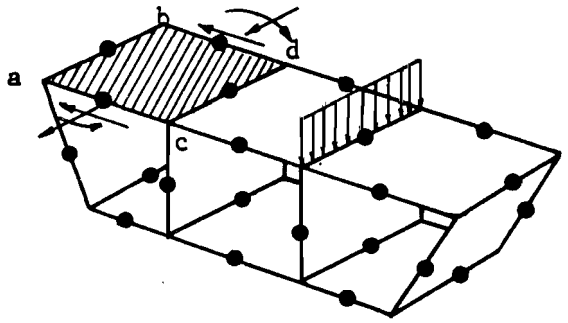

(b) Typical complete finite segment

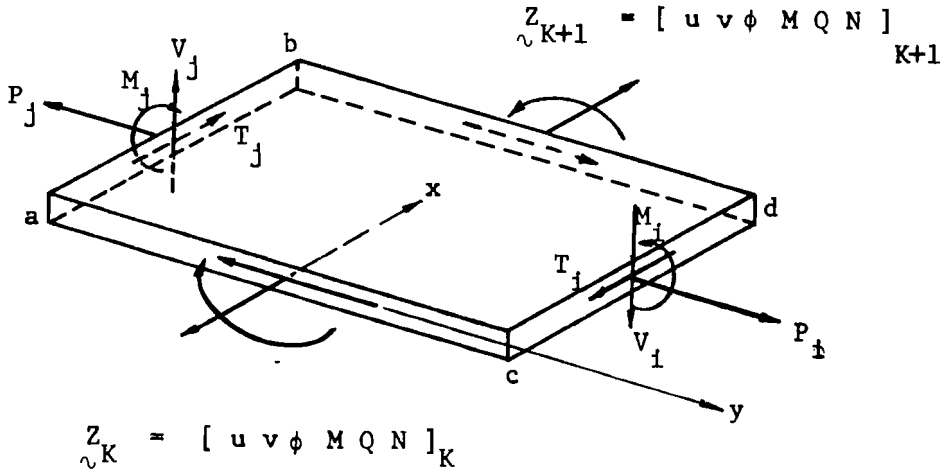

(c) Typical finite plate element

Fig. 2.1. Finite segment model. (Adapted from Ref. 19.)

recommended in Ref. 25 for the approximate analysis of folded plates. They are as follows:

(a) Each basic element is rectangular, of uniform thickness, and is elastic, homogeneous, and isotropic.

(b) The force-displacement relationship is linear.

(c) Slab bending is essentially a one-way phenomenon occurring in the transverse direction; the effect of longitudinal slab bending is negligible.

(d) The torsional stiffness of each plate of the structure is neglected; therefore, plate torsional and longitudinal moments are ignored.

(e) Stresses and displacements in the plane of the element (membrane action) are determined by treating each element as a beam in the longitudinal direction; thus longitudinal membrane stresses vary linearly over the element width.

(f) Poisson's Ratio is zero.

Several additional assumptions which are unique to the finite segment formulation are:

(g) Applied loads and element edge forces are uniformly distributed over the length of the element.

(h) The effects of membrane shear and transverse membrane stresses are included for the calculation of element in-plane displacements.

2.3 Element Forces and Displacements

The free body diagram of Fig. 2.1(c) indicates that the stresses surviving the simplifying assumptions may be resolved into 14 stress resultants. On the constant y edges of the element (element edges i and j) there are both membrane and slab resultants acting. The resultants governing the one-way slab behavior of the element are the transverse bending moments per unit length, M_i and M_j, and the normal shear forces per unit length V_i and V_j. The membrane behavior of the element is governed by the membrane edge shears per unit length, T_i and T_j; the transverse membrane stresses per unit length, P_i and P_j; and the actions (forces and

displacements) at the constant x edges (end stations K and K+1) of the element. The actions at the end stations of the element completely describe the stress and displacement state of the element at the particular station; consequently, these are termed the "state vector" for the element. The element state vector is defined as:

$$\underset{\sim}{z} = [u \; v \; \phi \; M \; Q \; N]^T$$

This vector is completely analogous to the state vector for a beam. The state vectors of all elements at a particular station, K, define a complete station state vector, and for a structure composed of q elements is given by

$$\underset{\sim}{Z}_K = [\underset{\sim}{z}_1 \; \underset{\sim}{z}_2 \; \cdots \; \underset{\sim}{z}_q]^T$$

The element edge force vectors are defined as

$$\underset{\sim}{S}_m = [T_i \; T_j \; P_i \; P_j]^T \tag{2.1}$$

and

$$\underset{\sim}{S}_s = [M_i \; M_j \; V_i \; V_j]^T \tag{2.2}$$

where the subscripts m and s denote membrane and slab action, respectively. The slab and membrane behavior will be considered separately since, for small displacements, they are independent.

The membrane behavior of the element may be described by four straining modes or "generalized displacements"--longitudinal extension, transverse extension, shear displacement, and longitudinal bending. These displacement quantities, taken at the longitudinal center of the element, define a generalized displacement vector

$$\underset{\sim}{\Phi} = [\bar{u} \; v' \; \bar{v} \; \bar{\phi}]^T$$

The generalized displacement vector, $\underset{\sim}{\Phi}$, is a function of the state vector, $\underset{\sim}{z}_K$, and the element edge force vector $\underset{\sim}{S}_m$. It is assumed that the actual element edge membrane forces may be computed as a combination of the

four element edge force patterns shown in Fig. 2.2. It will be assumed, in the determination of the effect of each force pattern, that the complete actions vector $\underset{\sim}{Z}_k$, is zero. Under this assumption it is seen that each force pattern corresponds to one component of $\underset{\sim}{\Phi}$; thus, a generalized edge membrane force vector is defined as

$$\underset{\sim}{Q} = [T' \; P' \; T'' \; P'']$$

For computational convenience it is desirable to define nodal point forces and displacements in terms of which the generalized forces and displacements may be expressed. The element edge nodal forces have been defined in Eqs. (2.1) and (2.2). The corresponding element edge nodal displacements are defined as

$$\underset{\sim}{u}_m = [u_i \; u_j \; v_i \; v_j]^T$$

and

$$\underset{\sim}{u}_s = [\theta_i \; \theta_j \; w_i \; w_j]^T$$

The components of $\underset{\sim}{u}_m$ and $\underset{\sim}{u}_s$ are defined at the longitudinal center of the element edges (element nodal points); however, the element edge forces are assumed to be uniformly distributed over the element edge. The nodal forces and displacements acting at the element end stations are the components of the state vectors $\underset{\sim}{z}_k$ and $\underset{\sim}{z}_{k+1}$. Positive directions of all element forces and corresponding displacements are shown in Fig. 2.3.

2.4 General Description of the Method

The objective of the analysis is to determine all the unknown stress resultants shown in Fig. 2.1(c), the associated displacements, and the element internal stresses. The state vector at station K, $\underset{\sim}{Z}_K$, is determined from the requirement that all $\underset{\sim}{z}_K$ must satisfy equilibrium and compatibility with elements from the previous segment or with a boundary or support condition at station K. The state vector $\underset{\sim}{Z}_{K+1}$ is determined as the superposition of two effects--the effect of $\underset{\sim}{Z}_K$ and the effect of the element edge forces and applied line loads over segment K. The actions at K+1 due to those at K are determined by a transfer matrix[28] procedure, and are expressed as a

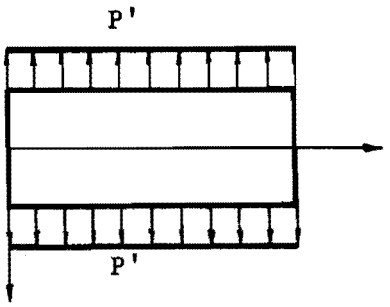

(a) P' - Symmetrical transverse membrane edge forces

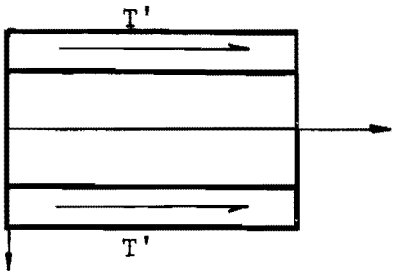

(b) T' - Symmetrical membrane edge shear forces

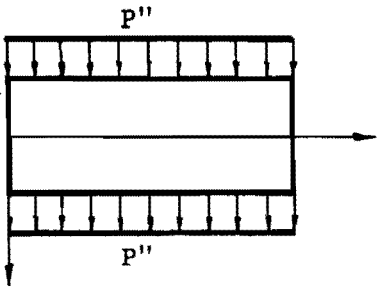

(c) P" - Antisymmetrical transverse membrane edge forces

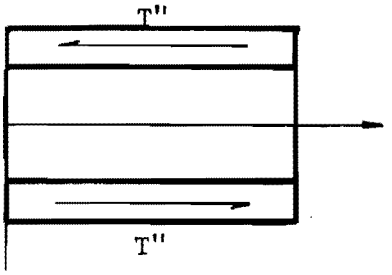

(d) T" - Antisymmetrical membrane edge shear forces

Fig. 2.2. Assumed generalized edge force patterns. (Adapted from Ref. 19.)

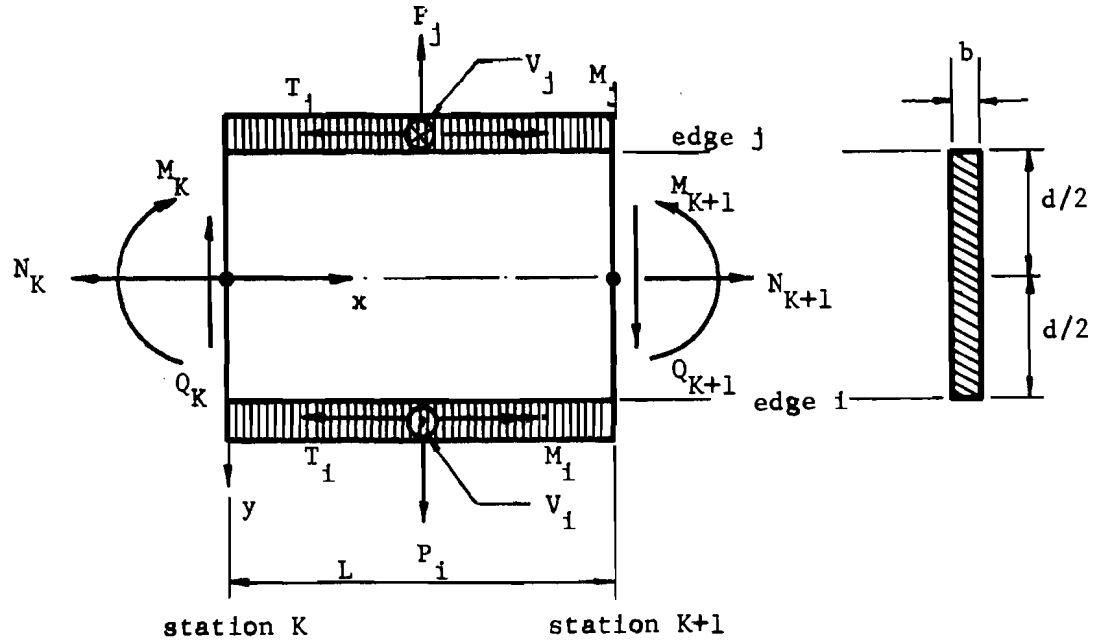

(a) Positive element forces in plate element coordinates

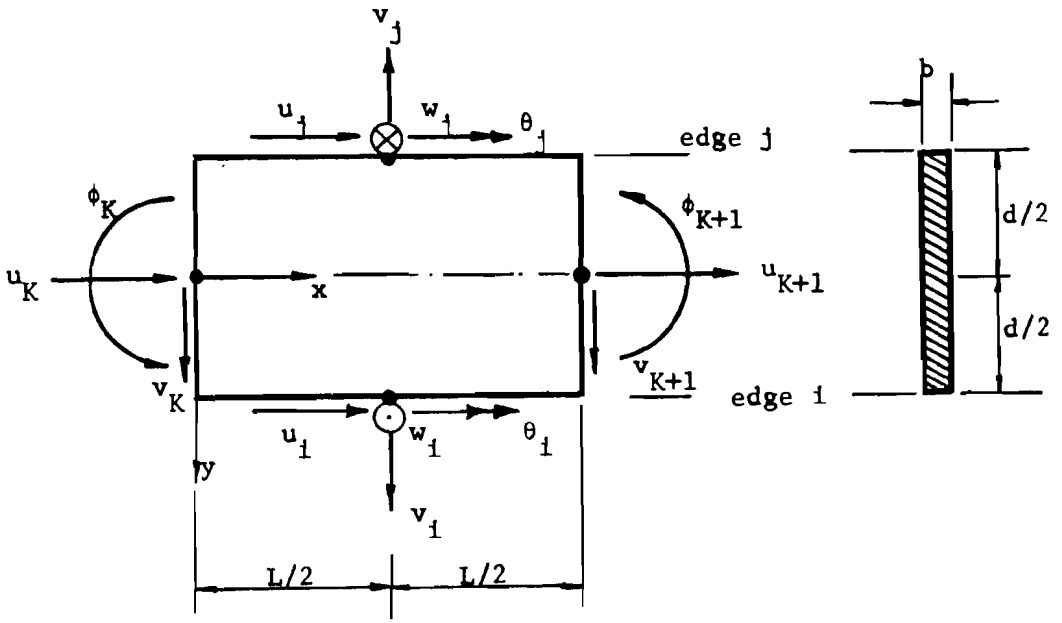

(b) Positive element displacements in plate element coordinates

Fig. 2.3. Positive element forces and displacements in plate element coordinates. (Adapted from Ref. 19.) NOTE: Positive Y axis direction toward element i edge.

function of $\underset{\sim}{Z}_K$. In order to determine $\underset{\sim}{Z}_{K+1}$ due to element edge forces and applied loads, consideration must be given transverse equilibrium and compatibility. Transverse equilibrium requires that, at a particular joint, the sum of all element edge forces from all elements connecting at the joint be in equilibrium with the externally applied line loads. Transverse compatibility requires that the nodal point displacements of all element edges connecting at the joint be equal. Explicit specification of these requirements effectively interconnects, transversely, all the elements in the segment. It should be noted here that transverse compatibility is maintained only at the element edge nodal points. Element edge forces are, therefore, determined as those forces necessary to establish transverse equilibrium and compatibility for a complete segment under the condition that $\underset{\sim}{Z}_K$ is equal to zero (since the effect of $\underset{\sim}{Z}_K$ at K+1 is determined separately). These forces are expressed as a function of $\underset{\sim}{Z}_K$ and the externally applied line loads; consequently, $\underset{\sim}{Z}_{K+1}$ due to the element edge forces is solved in terms of $\underset{\sim}{Z}_K$ and the externally applied line loads. Superposition of effects results in an equation for $\underset{\sim}{Z}_{K+1}$ in terms of $\underset{\sim}{Z}_K$ and the externally applied loads. Application of this procedure to each segment in the span results in a system of linear algebraic equations relating the state vector at the origin, $\underset{\sim}{Z}_o$, to the state vector at the end, $\underset{\sim}{Z}_e$. The known boundary conditions provide sufficient equations for the solution of $\underset{\sim}{Z}_o$ and $\underset{\sim}{Z}_e$. By progressing over the structure once again all state vectors and element edge forces and displacements are solved.

2.5 Coordinate Systems

In order to determine element membrane stiffness equations relating the generalized membrane element edge forces, $\underset{\sim}{Q}$, to the generalized displacements, $\underset{\sim}{\Phi}$, it is convenient to work in the plane of the element--the element relative coordinate system. For a synthesis of element properties it is necessary to refer to a coordinate system which is consistent for all elements--the global coordinate system. Both the element relative and global coordinate systems are defined in Fig. 2.4. Element nodal displacements and edge forces in both coordinate systems are shown in Fig. 2.4.

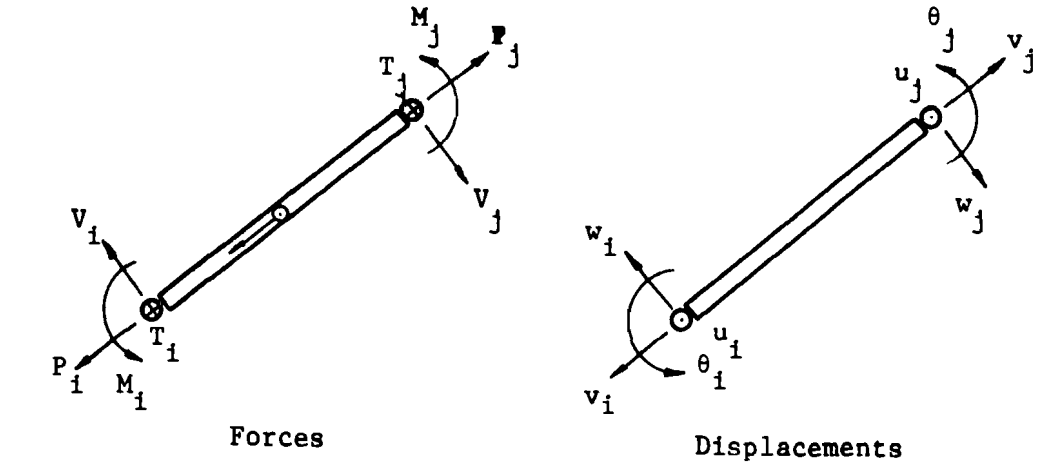

(a) Positive element edge forces and displacements in element relative coordinate system

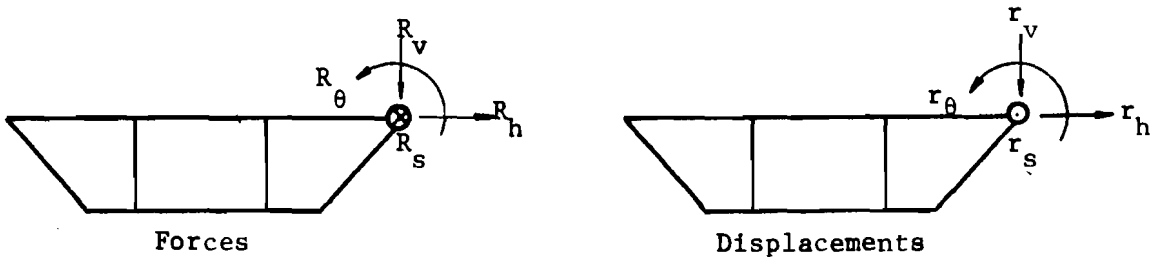

(b) Positive joint forces and displacements in the global coordinate system

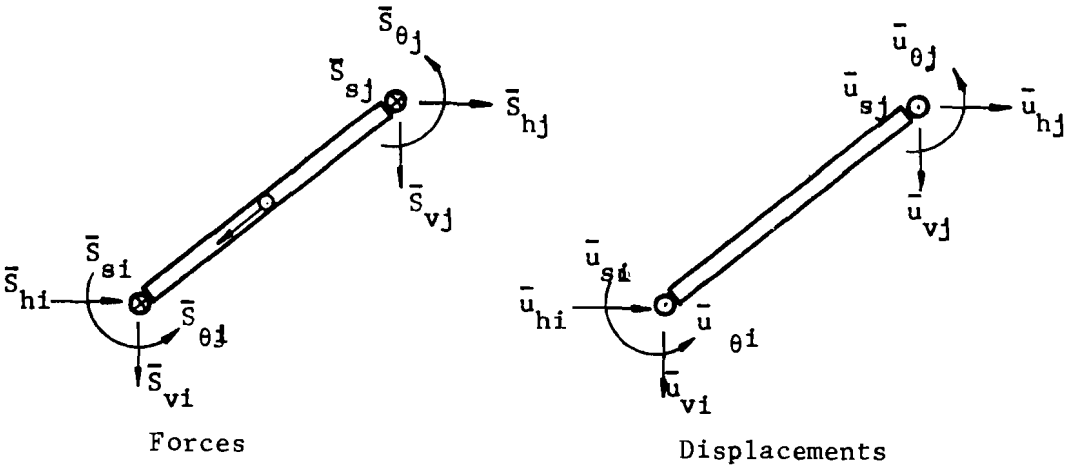

(c) Positive element edge forces and displacements in the global coordinate system

Fig. 2.4. Sign convention and positive direction of element relative coordinates. (Adapted from Ref. 19.)

2.6 Derivation of Equations for the Finite Segment Method

The equations with expansion for this case are derived in Ref. 32. This derivation is not repeated herein.

2.7 Special Considerations Required by Interior Supports

There are several ways to account for the restraint imposed upon the superstructure by interior supports. The technique to be utilized will be dictated by nature of the support.

2.7.1 Simple Pier Support. If the structure is continuous but simply supported over a rigid support; i.e., the support does not restrain longitudinal rotation of the cross section, the basic equations and procedures require no modification. The support restraint may be modeled by specifying the appropriate components of the global joint displacement vector, $\underset{\sim}{\bar{r}}$ as zero for the segment in which the support occurs. Several assumptions implicit in this approach are:

(a) Reactions from the support are applied as a uniformly distributed force, over the segment length, along the restrained joints only.

(b) Joint displacements are restrained to zero at the longitudinal center of the segment (element nodal points).

2.7.2 Interior Diaphragms and Elastic Supports. Should an interior diaphragm exist at the support station or the support offer partial elastic restraint, the basic analysis procedure and equations must be modified. The assumptions regarding the interaction of the support and superstructure are:

(a) Support restraint is specified independently for each element of the cross section in terms of restrained displacement components of the element state vector, or in terms of support stiffness coefficients corresponding to those displacements.

(b) The support reactions for each restrained element correspond to the force components of the element state vector. These support reactions act at the station of the interior support.

(c) There are no restraining forces applied to the joints at the support station.

Detailed derivations of the appropriate equations and the solution utilized are given in Ref. 32.

2.8 The Stopover

The coefficients relating the actions at the two ends of the structure result from a number of matrix multiplications. Therefore, for large systems round-off error can render the coefficients inaccurate. In order to reduce the possibility of such inaccuracies, the displacement components of the complete state vector at certain stations are taken as intermediate unknown vectors. The station at which intermediate unknown vectors are formed are termed stopovers. The matrix operations required at a stopover are the same as those employed at an interior support. The segment progression is then continued using the displacements at the stopover as the unknown vector until a diaphragm support, another stopover, or the end of the structure is encountered. Intermediate unknown vectors, unknowns at interior supports, and finally, the unknown origin boundary actions, $\underset{\sim}{Z}_{ou}$, are solved by a sequence of back substitutions.

C H A P T E R 3

PROGRAM SIMPLA2

3.1 Introduction

The previous chapter outlined a technique for solution of linear equations relating actions at the boundaries of the structure. These equations and known boundary conditions are sufficient for analysis of the structure, subject to general loading and boundary conditions. Utilizing this approach, a FORTRAN IV language computer program, SIMPLA2, was written for the analysis of segmentally constructed, post-tensioned box girders. The mathematical model upon which SIMPLA2 is based was initially developed for the analysis of prismatic plate systems of a given configuration under given loading, boundary, and support conditions. A computer program, SIMPLA,[8] had been written under the direction of Professor A. C. Scordelis to execute the analysis outlined in the previous chapter for completed structures. Subroutines SOLV and STEP, which perform the segment progression and back-substitution, were adapted from SIMPLA for use in SIMPLA2. Subroutine STIFF, which generates the element stiffness matrix, was adapted from SIMPLA without modification. The time and effort required to develop the computer program reported herein was significantly reduced by the availability of SIMPLA and the associated subroutines mentioned above. This material, and invaluable explanation, was provided the authors by Professor A. C. Scordelis.

The unique feature of SIMPLA2 is the capability to deal with a continuously changing structural system, providing a complete analysis at each stage of construction. The program also monitors and updates stresses in all tendons, at any specified stage of construction. At every stage of construction changes which have occurred in the system, i.e., addition of segments, changes in loading, boundary conditions, or interior supports, are specified by "stage control data" and "code words."

The configuration of post-tensioning tendons stressed at the particular stage is specified, and equivalent loadings are calculated. When all loading and boundary conditions are made consistent with those existing at the stage under consideration, the complete analysis of the updated structural system is made by the finite segment method. Each stage of construction, including closure, is considered. Analysis after the structure is made continuous requires additional considerations, as discussed in this chapter. The program is an analysis tool; thus the complete configuration of the system at each stage (loads, boundary conditions, support conditions, prestressing and structural dimensions) and the complete construction sequence must be known.

The purpose of this chapter is to describe SIMPLA2 in detail. The organization of the program and the primary functions of each subroutine are discussed. The additional concepts and equations necessary for the analytical treatment of post-tensioning and stage construction are presented. Finally, several limitations of the program are given. A detailed guide for the specification of input data and interpretation of printed results is given in Appendix B.

3.2 Program Organization

SIMPLA2 is written in FORTRAN IV for the CDC 6600 computer, but has a version programmed in FORTRAN IV for the IBM System 360 computer of the Texas Highway Department. The complete program is composed of nine subroutines and a master program. Detailed flow charts for the program are given in Appendix B.

The program employs seven disc files for temporary data storage during execution. The purpose of each disc file is shown in the flow charts.

The driver program, entitled SIMPLA2, performs three primary functions. The routine accepts the "structure control data" and processes this information to compute "structure constants." The term "structure control data" is reserved for those data which are characteristic of the

girder cross section and, therefore, remain constant for all stages of construction. The number of plate elements making up the cross section (NEL) and the number of joints in the cross section (NJT) are examples of structure control data. The number of degrees of freedom of the structure (4 x NJT), and the coefficients of the transformation matrix are examples of structure constants. Secondly, SIMPLA2 accepts and processes "stage control data" to compute "stage constants." Stage code words (see Appendix B) such as KODJA, KODBC, KODSPT, KREF, and KODTS are read: these control data and code words control the modifications to the loading, boundary conditions, support conditions, and structure to be made at the particular stage. Finally, the routine performs its function as a driver and calls the main solution routines STAGE, STEP, and SOLV, in turn. Data read and computed in SIMPLA2 are used to control the computations of the main solution routines to accomplish the complete solution.

The effects of prestress on the structure are accounted for by use of the equivalent load concept. It is the function of subroutine STAGE to accept tendon control data, and using these data to compute the tendon nodal point coordinates (Y), the tendon nodal point forces after friction losses have been taken into consideration (F), tendon slope at each station across which the particular tendon passes (THET) and, finally, the equivalent joint force and anchorage force vectors imposed upon the structure by the tendon. A detailed presentation of these calculations is contained in Sec. 3.3.

These routines perform computations and data manipulations which could generally be categorized as modifications to the loading, structure, and boundary conditions from one stage of construction to the next. Once these modifications have been made, the analysis of the modified system under the specified conditions can begin. Subroutines STEP and SOLV perform the finite segment analysis of the modified system.

The final subroutine of major significance is entitled CSTRAIN and recomputes tendon nodal point strains in each tendon at each stage of construction.

Two library subroutines are used in conjunction with STEP and SOLV. Subroutine DSYNINV is for the inversion of a square symmetric banded matrix, and is used in STEP for the inversion of the segment stiffness matrix. DSIMEQ is a general equation solver which is employed in both STEP and SOLV.

Subroutine PLFDS is for the computation of element edge stresses from the element internal stress resultants and the output of results only.

The SIMPLA2 CDC 6600 version also utilizes a routine, IOBIN, which is a system routine unique to The University of Texas at Austin Computation Center. IOBIN allows the programmer to randomly access the disc files in order to read, write, or rewrite a particular logical record without the necessity of using elaborate disc-positioning procedures. The fact that IOBIN is unique to The University of Texas Computation Center does not limit the general use of the program, since most large computer systems do have random access capability. A programmer should examine the program before use on another system.

The SIMPLA2 version for the IBM System 360 uses the IBM Random input/output to replace IOBIN. Some files were split to reduce record lengths and common blocks were reordered.

3.3 Analytical Treatment of Prestressing

3.3.1 The Equivalent Load Concept. Prestressing a structure may be described as the application of engineered forces to the structure producing stresses and displacements which offset the stresses and displacements induced by the applied loads. This concept of prestressing is the basis of a general technique for the analysis of prestressed structures, wherein all forces applied to the structure by the prestressing tendon are considered as applied loads. The analysis of the structure for these loads yields the stresses and displacements due to prestressing. The procedure described above is "the equivalent load concept" and has been used extensively for the analysis of prestressed structures.[26,27] The equivalent load concept is applicable without regard to the condition of determinacy, the only absolute requirement being that all the forces produced by the tendon on the structure be considered.

3.3.2 Forces Induced by Prestressing Tendon. In this report the term "post-tensioned" will imply that the prestressing tendon is located within the member cross section and that after the tendon is stressed it is anchored against the member itself. It is also implied that the tendon is unbonded during stressing. The assumption is made that the coefficients of friction between the tendon and duct material are known. Since this study deals exclusively with post-tensioned construction, the terms "prestressed" and "post-tensioned" will be considered synonymous.

The simplified example structure shown in Fig. 3.1 contains one tendon which has a general draped profile, $Y = f(x)$, and which is stressed to some specified value, f_{si}, at the jacking (live) end. In this example it is assumed that $F(0) = F(\ell) = f_{si} \times A_s$, implying that the tendon is stressed from both ends. Figure 3.1 illustrates all the forces exerted on the member by the tendon. When the specified jacking force is reached the tendon is anchored against the end of the beam, inducing concentrated forces at the anchors tangent to the tendon. As the tendon is stressed, it will attempt to straighten; the member prevents this straightening, thus receiving radial pressure, p, from the tendon. The tendon will also elongate, mobilizing a friction force between the duct and tendon. The frictional force is generally associated with a change in direction of the tendon and is a function of the coefficient of friction and the geometry of the tendon profile. A more complete discussion of friction forces is presented in Sec. 3.3.4. The friction will cause the tendon force to vary along the tendon length. Fig. 3.2 is a free body diagram of a length, ds, of the tendon. Considering equilibrium of all forces in the direction of the normal to the curve, n,

$$(F)(\sin d\theta/2) + (F + dF)(\sin d\theta/2) - N = 0 \qquad (3.1)$$

where N is the summation of all n-components over ds; i.e., $p = N/ds$. With small angle geometry and neglecting second order terms,

$$(F)(d\theta) = N \qquad (3.2)$$

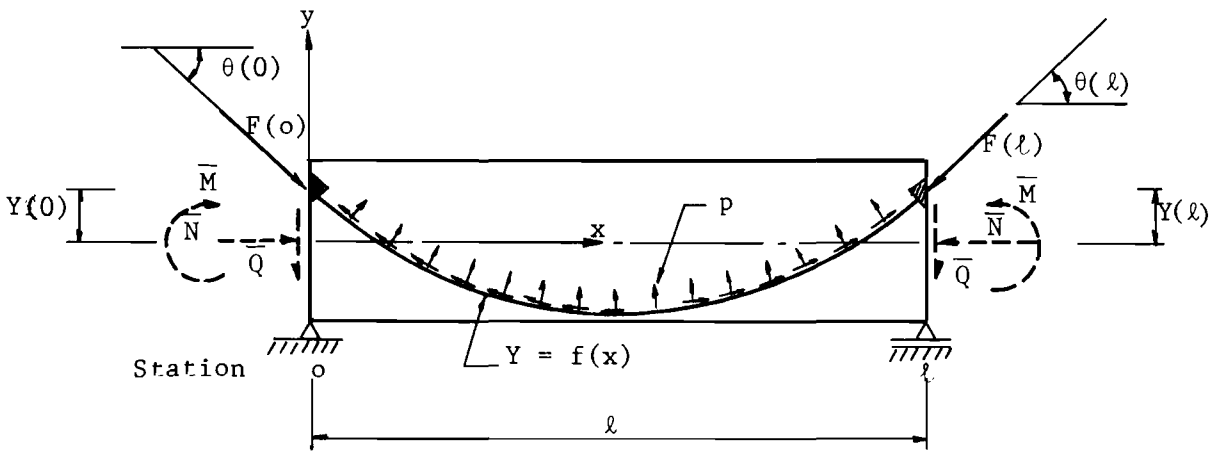

Fig. 3.1 Forces induced by tendon.

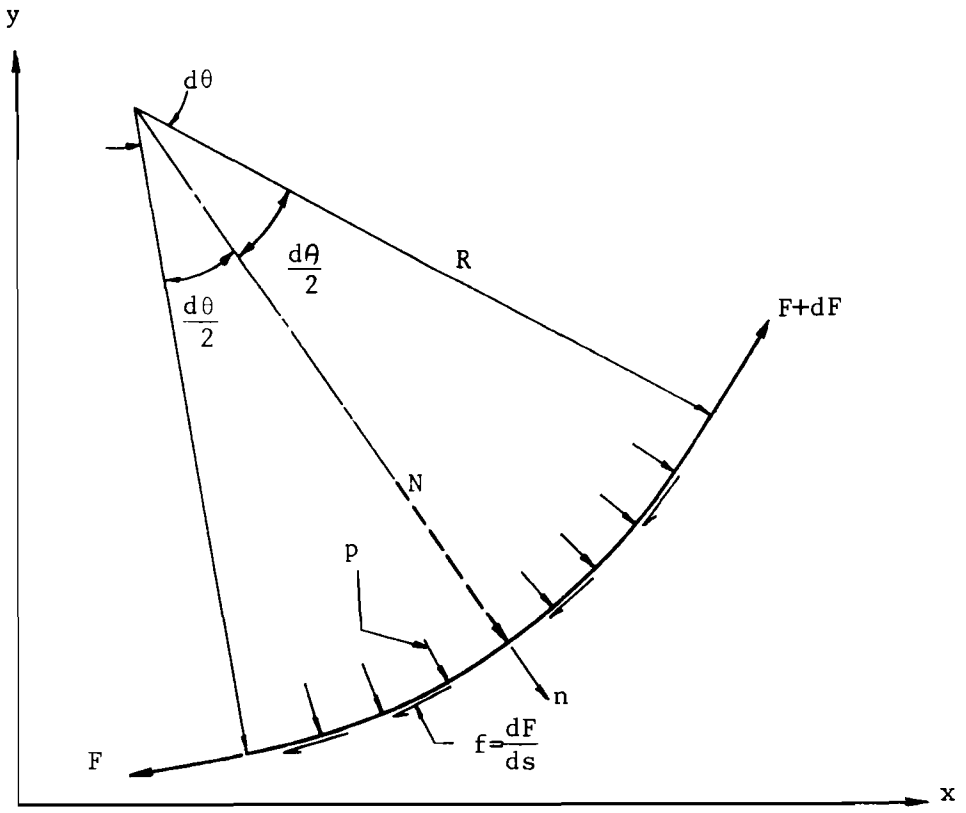

Fig. 3.2 Free body diagram of tendon increment.

and, therefore, the radial pressure per unit length is

$$p = N/ds = (F)(d\theta/ds) = F/R \tag{3.3}$$

Equation (3.3) indicates that the radial force per unit tendon length at any point along the tendon is a function of tendon force and tendon radius of curvature at that point. Figure 3.1 indicates that the anchor forces $F(0)$ and $F(\ell)$ are acting at eccentricities $Y(0)$ and $Y(\ell)$ and are directed at angles $\theta(0)$ and $\theta(\ell)$, respectively. The most convenient method to treat these anchor forces analytically is to resolve them into equivalent force systems acting at the centroid of the element. These equivalent forces, shown by the dashed vectors in Fig. 3.1, are termed "the anchorage force vector" and are given by

$$\begin{bmatrix} \bar{M} \\ \bar{Q} \\ \bar{N} \end{bmatrix} = F(0) \begin{bmatrix} Y(0)\cos\theta(0) \\ \sin\theta(0) \\ \cos\theta(0) \end{bmatrix} \tag{3.4a}$$

and

$$\begin{bmatrix} \bar{M} \\ \bar{Q} \\ \bar{N} \end{bmatrix} = -F(\ell) \begin{bmatrix} Y(\ell)\cos\theta(\ell) \\ \sin\theta(\ell) \\ \cos\theta(\ell) \end{bmatrix} \tag{3.4b}$$

It is reasonable to assume that the friction forces can be neglected in arriving at an equivalent prestress load system[26]; therefore, the radial forces, Eq. (3.3), and the anchorage force vectors, Eqs. (3.4), constitute the complete equivalent loading.

3.3.3 Geometry of the Tendon Profile. Before the equivalent forces can be evaluated numerically, the geometric characteristics of the tendon profile and the tendon force distribution must be known. A continuous function may be used to approximate arbitrary tendon profiles. It is

assumed that an entire tendon profile may be made up of one or more distinct curves. The profile illustrated in Fig. 3.3 is composed of five distinct curves: a curved portion labeled "Curve 1," a straight portion labeled "Curve 2," and a second curved portion labeled "Curve 3." Since the profile is symmetrical about the centerline, only half is shown. The tendon, N, is shown lying entirely in one plate element of the structure and spanning between stations 1 and 17 (the end of the structure). Each of the distinct curves can be represented by a polynomial expression of the general form:

$$Y = A_o + (A_1)(x) + (A_2)(x)^2 + ... + (A_m)(x)^m \qquad (3.5)$$

If the degree of the polynomial is assumed, m, and a sufficient number of points, m + 1, are selected along the curve, then the unknown coefficients (A_i) in Eq. (3.5) are easily determined.

For purposes of this computer program it is assumed that the entire tendon profile can be adequately described by selecting a combination of straight line and parabolic curves. Higher order approximations would require more input data. The points on each curve are provided by input values of "control coordinates." Curve 1 of Fig. 3.3, for example, is assumed to be parabolic; thus three control coordinates are required. The coordinates used are (NXL (1), YL (1)), (NXR (1), YR (1)), and (XM(1), YM(1)). The first two coordinates locate the end points of the particular curve. These are provided for both parabolic and straight line curves. The third point represents some interior point on the curve under consideration. Its selection should be made carefully so that a reasonable parabola, approximating the tendon, results. The control coordinates are measured in the element coordinate system, as shown in Fig. 3.3. Each distinct curve (Curve 1) begins (station 1) and ends (station 4) at a station rather than between stations.

It is quite important to the accuracy of the analysis that the input control coordinates be carefully checked by the user.

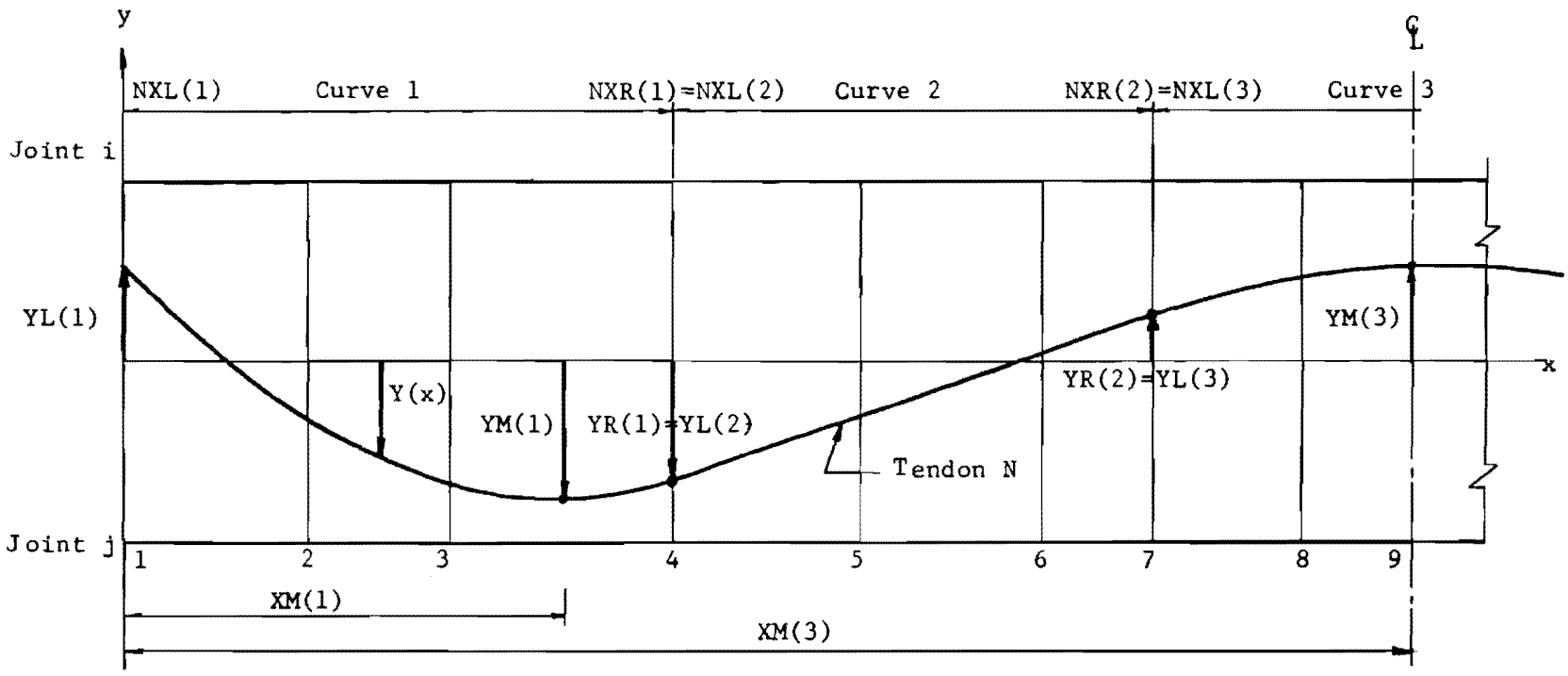

Fig. 3.3. Typical tendon profile.

3.3.4 Tendon Force Function and Friction Loss. In post-tensioned construction there are numerous sources of loss of prestress force, such as:

(1) Deformation and seating of the anchorage hardware upon transfer of the prestress force from the jack to the anchorage.

(2) Creep and shrinkage of the concrete.

(3) Stress relaxation of the steel.

(4) Friction between the tendon and the tendon duct material.

Due to the variety of anchorage hardware, it is impractical to attempt a rigorous analytical approach to compute anchorage take-up losses. Creep and shrinkage of concrete and stress relaxation in the tendons each present formidable analytical problems for all but the simplest cases. Due to the general complexity of these phenomena, and to the fact that they are functions of many variables, precise analytical evaluation of prestress losses due to creep, shrinkage, and stress relaxation is seldom undertaken. Creep and shrinkage losses depend heavily on the age and curing histories of the structure. These losses are much less severe in reasonably mature precast sections, especially in comparison with expected values when cast-in-place segmental construction is used. The most typical approach, as with present design codes,[1,27] is to deduct some precentage of the jack force or some fixed value of strain (stress), or a combination of both to account for these losses.

SIMPLA2 accepts all prestressing information in terms of force rather than stress, and the only occasion on which the program deals with tendon stress is for output. "Temporary maximum jacking force" is the maximum force to which the tendon is initially jacked when a temporary overstress and release-back approach is used for overcoming friction losses. "Jacking force" is the force being exerted by the jack just prior to transfer of prestress. "Initial prestress" is the jacking force less the force loss due to seating and deformation of the anchorage hardware. "Effective prestress force" or "prestress force" will generally vary along the tendon and is defined as the initial prestress less friction losses.

SIMPLA2 input deals only with the temporary maximum jacking force and initial prestress force. The program makes no allowance for losses due to shrinkage and creep. Consequently, losses of prestress force due to anchorage deformation and seating, shrinkage, and creep effects must be estimated or otherwise accounted for by the user.

Friction loss is a function of several well-defined variables and can be evaluated analytically from generally applicable equations. Figure 3.4(a) illustrates a typical tendon located in one plate element of the cross section and spanning through segments K and K+1. Figure 3.4(b) shows the free body diagram of an increment of this tendon which spans the interval $a \leq x \leq b$. The forces shown acting upon this increment are the effective prestress force at each end, F(a) and F(b), radial force per unit length, p, and the friction force per unit length, dF. From elementary mechanics:

$$dF/ds = (\mu)(p) \tag{3.6}$$

where μ is the coefficient of friction. Substituting Eq. (3.3) into Eq. (3.6) yields

$$dF/ds = (\mu)(F/R) \tag{3.7}$$

Substituting $(R)(d\theta)$ for ds in Eq. (3.7) leads to:

$$dF/F = (\mu)(d\theta) \tag{3.8}$$

Integrating both sides of Eq. (3.8) from a to b gives

$$F(b) = [F(a)][e^{\pm\mu\Delta\theta}] \tag{3.9}$$

where e is the base of natural logarithms, and the sign of the exponent depends upon the relative magnitudes of F(a) and F(b). The total friction loss over a tendon length is generally considered in two parts--that due to tendon drape and that due to deviations from the intended tendon plane (wobble). In order to account for both effects, Eq. (3.9) may be written as

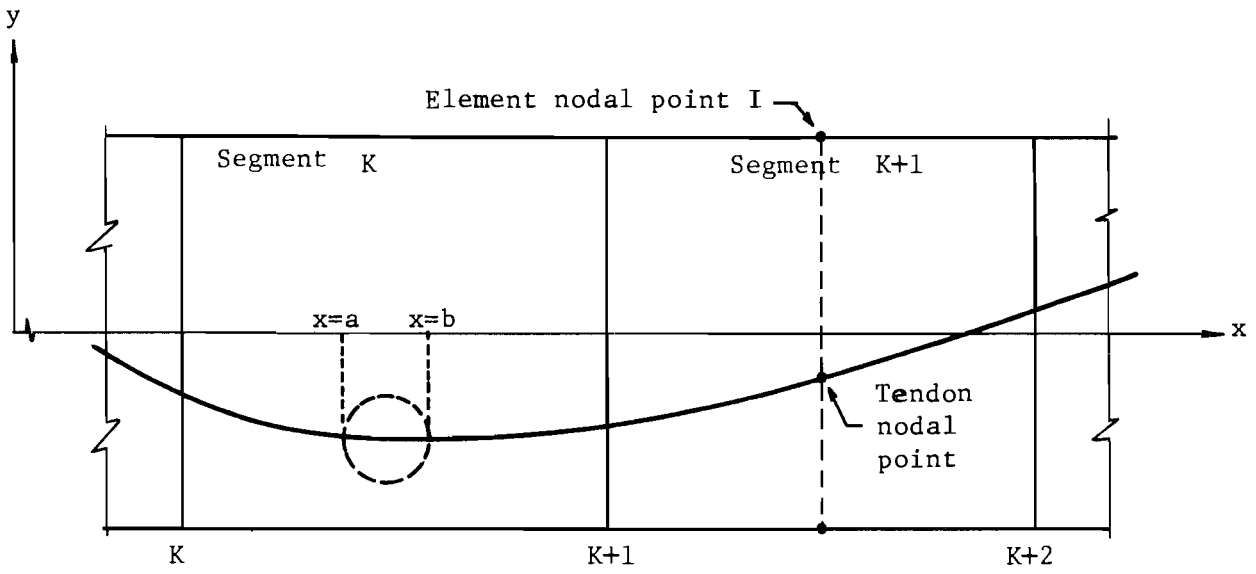

(a) Tendon spanning segments K and K+1

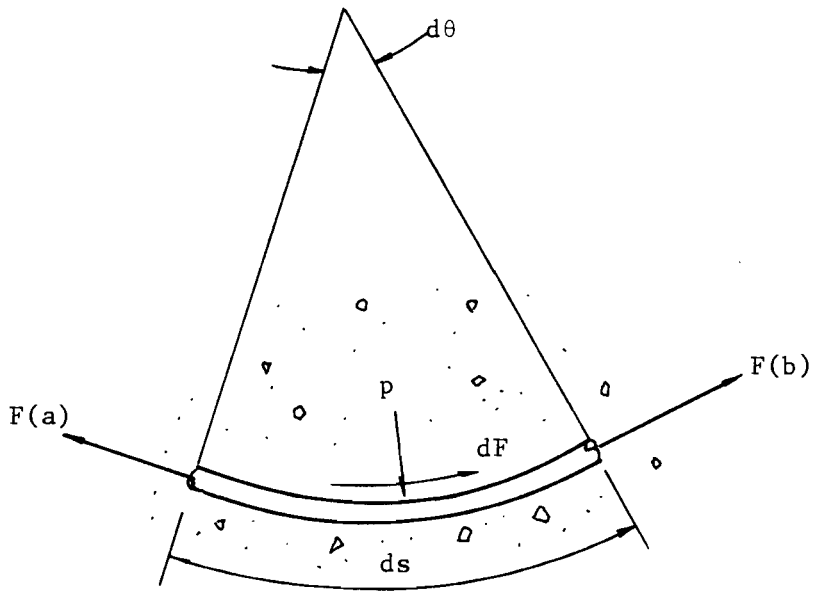

(b) Tendon in interval $a \leq x \leq b$

Fig. 3.4 Typical tendon.

$$F(b) = [F(a)][e^{\pm(\mu\Delta\theta+\lambda s)}] \tag{3.10}$$

where λ is the wobble coefficient and s is the tendon length over the interval.

Equation (3.10) is a continuous function for effective prestress force which takes into account the variation of F and variation of p throughout the interval. However, if F can be assumed constant over the interval, an approximate form of Eq. (3.10) may be derived to facilitate computer calculation. Assuming F is constant throughout the interval and equal to F(a), Eq. (3.8) can be rewritten as:

$$dF = [F(a)](\mu)(d\theta) \tag{3.11}$$

Integration over the interval yields:

$$F(b) = F(a)[1 \pm (\mu)(\Delta\theta)] \tag{3.11a}$$

and generalizing the equation to include the effects of wobble yields,

$$F(b) = F(a)[1 \pm (\mu)(\Delta\theta) \pm (\lambda)(s)] \tag{3.11b}$$

Extending the interval to include the entire K^{th} segment (Fig. 3.4(a)), the above equation can be written:

$$F(K+1) = F(K)[1 \pm (\mu)(\Delta\theta) \pm (\lambda)(\Delta X)] \tag{3.12}$$

where F(K+1) and F(K) are effective prestress values at stations K+1 and K, $\Delta\theta$ is the change in the tendon tangent angle between stations K and K+1, and ΔX is the horizontal projection of the tendon length between K and K+1.

Equation (3.12) is a close approximation of Eq. (3.10) if the friction loss over the interval is "small." According to several authorities,[1,26,27] Eq. (3.12) yields accurate results if F(a) and F(b) do not differ by more than approximately 15 percent. SIMPLA2 employs Eq. (3.12) to calculate effective prestress force at each station. For all problems

solved to date, the use of Eq. (3.12) rather than Eq. (3.10) has seemed justified since the tendon is broken into a number of short segments.

Numerous techniques may be used to reduce friction loss. One sure technique is to overtension the tendon to a temporary maximum jacking force, and then release back to a specified force, reversing the direction of the friction force. A second approach is to stress the tendon from both ends simultaneously. An even more effective method is to combine these two methods. The variation of effective prestress force over the tendon length depends upon the stressing option selected. Figure 3.5 illustrates, qualitatively, the variation of effective prestress force for the stressing options mentioned above.

SIMPLA2 is capable of modeling all stressing options shown, with the exception of the repeated jacking and release-back method. The tendon stressing option to be modeled is completely described by one input parameter identifying the live end of the tendon (KEEP), and two force values--the temporary maximum jacking force (PIP) and the initial jacking force (PIPP).

The friction coefficients and stressing option are both known input quantities and the tendon geometry is input for the particular tendon. Calculation of effective prestress force at any station along the tendon is accomplished by use of Eq. (3.12).

3.3.5 Calculation of Equivalent Loads. Post-tensioning induces two types of forces on the structure--radial pressures and anchorage forces--both of which depend on the geometry of the tendon profile and effective prestress force. With continuous functions representing tendon eccentricity and effective prestress force for each tendon, the radial pressures and anchorage force vectors are easily computed in force components compatible with those used in the finite segment method.

Equivalent Joint Loads - The PJP Array

A prestressed box girder structure is illustrated in Fig. 3.6(a). The structure is prestressed with two draped tendons (one per web) anchored

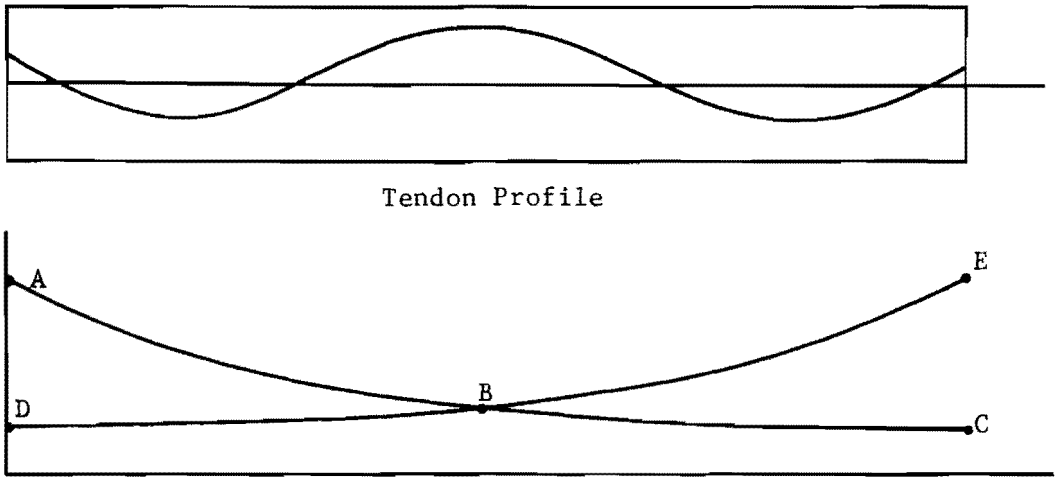

(a) Tendon Force - Jacking from one (ABC or EDB) or both ends (ABE)

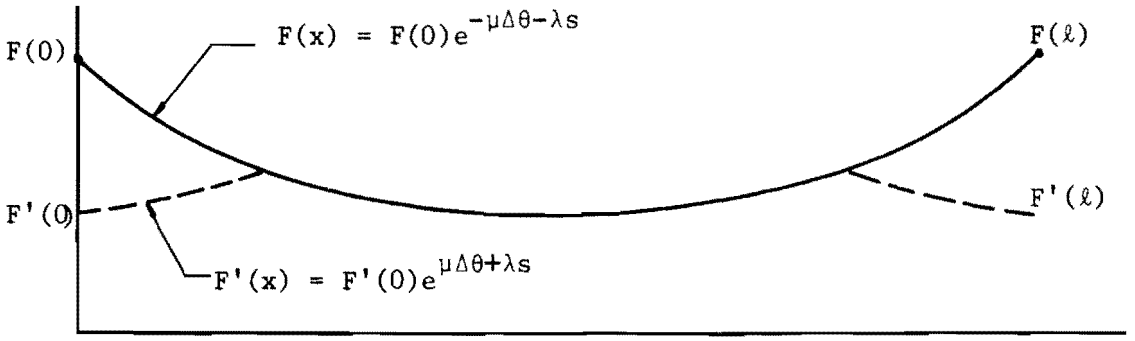

(b) Tendon Force - Jacking from both ends and releasing back

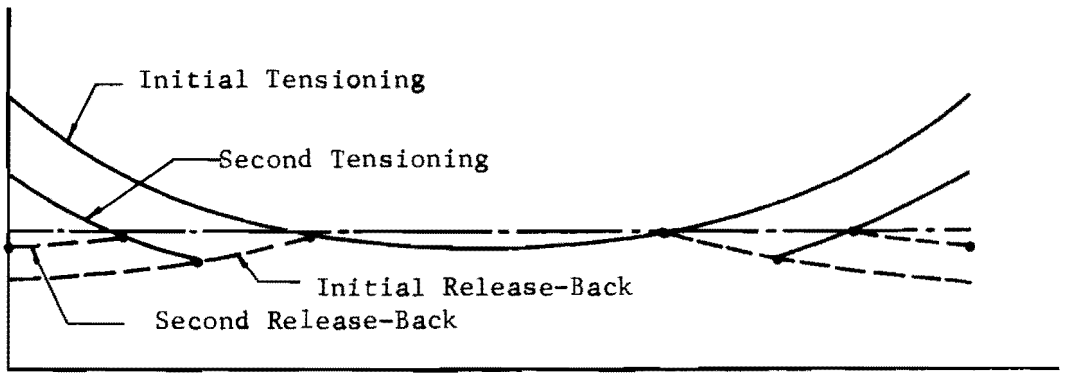

(c) Tendon Force - Repeated overstress release back

Fig. 3.5 Tendon force variation.

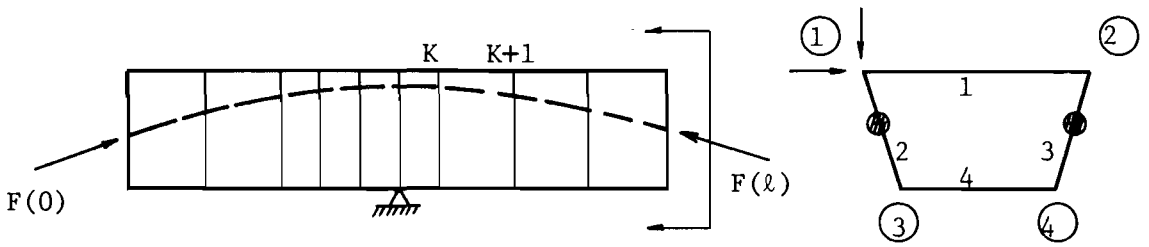

(a) Elevation and cross section of structure

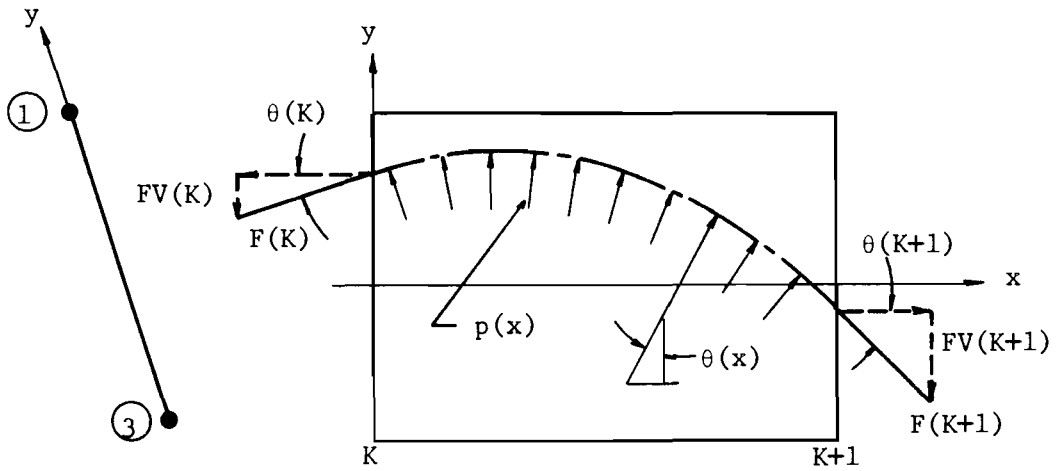

(b) Free body diagram of tendon segment

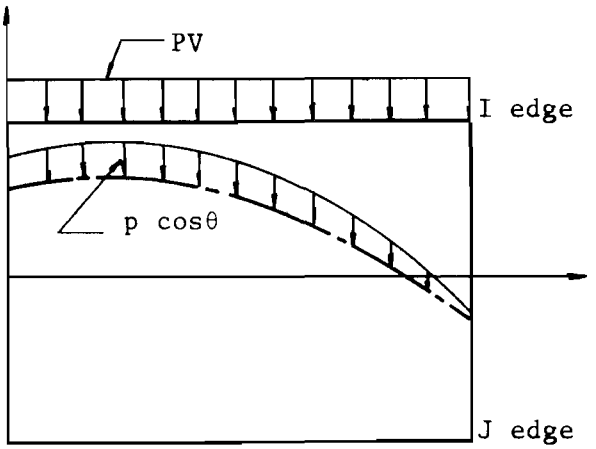

(c) Equivalent tendon pressure on structure

Fig. 3.6. Equivalent loads.

in the same web plate elements containing them. Figure 3.6(b) shows the free body diagram of segment K of one tendon in the plane of the plate element containing it. The effective prestress forces, F(K) and F(K+1), and the tendon slopes, $\theta(K)$ and $\theta(K+1)$, are evaluated by Eq. (3.12) and derivatives of the tendon layout polynomial, respectively. Considering the equilibrium of the tendon segment in the element y-direction:

$$\int_{K}^{K+1} (p)(\cos\theta)(ds) = F(K)\sin\theta(K) - F(K+1)\sin\theta(K+1) \qquad (3.13)$$

The vertical components of the radial pressure, $(p)(\cos\theta)$, act along the axis of the tendon, as shown in Fig. 3.6(c), and are distributed over the segment length as $\cos\theta$. The mathematical model adopted for the analysis requires that applied forces act on the joints (edges of the elements) and be uniformly distributed over the segment length. Obviously, an approximation is required. The equivalent force applied to the structure is calculated by

$$PV = [FV(K) - FV(K+1)]/[X(K+1) - X(K)] \qquad (3.14)$$

and is applied at the I-edge of the element, as shown in Fig. 3.6(c). The approximations introduced to the assumed uniform distribution over the element length are probably insignificant, since generally $\theta(K)$ and $\theta(K+1)$ do not differ considerably. Since, in this study, the macroscopic response of the structure is of primary concern, the effects of changing the point of application of the radial force components are negligible. For the same reason, the horizontal components of the radial forces are neglected in deriving the equivalent force system. The positive direction of PV is the positive y-direction of the element containing the tendon. Since PV is in the plane of the element and applied at the I-edge of the element, the equation used to transform the element edge forces into joint forces may be used to transform PV into an equivalent joint load. The complete transformation is represented symbolically as:

$$\begin{bmatrix} \bar{S}_i \\ \bar{S}_j \end{bmatrix} = \begin{bmatrix} A_{11} & A_{12} \\ A_{21} & A_{22} \end{bmatrix}^T \begin{bmatrix} S_s \\ S_m \end{bmatrix} \tag{3.15}$$

For transformation of PV, Eq. (3.15) may be condensed to:

$$\begin{bmatrix} \bar{S}_{hi} \\ \bar{S}_{vi} \\ \bar{S}_{\theta i} \\ \bar{S}_{si} \end{bmatrix} = \begin{bmatrix} A_{12} \end{bmatrix}^T \begin{bmatrix} 0 \\ 0 \\ PV \\ 0 \end{bmatrix} \tag{3.16}$$

This transformation results in a horizontal and vertical joint force acting at Joint I, representing the contribution of the single tendon under consideration to the complete equivalent joint load vector for segment K. The components may then be summed into a complete equivalent joint load vector which contains force contribution from all tendons in segment K. Treating all tendons in segment K in the same manner, the complete equivalent joint load vector is written as:

$$R_P = PJP(K) = \begin{bmatrix} R_{P1} \\ R_{P2} \\ \cdot \\ \cdot \\ \cdot \\ R_{Pn} \end{bmatrix} \tag{3.17}$$

where the subvectors R_{Pi} are of the form

$$R_{Pi} = \begin{bmatrix} \Sigma\bar{S}_{hi} \\ \Sigma\bar{S}_{vi} \end{bmatrix} \tag{3.18}$$

The summation indicates that the contributions from all tendons in the segment K, at the stage under consideration, to the equivalent joint load

vector at Joint I have been summed. An equivalent joint load vector is formed for each segment in the structure; therefore, the complete equivalent joint load array at each stage is of the form:

$$[PJP] = [\underset{\sim}{PJP}(1) \quad \underset{\sim}{PJP}(2) \ldots \underset{\sim}{PJP}(K) \ldots \underset{\sim}{0}\ \underset{\sim}{0}\ \underset{\sim}{0}] \qquad (3.19)$$

for a structure with n joints and K segments. Equation (3.19) implies that the array of equivalent joint load vectors, [PJP], is of dimension (2nx50). It should also be noted that the equivalent joint load vectors are now in a convenient form to be summed with the applied joint loads.

The Anchorage Force Vector - The PBAR Array

Each tendon imposes two anchorage force vectors onto the structure: one at the left (IXT), and one at the right (JXT) terminal station of the particular tendon. The vector imposed at the left terminal station, $\underset{\sim}{\bar{P}}_o$, is given by Eq. (3.4a) and that imposed at the right terminal station, $\underset{\sim}{\bar{P}}_e$, is given by Eq. (3.4b). For the general case of a structure consisting of q elements, both $\underset{\sim}{\bar{P}}_o$ and $\underset{\sim}{\bar{P}}_e$ are composed of q subvectors, each subvector being given by Eqs. (3.4a) or (3.4b). The general form of the anchorage force vector for a structure with q elements containing tendons in elements i and j only is:

$$\underset{\sim}{\bar{P}} = \begin{bmatrix} 0 \\ 0 \\ \vdots \\ \underset{\sim}{\bar{P}}_i \\ \vdots \\ \underset{\sim}{\bar{P}}_j \\ \vdots \\ 0 \end{bmatrix} \qquad (3.20)$$

where the vector dimension is (3qx1). Each anchorage station has associated with it a complete anchorage force vector as given by Eq. (3.20), or each $\underset{\sim}{\bar{P}}$ is associated with a particular station, either IXT or JXT.

It is assumed that all tendons stressed during a single stage of construction have the same terminal stations; therefore, $\underset{\sim}{\bar{P}}_o$ and $\underset{\sim}{\bar{P}}_e$ contain the contributions of all tendons stressed at that stage to the complete anchorage force vectors which are associated with the terminal stations for that stage. As $\underset{\sim}{\bar{P}}$ is computed, it is summed into the PBAR array. PBAR is an array composed of a $\underset{\sim}{\bar{P}}$ for each station in the structure, and is of the general form:

$$\text{PBAR} = [\Sigma\underset{\sim}{\bar{P}}_1 \quad \Sigma\underset{\sim}{\bar{P}}_2 \quad . \quad . \quad . \quad . \quad \Sigma\underset{\sim}{\bar{P}}_{K+1}] \tag{3.21}$$

The subscripts indicate the station number at which the $\underset{\sim}{\bar{P}}$ is applied. The summation indicates that the $\underset{\sim}{\bar{P}}$ associated with a particular station for the stage under consideration is summed with $\underset{\sim}{\bar{P}}$ applied at the station from all previous stages. PBAR is therefore an array containing all $\underset{\sim}{\bar{P}}$ acting on the structure at any stage and is updated with each subsequent tendon stressing. The column location of each vector indicates the station at which it is to be applied. Figure 3.7 illustrates segments K-1 and K of a one-plate element structure with $\underset{\sim}{\bar{P}}$ acting at station K. The force components of the state vector just to the left of the station are:

$$\underset{\sim}{p}_K^{\ell} = \begin{bmatrix} M \\ Q \\ N \end{bmatrix}_k^{\ell} \tag{3.22}$$

and those just to the right:

$$\underset{\sim}{p}_K^{r} = \begin{bmatrix} M \\ Q \\ N \end{bmatrix}_k^{r} \tag{3.23}$$

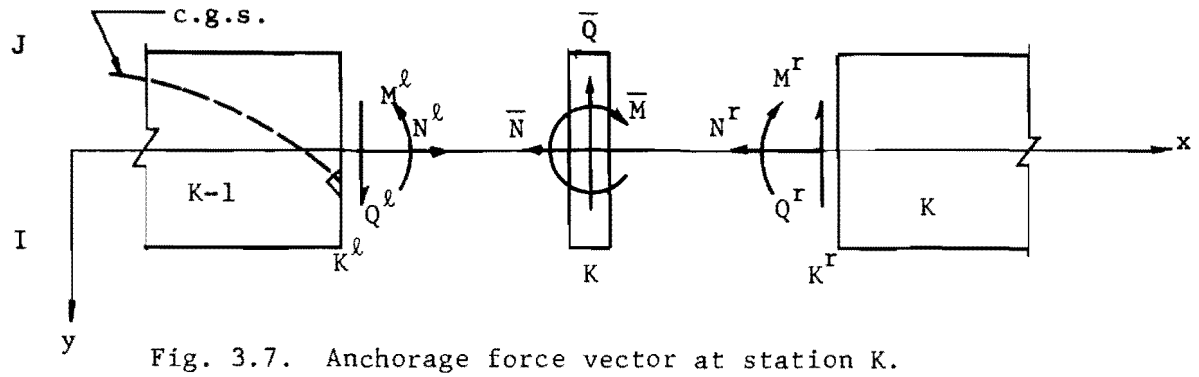

Fig. 3.7. Anchorage force vector at station K. Forces shown in positive direction.

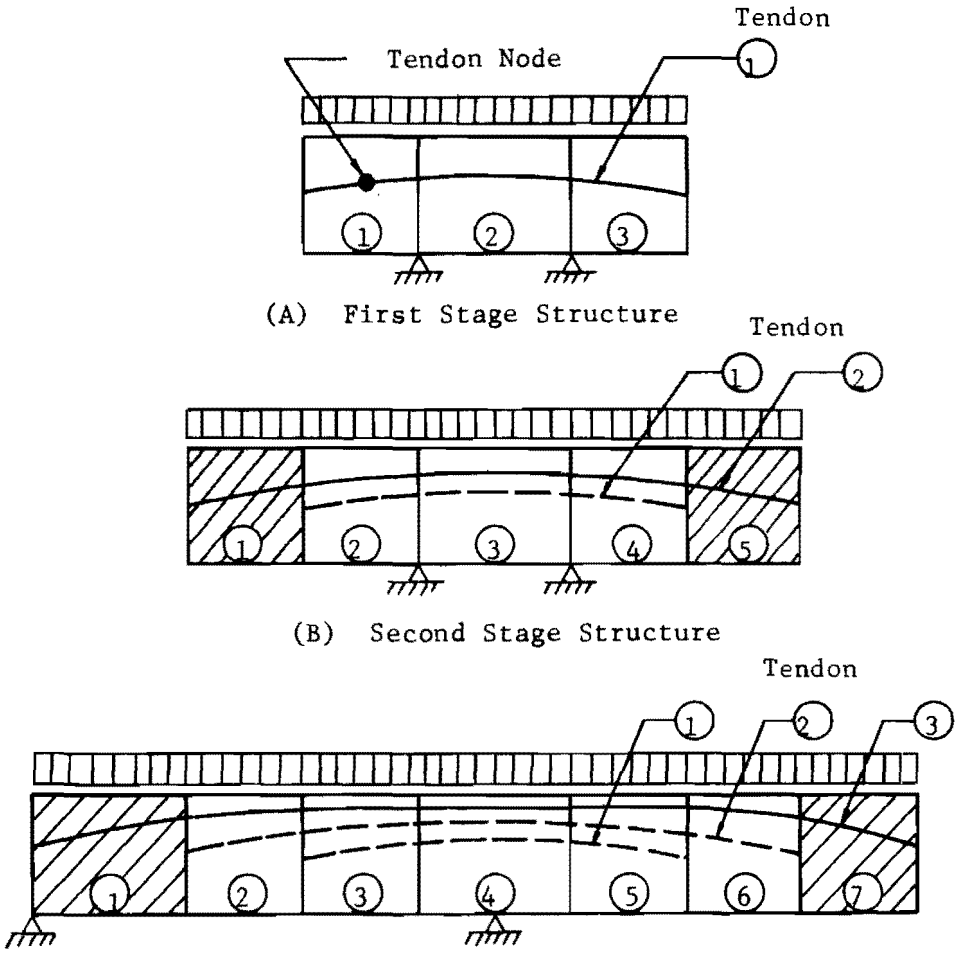

Fig. 3.8. Staging of the structure.

The anchorage force vector illustrated is given by

$$\underset{\sim}{\bar{P}}_K = \begin{bmatrix} \bar{M} \\ \bar{Q} \\ \bar{N} \end{bmatrix} = -F(K) \begin{bmatrix} Y(K)\cos\theta(K) \\ \sin\theta(K) \\ \cos\theta(K) \end{bmatrix} \tag{3.24}$$

since K is shown as the right terminal station for the tendon. All quantities are positive as shown. For equilibrium of the station:

$$\underset{\sim}{P}^r_K = \underset{\sim}{P}^\ell_K + \underset{\sim}{\bar{P}}_K \tag{3.25}$$

and for compatibility of displacements across the station:

$$\underset{\sim}{d}^r_K = \underset{\sim}{d}^\ell_K = \underset{\sim}{d}_K \tag{3.26}$$

where the subvector $\underset{\sim}{d}$ is the displacement component of the state vector for station K. Therefore, to take account of the anchorage force vector applied at station K, the state vector applied to segment K must be modified by the following equation:

$$\underset{\sim}{Z}^r_K = \underset{\sim}{Z}^\ell_K + \begin{bmatrix} \underset{\sim}{0} \\ \underset{\sim}{\bar{P}} \end{bmatrix}_K \tag{3.27}$$

To account for $\underset{\sim}{\bar{P}}$ in the general case, each element of the cross section is considered independently and the subvector associated with the particular element is added into the complete state vector using Eq. (3.27).

$$\underset{\sim}{Z}^r_K = \underset{\sim}{Z}^\ell_K + \begin{bmatrix} \underset{\sim}{0} \\ \underset{\sim}{\bar{P}}_1 \\ \underset{\sim}{0} \\ \underset{\sim}{\bar{P}}_2 \\ \vdots \\ \underset{\sim}{0} \\ \underset{\sim}{\bar{P}}_q \end{bmatrix} \tag{3.28}$$

The PJP and PBAR arrays completely describe the equivalent loading from the tendons stressed at the stage under consideration and all previous stages. For every subsequent tendon stressed, both arrays are modified to account for the additional equivalent loads.

3.4 Analytical Treatment of Stage Construction

3.4.1 Basic Approach. The capability of SIMPLA2 to analyze the structure for each stage of construction depends entirely on modifications made to the various force vectors, and boundary condition and support arrays. Once these modifications are made, the structure is completely analyzed once again. Since the basic analysis procedure deals with each segment independently in turn, accounting for segments added to the structure is simply a matter of specifying the number of segments added and their length. It may be concluded that the analysis of a structure which is constructed in L stages amounts to L separate analyses with the input data required for the Kth stage being deduced from that for the (K-1)th stage, using a minimum amount of additional user-generated input data.

The approach outlined above depends for its validity on several assumptions. With reference to Fig. 3.8, it is obvious that stressing tendon number 2 during the second stage of construction will cause the effective prestress force at all points along tendon number 1 to vary from the values calculated by Eq. (3.12). The variation in effective prestress force causes variation in the equivalent load vectors. The assumption is made that this change in equivalent load will be of secondary importance to the structural analysis and no account is made for this change. In order to check the validity of this assumption, SIMPLA2 is equipped with the capability to recompute tendon stresses for all tendons at any stage of construction. Further attention will be given this matter in the discussion accompanying the example problems in Chapter 4. The analysis performed at each stage assumes the structure to be completely continuous. However, in fact, the stations located at the most recently placed epoxy joints mark sections at which complete structural continuity

does not exist until the jointing material develops its design strength. The assumption of complete structural continuity may be justified by several practical considerations. It has been recommended that structures of this type be designed under a "no tension" criterion,[6] meaning that no longitudinal tensile stresses be allowed at any section of the structure at any stage of erection. A design allowing longitudinal tensile stresses at some locations in the structure would be obviously unacceptable if the "wet" joint were required to carry tensile stresses. In some designs (as Example 3 of the following chapter), where prestressing would induce temporary tensile stresses at a wet joint, temporary tensile fasteners may be provided to accommodate these stresses while the epoxy sets. With these considerations in mind, it is assumed that only shear and direct compressive stresses need be transmitted across the joint. The physical discontinuity in the structure will have no effect on the transmission of compressive stresses across the joint. In the type problems of primary concern in this study (Example 3 of the following chapter) the most significant shear forces are carried across the joint by web elements which are generally provided with shear keys. In many cases the flange elements are also provided with shear keys for alignment purposes. In view of these considerations, it is assumed that the element shear forces will be transmitted across the joint as if the structure were completely continuous, and thus, that the analysis of a continuous structure leads to results which are accurate in a macroscopic sense.

3.4.2 Stage Control Data and Code Words. The basis of the staging capability of SIMPLA2 is the modification of the various force and boundary condition arrays. These modifications are in turn governed by the input "stage control data" and "stage code words." The stage control data describe the number of segments added to the structure at the left and right ends (NSAL and NR, respectively), the number of tendons stressed at this stage (NCBA), and the terminal stations (NXTL and NXTR) for the tendons stressed. It is assumed that all tendons stressed at one stage have the same terminal stations. Therefore, at any stage of construction, any number of tendons (up to a maximum of six) may be stressed, and each

of these tendons may have an arbitrary profile. It is required, however, that each of the tendons be anchored at the same stations along the girder in order to be considered in one stage. The parameter NSAL is used not only to determine the total number of segments to be considered at this stage, but also to relocate the origin of the structure and relocate all force vectors within the force arrays. NSAL and NR determine the total number of segments in the structure at the particular stage; either or both of these parameters may be zero. The parameters NCBA, NXTL, and NXTR are associated with all tendons stressed at the particular stage. NCBA may be zero, in which case the NXTL and NXTR parameters are undefined, and NSAL and NR must be zero. NXTL and NXTR locate the columns of PBAR into which the anchorage vectors for this stage will be summed, and also the columns of the PJP array which will receive force contributions from the tendons stressed at this stage. Stations and segments are renumbered at each stage (except when NSAL = 0). Input and output at each stage are referred to the station and segment numbering scheme for the particular stage.

Stage code words, KODJA, KODBC, and KODSPT indicate how the problem has changed with respect to applied joint actions, boundary conditions, and support restraint conditions from the previous stage of construction. KREF identifies the last stage of cantilever construction; the significance of identifying this stage will become apparent in the following. Specific information concerning appropriate numerical values of these data is found in Appendix B.

3.4.3 From Cantilevered to Continuous Structures. By virtue of the very nature of cantilever segmental construction, the structural system under analysis will at some point change from two separate cantilevered systems to one continuous system. It is not unlikely that this transition may occur as an intermediate stage of the complete construction, as in Example 3 in the following chapter. Prior to closure SIMPLA2 deals with one cantilever of the completed structure. The effects of all actions on the structure following closure must be determined from an analysis of the continuous structure; however, portions of the continuous structure (all

segments except the closure segment) are experiencing "locked in" stresses and displacements. Therefore, to obtain a complete solution for any stage following achievement of continuity requires additional consideration. The approach taken by SIMPLA2 is to consider the complete solution, at any stage after continuity, as the superposition of two component solutions, the "reference solution" and the "continuous solution."

Figure 3.9(a) illustrates the situation at the time the two independent cantilever systems have been constructed to their full extension, and all preparations for placing the closure segment have been made. Stresses and displacements in the cantilevers result from dead load, live load applied at this stage, and prestressing applied at this and all previous stages. These stresses and displacements are those referred to earlier as being "locked in," and constitute the reference condition for the continuous structure. Henceforth these stresses and displacements will be designated "the reference solution" and this stage (the stage just prior to closure) will be termed "the reference stage." Figure 3.9(d) illustrates placing the closure strip and tensioning the first of the continuity tendons. The stresses and displacements induced by this tendon must be determined from the analysis of the continuous structure [Fig. 3.9(c)], i.e., the "continuous solution." The figure implies that only the action of the first closure tendon and the dead weight of the closure segment are considered in arriving at the continuous solution. Alternatively stated, at every stage after achieving continuity, only the effects of changes in action (from the reference condition actions) are considered, and these changes are applied to the continuous structure [Fig. 3.9(c)]. Under these circumstances, the continuous solution will determine changes in the reference solution due only to those actions applied to the structure after continuity is achieved. The complete solution for any segment (with the exception of the closure segment) is the superposition of the reference and continuous solutions.

There are two approaches which can be taken in the program for analysis of the structure during the closure phase. The first is to consider the complete problem as three separate problems. The first problem

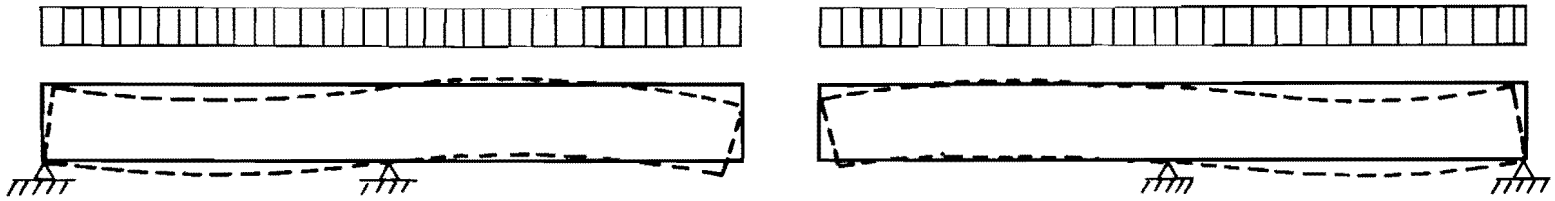

(a) Reference Stage - Left Cantilever

(b) Reference Stage - Right Cantilever

Δ_R

+

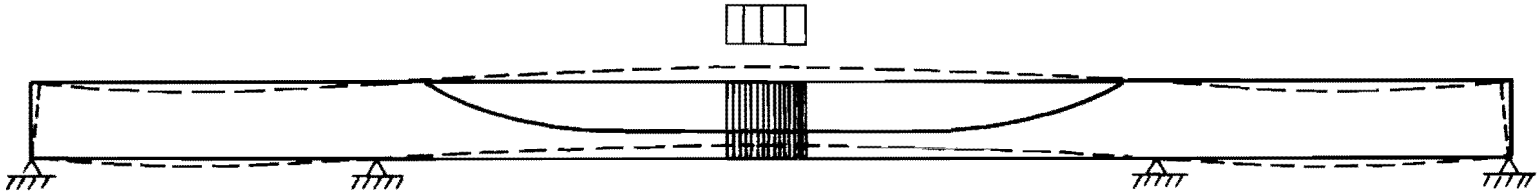

Δ_C

(c) Continuous Structure at First Stage of Closure

=

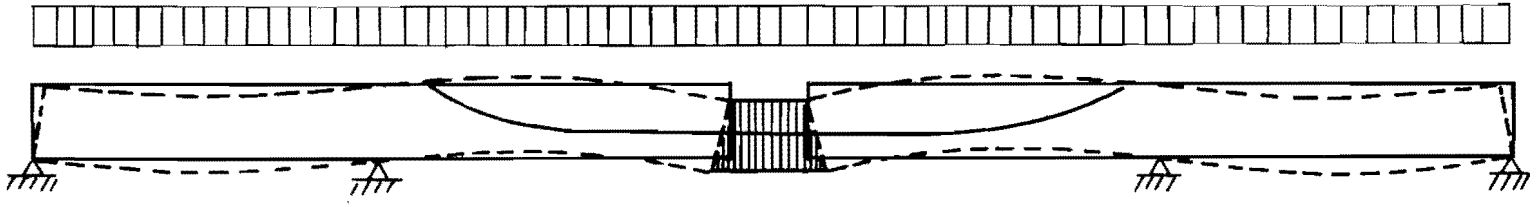

Δ

(d) Superposition of Reference and Continuous Solutions at First Stage of Closure

Fig. 3.9. Superposition of solutions.

considers the stage construction of the left cantilever [Fig. 3.9(a)], the last stage being the reference stage for the left cantilever. The second problem treats the right cantilever [Fig. 3.9(b)] in an identical fashion, resulting in the reference solution for the right cantilever. The third problem deals with the complete continuous structure [Fig. 3.9(c)] and the actions applied during the closure phase of construction in their proper sequence. Once the three solutions are in hand, the complete solution for either cantilevered portion at every stage is readily obtained by superposition of the appropriate solutions. Since SIMPLA2 has no provision for obtaining two reference solutions in a single run, the superposition has to be done external to the computer in this case. A second disadvantage with this approach is that variations of effective prestress force in tendons stressed during the cantilevering phase of construction, due to actions applied after continuity is attained, cannot be determined automatically. This method may be used to advantage to determine the best sequence in which to apply the various forces (prestress) and displacements which are applied during the closure phase of construction. These actions may be applied to the continuous structure individually to determine the influence of each, then superimposed in various sequences to arrive at the most desirable.

The alternative utilizes the capability of SIMPLA2 to perform a complete analysis in one continuous run, superimposing reference and continuous solutions automatically at all stages of closure. The closure stages are considered as additional stages in the segmental construction of the cantilevers. Analysis at each closure stage provides changes in the reference solution for the cantilever due to the actions associated with the particular stage of closure. These changes are then automatically superimposed on the reference solution to yield the final solution for the cantilevered portion of the continuous structure. The procedure is to first arrive at the reference solution for the particular cantilever being considered by a straightforward use of SIMPLA2. Assuming the third stage of construction is the reference stage for the structure illustrated in Fig. 3.8, this would require an analysis of the structure at stages 1, 2,

and 3 [Figs. 3.8(a), (b), and (c), respectively]. Since the fourth stage of construction involves making the two cantilevered systems one continuous structure [Fig. 3.9(d)], the description of the mathematical model must change from that of Fig. 3.8(c) to that of Fig. 3.9(c). The user specifies the continuous structural configuration by the stage control data; the closure segment plus the entire right cantilever system are considered as segments added at the right of the cantilever in Fig. 3.8(c). Since the continuous solution is to reflect only changes due to actions applied after continuity is achieved, the various force vectors which are held common from stage to stage must be modified. This is accomplished automatically by the program before analysis of the continuous structure is begun. All force vectors (PBAR, PJP, and AJP) are initialized and progressive assembly of the various force arrays begins over again with the analysis of the continuous structure for the first stage of closure. Both the applied joint actions array, AJP, and the associated indicator array, LIND, are initialized. Applied joint actions, therefore, must be completely respecified at the first stage of closure. Once the description of the structure and the force arrays have been modified, as discussed above, the continuous structure is analyzed and results pertinent to those segments comprising the left cantilever portion of the complete structure [Fig. 3.8(c)] are superimposed with the reference solution. SIMPLA2 is capable of modeling the segmental construction of only one cantilever at a time. Therefore, unless advantage can be taken of symmetry, analysis of the complete structure requires two separate runs of the program.

Adopting the latter approach for analysis of the closure stages has several advantages over the former method. The primary advantage is that superposition of solutions is accomplished automatically. Since in this case analysis is performed for all stages including closure in one continuous run, variations of effective prestress force in all previously stressed tendons may be obtained automatically at any stage of construction.

Example Problems 1 and 3 in the following chapter employ the latter approach for analysis during closure. Discussion accompanying Example Problem 1 offers further comments and explanation on the technique.

3.4.4 Effective Prestress Force. Initial effective prestress force at all tendon nodal points of a given tendon is determined by Eq. (3.12) at the time the tendon is stressed. As segmental construction proceeds and the girder is strained under the action of further loads and prestress, effective prestress forces in the tendon will vary from values computed by Eq. (3.12). Referring to Fig. 3.8, it may be seen that at stage 2 as tendon number 2 is stressed and the additional loads are applied to the structure, the strained configuration of segments 2, 3, and 4 change from that existing at stage 1. It is assumed that after initial stressing tendons are bonded and there exists strain compatibility between the structure and tendon; therefore, strains in tendon number 1 will also vary. It may be seen also that at every subsequent stage strains in tendon number 1 are again altered.

SIMPLA2 has the capability to compute at any stage actual tendon stresses in all tendons stressed at previous stages. The calculation is dependent upon the assumption that strain compatibility exists after initial stressing of the tendon; that is, the tendon is grouted immediately after stressing. Element edge normal stresses, SX(I) and SX(J), are computed as a matter of routine in the analysis [Fig. 3.10(b)]. Tendon nodal point coordinates, Y, are computed. This information, coupled with the assumption of linear strain variation across the element width, is sufficient to calculate element normal strain, $\epsilon_L(K)$, at the location of the Kth tendon nodal point, at any stage L, by the relation:

$$\epsilon_L(K) = \frac{SX(I) - SX(J)}{dE} (Y) + \frac{SX(I) + SX(J)}{2E} \qquad (3.29)$$

where d is the width and E the modulus of elasticity of the element containing the particular tendon. This calculation is performed at each stage for all nodal points of all tendons stressed at this stage. These strain values are the initial nodal point strains, $\epsilon_o(K)$, in the structure at the Kth tendon nodal point. To calculate tendon stress for these

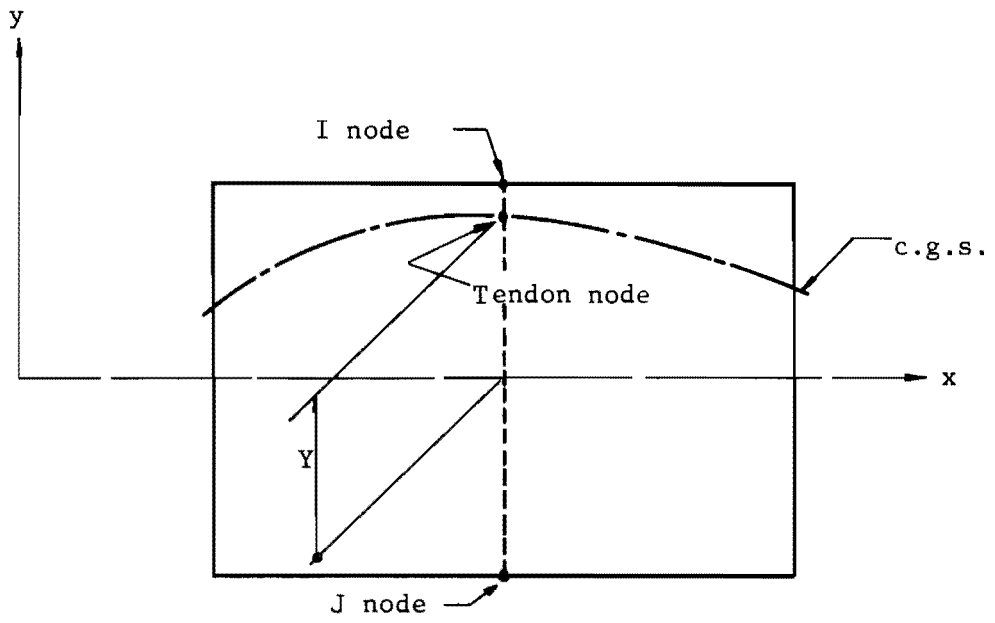

(a) Typical element and tendon segment

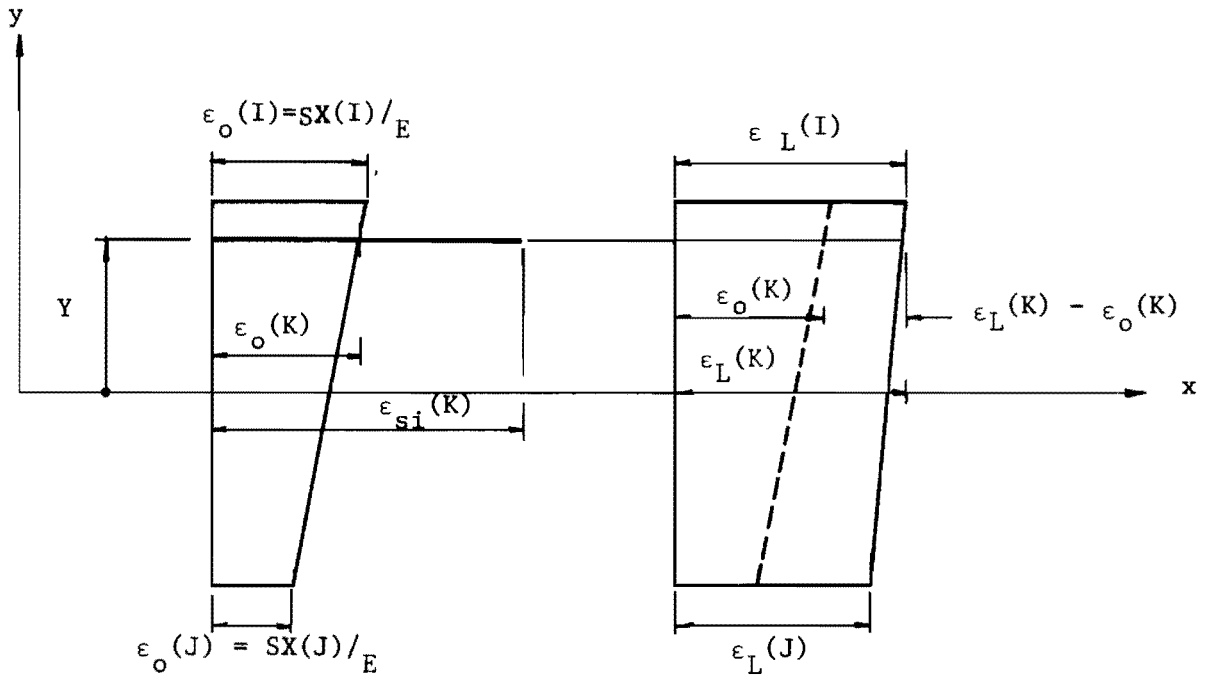

(b) Strain diagram at initial tendon stressing

(c) Strain diagram at stage L

Fig. 3.10. Changes in tendon stress.

tendons at any future stage, L, only requires calculation of new strain values, $\epsilon_L(K)$, at the location of tendon nodal points by Eq. (3.29). Since strain compatibility exists between tendon and structure, tendon stress S_t, at any nodal point K, is simply (see Fig. 3.10):

$$S_t(K) = \epsilon_{si}(K)E_s + E_s[\epsilon_L(K) - \epsilon_o(K)] \tag{3.30}$$

where $\epsilon_{si}(K)$ is the initial tendon strain given by

$$\epsilon_{si}(K) = F(K)/A_sE_s \tag{3.31}$$

and F(K) is calculated by Eq. (3.12). The user specifies those stages at which this calculation is to be performed. When the calculation is called for, revised tendon stresses for all tendons stressed prior to this stage are computed. This calculation requires retrieving initial nodal point strain values, tendon coordinates, and initial tendon forces from auxiliary storage units, and thus this operation can become quite time-consuming.

3.5 Program Limitations

Any analytical technique of structural analysis is limited by the assumptions made in arriving at the mathematical model. Throughout Chapters 2 and 3, the assumptions made to arrive at the finite segment and prestressing tendon models were discussed and will not be repeated. The user should be aware of them and recognize the associated limitations.

SIMPLA2 has been written with a specific class of problems in mind (see Example Problem 3 in the following chapter). Array dimensions are established to render the program capable of handling a reasonably large problem of this category. With the presently specified array dimensions, the CDC 6600 version of SIMPLA2 requires approximately 130000 storage locations to compile and execute. Limitations on the input variables are:

(1) Maximum numbers of elements and joints are 15 and 16, respectively.

(2) Maximum number of plate types is 15.

(3) The longitudinal span may be divided into a maximum of 50 segments.

(4) A maximum of 4 interior supports may occur along the longitudinal span.

(5) A maximum of 10 segments may be added to either or both ends of the structure at each stage.

(6) The maximum number of stages in the erection sequence is 25.

(7) The maximum number of tendons stressed in one stage is 6.

(8) The total number of tendons must not exceed 25.

(9) The difference in joint numbers of the two joints connecting one element must not exceed 4.

(10) The number and locations of stopovers is arbitrary and the minimum number required for accuracy depends on the size of the structure. For a suitable choice some experience is required. The number of stopovers used should be minimized, since at each stopover a number of extra calculations are required.

(11) The numerical difficulties encountered with the finite segment method are due to round-off error. Lo[8] states that using an IBM 7090/7094 system (9 digit word length), the use of double precision calculation was necessary for accurate results. The IBM system 360 version was converted to a double precision calculation throughout and indicates a comparable degree of accuracy to the CDC 6600 version. It has been the authors' experience with a CDC 6600 system (15 digit word length) that for problems approaching the dimension limits above and similar to Example Problem 3 in Chapter 4 accurate results were obtained without the use of double precision calculation.

(12) SIMPLA2 is equipped with very few automatic error checks; therefore, the user should prepare and check all input data carefully.

3.6 Program Extensions

Subsequent to completion of Project 3-5-69-121, the Texas Highway Department began the preliminary design of a much larger bridge than the one presented in Example Problem 3 in the following chapter. In the analysis of that bridge, limitations (6) and (8) as given in Sec. 3.5 were exceeded. The program was redimensioned to increase the maximum number of stages to 75 and the total number of tendons to 100.

The increased number of stages made it overly inefficient to always run the program from the start of all construction when effects of a specific action late in the construction sequence had to be examined. In reprogramming a restart capability was added, so that results of intermediate stages

were able to be saved on permanent file. In that way the problem could be run to a certain stage, output examined, new input developed, and then the analysis restarted at the last stage and with the conditions previously analyzed. This greatly expedites analysis of large structures where results of intermediate stages must be known to decide construction operation values in later stages.

During the analysis of the larger structure, at a point where the number of unknown joint-segment displacements being solved was approximately triple the maximum number in Example Problem 3, numerical accuracy problems were encountered using CDC 6400/6600 single precision arithmetic. The program was converted to double precision and the numerical accuracy problems did not reappear, even though the final stages involved about five times the maximum number of unknowns of Example Problem 3.

The CDC 6400/6600 version of this revised program SIMPLDP requires approximately 65,000 storage locations to compile using compiler MNF and 175,000 storage locations to execute.

C H A P T E R 4

EXAMPLE PROBLEMS

4.1 Introduction

In this chapter the results of three example problems are presented. The first example illustrates for a rectangular cross section the input data required for segmentally constructed, post-tensioned girders to show data coding for stage construction.

The second example gives a comparison of results obtained by the programmed finite segment method with those obtained by the more exact folded plate method to assess the accuracy of the mathematical model of the composite structural system. This example demonstrates several characteristics of the SIMPLA2 program without the complications of stage construction.

The final example shows the capability of SIMPLA2 to analyze a major segmental box girder structure. The example structure is the Texas Highway Department's three-span box girder structure over the Intracoastal Canal in Corpus Christi, Texas. This bridge was the first of this type constructed in the United States.

4.2 Example Problem 1 - Stage Construction of a Rectangular Girder

The purpose of this example is to show the specification of input data and interpretation of the printed output. A listing of the complete input data and partial output for this problem is given in Appendix C. This example was selected to demonstrate the input required for segmentally constructed post-tensioned structures, without the additional complications of a complex multi-element cross section.

The completed structure (Fig. 4.2) is a three-span continuous rectangular beam composed of two individual precast segmentally constructed

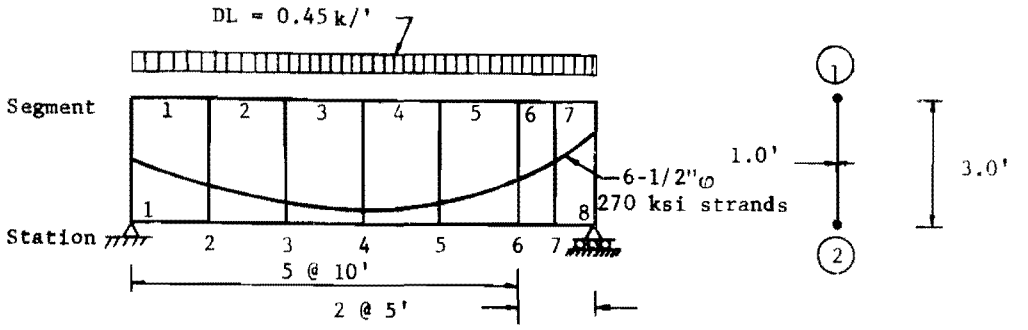

(a) Initial stage

(b) Cross section idealization

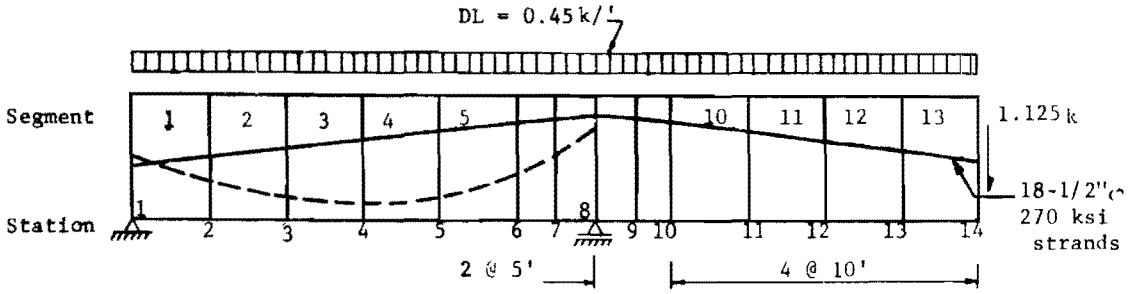

(c) Second stage - the reference stage

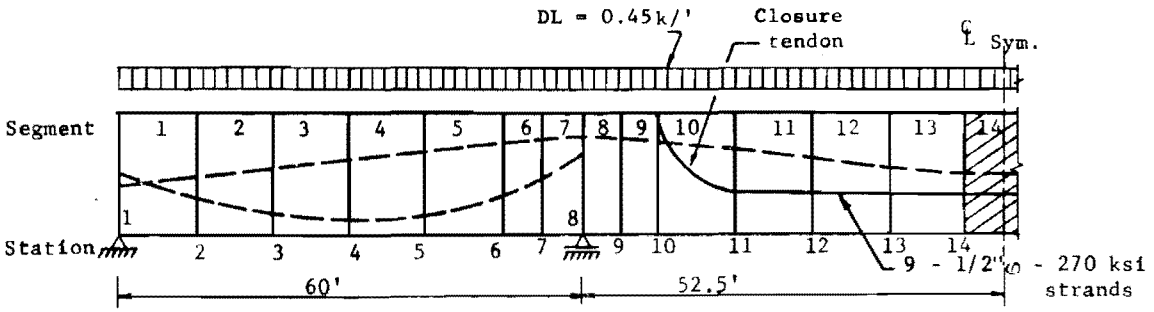

(d) Final stage of construction

Fig 4.1. Example problem 1 - construction sequence.

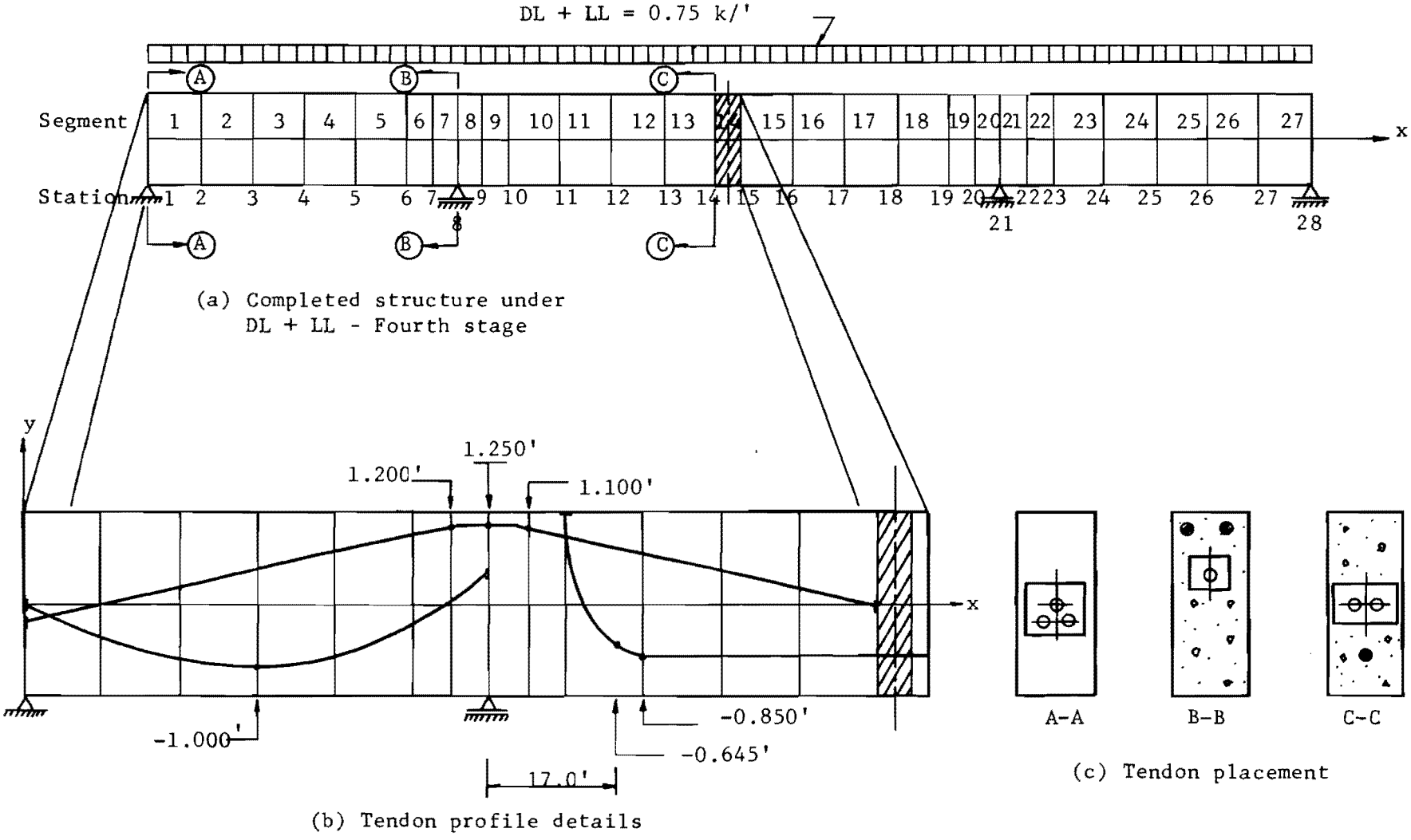

Fig. 4.2. Example Problem 1 construction.

cantilevered systems, made continuous by a cast-in-place closure segment and post-tensioning. The structural configuration to be analyzed at each stage is shown in Fig. 4.1. The sequence of construction is as follows:

(1) In the first stage the anchor span is placed and post-tensioned as in Fig. 4.1(a).

(2) In the second stage the cantilever arm is positioned as in Fig. 4.1(c), an epoxy joint is prepared at Station 8, and the cantilever arm is post-tensioned to the anchor span. The closure segment is then cast-in-place. The weight of the cast-in-place closure segment is represented by a 1.125 kip load, as shown in Fig. 4.1(c). Addition of the cantilever arm and placement of the closure segment would actually be accomplished in two stages; however, for purposes of this example these events are considered to occur in one stage.

(3) In the third stage the closure tendon is stressed, as shown in Fig. 4.1(d).

(4) In the fourth stage the completed girder is analyzed for a uniform live load of 0.30 kip per ft.

The closure tendon is designed to prevent tensile stresses in the closure segment and segments adjacent to the interior support under live load. The coefficient of friction and wobble coefficient have been assumed to be zero.

4.2.1 Input Data. The main purpose of this example is to clarify the method of inputting data for stage construction. A detailed explanation of the data coding for Example Problem 1 is given to show the application of SIMPLA2 in this case. The card titles and card numbers referred to are the titles and numbers assigned in the SIMPLA2 program input guide in Appendix B. A listing of the actual data cards for Example 1 is given in Appendix C.1. The card sequence number and type is identified in the left-hand margin of this appendix so that the ordering of the deck and the classification of the card can be easily seen. In inputting data, all

physical quantities must be input in consistent dimensions. In this example force is input in KIPS and distance in FT. Hence, distributed loads are input in KIPS/FT and stresses are in KIPS/SF. Dead load is split evenly between the two joints of a plate element.

As can be seen in the SIMPLA2 Data Input flow charts in Figs. B.3, the data input for the initial stage differs slightly than for subsequent stages. The input consists of 101 cards. Sequence and remarks for each card are given in Table C.2.

The input data required to specify the cross-sectional configuration and elastic properties (cards 2 and 3), the plate element connectivity (card 4), and tendon constants (card 5) is straightforward. At the initial stage each segment requires an INITIAL SEGMENT ACTIONS CARD, 12(A), since none of the segments has been considered previously. An interior support is called for at station 8; i.e., ISTOP(7)=-1, since this station will locate an interior support at every subsequent stage. However, an INTERIOR SUPPORT/DIAPHRAGM RESTRAINT CONDITIONS CARD, 14, will not be provided at this stage, since station 8 also locates the end boundary of the structure (see Appendix B.2, card 12(B), Remarks 6 and 7). An END BOUNDARY CONDITIONS CARD, 15, is required at this stage.

At the second stage the configuration is altered by the addition of six mathematical segments at the right end of the structure and the addition of one tendon spanning from station 1 to station 14, as illustrated in Fig. 4.1(c). None of the joint actions acting on that portion of the structure comprising the initial stage structure (segments 1-7) are altered; therefore, KODJA = 0. The boundary conditions have obviously been altered, since the end boundary at the initial stage was restrained in the vertical direction, but the end boundary at the second stage is completely free and subject to a shear force representing the dead load of the closure segment. Therefore, KODBC = 1. It will be necessary to respecify boundary conditions for both boundaries. The interior support restraint conditions are thought of as being changed, since at the initial stage there are no interior support restraints specified for station 8, whereas at the second stage support restraints must be specified. The

support code, KODSPT, is therefore 1. Since the joint actions applied to those segments comprising the anchor span are unaltered (KODJA = 0), only the INITIAL SEGMENT ACTION CARDS, 12(A), are required for segments 8-14. The segment progression routine requires that the structure always be specified from extreme left to right, beginning with the origin boundary conditions. Each segment is considered in turn, as described in Chapter 2. It becomes evident why, after tendon data are specified, the structure is specified beginning with the origin in card 33, skipping segment cards for segments 1-7, since they remain unchanged from the previous stage, specifying the new interior support at station 8, with a type 14 card in card 34, and continuing with new segment and end boundary cards. The second stage is the final stage at which the effects of additional actions will be determined from consideration of a cantilevered system (the reference stage); thus, KREF = 1.

The third stage is the stage at which continuity is achieved and is the first (and last) stage of closure. The structure to be analyzed has the longitudinal configuration illustrated in Figs. 4.1 and 4.2--the STAGE CONTROL DATA are specified accordingly. The sole purpose of modeling the complete right portion of the structure (segments 14-27) is to provide the proper boundary conditions for the left portion (segments 1-13) which is under analysis. For this particular example (longitudinally symmetrical), the correct boundary condition may be specified directly quite simply. However, in the general case of a longitudinally and transversely unsymmetrical box girder, such direct specification is quite difficult.

It is important for the user to recall that the final solution for this stage is the superposition of the reference stage solution and continuous solution which includes effects of actions applied after continuity is achieved; and that the force arrays, PBAR and PJP, the joint actions array, AJP, and the associated indicator array, LIND, are all automatically initialized at this time (the first stage of closure). Therefore, unless otherwise specified at the first stage of closure, the continuous structure is analyzed for the effects of continuity prestressing only. For this particular problem it is appropriate for all applied joint actions

to be zero force quantities (the condition imposed by initializing AJP and LIND). Therefore, KODJA = 0, and no joint actions specification is necessary at this stage. The boundary conditions are changed, since the end of the structure becomes simply supported, and the existing interior support restraint conditions are unaltered; thus, KODBC = 1 and KODSPT = 0 for this stage.

The completed structure is analyzed for a fixed live load of 0.30 kips per ft. as a fourth stage. The single modification required is the specification of the applied load by setting KODJA = 1 and furnishing a MODIFIED SEGMENT ACTIONS CARD, 12(B), for each segment.

4.2.2 Computed Results. In order to illustrate the interpretation of computer output using the guide found in Appendix B.4, some of the significant items of the computed results for Example Problem 1 are discussed briefly. A partial listing of the computer output is furnished in Appendix C.3.

4.2.2.1 Element Stresses. Element force resultants, as shown in Fig. B.4, and subsequently element edge normal stresses, SX(I) and SX(J), are computed for each element in every segment. The rectangular cross section structure in this case is represented by a single plate element. Therefore, the element edge stresses computed are the top (I or 1-edge) and bottom (J or 2-edge) fiber normal stresses. The stress distribution across the plate element is linear according to the assumptions of the finite segment method.

Several sections at which it is desirable to monitor the normal stresses as construction proceeds are shown in Fig. 4.3. The longitudinal center of segment 2 (x = 15.0 ft.) is the nearest section at which results are computed to the point of maximum live load moment in the anchor span (x = 16.85 ft.). The maximum moments, both dead load and live load, occur at station 8, which also marks the location of the epoxy joint. The centerline of the main span (segment 14) is the location of maximum negative moment due to stressing the closure tendon and maximum positive live load moment.

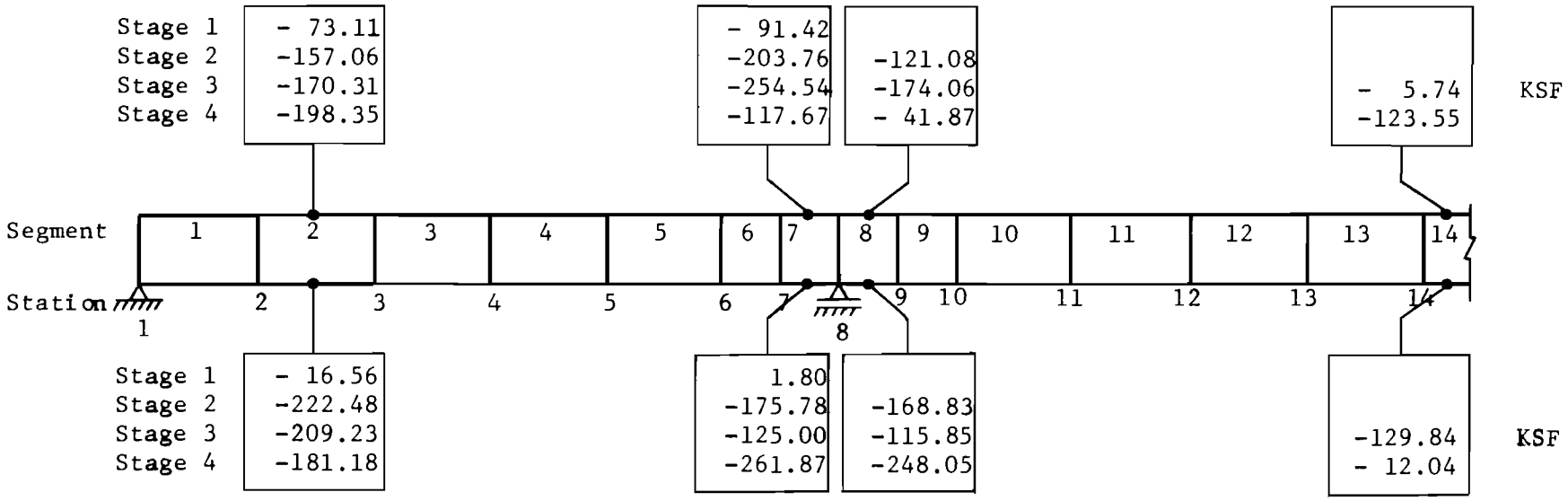

Fig. 4.3. Normal stress of each stage of construction (KSF).

Sign Convention
- Compression

Computed stresses at each of these sections for each stage of construction are given in Fig. 4.3. The tendon coordinates at each of these sections and the tendon forces are given in the table below.

TENDON - FORCE (Kips)	SEG. 2 Y (ft.)	SEG. 7 Y (ft.)	SEG. 8 Y (ft.)	SEG. 14 Y (ft.)
1 - 135	-0.813	0.280	--	--
2 - 435	0.146	1.25	1.25	--
3 - 225	--	--	--	-0.850

The secondary reactions induced by stressing the third tendon are 1.325 kips upward at station 1 and 1.325 kips downward at station 8. With these data the computed normal stress values have been independently verified with excellent agreement by use of the following equations:

$$M = M_G + P \cdot y + M_s$$

and;

$$S(X) = - 0.333P + 0.667M$$

where;

M_G = Gravity load moment

M_S = Secondary moment induced by prestressing a continuous beam

P = Tendon force

y = Tendon coordinate

In using the output data to determine such computed quantities such as end reactions, care must be taken to correctly add the vertical components of tendons anchored at the origin or end to the plate transverse shears. For instance, in stage 1 the origin reaction is 0.45 x 30 = 13.5 kips. Calculation of the vertical component of the force in tendon 1 using differentiation of a parabolic curve through the given tendon profile indicates the vertical component to be 10.1 kips. Thus, the net shear at the origin is 13.5 kips - 10.1 kips, or 3.4 kips. This is the value shown

on the output of stage 1 for the transverse shear at the origin in element. If the output was used for computing reactions, the 3.4 kips and 10.1 kips would have to be summed.

4.2.2.2 Joint Displacements. The four components of the joint displacement vector are printed for each joint in the structure at each stage. Only vertical components are of interest for this problem. Figure 4.4 illustrates the displaced configuration of the structure at each stage of construction and under live load. The displacements of joints 1 and 2 are essentially the same; therefore, only those of joint 1 are presented. It should be noted that although the stresses for segment 14 (the closure segment) are given directly the joint displacements are not. Displacement quantities computed for the closure segment are the displacements (computed from a zero reference) of the continuous structure due to the actions applied after continuity is achieved. For this example the displacements computed for segment 14 at stage 3 are the displacements of the continuous structure, from a zero datum, due to the action of the continuity tendon. As described in Chapter 1, the closure segment is in general only a cast-in-place strip approximately 24 in. in length, thus the inability of the program to compute closure segment displacements directly is not a serious disadvantage. For this example, closure segment joint displacements have been computed approximately and are indicated in Fig. 4.4 by the dashed curve extensions. The computation of these values is accomplished by using the computed end transverse displacement at stage 2 (-5.645×10^{-2} ft.) as a reference datum. Superimposing this value with those vertical joint displacements computed for segment 14 at stages 3 and 4 results in the values indicated.

It may be easily seen that the displacement diagrams shown in Fig. 4.4 are reasonable by considering the equivalent loadings from the three stages of prestressing. The equivalent loadings are sketched in Fig. 4.5. It should be noted that the structure is lightly prestressed at stage 1; therefore, the dead load is not completely balanced and downward displacements result.

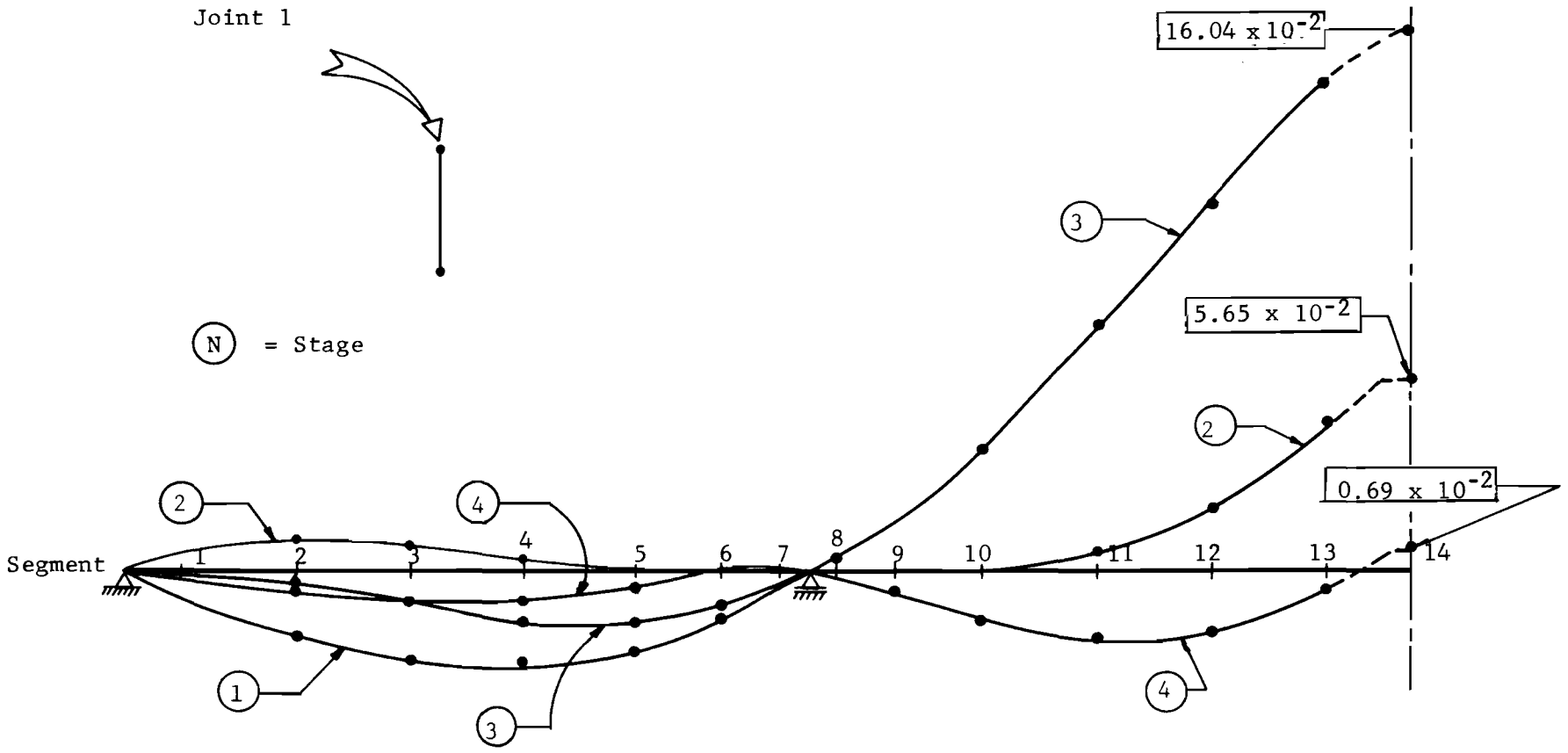

Segment / Stage	Vertical Displacement (ft. x 10^{-2})												
	1	2	3	4	5	6	7	8	9	10	11	12	13
1	0.692	1.915	2.707	2.876	2.305	1.365	0.501	-	-	-	-	-	-
2	-0.493	-0.859	-0.716	-0.374	-0.068	0.042	0.032	0.000	0.048	0.082	-0.413	-1.877	-4.256
3	-0.087	0.291	0.974	1.514	1.542	1.048	0.415	-0.435	-1.410	-3.575	-7.184	-10.80	-14.38
4	0.082	0.595	1.002	0.950	0.477	0.084	-0.031	0.169	0.761	1.507	2.017	1.887	0.475

Fig. 4.4 Vertical displacements at each stage - Example Problem 1.

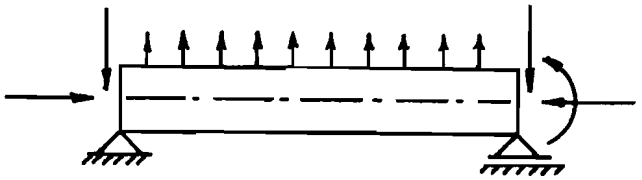

(a) Equivalent loading - Stage 1 (P = 135k)

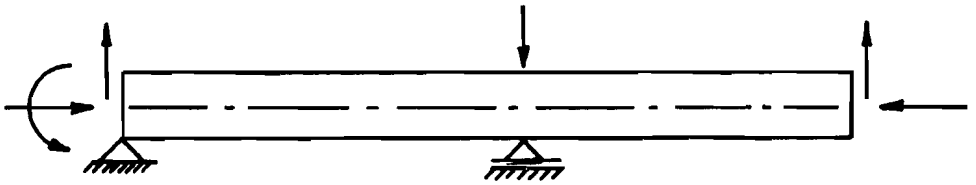

(b) Equivalent loading - Stage 2 (P = 435k)

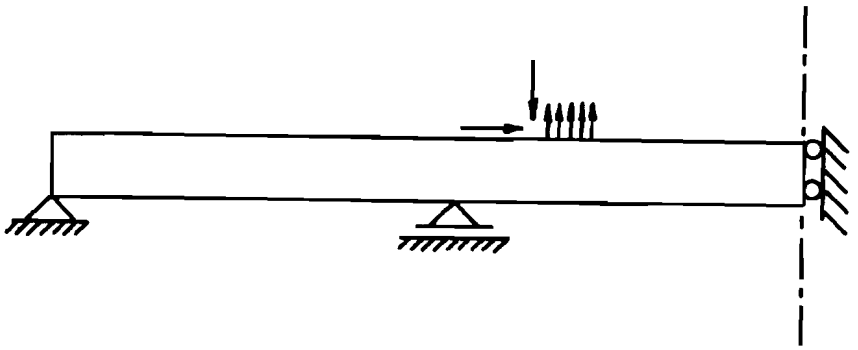

(c) Equivalent loading - Stage 3 (P = 225k)

Fig. 4.5. Equivalent loadings.

4.3 Example Problem 2

The general validity of the finite segment method has been quite adequately demonstrated[8,19] and will not be discussed herein. The objective of this example is to demonstrate the validity of the technique used to model the prestressing forces on the structure in conjunction with the finite segment method.

The structure selected for analysis, illustrated in Fig. 4.6, is a three-cell, two-span, continuous box girder. The structure is prestressed by four tendons, one per web, each having a profile composed of six parabolic curves [Fig. 4.7(c)]. The cross section idealization, shown in Fig. 4.6(c), is composed of 14 elements and 12 joints. The structure will be considered under two separate loading conditions--the prestress load and a combination of prestress and a live load applied to joint 1, as shown in Figs. 4.6(a) and 4.6(c).

The structure is analyzed by two techniques for each loading condition. A computer program entitled MUPDI, developed by Scordelis,[18] based on the folded plate method, is used for the first analysis. As mentioned in Chapter 1, the folded plate method is considered the most accurate analysis presently available; therefore, the results of this analysis will be used as a standard for comparison. The second analysis is performed using the SIMPLA2 program.

To account for the effects of prestressing in the MUPDI analysis, equivalent joint loads were computed as the product of the tendon curvature and tendon force, and applied at the juncture of the web and top flange. This simplified representation should be quite accurate for this example, since the tendon curvatures and slopes are very small. Because the end slope is slight and end eccentricity is zero, the anchorage force from each tendon is applied as two longitudinal joint forces, each one-half the tendon force in magnitude, and applied at the web flange juncture. Application of the equivalent prestress forces to the structure using this approach required the specification of 36 individual joint loads.

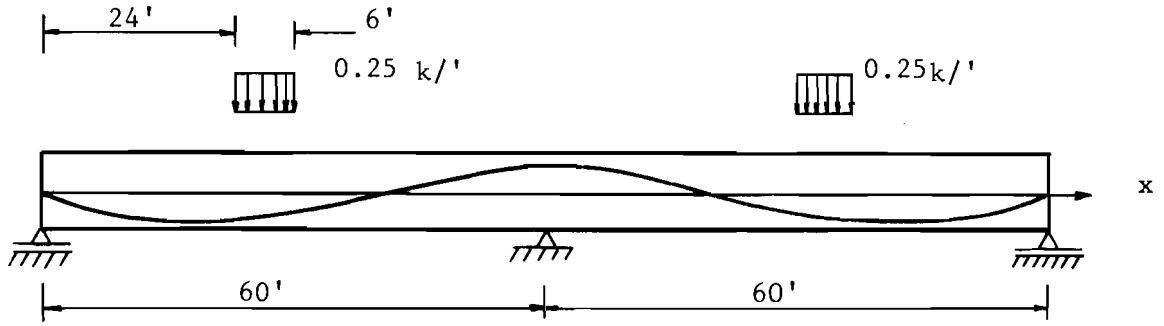

(a) Example Problem 2 - Elevation

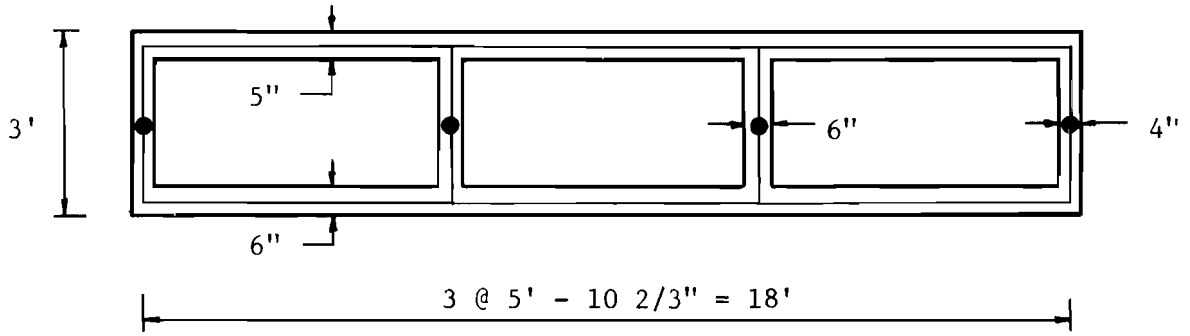

(b) Example 2 - Cross Section

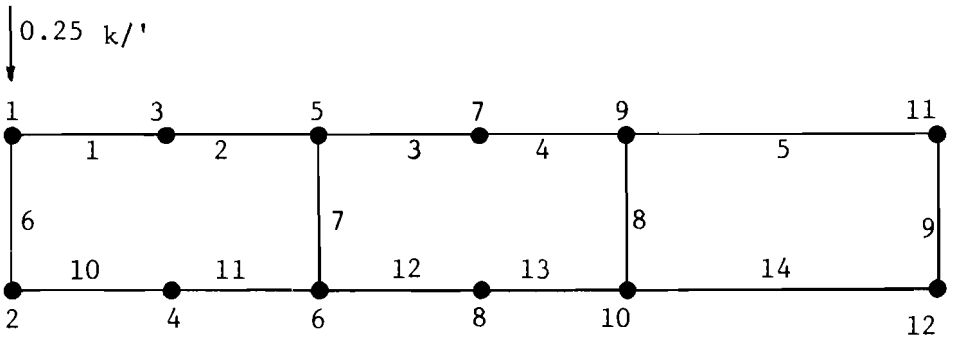

(c) Example 2 - Cross Section Idealization

Fig. 4.6. Example Problem 2.

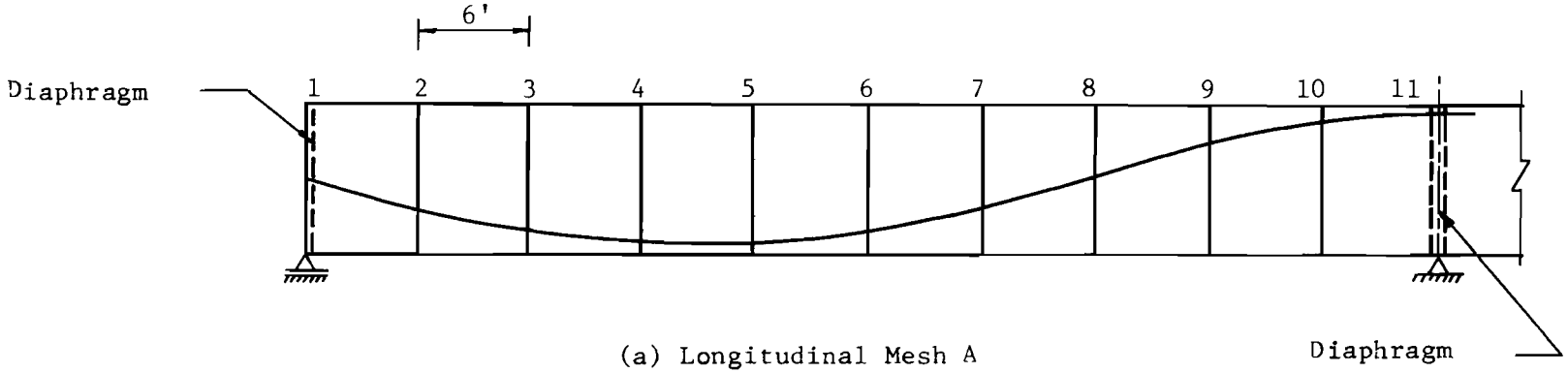

(a) Longitudinal Mesh A

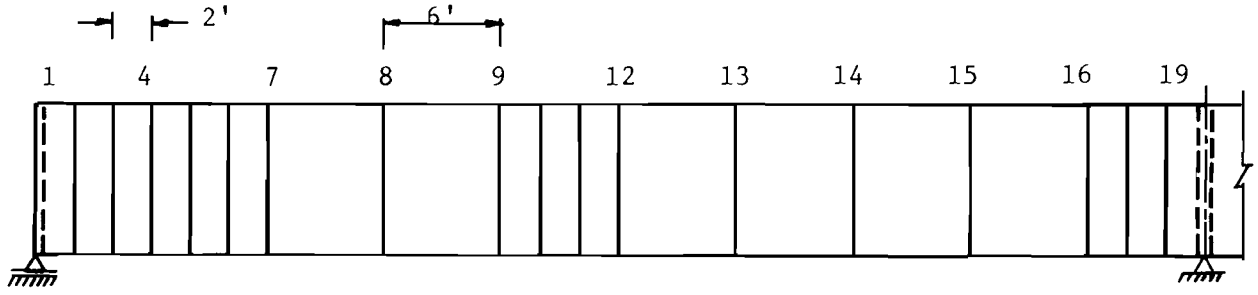

(b) Longitudinal Mesh B

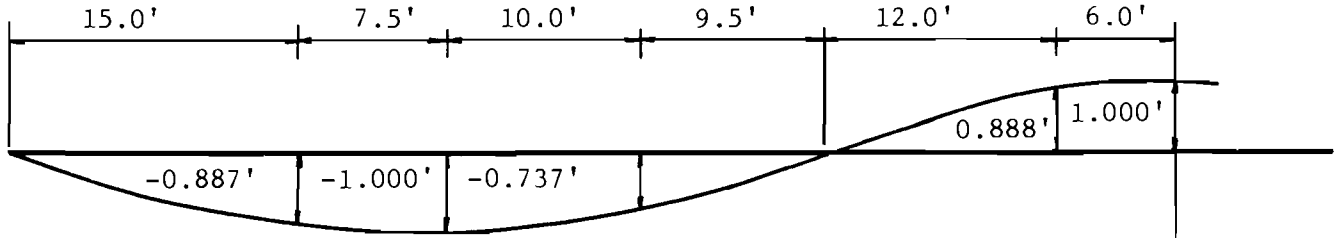

(c) Tendon Profile

Fig. 4.7. Example Problem 2 - Elevation.

Scordelis[19] has shown that results obtained by the finite segment method approach the results of more "exact" analysis techniques as the cross section idealization is refined; i.e., more elements are included in the cross section. The effect of refining the longitudinal idealization, i.e., including additional finite segments in the span, will be briefly examined here. To do this, the example was solved by SIMPLA2 using two different longitudinal subdivisions of the span, shown in Figs. 4.7(a) and 4.7(b), and denoted Mesh A and Mesh B. It was necessary to solve only one span of the structure with the SIMPLA2 program, since a fixed boundary condition can be modeled. The same cross section idealization is used for the three analyses. The modulus of elasticity is assumed to be 432,000 kips per sq. ft. and Poisson's ratio of 0.0 is used. The coefficient of friction and wobble coefficients are both assumed to be zero.

4.3.1 Prestressing Load. In order to assess the accuracy of the method used to model prestress forces, results from the MUPDI and SIMPLA2 analyses are compared. The following section treats the structure under the action of prestress only.

4.3.1.1 Vertical Joint Displacements. The variation of the vertical joint displacement along the span is illustrated in Fig. 4.8 for two joints of the cross section. The elastic curve for all joints is similar to those presented. The values of displacement computed by MUPDI and SIMPLA2 are given at the centers of the segments denoted Mesh A in Fig. 4.7(a).

The computed displacements compare favorably both in terms of magnitude and variation along the span. In all cases the displacements computed by SIMPLA2 are high. This indicates that the overall stiffness of the SIMPLA2 structural model is less than that of the more exact MUPDI model. The difference is on the order of 4 percent of maximum deflection.

The transverse distribution of vertical joint displacements is illustrated in Fig. 4.9(a). The displacements given are for the joints located on the top flange at a section 27.0 ft. from the left support.

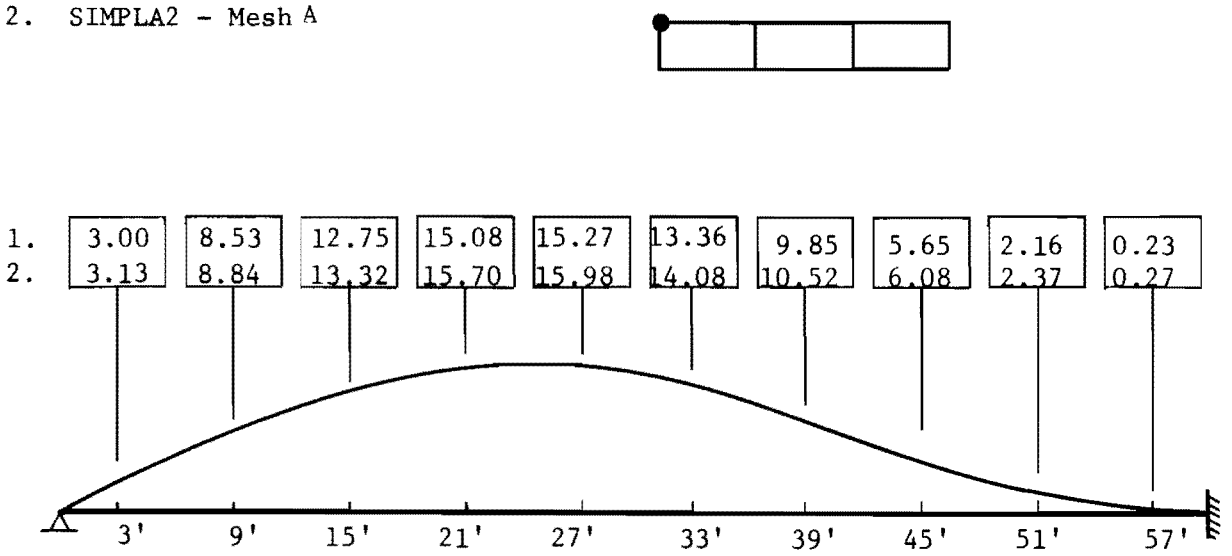

(a) Vertical Displacement at Joint 1 - Ft. x 10^{-3}

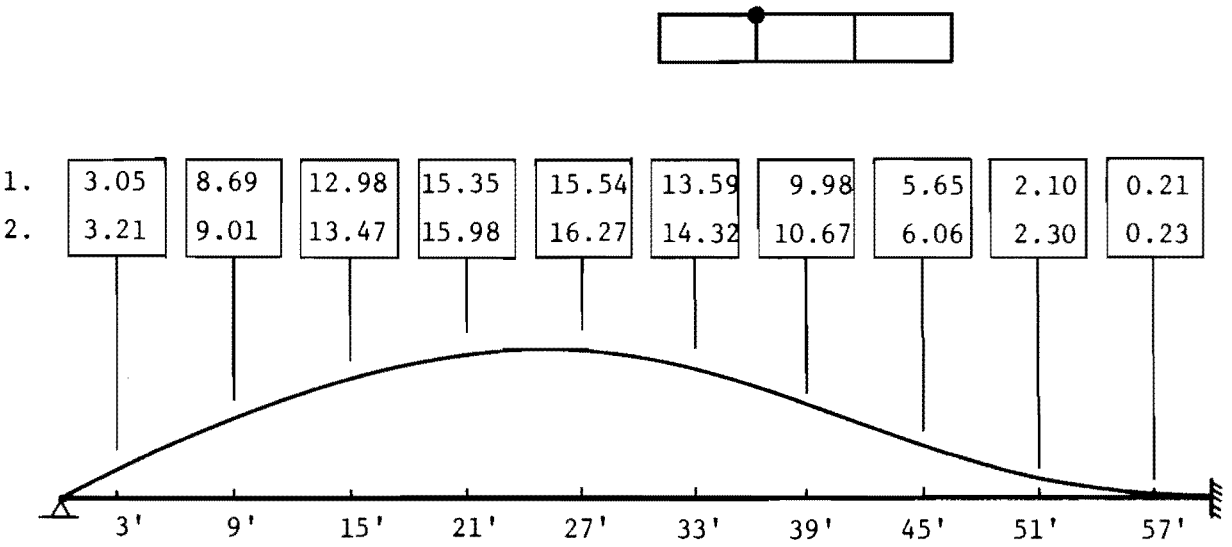

(b) Vertical Displacement at Joint 5 - Ft. x 10^{-3}

Fig. 4.8. Comparison of vertical joint displacements under prestress only.

1. MUPDI
2. SIMPLA2 - Mesh A
3. SIMPLA2 - Mesh B

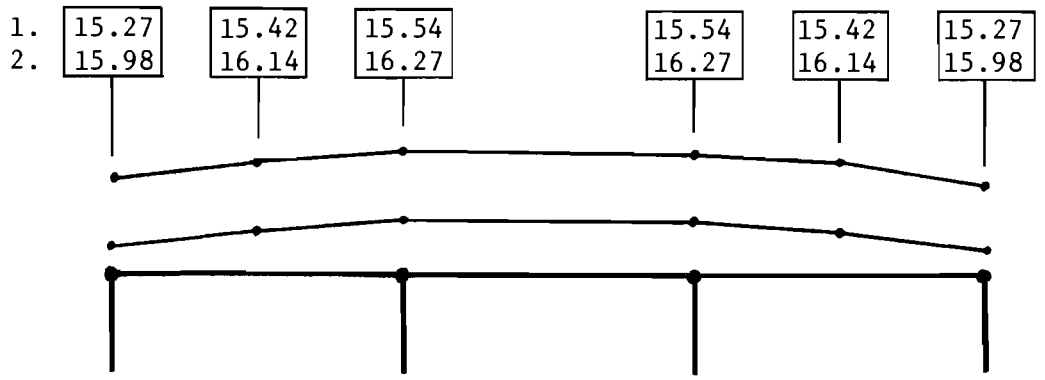

(a) Under Prestress Only - x = 27'.

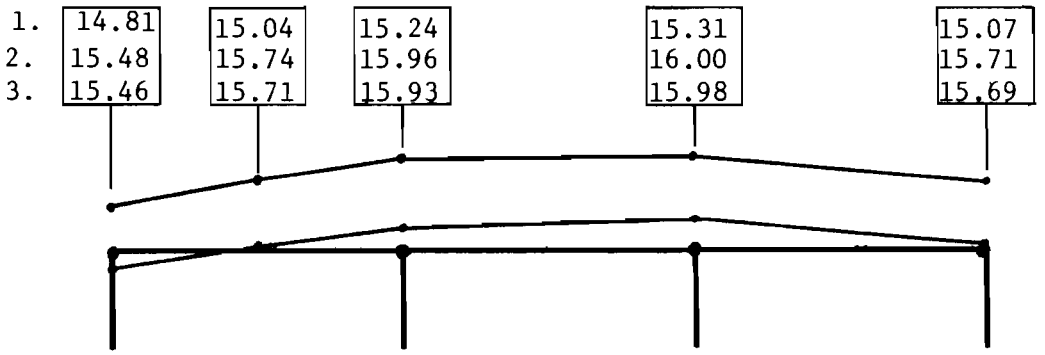

(b) Prestress Plus 1.5 kip Load - x = 27'

Fig. 4.9. Transverse distribution of vertical joint displacements (ft. x 10^{-3}).

Displacements are plotted from a base of 15.00×10^{-3} ft. Again, the displacement comparison is favorable. The same relationship is exhibited between the computed values as discussed in connection with Fig. 4.8.

4.3.1.2 Longitudinal Membrane Stress. The transverse distribution of longitudinal membrane force per unit length, NX, is presented in Fig. 4.10. Since the top and bottom flanges are of constant thickness, these plots also illustrate the transverse variation of longitudinal membrane stress, SX. The force distributions are observed at sections 21.0 ft. and 57.0 ft. from the left support. The MUPDI analysis produces a continuous variation of NX across the width of the section with stress concentrations at the web flange juncture. The SIMPLA2 analysis is seen to approximate the transverse distribution of NX under the constraint that the distribution across each element must be linear. The comparison between NX distributions and magnitudes obtained by the two analyses is satisfactory.

4.3.1.3 The Anchorage Force. The cross-sectional area of the anchor plates is generally quite small compared to the cross-sectional area of the member; therefore, anchorage forces are applied to the structure as nearly concentrated forces. Within some distance from the anchorage, termed the anchorage zone, the stress distribution is very non-uniform and complex. Analytical determination of the stresses within this zone is very complicated for even the simplest cases. Clearly this problem is beyond the scope of the segmental analysis program. Various researchers[26] have determined, both experimentally and analytically, the length of the anchorage zone to be approximately equal to the section depth for a rectangular section with the tendon anchored at the centroid.

The objective of the following discussion is to point out the characteristic manner in which anchorage forces are distributed into the cross section by the SIMPLA2 program and to clarify the effect of the anchorage force on computed stresses. This effect manifests itself in computed stress inconsistencies at points connecting two elements. Nodal point computed stress inconsistencies are characteristic of finite element displacement formulations. In regions of gentle stress gradients,

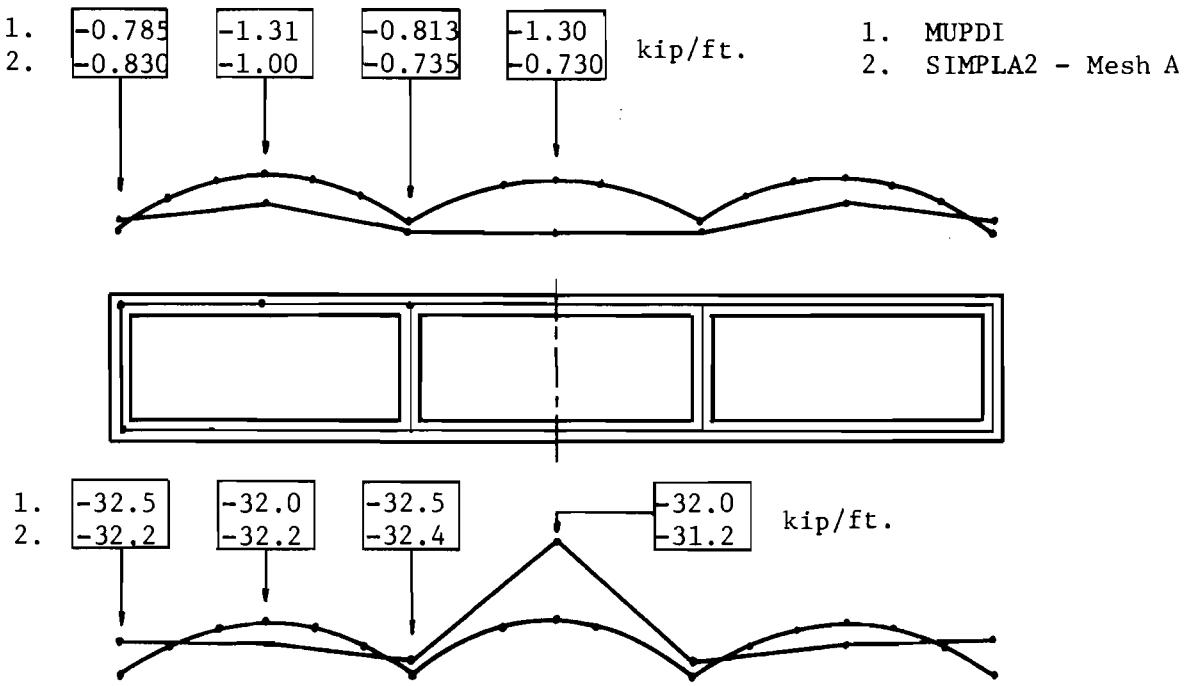

(a) Normal Force per Unit Length - x = 21'

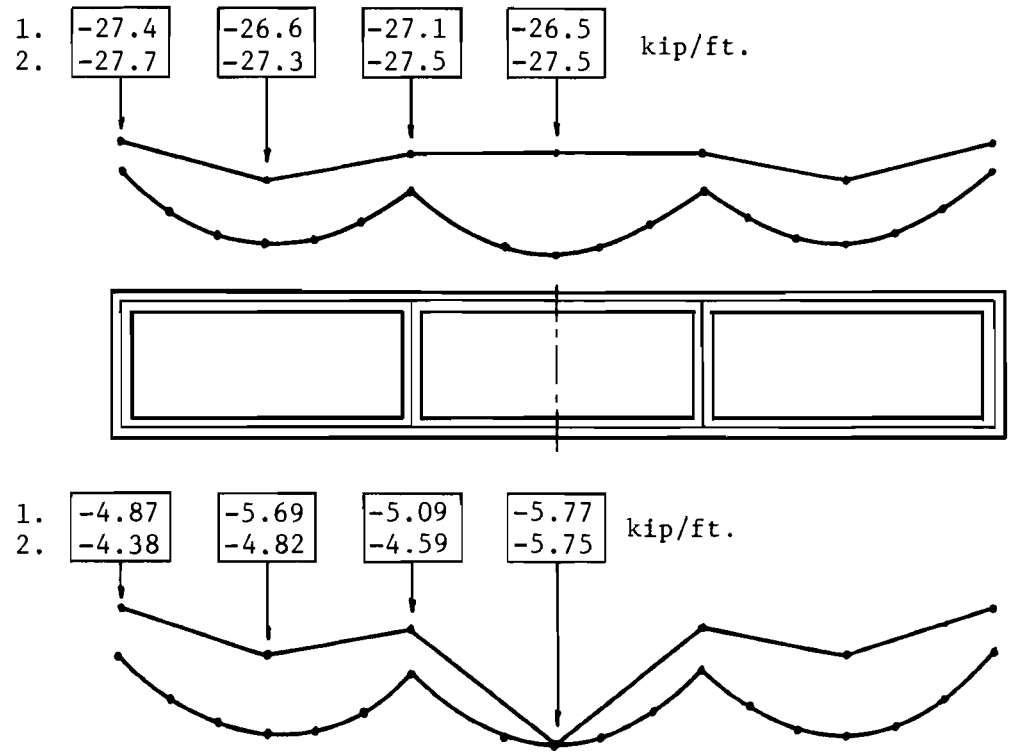

(b) Normal Force per Unit Length - x = 57'

Fig. 4.10. Comparison of longitudinal membrane force.

incompatibilities are for practical purposes negligible and in the vicinity of stress concentration the element size is generally refined to largely eliminate significant incompatibilities. The unique problem faced here lies in the fact that in the general case (as in the following example) there are many anchorage points to consider; thus a refinement of the mesh size in order to reduce computed stress inconsistencies is not feasible. It has been suggested that an arithmetic average (or possibly a weighted average) of the inconsistent stress values will yield satisfactory results.[29]

The problem is illustrated in Fig. 4.11. The I-edge of element 6 and the I-edge of element 1 are, in fact, the same point on the cross section [see Fig. 4.6(c)]. However, the normal longitudinal stress values computed by SIMPLA2 for element 1 at joint 1, and those computed for element 6 at joint 1 (denoted points A and B, respectively) are noticeably different initially and for all practical purposes converge at a distance from the left end of approximately 20 ft. It should be noted that the anchorage zone is assumed to extend approximately 3 ft. from the anchorage; therefore, no stresses are given in this interval. The stress variations shown for the flange and web elements are characteristic of the SIMPLA2 program. Stress concentrations are evident at element edge nodal points (the longitudinal center of a segment), since it is at these points that transverse compatibility is enforced. The web and flange stress computed by SIMPLA2 are also seen to oscillate about one another, and about the MUPDI value in the first several segments past the anchorage. The disturbance caused by the anchorage force, for all practical purposes, disappears in the third segment (at 15 ft. from the end) and the stress inconsistencies remaining are those characteristic of the formulation.

Figure 4.11 also shows a plot of the weighted average of the flange and web stresses. The agreement between the average values and the MUPDI values is excellent. The same relationships between computed flange and web stresses is exhibited at joint 5, as shown in Fig. 4.12. In this case the "average" curve represents a simple arithmetic average of the three

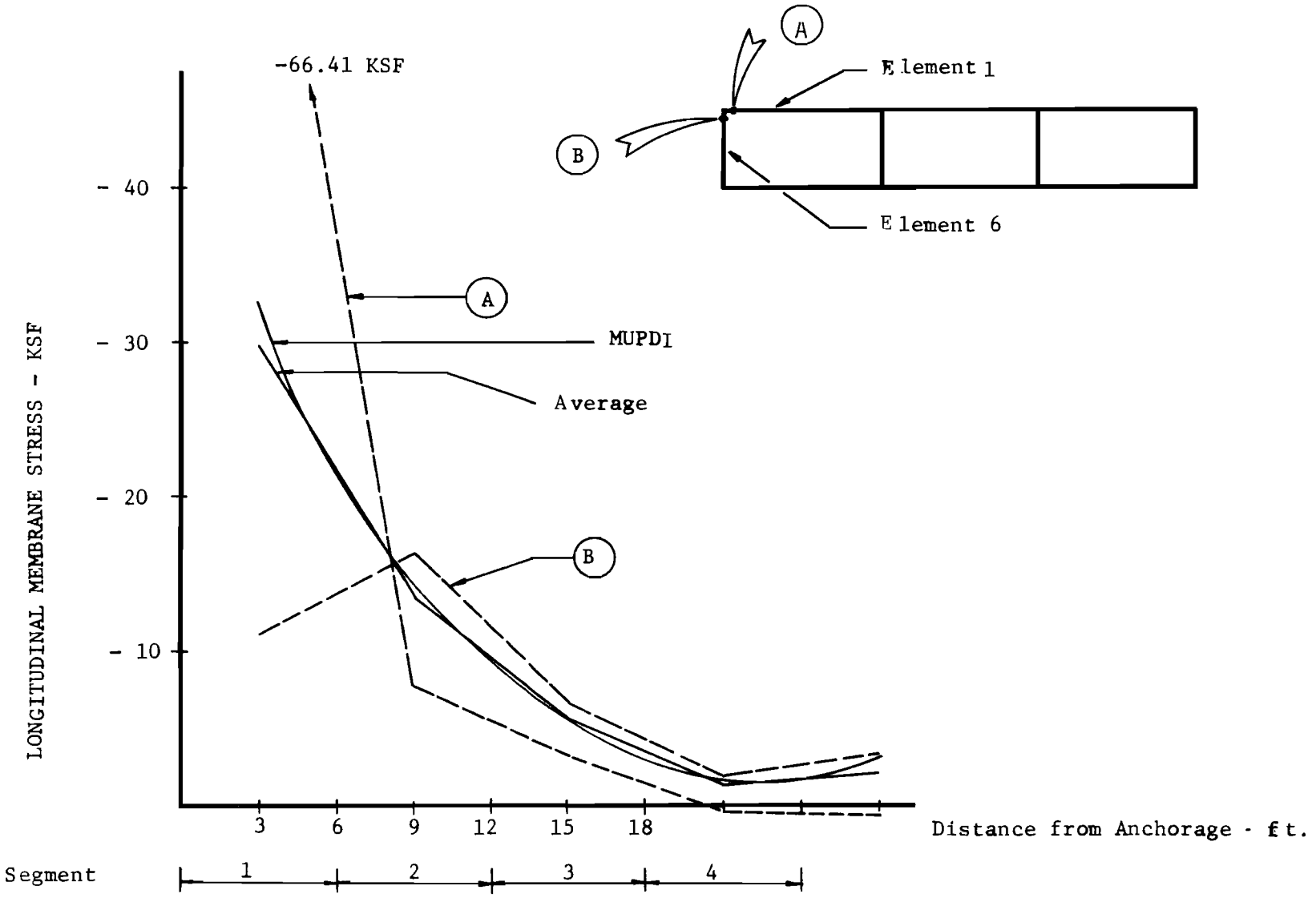

Fig. 4.11. Anchorage force effect on SX.

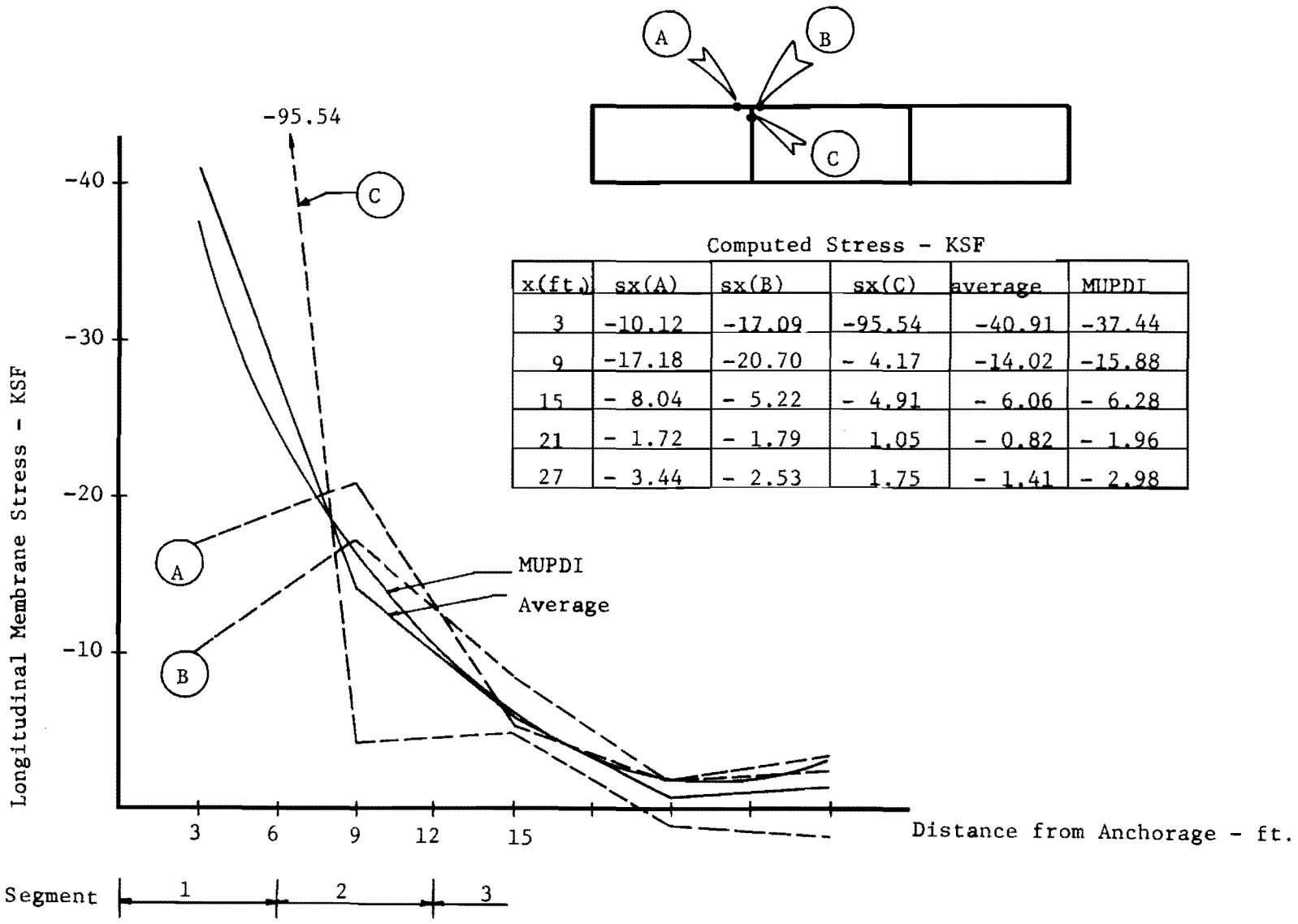

Computed Stress - KSF

x(ft.)	sx(A)	sx(B)	sx(C)	average	MUPDI
3	-10.12	-17.09	-95.54	-40.91	-37.44
9	-17.18	-20.70	- 4.17	-14.02	-15.88
15	- 8.04	- 5.22	- 4.91	- 6.06	- 6.28
21	- 1.72	- 1.79	1.05	- 0.82	- 1.96
27	- 3.44	- 2.53	1.75	- 1.41	- 2.98

Fig. 4.12. Anchorage force effect on SX.

computed values. The agreement between the average stress values and those computed by MUPDI is satisfactory.

4.3.2 Longitudinal Mesh Variation. To show the significance of variations in the longitudinal mesh size, a line load is applied to the prestressed structure at joint 1, as shown in Fig. 4.6(a). The total magnitude of the load is 1.5 kips.

4.3.2.1 Vertical Joint Displacement. Plots illustrating the longitudinal variation of vertical joint displacement are given in Fig. 4.13. A comparison of the displacement values given indicate good agreement between the results of the MUPDI and SIMPLA2 analyses under this loading condition. The effect of refining the longitudinal mesh may be observed by comparison of the second and third sets of displacements. It is seen that refining the longitudinal mesh does improve the computed displacement values; however, the improvement is slight. At all stations the displacements computed with mesh B are less than those computed with mesh A, reflecting the fact that with the refined mesh transverse compatibility is maintained at more points on the structure; therefore, the overall stiffness of the analytical model is increased.

The transverse variation of vertical joint displacements under the combined effect of prestressing and eccentric load is illustrated in Fig. 4.9(b). The three sets of displacements exhibit the same relationship to each other as discussed in connection with Fig. 4.13.

4.3.2.2 Transverse Moments. The longitudinal distribution of transverse moment at joint 1 is shown in Fig. 4.14. SIMPLA2 does not compute transverse moments at the end of the structure; consequently, the SIMPLA2 curve is terminated 57.0 ft. from the left end. Comparison of the three sets of values given indicates satisfactory agreement between the two SIMPLA2 and MUPDI analyses. The poorest correlation is obtained in the sensitive regions near the concentrated load and the interior diaphragm support, where torsional moments are largest. Comparison of the values obtained from the two SIMPLA2 analyses indicates that the transverse moments are not very sensitive to the longitudinal mesh size. Although

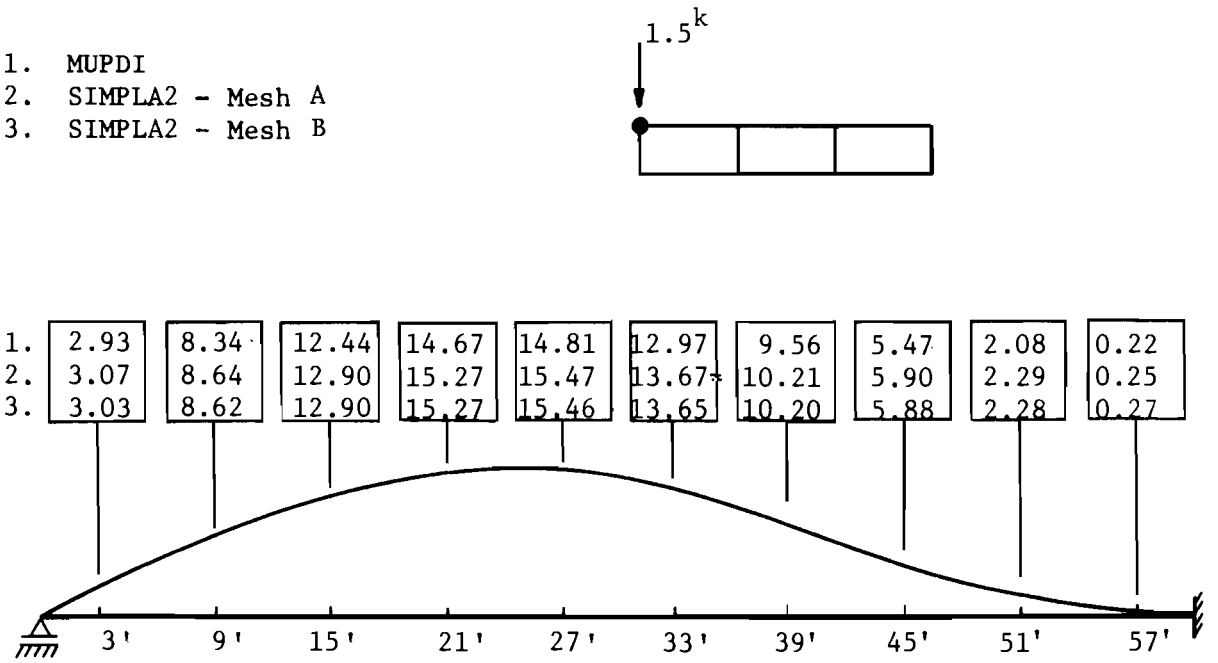

(a) Vertical Displacement at Joint 1 - Ft x 10^{-3}

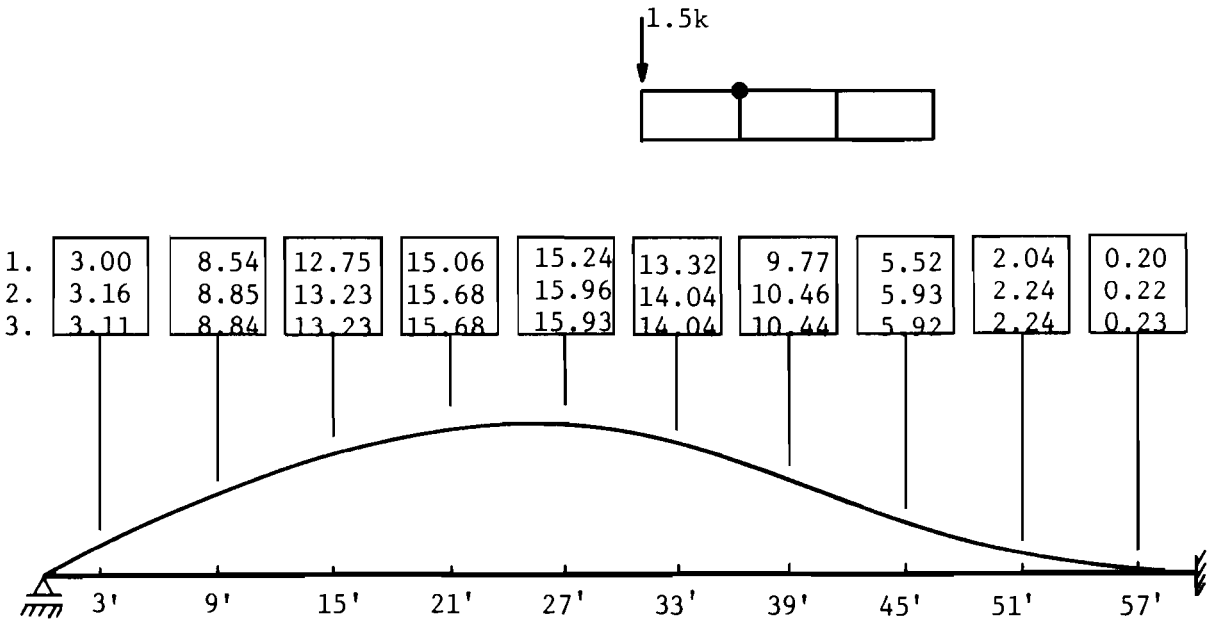

(b) Vertical Displacement at Joint 5 - Ft. x 10^{-3}

Fig. 4.13. Comparison of vertical joint displacements. Prestress plus 1.5 kip load.

1. MUPDI
2. SIMPLA2 - Mesh A
3. SIMPLA2 - Mesh B

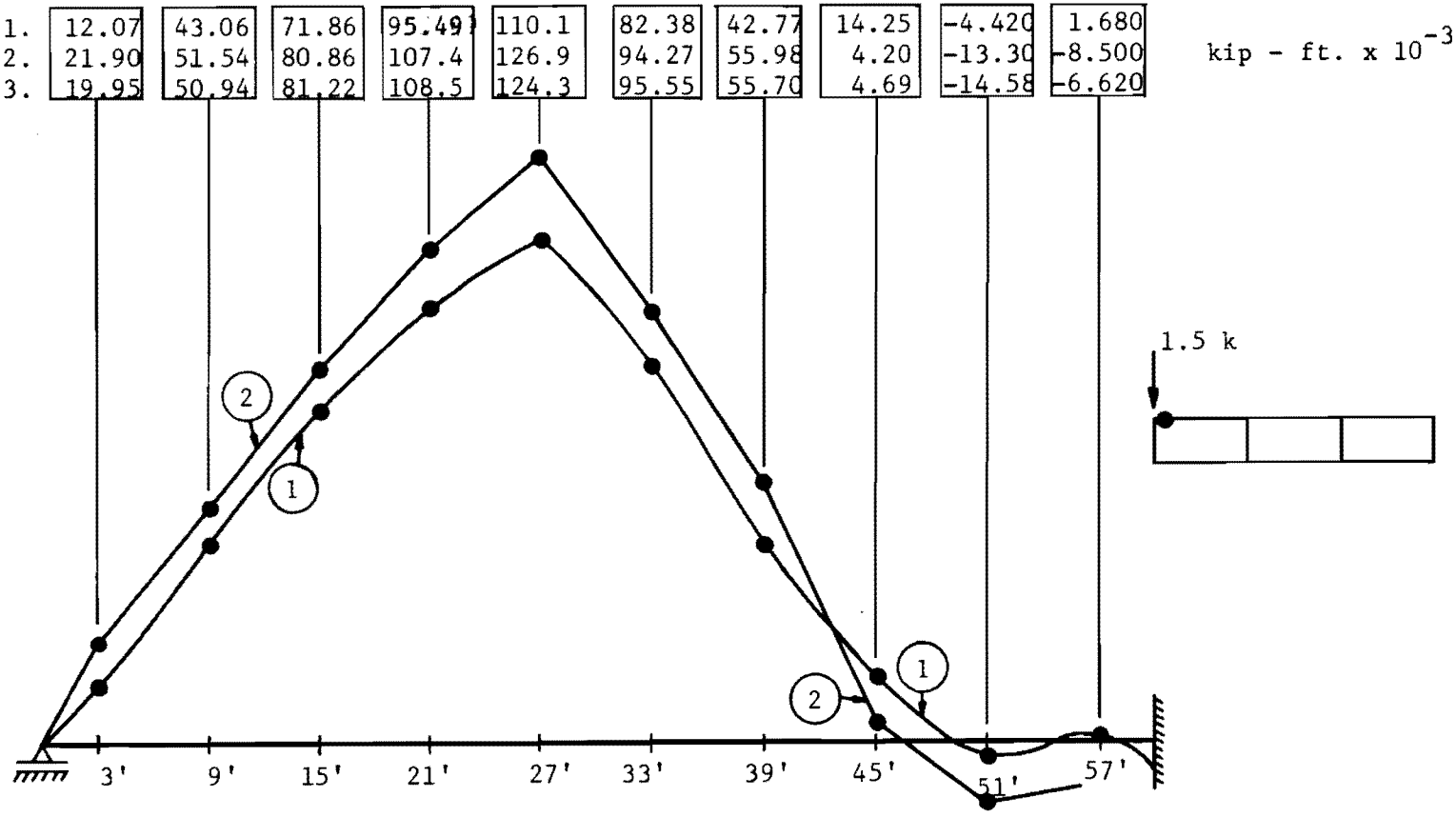

Fig. 4.14. Comparison of transverse moment.

the results obtained with mesh B differ from those obtained with mesh A in every segment, the differences are small in all cases. It is also noticeable that the results obtained using mesh B are not better for all segments than those obtained using mesh A. For either case, however, the results are satisfactory for design purposes, the maximum difference from the MUPDI values being 16.8 ft.-kips.

The variations in longitudinal normal stress due to the longitudinal mesh refinement are insignificant and are not shown.

4.3.3 Conclusions. This example shows the suitability of the composite mathematical model for the analysis of prestressed box girders. It is shown that the anchorage force causes significant inconsistencies in computed stresses; however, this effect is localized and damps out rapidly. For those segments near the anchorage, satisfactory stress values may be obtained by averaging the inconsistent values.

4.4 Example Problem 3--The Intracoastal Canal Bridge, Corpus Christi, Texas

This example deals with the analysis of a precast, prestressed segmentally constructed box girder bridge superstructure. The completed structure is a three-span, continuous, double-cell box girder. The spans are 100 ft., 200 ft., and 100 ft.; an elevation of the left half of the longitudinally symmetrical structure is shown in Fig. 4.15(a). This example is from an intermediate stage in the design of the bridge. Some small differences exist between the example and the tendon layout as constructed.

4.4.1 Construction of the Prototype. The entire bridge superstructure is precast as segments 10 ft. in length and comprising one-half of the complete cross section, as shown in Fig. 4.15(b). The complete structure as shown in Fig. 4.15(c) is constructed as two independent box girders side by side, each being one cell of the double cell completed box girder. In the final phases of construction the two independent box girders are joined transversely by a longitudinal cast-in-place strip, resulting in a two-cell monolithic box girder bridge. Since the sequence

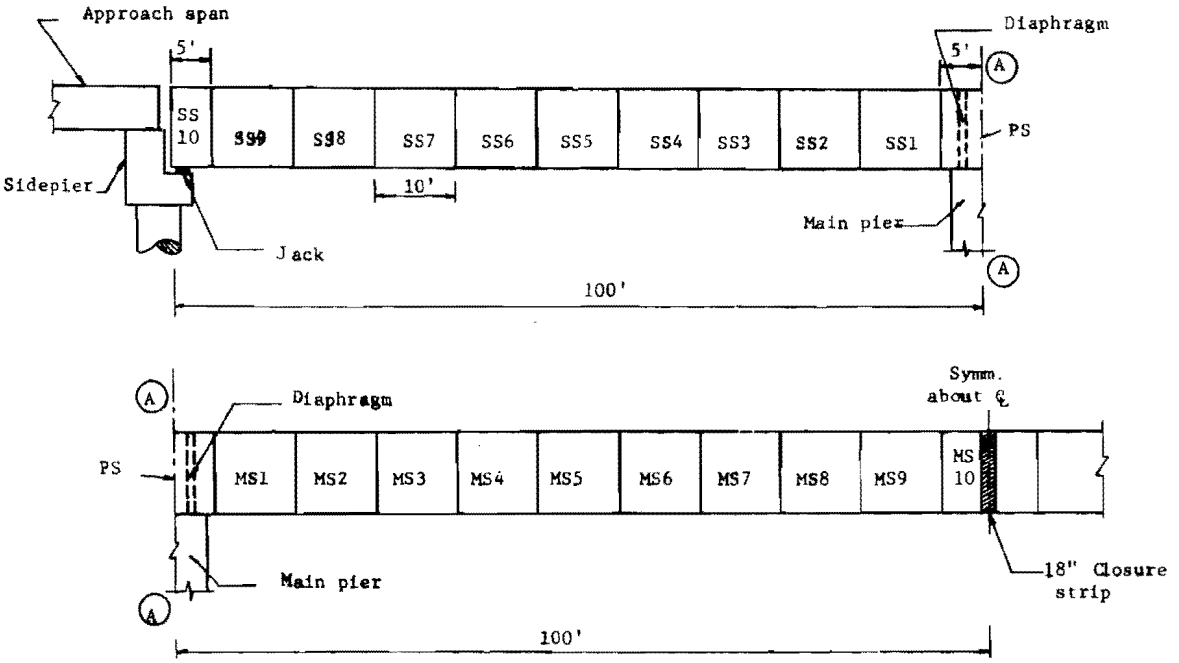

(a) Erection sequence

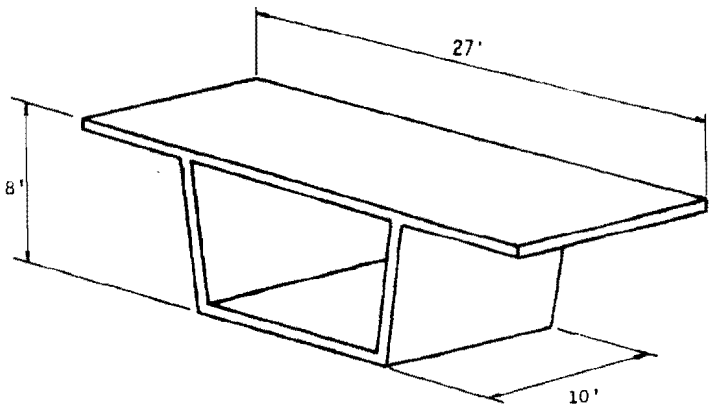

(b) Typical precast segment

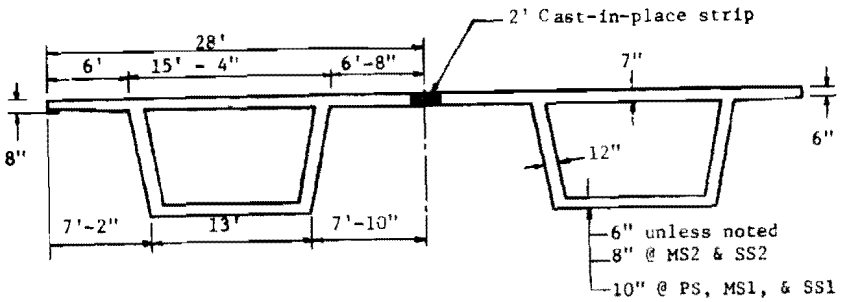

(c) Complete cross section

Fig 4.15. Intercoastal Canal Bridge - details.

of construction, prestressing, and loading are identical for each box girder, it is necessary to consider only one acting independently of the other for analysis during construction.

Design details are presented in Ref. 31. Full explanations of the calculation procedures and reasons for various closure steps are given in that reference. Only enough detail is presented here to allow correct modeling of the construction procedure.

Each girder is constructed as a balanced cantilever. Construction proceeds from the main pier outward in both directions simultaneously toward the end pier and central span centerline. Site conditions are such that the contractor may work from the area subadjacent to the superstructure and avoid the necessity of subjecting the partially constructed girder to heavy construction loads.

Construction of each girder is initiated by placing the pier segment [labeled "PS" in Fig. 4.15(a)]. A temporary moment connection to the pier is made by means of 3 in. diameter anchor bolts extending from the top flange of the girder through the diaphragms into the pier, as shown in Fig. 4.16. The cantilevering phase of the construction sequence begins by applying epoxy resin to the joint surfaces, positioning segments MS1 and SS1, and tensioning tendon B1 (Fig. 4.17). The same procedure is repeated through the placing of segments MS9 and SS9, and stressing tendon B9. The next step is to place the end half-segments, labeled MS10 and SS10. Tendons B10, C4 and C3 are stressed in order to place these segments. Tendons C1 and C2, which are designed to accommodate positive moment in the side span induced by further prestressing in the central span and by live load, are then stressed. A hydraulic jack (Fig. 4.15) is then brought into contact with the end segment. The function of the jack at this stage is simply to restrain further vertical displacement of the end of the girder while stressing the A-series tendons. There is no jacking done at this stage.

The cantilevering phase of construction is conducted from both main piers. At completion of the cantilevering, the structure is in the configuration of two independent cantilevered systems, each having a

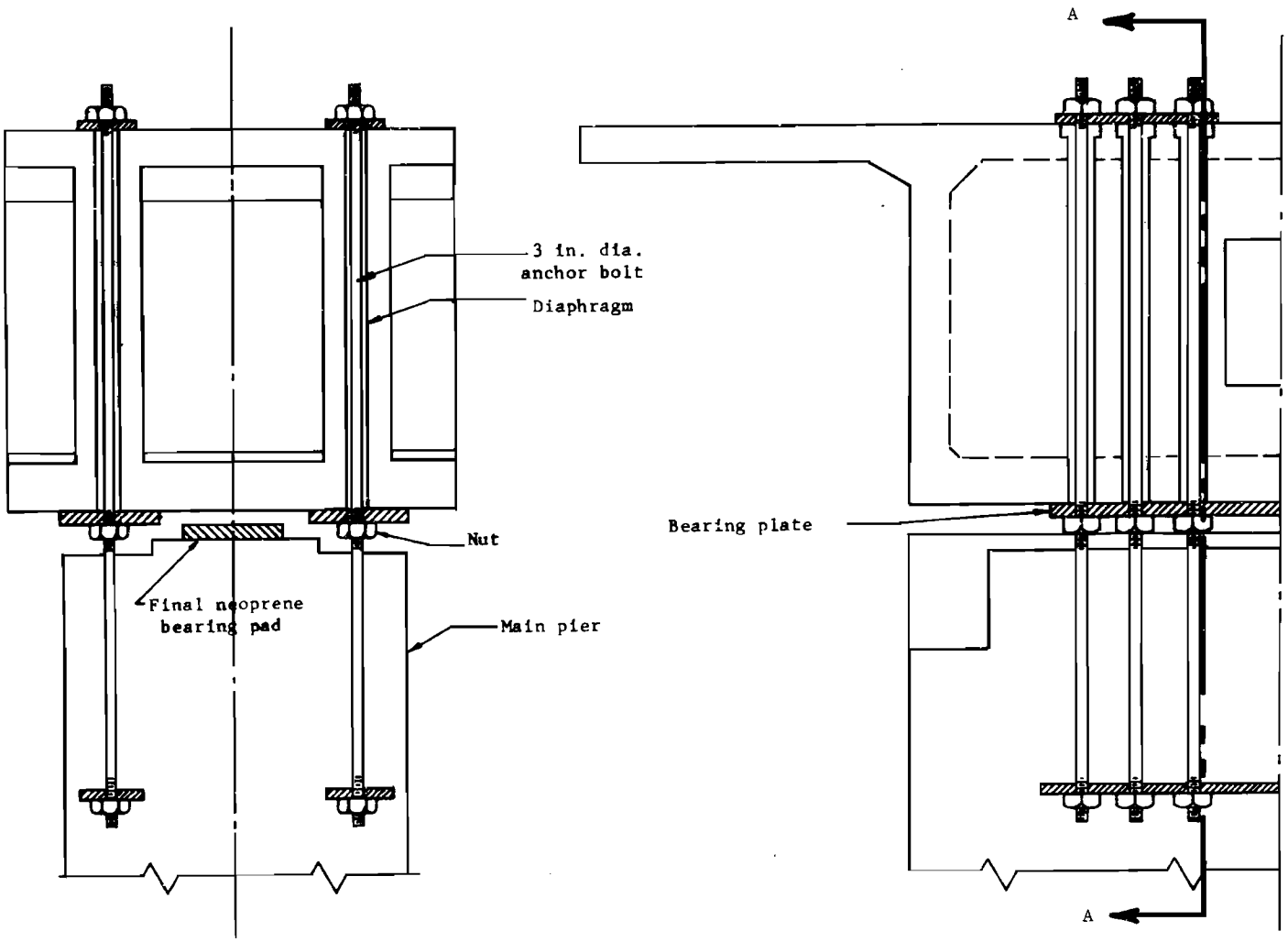

(a) Section A-A

(b) Typical section through restraining bolts

Fig 4.16. Details of pier connection.

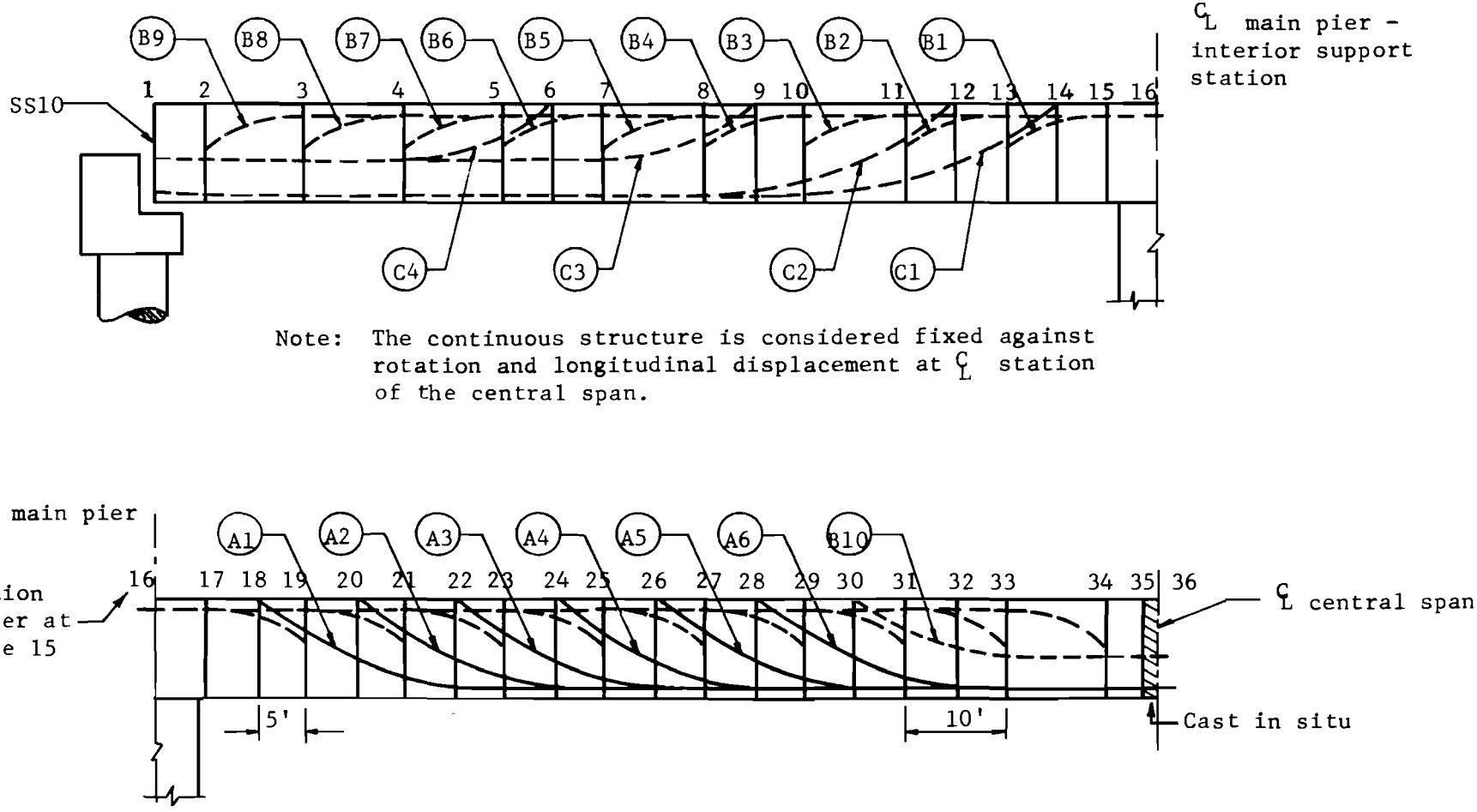

Fig. 4.17. Tendon layout and mathematical segments.

100 ft. anchor span and a 100 ft. cantilever arm (Fig. 4.15). The opposite end faces of the two central span cantilever arms are approximately 18 in. apart; the system is ready for longitudinal closure. A cast-in-place closure segment is placed and the series A tendons are stressed. In order to prevent tensile stresses in the top flange of the central span (due to stressing the A series), several intermediate operations must be performed while stressing. After tensioning tendon A4, the rotational restraint provided at the main piers (by means of the anchor bolts) is released, then the end reaction is increased from 31.6 kips to 51.6 kips. The remaining tendons, A5 and A6, are tensioned.

The final step in the erection sequence is to adjust the elevation of the end of the girder. The primary purpose of this adjustment is to bring the top deck of the segmental span at the ends to the correct elevation relative to the approach span. The criterion for the final adjustment employed is that the end of the segmental girder (segment SS10) has zero vertical displacement; i.e., the elevation of segment SS10 be equal to the elevation of the pier segment. This elevation adjustment is accomplished by incrementing the end reaction by means of the hydraulic jack under the end segment. For this structure under this analysis procedure the final adjustment requires increasing the end reaction for each box girder from 51.6 kips to 64.8 kips. Determination of these values will be explained in the next section.

4.4.2 The Analytical Model. The construction sequence outlined has been modeled as 22 separate construction stages for purposes of the SIMPLA2 analysis. A summary of the analytical stages of construction is given in Table 4.1.

Transverse symmetry of each box girder with respect to both cross section and loading makes it possible to use one-half the box girder cross section for the analytical model and greatly reducesthe analysis effort. The cross section and loading idealizations are shown in Fig. 4.18. Because the program is limited to dealing with prismatic plate elements,

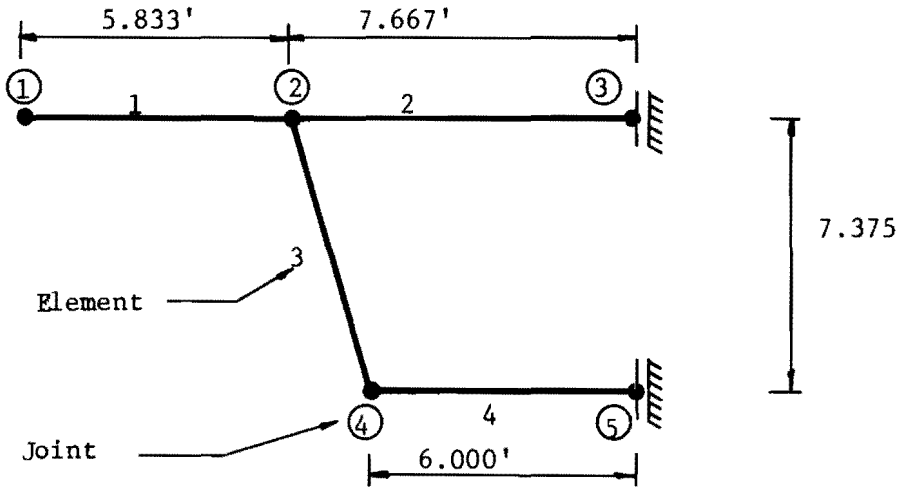

(a) Cross section idealization

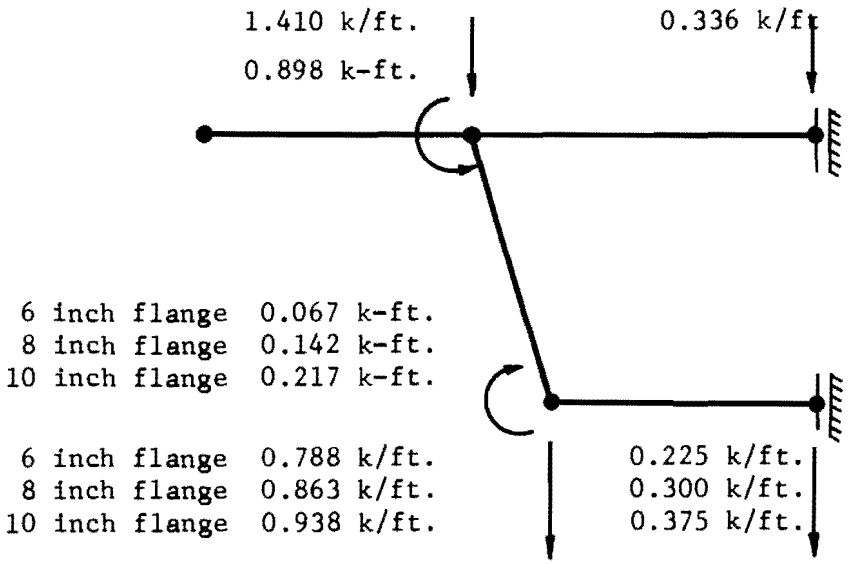

(b) Equivalent dead loads

Fig. 4.18. Example 3 - Analytical model.

TABLE 4.1. ANALYTICAL STAGES

STAGE	ACTION
1-9	Addition of segments SS1 through SS9 and MS1 through MS9; stress tendons B1 through B9.
10	Addition of segment MS10; stress tendon B10.
11	Addition of segment SS10; stress tendon C4.
12-14	Stress remaining C series tendons in the order C3, C2, C1.
15	First stage of closure. Place jack under SS10; stress tendon A1.
16-18	Stress tendons A2-A4
19	Release restraining nuts at main pier; increment end reaction by 20 kips/box to 51.6 kips/box .
20-21	Stress tendons A5 and A6.
22	Adjust elevation of SS10 to relative zero.

all plates are so idealized. The joint loads shown are equal in magnitude and opposite in direction to the dead load fixed end moments and shears for each element. The bottom flange thickness of the prototype structure is stepped, as shown in Fig. 4.15(c). For the analysis the bottom flange was assumed to be 8 in. thick throughout; however, the dead load for each segment was computed based on the actual section. The computed bottom flange stress results have been adjusted to reflect the actual bottom flange thickness.

The longitudinal idealization used in this example is shown in Fig. 4.17. At the stage in which the girder becomes continuous (stage 15) and all subsequent stages, the girder is assumed longitudinally symmetrical about the centerline of the central span. Taking advantage of both longitudinal and transverse symmetry, only one-quarter of the structure need be considered for analysis at stages 15 through 22. Figure 4.17 shows that the complete analytical model is subdivided into 34 mathematical segments. The longitudinal subdivision shown incorporates the least number of stations (therefore the least number of segments) required to

specify the tendon layout for this example. A more accurate symmetrical layout would increase accuracy. Prestressing details are given in Table 4.2. Several dual tendons in the actual structure have been combined into single equivalent tendons to simplify this example.

TABLE 4.2. PRESTRESSING DETAILS

Stage	Tendon Number	1/2"ϕ, 270^k Strands per Tendon	Area of Steel (S.F.)	Maximum Force = $0.75f'_sA_s$(k)	Initial Force = $0.6f'_sA_s$(k)
1	B1	24	0.02554	744.0	595.0
2-3	B2-B3	22	0.02340	683.0	546.0
4-6	B4-B6	12	0.01277	372.0	298.0
7	B7	7	0.00745	218.0	174.0
8-10	B8-B10	6	0.00638	186.0	149.0
11-14	C4-C1	6	0.00638	186.0	149.0
15-21	A1-A6	8	0.00850	248.0	198.0

The effects of the interior support, at the main pier, are assumed to be acting at the station marking the centerline of the pier. The main piers consist of two 8 ft. deep by 13 ft. wide rectangular sections (one supporting each box girder) and rise 100 ft. above the pile cap. The lateral and rotational stiffness of the pier was computed on the basis of an effective pier height of 130 ft. to allow for base rotation. The effects of the pier stiffness on the girder are modeled by assuming that the lateral stiffness acts as an axial elastic restraint on the bottom flange element and the rotational stiffness acts as a rotational elastic restraint on the web element at the interior support station, as shown in Fig. 4.19. The calculation of the lateral and rotational stiffness coefficients are given in Fig. 4.20. The rotational stiffness reflects both the pier flexural stiffness and the flexibility of the bolt connections (see Ref. 33). Unless the anchor bolts are prestressed, rotations due to elongations of the bolts have to be computed. Moreover, since the neoprene

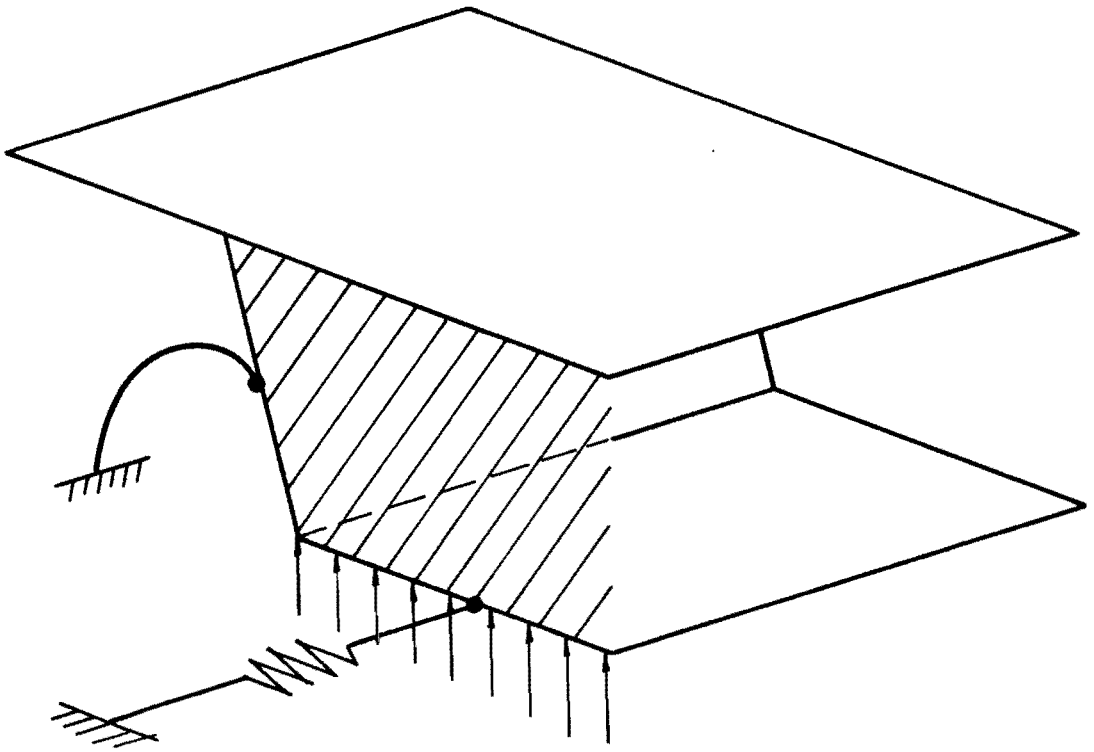

Fig. 4.19. Mathematical model of support condition - Example 3.

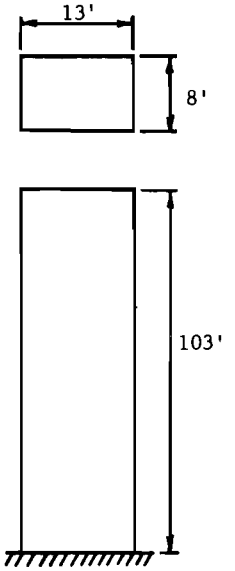

Pier stiffness

$$\frac{M}{\theta} = \frac{4\,EI}{L}$$

$$E_c = 3\times10^6 \text{ psi} = 432\times10^3 \text{ ksf}$$

$$I = \frac{13\cdot8^3}{12} = 555 \text{ ft.}^4$$

$$\frac{M}{\theta} = \frac{4\times4.32\times10^5 \times 555}{130} = 7.38\times10^6$$

Use KL = 130'

One-half of rotational stiffness applies to 1/2 box of Fig. 4.19 = 3.69×10^6.

(a) Pier stiffness

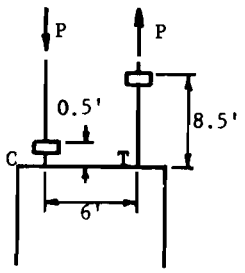

3 - 3"ø bolts
A = 0.147sf
$E_s = 29\times10^6$psi = 4.18×10^6ksf

$$\Delta_1 = \frac{PL}{AE} = \frac{P \times 0.5}{0.147 \times 4.18 \times 10^6} = 8.14 \times 10^{-7}\ P$$

$$\Delta_2 = \frac{PL}{AE} = \frac{P \times 8.5}{0.147 \times 4.18 \times 10^6} = 1.38 \times 10^{-5}\ P$$

$$\theta = \frac{\Delta_1+\Delta_2}{6} = 2.44 \times 10^{-6}P \qquad \frac{M}{\theta} = \frac{6P}{2.44 \times 10^{-6}P} = 2.46 \times 10^6$$

(b) Bolt stiffness

$$\frac{1}{K_1} + \frac{1}{K_2} = \frac{1}{K_3}$$

$$\frac{1}{3.69 \times 10^6} + \frac{1}{2.46 \times 10^6} = \frac{1}{K_3} \qquad K_3 = 1.48 \times 10^6 \ \frac{\text{ft.-k}}{\text{rad.}}$$

(c) Rotational stiffness of pier and bolts

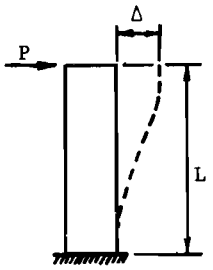

$$M = \frac{6\,EI\,\Delta}{L^2} = \frac{PL}{2}$$

$$P/\Delta = \frac{12\,EI}{L^3} = \frac{12 \times 432 \times 10^3 \times 555}{(130)^3}$$

$$P/\Delta = 1.31 \times 10^3 \text{ k/ft.}$$

One-half of lateral stiffness applies to 1/2 box of Fig. 4.19 = 655 k/ft.

(d) Lateral stiffness of pier

Fig 4.20. Computation of restraint coefficients.

bearing pad between the top of the pier and the pier segment has very little shear stiffness, it is questionable that the superstructure will feel the full effect of the lateral stiffness of the pier. The rotational and lateral stiffness coefficients used for this analysis are 1.48×10^6 ft.-kips per radian and 655.0 kips per ft., respectively, for the half-box section modeled. The pier is assumed to be axially rigid. The combined effects of the axial rigidity of the pier and the diaphragms are modeled as restraints preventing horizontal displacement and rotation of joints 2, 3, 4, and 5 in the segments containing the diaphragm.

The boundary condition required to model longitudinal symmetry of the girder for stage 15, and all subsequent stages, is obtained by restraining all degrees of freedom at the end station (centerline of the central span) except the shear displacement of the web element.

For purposes of analysis it is assumed that the compressive strength of superstructure concrete is 6000 psi and the ultimate strength of the prestressing steel is 270 ksi. When the duct material is metal sheathing and tendons are made up of wire cables, it has been suggested that the coefficient of friction may vary between 0.15 and 0.35, and the wobble constant may be from 0.0005 to 0.0030.[1] Since tendon ducts can be placed with a higher degree of quality control, a lower wobble constant was assumed for this analysis. Values used for friction and wobble constants were 0.25 and 0.0002, respectively.

A complete listing of the data input for this example is included in Appendix C.4. The input is identified by stages corresponding to Table 4.1, and in each stage the card types are identified corresponding to the classification used in the Input Guide of Appendix B.2.

Stage 0 designates the input data for the general structural constants. In Stage 1, the type 11 and 15 cards indicate free boundaries at the origin and end for the cantilevering phase. The type 14 cards impose the rotational and longitudinal restraint of the pier-bolt system at the interior support and act with the type 13 cards for segment 3 to define the diaphragm restraint conditions. The 0 in column 8 of the

type 12A card for segment 4 imposes the same diaphragm restraints on it as used with segment 3. Cantilevering proceeds through stage 9 in a balanced manner. In stage 10 the joint conditions for the interior diaphragms located in segments 14 and 15 are slightly modified to allow elastic vertical movement so as to keep from preventing rotation of the pier segment under subsequent unsymmetrical stressing operations prior to closure.

Stage 14 is the last stage of cantilevering so the indicator KREF in column 16 of card type 7B is set equal to 1 to indicate that this is the reference stage and that further stages will involve the analysis of the continuous structure.

Stage 15 contains extremely important changes in the boundary conditions. The type 11 cards indicate that vertical displacement of the origin is prevented to simulate the jacks being placed under the girders at the left hand piers before stressing of the center span positive moment tendons. The type 13 cards for segments 1 and 17 contain no dead load effects at this stage, since these effects are completely included in the reference solution and the closure analysis needs only the continuity loading data. Segments 15 and 16 at the center pier continue to be restrained against horizontal and rotational movement by their type 13 cards, reflecting the diaphragm effect. The type 15 cards impose the condition of symmetry at the closure segment which allows significant reduction in the data input and analysis time. Free vertical movement of the web at the closure is still allowed.

Stages 16 to 18 correspond to the same continuous structure with vertical displacement at the origin still prevented. Since there are no changes in the origin boundary card, the origin is held at the same level as in stage 15 after completion of cantilevering. This is a design choice and could be altered in other applications.

Stage 19 encompasses several major changes to the structure and indicates that the SIMPLA2 program can realistically model construction steps, but needs considerable design guidance either from other calculation procedures or from multiple runs of the SIMPLA2 program. In stage 19 the restraining nuts at the main pier are released, causing the reaction at the

origin to increase. Furthermore, in order to control midspan tensile stresses during stressing, the designers (Ref. 31) had recommended that the origin reaction (31.6 kips per box) be further increased 20 kips per box. The effect of this combination was precalculated and was input as 25.8 kips for the half-box model in the element 3, type 11 card. The reaction at the support at the end of stage 18 corresponded to 24.5 kips/box. The type 14 cards release the moment connection and the longitudinal restraintat the central pier, keeping only the diaphragm support.

Origin deflection at the completion of stage 14 was 0.140 ft. downward from the original baseline through the pier supports. This constitutes the reference stage for the continuous structure. At completion of stage 19, the origin deflection was 0.032 ft. downward from the original baseline. However, this would be 0.140 ft.-0.032 ft., or 0.108 ft. upward from the reference solution. In stage 20, the origin pier jacks hold the segment in vertical position as the tendon is stressed so the type 11 card for the origin is given a fixed displacement coordinate of +0.108 ft. from the reference baseline. Similarly, in stage 22, when the origin is brought back to essentially a zero deflection position relative to the piers, a fixed displacement is specified at the origin which corresponds to the reverse of the deflection at the origins at the reference stage 14. A very slight error is shown on the card as the correct number should be 0.140 ft.,* not 0.1369 ft.

The techniques used to model the specified closure and final adjustment sequence require detailed knowledge of intermediate solutions for reactions and displacements. Either the specific values must be known beforehand from other design or calculation procedures, or multiple runs of the SIMPLA2 program are required. In the absence of previous calculations, all analysis could be performed through stage 18, with a special stage 19 in which the deformation constraint at the origin was maintained but the center pier rotation restraint was released. This

---

*The Input Guide in Appendix B.2 specifies that boundary conditions at the ends of the structure are input referenced to the element relative coordinate system. Hence, the sign of the displacement depends on whether the lower numbered joint is on the top edge or the bottom edge of the plate.

would indicate the value of the reaction after stage 18 and the change in reaction due to release of pier restraint. This value could then be supplemented by the indicated 20^{k}/box additional increment at the origin. The new force would then provide the input for stage 19 in the program input as outlined in Appendix C.4. The program would then be rerun through stage 19, which would yield the correct deflection for computation of the origin boundary condition for stages 20 and 21. Another pass would then be required for the complete solution as given. Any problem where the boundary conditions for all stages are known beforehand or can be determined by auxiliary elastic calculations allow the entire erection sequence to be programmed and the solution obtained with a single execution of the program.

4.4.3 Discussion of Results. During erection of the structure calculated displacement curves as shown in Figs. 4.21 and 4.22 can prove useful if displacements are large enough to be accurately observed. Since, during erection the girder is subject only to dead load and prestress, the transverse membrane stresses, transverse bending moments, and normal shears are all quite small. Because the girder is not subject to torsion, the flange membrane shears are also small; consequently, stress quantities considered significant are the longitudinal membrane stresses and web membrane shears.

4.4.3.1 Displacement during Erection. Figure 4.21 illustrates the computed displaced configuration of the girder at various stages of cantilevering. Through the first nine stages of the erection sequence, the girder is symmetrical about the main pier; therefore, the displacements of only one cantilever arm are shown. Displacement curves for stages 1, 2, 3, and 5 fall between those for stages 4 and 7, and are omitted for the sake of clarity. Because under dead load the joints displace almost uniformly, displacement of only one joint is reported. The

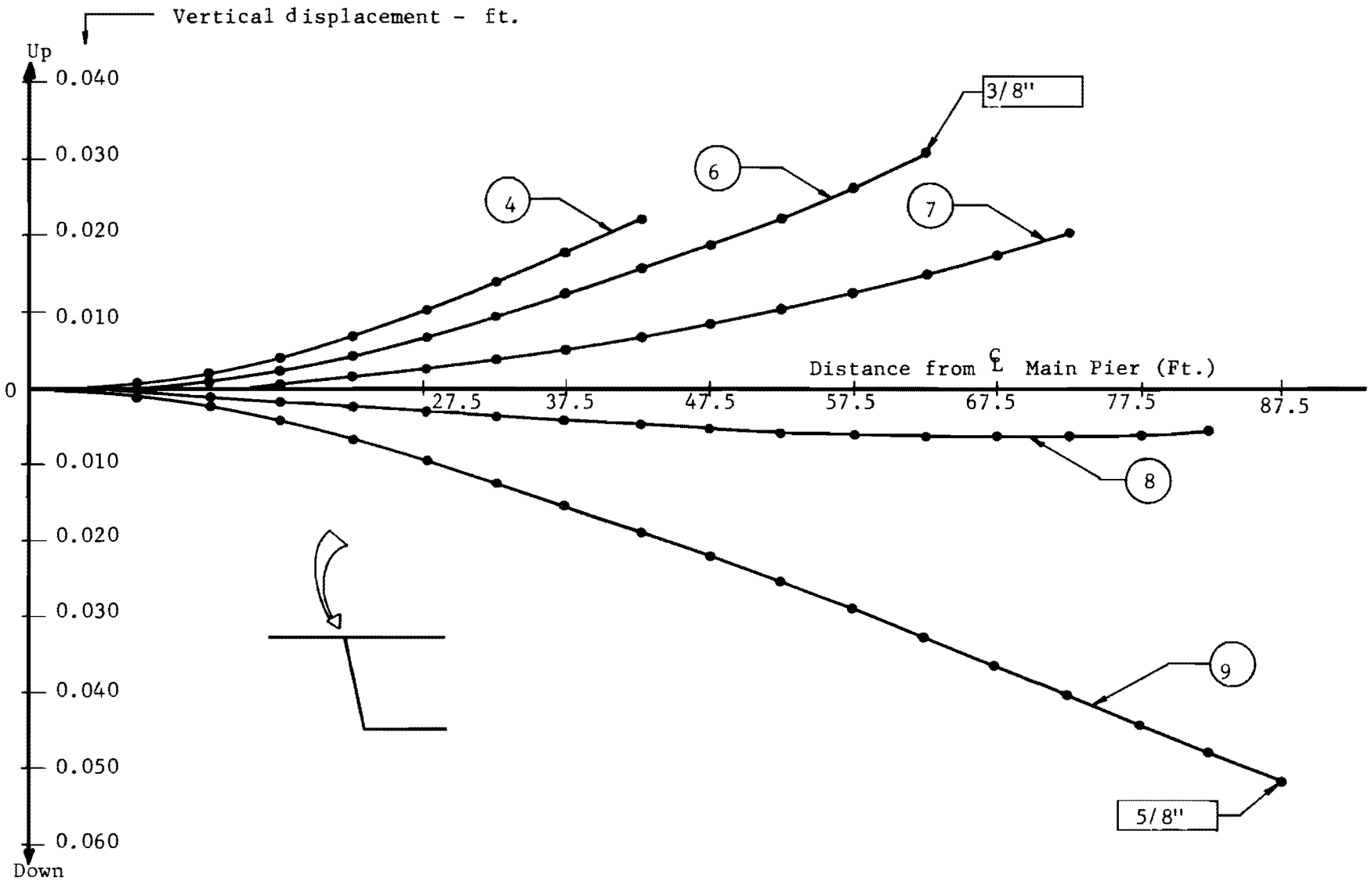

Fig. 4.21. Intracoastal Canal Bridge - Displacements during erection.

end of the girder displaces upward through the first seven stages of erection. With the addition of the final three full segments (stages 7, 8, and 9), the girder displaces downward. The very small deflection values in the long cantilever arms indicate the stiffness of the design and the efficiency of load balancing.

Figure 4.22 illustrates the displaced configuration of the girder at the full cantilevered reference stage (stage 14) and at various stages of the closure sequence. With the addition of segment MS10 and stressing of tendon B10, the problem becomes unsymmetrical and it is necessary to observe both cantilever arms. Figure 4.22 shows the maximum displacement occurs at the end of the left cantilever arm (segment SS10) and is approximately 1-5/8 in. downward. Vertical displacement of the right end (segment MS10) is 1-1/8 in. downward. This difference in end displacements reflects the effect of the series C tendons. Stressing tendons A1 through A4 (stages 15 through 18, respectively) reduces the vertical displacement at segment MS10 to about 1/2 in. while increasing vertical displacements throughout the side span slightly. Incrementing the origin reaction at stage 19 reduces the displacement at SS10 to 3/8 in. downward and increases that at MS10 to almost 1 in. downward. The final configuration of the completed girder shows that under dead load and prestress the completed girder is cambered upward about 1/16 in. at the center of the side span and downward about 3/4 in. at the center of the central span.

Figures 4.21 and 4.22 reflect the fact that the tendon forces were designed to balance approximately 60 percent of the dead load and, therefore, control dead load displacements. The maximum dead load displacement to span ratio for the completed girder is 1/3000, indicating that the design is, indeed, well-balanced.

When the 18 in. cast-in-place closure strip between cantilever arms is placed (stage 15), an angular discontinuity is effectively "locked" into the girder at the center of the central span. Since the design is well-balanced, i.e., dead load displacements are quite small, this angular discontinuity is also quite small.

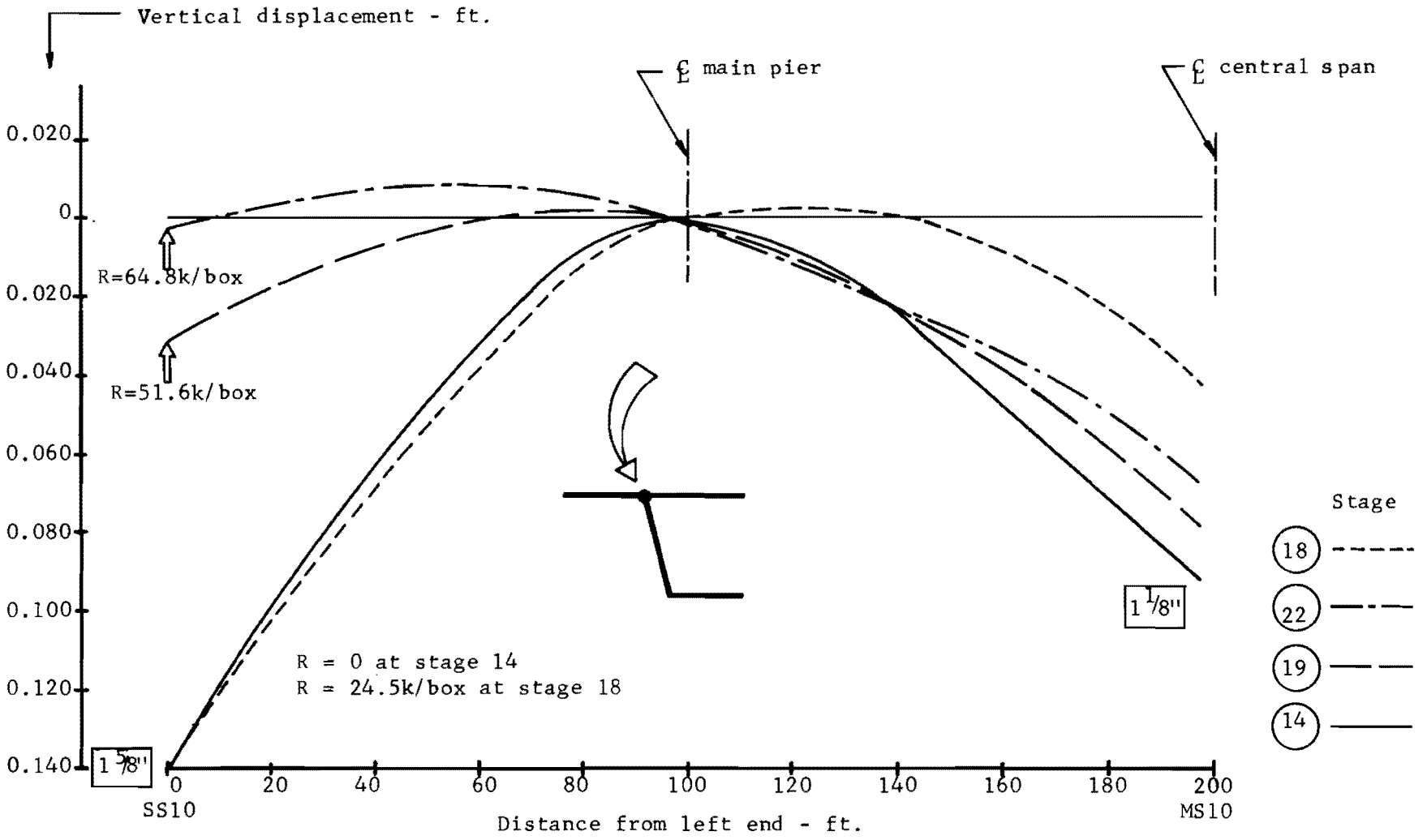

Fig. 4.22. Elastic curve at various stages of closure.

4.4.3.2 Normal Stresses during Erection. Normal stresses are computed for each edge of all elements at every stage of erection. During the cantilevering phase the critical section will be near the face of the pier segment. However, the pier segment is fully supported and due to the involved support condition imposed it is likely that the stresses computed at the pier segment may be distorted. Consequently, the midpoint of the next mathematical segment (a section 7.5 ft. to the right of the pier centerline) is selected for observation. This section will be henceforth referred to as the pier section. During closure, both the pier section and the cast-in-place closure strip are critical. Stresses at web flange junctures are computed by averaging stresses from the connecting elements, as discussed in Sec. 4.3.1.3. In the following presentation all computed flange forces at the pier section have been given as stresses on the actual 10 in. bottom flange thickness.

Figure 4.23 illustrates the maximum and the minimum stress envelopes for the girder at the pier and at the closure sections. It is obvious that all stresses are conservative throughout erection when compared to the allowable compressive stress (345 KSF). This is fairly typical of designs approached from a load balancing point of view. The bottom flange at the pier experiences tensile stresses during the first three stages of erection in violation of the design criteria. These tensile stresses must be controlled during erection by the use of auxiliary external prestressing which may be removed at a later stage. The minimum stresses in the top flange occur at stage 1, and the maximum at stage 6. The nonuniform distribution of stress in the top flange results from shear deformation of the flange (shear lag) caused by high compressive web stresses around the anchors. Maximum stress in the bottom flange occurs at stage 11 when each cantilever arm is complete.

The minimum stresses in both flanges at the closure strip occur at stage 15 when the first closure tendon (A1) is stressed. The maximum stresses in the top flange occur at stage 22 as a result of adjusting the end reaction, and in the bottom flange at stage 21. Stresses existing at the two sections under consideration at the completion of erection are shown in Fig. 4.24.

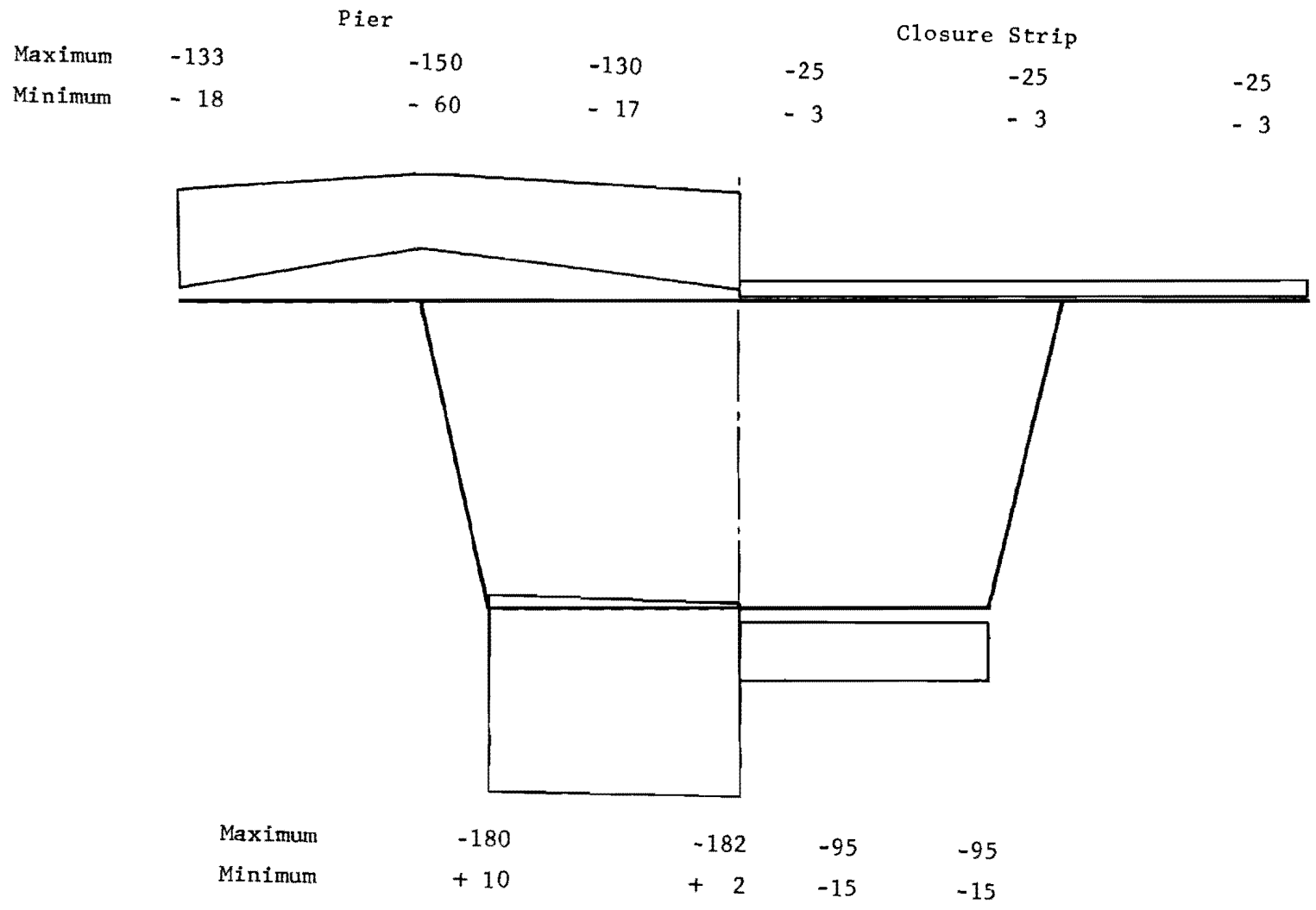

Fig. 4.23. Stress envelopes during erection (KSF).

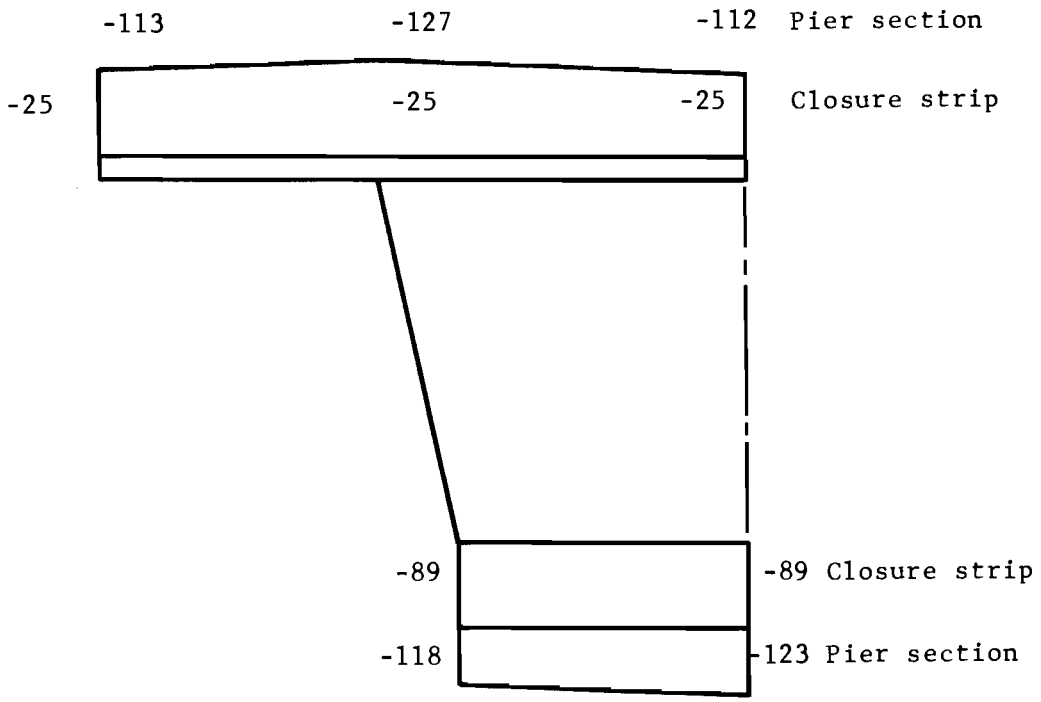

Fig. 4.24. Stress distribution at completion (KSF).

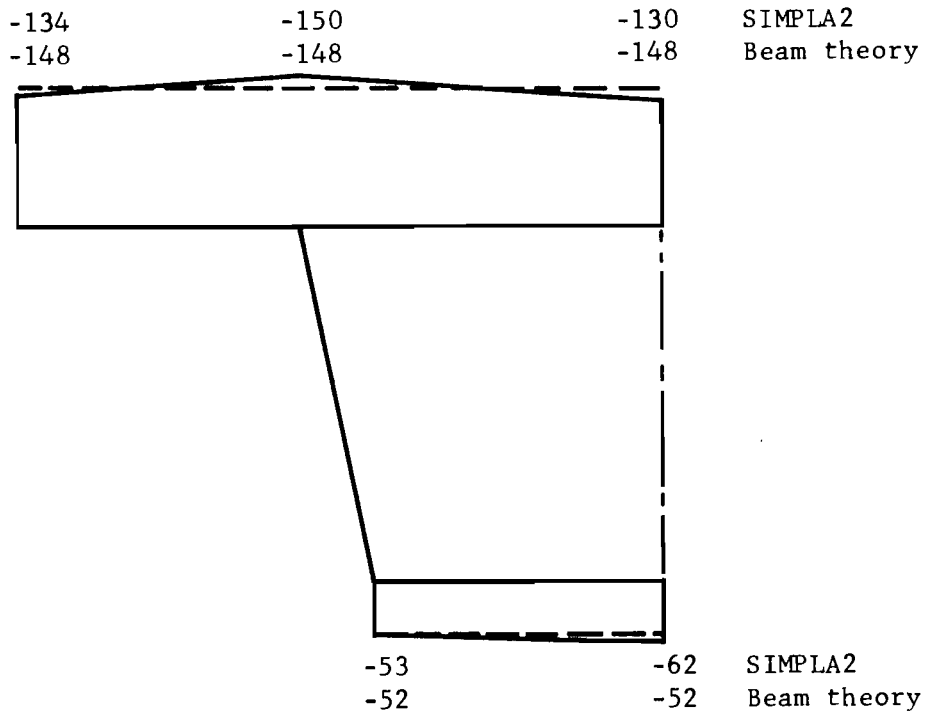

Fig. 4.25. Stress at pier section at completion of Stage 6 - comparison to beam theory (KSF).

Various causes for nonuniform flange stress distribution were discussed briefly in Chapter 1. Since in this case there are no load components to twist or distort the girder, nonuniformities in flange stresses are caused by shear lag. Figures 4.23 and 4.24 indicate that throughout most of the erection sequence the flange stresses are distributed nearly uniformly at the sections under consideration, the exception being at the pier section at stage 1. The apparent absence of shear lag effects at the pier section (which would ordinarily experience the most significant effects) may be attributed to the fact that the design is well-balanced; therefore, a large percentage of the total stress at the section is due to distributed axial load. This indicates that for similar examples a reasonably accurate analysis for longitudinal membrane stresses may be based upon ordinary flexural theory. A comparison of longitudinal membrane stresses as computed by ordinary flexural theory to those from the SIMPLA2 analysis is shown in Fig. 4.25 for a typical stage (stage 6). The "beam theory" values are obviously accurate enough for design purposes. It should be emphasized, however, that under other load and cross section configurations shear lag can account for significant stress nonuniformities[15,17] and the use of ordinary flexural theory must be used with care.

Due to the nearly uniform distribution of longitudinal normal stresses at the pier section, the average top and bottom flange stress at each stage is a significant design parameter. Observing changes in average top and bottom flange stresses as erection advances, provides further insight into the behavior of the girder during erection. Figures 4.26 and 4.27 show the variation of the average stress in the top and bottom flanges, respectively, as erection proceeds. At stages 11, 12, 13, and 14, the stresses at the pier section do not change. This result is expected, since the structure at these stages is statically determinate. Therefore, only the region spanned by tendon C1 should experience stress variation.

Figures 4.26 and 4.27 illustrate the effect of the closure sequence upon the pier section. Each stage of the closure sequence

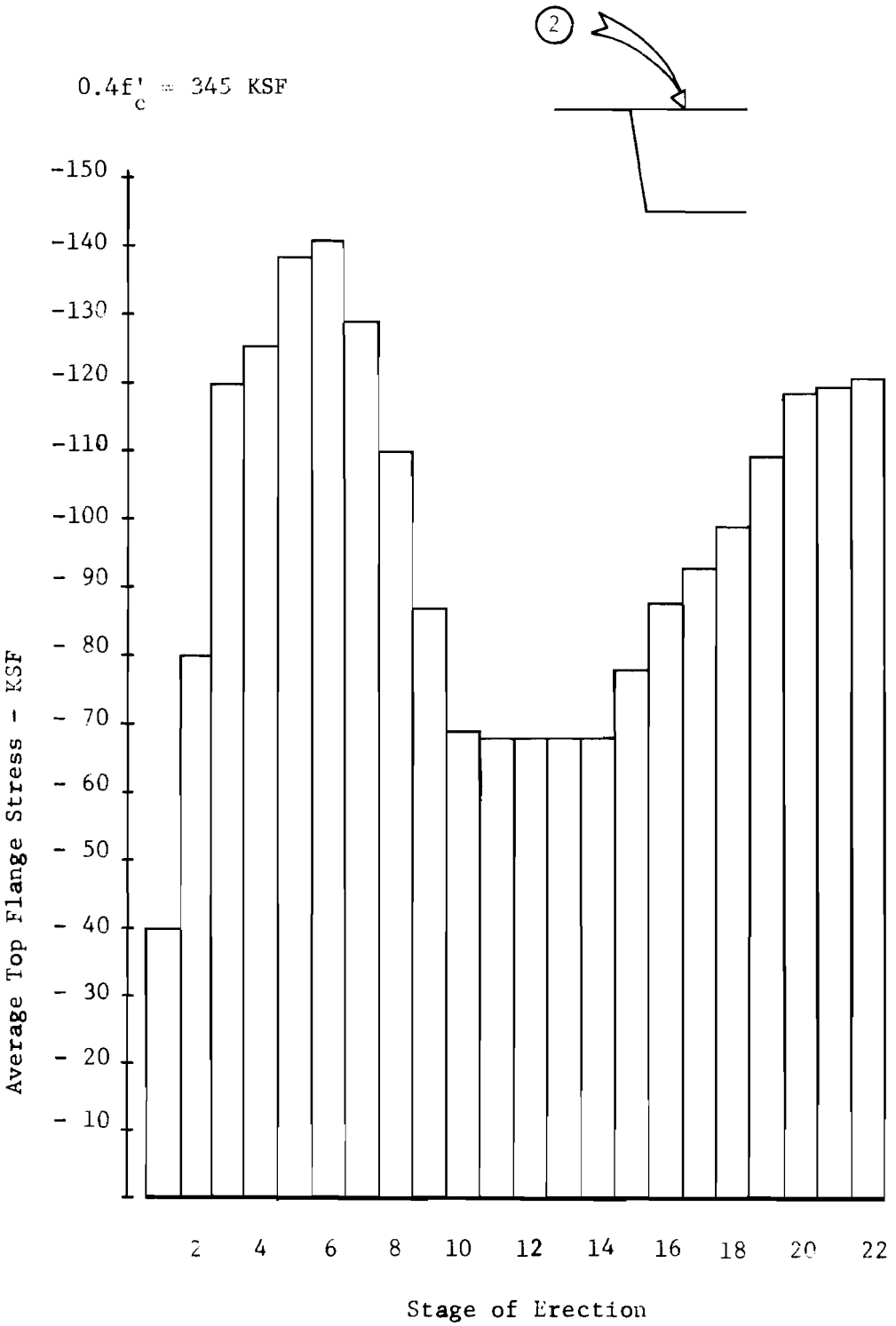

Fig. 4.26. Variation of average top flange stress at pier section.

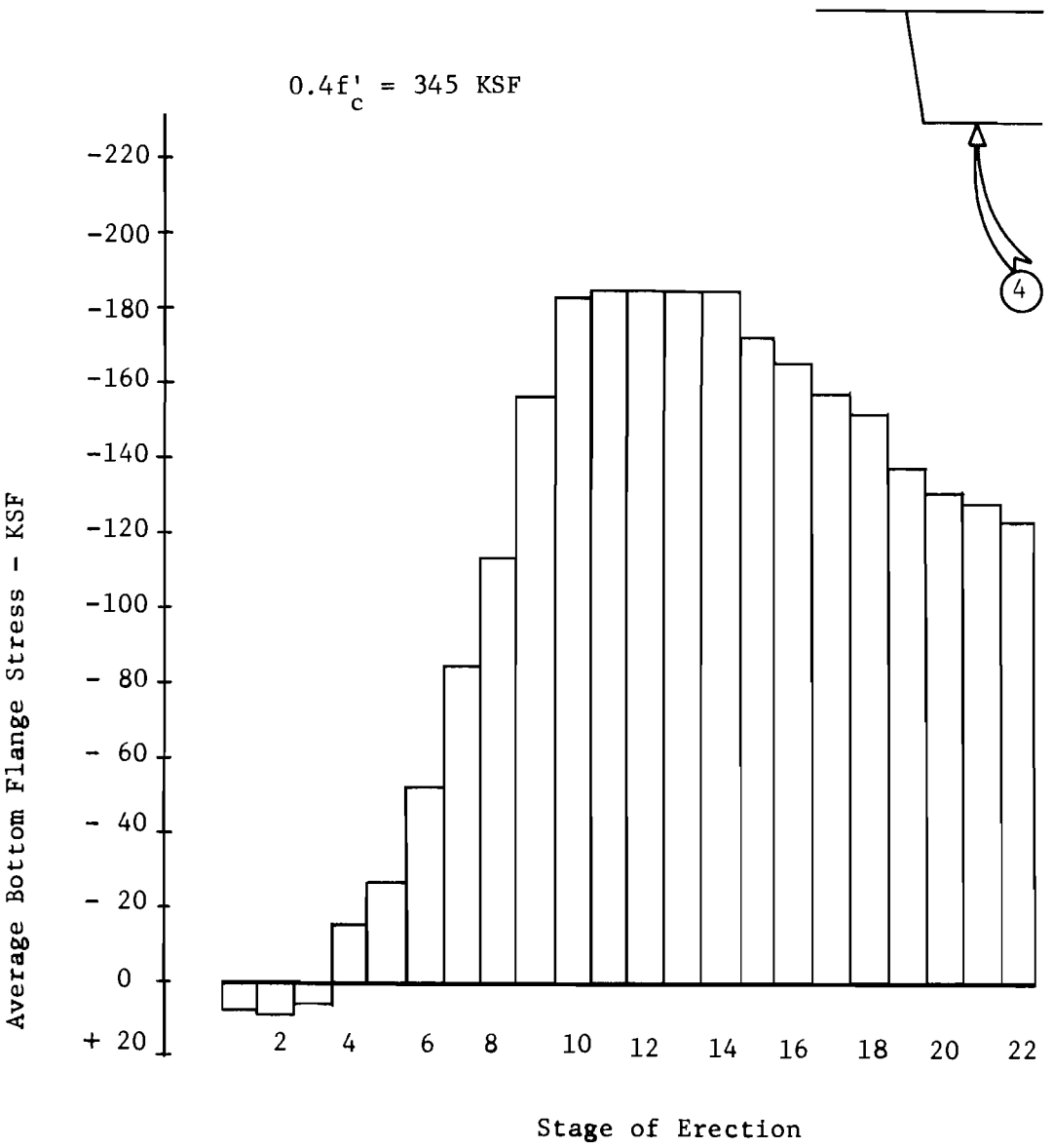

Fig. 4.27. Variation of average bottom flange stress at pier section.

(stages 15 through 22) induces positive moment at the pier section as can be seen by considering the equivalent loads associated with each stage. These graphs illustrate vividly that the flange stresses are conservative at all stages of erection.

4.4.3.3 Web Shear Forces. The precast segment is provided with a shear key in each web to carry the shear force across the interface until the epoxy jointing material develops its design strength. In order to evaluate the adequacy of the shear key provided, web membrane shears must be determined at the interface. Referring to Fig. 4.17, it is seen that the tendon profile has a horizontal tangent at the station marking the interface of the segment being added and the standing portion of the structure. By considering a free body diagram of the curved portion of the tendon, it is seen that the vertical component of the anchorage force must be equilibrated by the vertical components of the radial pressures applied to the tendon by the web. Therefore, during erection, the web shear at an interface is simply the shear force due to dead load--that due to prestressing is zero.

Should the tendon profile, cross section, or construction loads be more involved, evaluation of the web shears at the epoxy joints would not be such a simple matter. Moreover, the anchorage force and tendon curvature cause significant variations in web shear between stations; thus the most effective means of studying web shear is to construct a web shear force diagram. Computer output from the SIMPLA2 analysis includes membrane shear forces for each element at the longitudinal center of the mathematical segment. These values are used to construct the web shear force diagram at a typical stage (stage 6) shown in Fig. 4.28. Vertical components of the anchorage force vectors are given as the transverse shear in the web element at the origin for the stage at which the particular tendon is stressed. Since element edge forces are assumed uniformly distributed over the length of one mathematical segment, membrane shear in each element is assumed to vary linearly over the segment length. Actual shears would depend on the tendon curvature. Consequently, construction of an approximate web membrane shear force

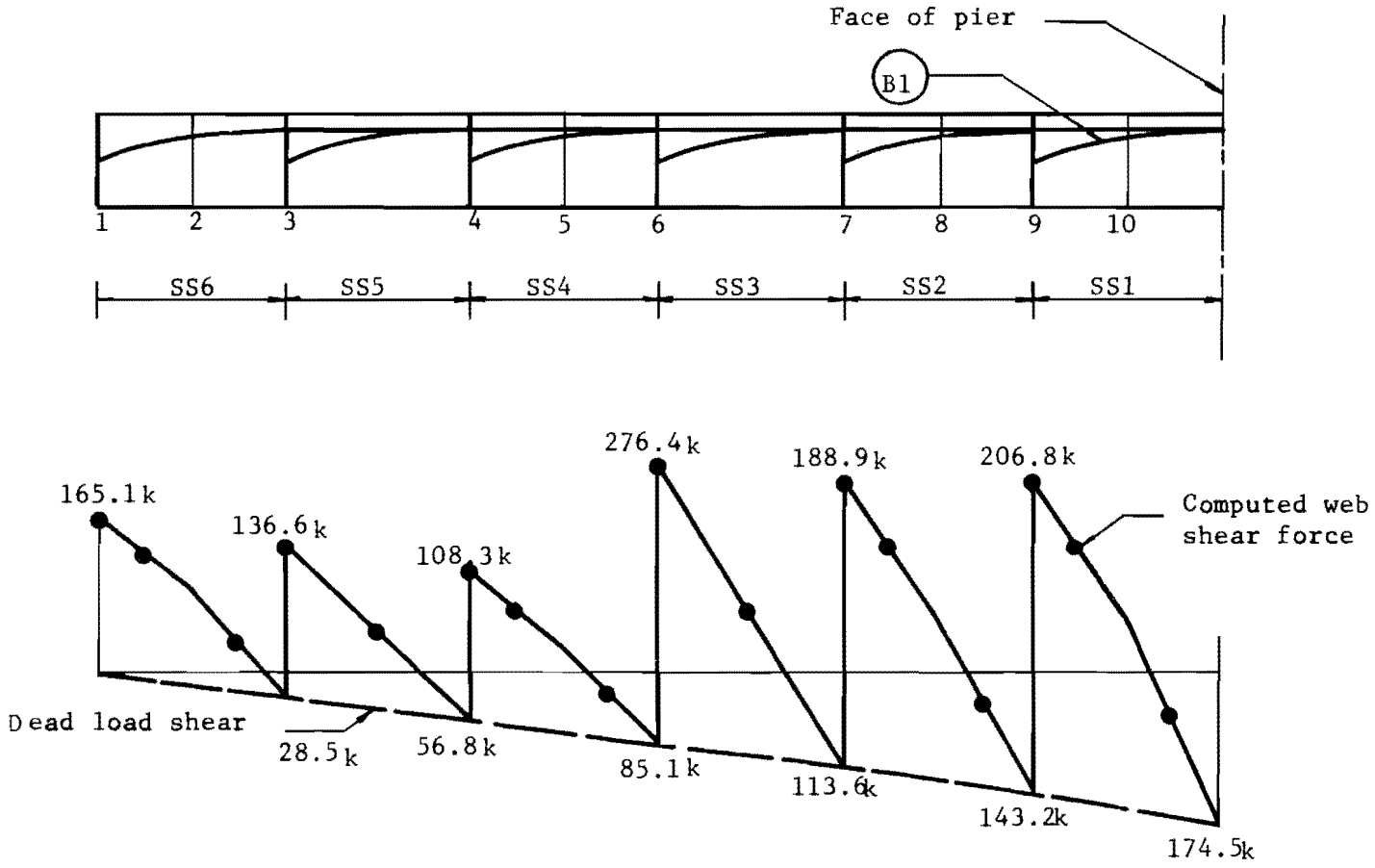

Fig. 4.28. Typical web shear force diagram - Stage 6.

diagram directly from computed values is a simple matter. Figure 4.28 shows that the dead load shear values (which were calculated independently) agree well with the values obtained from the shear diagram constructed in this manner, indicating reasonable accuracy of computed values.

Computed results indicate that during erection the critical web shear is 350 kips and occurs at the anchorage ends of the structure at the initial stage. This maximum shear force is a direct result of the large prestress force employed at the initial stage, and acts temporarily upon a section at the anchorage end of segment SS1. The maximum shear force acts temporarily, since at each stage subsequent to Stage 1 the shear force at this section is reduced by the dead load of the segments to the left of segment SS1 (see Fig. 4.28). At Stage 6, Fig. 4.28 indicates that the shear force at this section is reduced from 350 kips to 206.8 kips by the dead load of segments SS2 through SS6.

4.4.3.4 Effective Prestress Forces. The total area of prestressing steel required during cantilevering is much too large to be placed in the web. Therefore, most of the B series tendons curve in plan out of the web into the top flange as they move away from the anchorage. Figure 4.29 illustrates a plan and an elevation view of a typical B series tendon. Because the tendon curves both in a horizontal and in a vertical plane, and since the curvature of the tendon in the vertical plane is relatively large, severe friction losses are observed over the first 20 ft. of the B series tendons. SIMPLA2 furnishes effective prestress at each tendon nodal point at the stage at which the tendon is stressed--initial effective prestress. The tendon may be monitored at some future stage of erection and revised effective prestress is computed as explained in Chapter 3. Figure 4.29 shows the variation of computed effective prestress for a typical B series tendon (tendon B6). The solid curve labeled "Stage 6" represents effective prestress at Stage 6 after the tendon has been pulled to a maximum jacking stress of $0.75f'_s$ and released back to $0.60f'_s$. The dashed curve labeled "Stage 9" represents the effective prestress in tendon B6 at the completion of Stage 9 of erection.

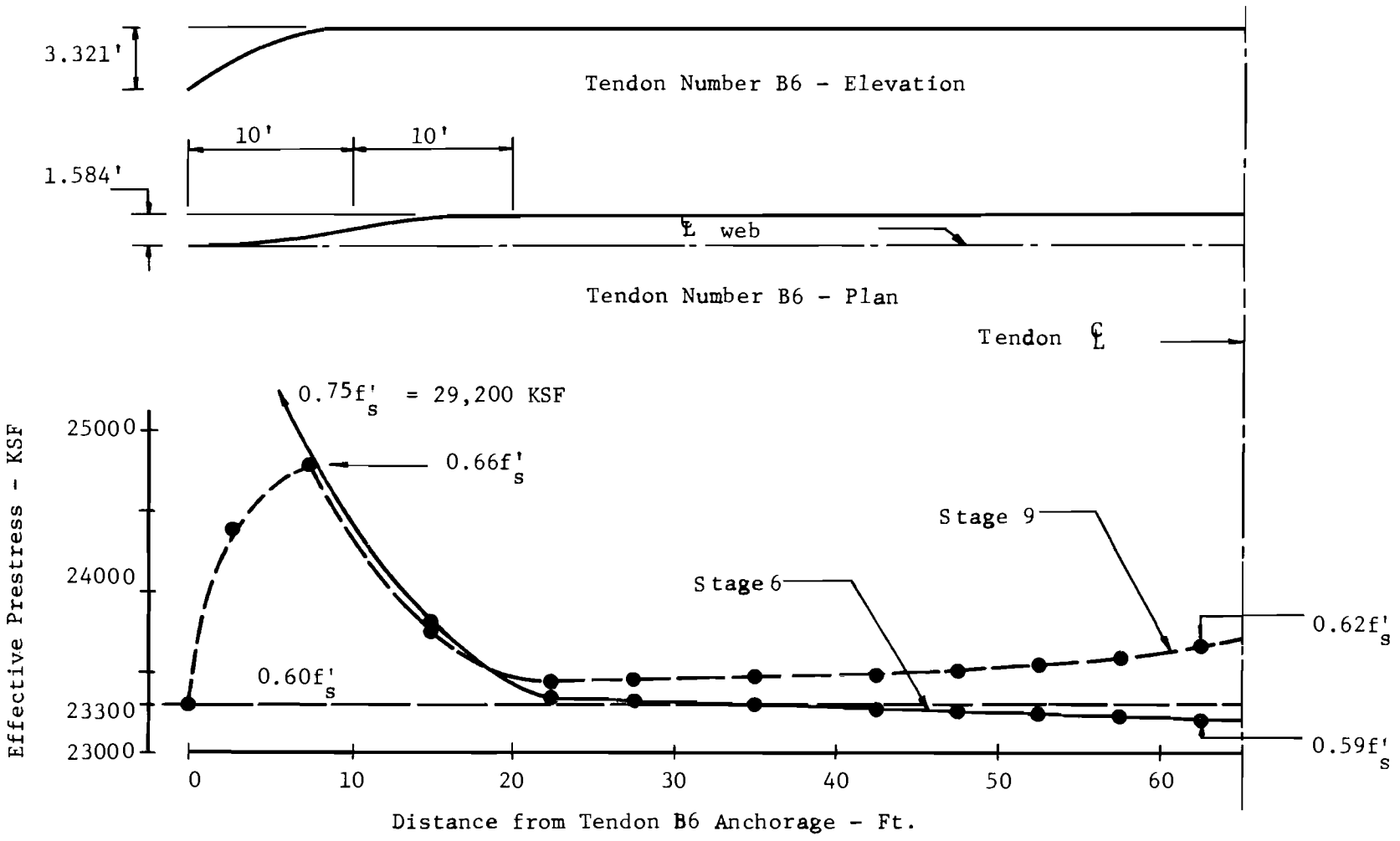

Fig. 4.29. Tendon stress variation due to friction loss and erection for typical B series tendon.

Several conclusions may be drawn from Fig. 4.29. In Chapter 3 the assumption was made that over the length of one segment friction loss would not exceed approximately 15 percent. This assumption allowed the use of an approximate prestress force function. Figure 4.28 indicates that the maximum friction loss over one segment length for tendon B6 is approximately 6 percent--the maximum friction loss observed for all B series tendons is approximately 9 percent, occurring in tendon B9. Since the assumption is not violated in this severe test, it may be concluded that adopting an approximate force equation rather than the more exact equation is justified.

Variations of tendon stress from initially computed effective prestress values have been discussed in Chapter 3 and are a result of elastic deformation of the structure due to sequential prestressing and dead load application. It has been assumed implicitly in the analysis that these tendon force changes are small and that equivalent joint loads computed from initial effective prestress values need not be recalculated to reflect these changes. For more conventional structures, variations in prestress force are for design purposes negligible.[26,27] In this more unusual application, however, it is conceivable that tendon force changes could be significant. The capability to monitor all previously placed tendons provides a convenient check on the assumption mentioned above and furnishes the designer a continuous account of the tendon stress status. The plot shown in Fig. 4.29 illustrates this capability. It is seen that at the completion of stage 9, tendon force in tendon B6 is increased by a maximum of 3 percent. The logic of this result may be deduced by inspection of Table 4.2 and Fig. 4.21. Figure 4.21 indicates that from stage 1 to stage 6 the prestress forces applied produce a positive moment in the pier segment. Alternatively stated, it can be said that at each stage, from 1 to 6, the positive moment increment induced in the pier segment by prestressing is greater than the negative moment increment induced by the dead load of the added segment. Table 4.2 indicates that from stage 6 to stage 9 the prestress force is reduced; thus at stages 7, 8, and 9 the additional increment of dead load moment is not

completely balanced. This fact is illustrated in Fig. 4.29. Since strain compatibility between the concrete and tendon B6 exists at stages 7, 8, and 9, it is obvious that the tensile strain in tendon B6 at the support segment must increase. Although tendon stresses have been increased to values slightly over the $0.60f'_s$ assumed, the excess is for all practical purposes negligible in view of creep losses. It is also evident that tendon force changes are insufficient to warrant a revision of equivalent joint loads contributed by tendon B6. Tendon B6 was selected as a typical example; however, from a limited study of tendon stress changes occurring during erection, it was found that the conclusions noted above are generally applicable for this structure.

The A and B series tendons each have characteristic tendon profiles. Furthermore, the profiles of all tendons within each series are similar. Thus, it is possible to evaluate the effectiveness of the suggested stressing procedure (a single overtensioning to $0.75f'_s$ and release back to $0.60f'_s$) by observing a single tendon from each series. It may be seen from Figs. 4.29 and 4.30 that the proposed stressing procedure results in effective prestress force of approximately $0.60f'_s$ over the entire tendon length. The distribution of prestress over the tendon length is considered satisfactory.

4.4.4 Summary. The application of SIMPLA2 to a practical example of a segmentally constructed box girder has been demonstrated. The analysis has furnished displacement diagrams which provide an insight into the structural behavior during erection. These diagrams illustrate that the design is well-balanced. Stress envelopes, readily obtainable from the computer output, show that throughout erection compressive stresses are quite conservative. Small tensile stresses are observed during the early stages of erection and appropriate temporary stressing should be used to control them, since the epoxy can take no tension at early ages. It is seen that in order to construct web shear force diagrams the effect of prestressing tendons must be taken into consideration, but such consideration is easily accomplished using computed results. For this structure, tendon stress changes due to stage erection are shown to be insignificant.

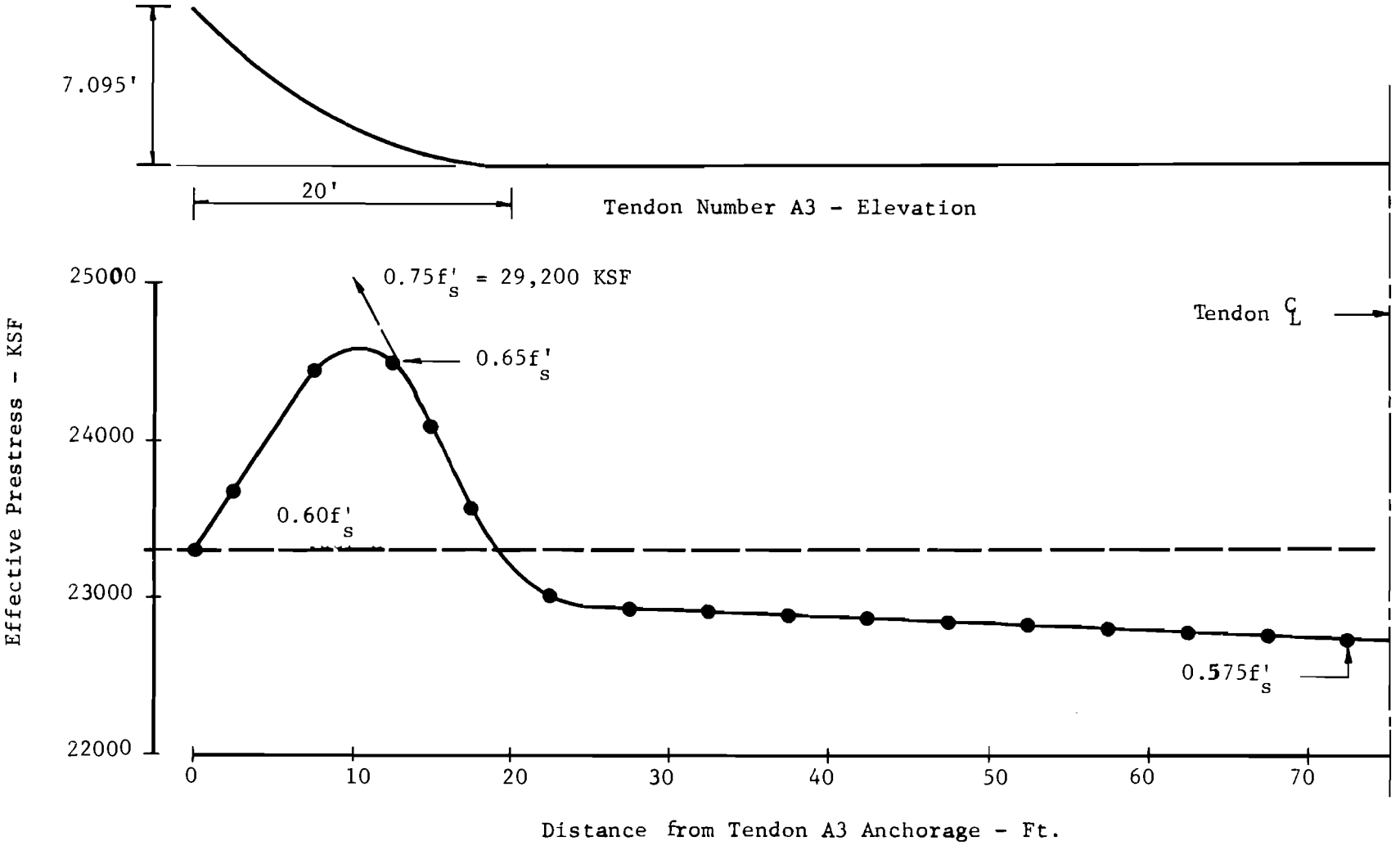

Fig. 4.30. Tendon stress variation in typical A series tendon.

The accuracy of SIMPLA2 has been further verified by comparison with detailed measurements made in tests of a realistic one-sixth scale structural model of the Corpus Christi bridge. The comparison will be presented in a subsequent report in this series. However, the comparison is generally quite favorable, showing the general applicability of SIMPLA2.

In order to judge the time and cost requirements of running SIMPLA2 for a practical case, the following times are of interest. A complete analysis run for the input data of Appendix C.4 for Example 3, using the CDC 6600 version and a FORTRAN program deck, used 108 seconds of central processor time and 318 seconds of peripheral processor time.

CHAPTER 5

SUMMARY, CONCLUSIONS, AND RECOMMENDATIONS

5.1 Summary of the Investigation

The objective of this research was to develop a mathematical model and an associated computer program for the analysis of segmentally constructed, prestressed box girders. The scope of this investigation was limited to the analytical consideration of constant depth, elastic, longitudinally prismatic plate assemblages such as box girders or folded plates.

From a number of available plate analysis models, the finite segment technique was deemed most appropriate for adaptation. Development of the segment progression computational technique was presented in Chapter 2. Chapter 3 derives the equations by which equivalent prestress forces are computed, and introduces the concepts used to model segmental erection and closure. The limitations of SIMPLA2 are enumerated.

In order to demonstrate the practical application, accuracy, and capabilities of SIMPLA2, three numerical examples are considered in Chapter 4. The example problems are solved and the results presented graphically.

5.2 Conclusions

5.2.1 General Conclusions. The main conclusion of this research is that SIMPLA2 is a useful tool for the analysis of segmentally erected, prestressed box girders. The program allows the designer to automatically model the erection of the structure, within the computer, in the same manner as he envisages the field erection. The results show the structural response of each step of the proposed erection sequence. SIMPLA2 can be utilized for the analysis of elastic, prismatic folded plate structures of arbitrary open or closed cross section. The program is applicable to

general conditions of loading and restraint, including diaphragms and elastic restraints. A wide variety of prestressing tendon profiles and stressing options may be considered.

The Texas Highway Department made use of SIMPLA2 during the design of the Intracoastal Canal Bridge at Corpus Christi, Texas, which was the first segmentally erected precast box girder bridge constructed in the United States. The program was used to check the final design at all stages of erection, including each step of the closure sequence, and to rapidly assess the feasibility of tendon layout changes suggested by the subcontractor.

5.2.2 Specific Conclusions. Example Problem 2 was solved by both the SIMPLA2 analysis and the more accurate folded plate (elasticity) method. A comparison of results indicates that the composite mathematical model employed in the development of SIMPLA2 adequately predicts the response of segmentally constructed, prestressed box girders.

Computed local stress inconsistencies are typical of finite element displacement formulations. The stress inconsistencies observed are insignificant, except in the vicinity of an anchorage. Large stress inconsistencies are observed at the flange web juncture in the vicinity of an anchorage and dissipate rapidly away from the anchorage. Within the anchorage zone an average of the inconsistent stress values provides satisfactory stress values for the flange web juncture. In cases where the juncture connects more than one flange element to a prestressed web element a weighted average was more appropriate.

Example Problem 3 demonstrated that the SIMPLA2 analysis can be applied to practical problems and showed the value of the technique as a design aid. The B series tendons were designed to balance approximately 60 percent of the dead load when the full cantilever condition is reached. With this percentage of dead load balanced, there is an adequate end reaction (51.6 kips) at completion of closure and the elevation of the end may be adjusted to zero without excessive jacking (final reaction of 64.64 kips is required). With 60 percent of dead load balanced, the

vertical displacement at the tip of the main span cantilever arm was less than 1 in. This amount of deflection presents no problems during the closure sequence. Utilizing this design criterion also satisfies working stress criteria except during the first three stages of erection when small tensile stresses are induced in the bottom flange. These tensile stresses can be easily controlled by temporary prestressing. Therefore, the design criteria requiring that approximately 60 percent of the dead load be balanced are satisfactory for this design and may be adopted for preliminary designs of similar girders.

In this example there were no load components to produce torsional deformations (with accompanying nonuniformity of longitudinal normal stresses). Moreover, since the design is well-balanced, a major portion of the stress at the pier section is due to axial load which is distributed along the span of the cantilever arm; hence the effects of shear lag are minimal. It can be concluded that under these circumstances a simplified longitudinal flexural analysis treating the girder as a beam will provide results adequate for design purposes. In cases where this simplification is applicable, it remains necessary to carefully evaluate equivalent prestress loads, since the characteristic tendon profile and high prestress forces induce high shear forces.

The results of this example also illustrate that effective prestress in a given tendon may be increased or decreased as a result of the stages of erection following the placement of the tendon. It is concluded that as a result of the stressing sequence employed for this design variations in tendon stresses from initial values are negligible for practical purposes. It can also be concluded that, unless the friction and wobble coefficients employed for this problem are seriously underestimated, a single overstress to $0.75f'_s$ and release back to $0.60f'_s$ will produce a satisfactory distribution of prestress force along the tendon.

5.3 Recommendations

5.3.1 Use of SIMPLA2. There is a definite disadvantage accompanying the neatly printed, well-organized, printout from a "canned"

computer program. All too frequently users are lulled by its official appearance into accepting whatever is printed on the paper as unquestionable fact. The strongest recommendation the authors can make to a potential SIMPLA2 user is to avoid this pitfall by using engineering judgment to constantly ensure that the computed results appear reasonable. The user is advised to carefully scrutinize the echo print of the input data to ensure that the input modeled what is intended. In order to minimize input errors, a carefully prepared sketch depicting what is to occur at each stage of erection is indispensable. In order to properly interpret the computed results, the user is urged to become familiar with all the assumptions upon which the analysis is based.

In some cases the box girder will respond essentially as a conventional beam; however, it is frequently difficult to recognize these cases. In such cases shear lag and cross-sectional distortion can justifiably be neglected and the longitudinal and transverse analysis conducted separately. However, the equivalent prestress forces represent a significant portion of the total load during erection. Moreover, web shears resulting from the vertical components of anchorage forces are quite large. These considerations demand that even in cases where the girder may be treated as a beam in the longitudinal direction, an accurate representation of the tendon profile and evaluation of equivalent prestress forces is still necessary. SIMPLA2 can be used effectively for such problems by use of an equivalent, one or two element cross-sectional idealization (rectangular beam or T-beam). This approach allows analysis of the longitudinal structural response, and an accurate automatic evaluation of equivalent prestress forces. Use of a simple cross-sectional representation allows a saving of computational effort. This technique will be of value when SIMPLA2 is used as a design aid.

Equivalent prestress forces are a function of the tendon profile. Therefore, the accuracy of the computed equivalent prestress forces depends largely upon how well the polynomial expression, generated from input control coordinates, represents the actual tendon profile. The user is advised to select and specify the tendon profile control coordinates with care.

5.3.2 Improvements to SIMPLA2. Unfortunately, hindsight is generally much better than foresight; this research is not an exception and experience suggests the following modifications to SIMPLA2. In order to obtain the analysis for a particular stage it is now necessary to first perform the analyses for all previous stages. By making several rather simple changes, this inefficiency could be eliminated. By including an additional branch within the driver program, it would be possible to have the program compute and compile equivalent prestress force vector contributions from any particular stage(or any number of stages) without going through the complete solution for each stage. This added flexibility could significantly reduce the execution times required for large problems at the expense of having a solution for every stage.

The segment progression procedure can be described as the numerical solution of a boundary value problem. The equations relating the actions at the ends of the structure are derived from the known origin boundary actions, unit values of the unknown boundary actions, and the applied loading. Due to the nature of the problem, the known boundary actions and the loading applied between two given stations may change from stage to stage. It is necessary, therefore, to rederive the relationship between the state vectors at the two stations for each stage of erection. The authors suggest an approach whereby the relationship between end actions is derived by assuming unit values for all boundary actions and applied loads. Utilizing this approach, the equation relating the actions between two stations would remain constant for every stage of construction; therefore, the segment progression would have to be performed only over those segments added at each stage. The solution would then be obtained by substituting the actual boundary conditions and loads into the equation.

5.3.3 Research Needs. The program developed herein is applicable to prismatic, constant depth, structures. In practice, however, constant depth box girders are not economically feasible for spans greater than approximately 250 to 300 ft. Moreover, bridge superstructures which are skewed with respect to their supports or curved in plan, or both, are not

at all uncommon. SIMPLA2 is applicable to neither curved nor skewed bridges. There is, therefore, an obvious need for additional research, both analytical and experimental, to study curved, skewed, and haunched segmentally constructed, prestressed box girders. Lo[8] suggests that the finite segment technique may provide a logical approach to the analysis of haunched structures. Variations of the traditional finite element method have been employed recently for analysis of curved and skewed box girders. Adapting one of these techniques for the basic analysis and an approach such as the one reported herein to model prestressing forces and segmental erection is a possible approach to mathematical analysis. Regardless of the scheme followed, experimental results with which to check the applicability of, and to inspire confidence in, the analytical technique is highly desirable.

5.4 Concluding Remarks

It should be recognized that the three examples reported do not fully demonstrate the versatility of the SIMPLA2 program. The examples presented are limited to simple loading, boundary, and support conditions in order to demonstrate the application of the program without unnecessary complications. The program was developed for analysis during erection; however, it is equally applicable for analysis of the completed structure under service loads. The work reported herein dealt primarily with cantilevered construction. However, the program is applicable to general support and boundary conditions; therefore, it may also be applied to girders being constructed on falsework. SIMPLA2 may be applied to a problem as simple as a simply supported prestressed beam, or as complex as an indeterminate, stage erected, prestressed folded plate subject to general conditions of loading and restraint. As with other analytical techniques, the range of problems to which SIMPLA2 can be applied depends partially upon the user's familiarity with the technique and his ingenuity.

R E F E R E N C E S

1. ACI Committee 318, Building Code Requirements for Reinforced Concrete (ACI 318-63), American Concrete Institute, Detroit, Michigan, 1963.

2. Structures Precontraintes, V Congres de la Federation Internationale de la Precontrainte, Paris, June 1966.

3. Abdel-Samad, S. R., Wright, R. N., and Robinson, A. R., "Analysis of Box Girders with Diaphragms," Journal of the Structural Division, ASCE, Vol. 94, ST10, Proc. Paper 6153, October 1968.

4. Atkins, W. D., "A Generalized Numerical Solution for Prestressed Concrete Beams," unpublished Master's thesis, The University of Texas at Austin, August 1965.

5. Denison, C., and Wedgwood, R. J. L., "Need for Diaphragms in Concrete Box Girders," Journal of the Structural Division, ASCE, Vol. 97, ST3, Proc. Paper 7965, March 1971.

6. Lacey, G. C., "The Design and Optimization of Long Span, Segmentally Precast, Box Girder Bridges," unpublished Ph.D. dissertation, The University of Texas at Austin, December 1970.

7. Lacey, G. C., Breen, J. E., and Burns, N. H., "Long Span Prestressed Concrete Bridges of Segmental Construction--State-of-the-Art," Journal of the Prestressed Concrete Institute, Vol. 16, No. 5, October 1971.

8. Lo, K. S., "Analysis of Cellular Folded Plate Structures," unpublished Ph.D. thesis, Division of Structural Engineering and Structural Mechanics, University of California at Berkeley, January 1967.

9. Lo, K. S., and Scordelis, A. C., "Finite Segment Analysis of Folded Plates," Journal of the Structural Division, ASCE, Vol. 95, ST5, Proc. Paper 6544, May 1969.

10. Malcolm, D. J., and Redwood, R. G., "Shear Lag in Stiffened Box Girders," Journal of the Structural Division, ASCE, Vol. 96, ST7, Proc. Paper 7409, July 1970.

11. Mattock, A. H., and Johnston, S. B., "Behavior under Load of Composite Box Girder Bridges," Journal of the Structural Division, ASCE, Vol. 94, ST10, Proc. Paper 6168, October 1968.

12. Mehrotra, B. L., Mufti, A. A., and Redwood, R. G., "Analysis of Three-Dimensional Thin-Walled Structures," Journal of the Structural Division, ASCE, Vol. 95, ST12, Proc. Paper 6966, December 1969.

13. Meyer, C., and Scordelis, A. C., "Computer Program for Prismatic Folded Plates with Plate and Beam Elements," Report No. SESM 70-3, Department of Civil Engineering, University of California, Berkeley, February 1970.

14. Muller, J., "Long Span Precast Prestressed Concrete Bridges Built in Cantilever," First International Symposium on Concrete Bridge Design, ACI Special Publication No. 23, American Concrete Institute, Detroit, Michigan, 1969.

15. Myers, D. E., and Cooper, P. N., "Box Girder Model Studies," Journal of the Structural Division, ASCE, Vol. 95, ST12, Proc. Paper 6966, December 1969.

16. Pierce, D. M., "A Numerical Method of Analyzing Prestressed Concrete Members Containing Unbonded Tendons," unpublished Ph.D. dissertation, The University of Texas at Austin, June 1968.

17. Reissner, E., and Hildehand, F. B., "Least Work Analysis of the Problem of Shear Lag in Box Beams," NACA Technical Note, U. 629, No. 893, May 1943.

18. Scordelis, A. C., "Analysis of Simply-Supported Box Girder Bridges," SESM 66-17, Department of Civil Engineering, University of California, Berkeley, October 1966.

19. Scordelis, A. C., "Analysis of Continuous Box Girder Bridges," SESM 67-25, Department of Civil Engineering, University of California, Berkeley, November 1967.

20. Scordelis, A. C., and Meyer, C., "Wheel Load Distribution in Concrete Box Girder Bridges," SESM 69-1, Department of Civil Engineering, University of California, Berkeley, January 1969.

21. Tung, D. H. H., "Torsional Analysis of Single Thin-Walled Trapezoidal Concrete Box Girder Bridges," First International Symposium on Concrete Bridge Design, ACI Special Publication No. 23, American Concrete Institute, Detroit, 1969.

22. Winter, G., "Stress Distribution in and Equivalent Width of Flange of Wide, Thin-Walled Steel Beams," Technical Note 784, National Advisory Committee for Aeronautics, 1940.

23. Wright, R. N., Abdel-Samad, S. R., and Robinson, A. R., "BEF Analogy of Analysis of Box Girders," Journal of the Structural Division, ASCE, Vol. 94, ST4, Proc. Paper 5394, August 1967.

24. ASCE-AASHO Task Committee on Flexural Members, Subcommittee on Box Girders, "Progress Report on Steel Box Girder Bridges, Journal of Structural Division, ASCE, Vol. 97, ST4, April 1971.

25. Task Committee on Folded Plate Construction, "Phase I Report on Folded Plate Construction," Journal of the Structural Division, ASCE, Vol. 89, ST6, Proc. Paper 3741, December 1963.

26. Leonhardt, F., Prestressed Concrete Design and Construction, Second Edition, Wilhelm Ernest and Sohn, Munich, Germany, 1964.

27. Lin, T. Y., Design of Prestressed Concrete Structures, Second Edition, John Wiley and Sons, Inc., New York, 1967.

28. Pestel, E. C., and Leckie, F. A., Matrix Methods in Elastomechanics, McGraw-Hill Book Company, Inc., New York, 1963.

29. Zienkiewicz, O. C., The Finite Element Method in Structural and Continuum Mechanics, McGraw-Hill Publishing Company, Ltd., London, 1967.

30. Lacey, G. C., and Breen, J. E., "Long Span Prestressed Concrete Bridges of Segmental Construction--State-of-the-Art," Center for Highway Research Report 121-1, The University of Texas at Austin, May 1969.

31. Lacey, G. C., and Breen, J. E., "The Design and Optimization of Long Span Segmentally Precast, Box Girder Bridges," Center for Highway Research Report 121-3, The University of Texas at Austin, November 1974.

32. Brown, Robert C., Jr., "Computer Analysis of Segmentally Constructed Prestressed Box Girders," unpublished Ph.D. dissertation, The University of Texas at Austin, June 1972.

33. Kashima, Satoshi, "Construction and Load Tests of a Segmental Precast Box Girder Bridge Model," unpublished Ph.D. dissertation, January 1974.

A P P E N D I X A

NOTATION

A	Cross-sectional area of element
A_s	Cross-sectional area of steel reinforcement.
b	Element thickness.
$\underset{\sim}{d}$	Displacement subvector of the state vector.
$\underset{\sim}{d}_K^{\ell}$	Displacement subvector of the element state vector just to the left of station K.
$\underset{\sim}{d}_K^{r}$	Displacement subvector of the element state vector just right of station K.
d	Element depth.
E_s	Modulus of elasticity of tendon steel.
e	The subscript indicates that the subscripted quantity is referred to the end station.
F	Effective prestress force.
FV	Vertical component of the effective prestress force F.
G	Shear modulus of element.
I	Moment of inertia of the element = $bd^3/12$.
I_s	Moment of inertia of slab strip of unit width = $d^3/12$.
L	Segment (element) length.
$\bar{L}$	One-half segment (element) length = 1/2 L.
$\underset{\sim}{M}$	Component of the fixed element edge force vector, $\underset{\sim}{S}_m$, due to the known origin boundary actions and the applied joint actions.
$\bar{M}$	Longitudinal bending moment component of the anchorage force vector, $\underset{\sim}{\bar{P}}$.
M_G	Gravity load moment.
M_S	Secondary moment induced by prestressing a continuous beam.
M_{K+1}	Longitudinal bending moment component of the element state vector at station K+1, $\underset{\sim}{Z}_{K+1}$.
M_i	Transverse bending moment component of the element edge force vector, $\underset{\sim}{S}$, at the element I edge. A corresponding moment component is defined at the element J edge. The components of $\underset{\sim}{S}$ are assumed to be uniformly distributed over the element edge.
$\bar{N}$	Axial force component of the anchorage force vector, $\underset{\sim}{\bar{P}}$.
N_{K+1}	Axial force component of the element state vector, $\underset{\sim}{Z}_{K+1}$.
o	This subscript is used to denote quantities associated with the origin boundary of the structure.
$\underset{\sim}{\bar{P}}$	The anchorage force vector.

P'	Symmetrical transverse membrane edge force component of the generalized element edge force vector, $\underset{\sim}{Q}$.
P''	Antisymmetrical transverse membrane edge force component of the generalized element edge force vector, $\underset{\sim}{Q}$.
P_i	Force component of the element edge force vector, $\underset{\sim}{S}$, associated with transverse extension of the element. A corresponding force component is defined at the element J edge. The components of $\underset{\sim}{S}$ are assumed to be uniformly distributed over the element edge.
$\underset{\sim}{\bar{P}}_e$	Anchorage force vector at the end station.
$\underset{\sim}{\bar{P}}_o$	Anchorage force vector at the origin station.
$\underset{\sim}{PJP}(K)$	The equivalent joint load vector exerted on segment K due to prestressing. These equivalent joint loads result from curvature of the tendon profile.
[PJP]	An array of equivalent joint load vectors, $\underset{\sim}{PJP}$.
PV	The equivalent vertical tendon pressure, uniformly distributed between two stations of the structure, applied at the element I edge.
p	Radial force per unit length, due to prestressing, acting at the interface of the tendon and the structure.
$\underset{\sim}{p}_K^{\ell}$	The force subvector of the element state vector just to the left of the anchorage station K.
$\underset{\sim}{p}_K^{r}$	The force subvector of the element state vector just to the right of the anchorage station K.
$\underset{\sim}{Q}$	The generalized element edge force vector.
$\bar{Q}$	Shear force component of the anchorage force vector, $\underset{\sim}{\bar{P}}$.
Q_{K+1}	Shear force component of the element state vector, $\underset{\sim}{Z}$.
q	The number of elements in the cross section.
R	Radius of curvature of the tendon profile.
$\underset{\sim}{R}_P$	The equivalent joint load vector, due to prestressing, for a complete finite segment.
$\underset{\sim}{R}_{pi}$	The equivalent joint load vector, due to prestressing for joint i.
$\underset{\sim}{r}$	The joint displacement vector for a complete finite segment. The components of $\underset{\sim}{r}$ occur at the element edge nodal points.
$\underset{\sim}{r}_i$	The joint displacement vector for a typical joint, i.
r_{hi}	The horizontal component of $\underset{\sim}{r}_i$. Similar displacement components in the vertical, longitudinal, and rotational directions are defined at joint i.
$\underset{\sim}{S}$	The element edge force vector referred to the element relative coordinate system.
$\underset{\sim}{S}_m$	A subvector of $\underset{\sim}{S}$ containing the element edge forces associated with membrane behavior of the element.

$\underset{\sim}{S}_s$ A subvector of $\underset{\sim}{S}$ containing the element edge forces associated with one-way slab behavior of the element.

$S_t(K)$ Tendon stress at nodal point K.

$\underset{\sim}{\bar{S}}$ The element edge force vector referred to the global coordinate system.

$\bar{S}_{hi}$ The horizontal component of $\underset{\sim}{\bar{S}}_i$. Similar force components in the vertical, longitudinal, and rotational directions are defined at joint i.

$\underset{\sim}{\bar{S}}_i$ A subvector of $\underset{\sim}{\bar{S}}$ containing the element edge force components at the element I edge. A corresponding subvector $\underset{\sim}{\bar{S}}_j$ is defined at the element J edge.

s Tendon length.

T' Symmetrical membrane element edge shear force component of the generalized edge force vector, $\underset{\sim}{Q}$.

T'' Antisymmetrical membrane element edge shear force component of the generalized edge force vector, $\underset{\sim}{Q}$.

T_i Membrane element edge shear force component of the element edge force vector, $\underset{\sim}{S}$. The force components of $\underset{\sim}{S}$ are assumed to be uniformly distributed over the length of a segment. A corresponding force component is defined at the element J edge.

$\underset{\sim}{u}$ The element edge nodal point displacement vector referred to the element relative coordinate system. The components of $\underset{\sim}{u}$ occur at the longitudinal center of the element edge.

$\bar{u}$ The longitudinal displacement component of the generalized element displacement vector $\underset{\sim}{\bar{u}}$. This displacement component is associated with the T' force component of the generalized element edge force vector $\underset{\sim}{Q}$.

$\underset{\sim}{\bar{u}}$ The element edge nodal point displacement vector referred to the gloval coordinate system. The components of $\underset{\sim}{\bar{u}}$ occur at the longitudinal center of the element stage.

u_i The element edge nodal point longitudinal displacement component of $\underset{\sim}{u}$ at the element I edge. A corresponding longitudinal displacement component is defined at the element J edge.

$\underset{\sim}{\bar{u}}_i$ A subvector of $\underset{\sim}{\bar{u}}$ containing the components of $\underset{\sim}{\bar{u}}$ occurring at the element I edge. A similar subvector is defined at the element J edge.

u_{K+1} The longitudinal displacement component of the element state vector of station K+1.

$\bar{u}_{hi}$ The horizontal displacement component of $\underset{\sim}{\bar{u}}_i$. Similar displacement components in the vertical, longitudinal, and rotational directions are defined at the element I edge

$\underset{\sim}{u}_m$ A subvector of $\underset{\sim}{u}$ containing the element edge nodal point displacement components associated with membrane behavior of the element.

$\underset{\sim}{u}_s$ A subvector of $\underset{\sim}{u}$ containing the element edge nodal point displacement components associated with one-way slab bending of the element.

V_i Element I edge normal shear force per unit length referred to the element relative coordinate system. A corresponding force component is defined at the element J edge.

v Vertical projection of the element depth, d. This is a signed variable.

v' Transverse extension displacement component of the generalized element displacement vector, Φ. This displacement component is associated with the P' force component of the generalized element edge force vector, $\underset{\sim}{Q}$.

$\bar{v}$ Vertical displacement component of the generalized element displacement vector, Φ. This displacement component is associated with the T'' P'' force components of the generalized element edge force vector, $\underset{\sim}{Q}$.

v_i Transverse extension displacement component of u at element I edge. A corresponding displacement component is defined at the element J edge.

v_{K+1} Shear displacement component of the element state vector at station K+1.

w_i Normal shear displacement component of the element edge nodal point displacement vector, $\underset{\sim}{u}$.

x Longitudinal distance measurement along the span of the structure. The x origin is located at the origin station of the structure.

Y The y coordinate of the tendon profile at any location, x, along the girder. Y is measured in the plane of the element containing the tendon.

y The element transverse coordinate. The y origin is located at the transverse center of the element.

$\underset{\sim}{Z}_K$ The complete station state vector at station K.

$\underset{\sim}{Z}_o$ The complete station state vector at the origin station. This vector is expressed as the sum of two components; the unknown components of the origin state vector $[L]\underset{\sim}{Z}_{ou}$, and the known components of the origin state vector, $\underset{\sim}{Z}_{ok}$

$\underset{\sim}{Z}_{ok}$ The known components of the origin state vector.

$\underset{\sim}{Z}_{ou}$ The unknown components of the origin state vector.

$\underset{\sim}{Z}_e$ The complete station state vector at the end station of the structure.

$\underset{\sim}{z}_K$ The element state vector at station K.

$\epsilon_L(K)$ The longitudinal normal strain in the structure at the location of the Kth tendon nodal point. The subscript L denotes that this strain value corresponds to a stage after the particular tendon has been stressed.

$\epsilon_o(K)$ The longitudinal normal strain in the structure at the location of the Kth tendon nodal point. The subscript o denotes that this strain value corresponds to the stage at which the particular tendon is stressed.

$\epsilon_{si}(K)$ The initial strain in the tendon at the Kth tendon nodal point.

θ Tendon profile slope at any point along the profile.

θ_i Element edge transverse bending displacement component of the element edge nodal point displacement vector, $\underset{\sim}{u}$, at the element I edge. A corresponding displacement component is defined at the element J edge.

λ Wobble coefficient.

μ Friction coefficient.

$\underset{\sim}{\Phi}$ Generalized element displacement vector.

$\underset{\sim}{\Phi}'$ Generalized element displacement vector ignoring the transverse extension displacement component of the element.

ω Longitudinal rotation component of the element state vector.

A P P E N D I X B

PROGRAM SIMPLA2

B.1 General

B.2 Guide to Input Data

B.3 Flow of Input Data

B.4 Computer Output

B.5 SIMPLA2 Flow Charts

B.6 Listing of SIMPLA2

B.1 - General

Identification

The computer program discussed within this appendix, entitled SIMPLA2, is written in the FORTRAN IV computer language with versions for use on the CDC 6600 computer and the IBM System 360 computer.

Application

The primary objective of the program is the structural analysis of segmentally constructed, post-tensioned, box girder bridges at each stage of construction. The generality of the program gives applicability to numerous other problems involving prestressed box girders and folded plates.

Coordinate Systems and Sign Convention

All joint actions are input and output referenced to the fixed coordinate system. Positive action directions are common for all joints (Fig. B.2). Internal beam-type and element edge actions, and boundary conditions at both ends of the structure, are input and output referenced to the element relative coordinate system (Figs. B.3 and B.4).

B.2 - Guide to Input Data

The program data are input by means of data cards. Each individual stage of construction may not require all the data cards listed below. The user supplies only those cards required for the particular stage. Extra data cards will result in erroneous execution. The order of data specified here must be strictly adhered to and consistent units must be used throughout. An asterisk indicates further comments are to be found in the "Remarks" concerning the particular card.

1. TITLE CARD - (12A6)

   Column 1-72 - TITLE (12), title of the problem. Any FORTRAN characters are acceptable.

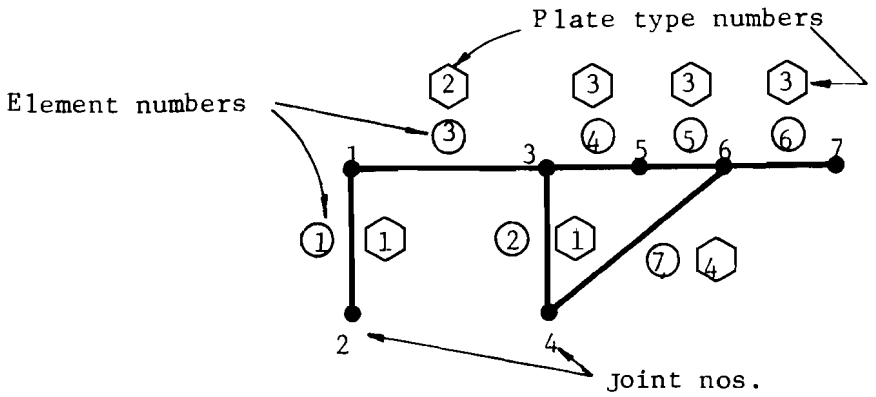

Fig. B.1. Cross section idealization showing plate type, element, and joint numbers--section taken looking toward origin (from Ref. 19).

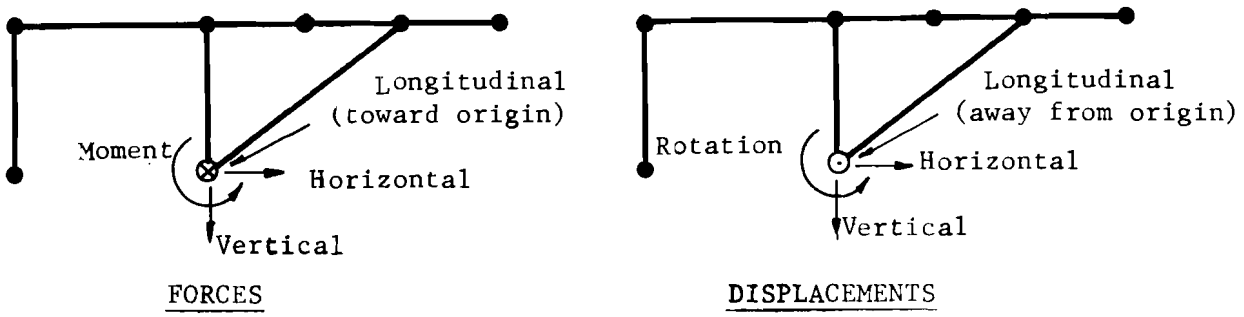

Fig. B.2. Positive joint actions (from Ref. 19).

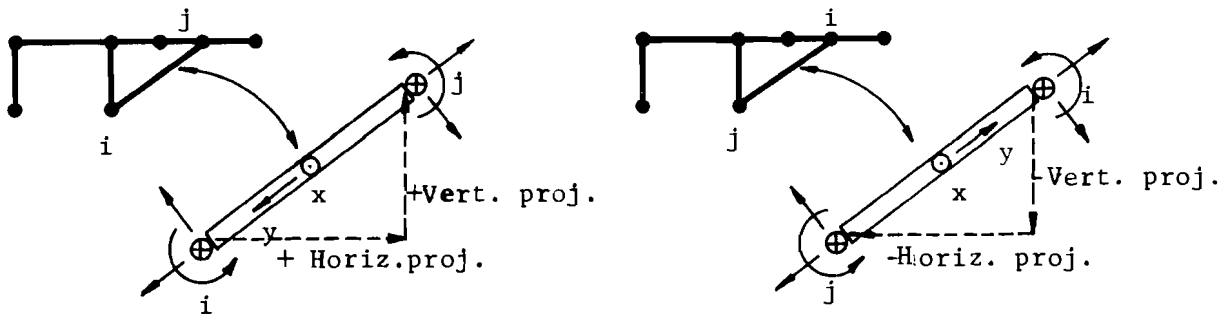

Fig. B.3. Sign convention for element projections, positive direction of element coordinate axes and edge forces (from Ref. 19).

2. CROSS SECTION CONTROL DATA - (3I4)

Column 1-4 - NPL, number of plate types in the cross section. (Maximum 15)

Column 5-8 - NEL, number of elements in the cross section. (Maximum 15)

Column 9-12 - NJT, number of joints in the cross section. (Maximum 16)

*3. PLATE TYPE DATA - (I10, 4F10.0)

Column 1-10 - I, plate type number.

Column 11-20 - H(I), horizontal projection of plate Type I.

Column 21-30 - V(I), vertical projection of plate Type I.

Column 31-40 - TH(I), thickness of plate Type I.

Column 41-50 - E(I), elastic modulus of plate Type I.

Remarks - Card 3

1. The horizontal and vertical plate projections must be input with the proper sign. See Fig. B.3 for sign convention.
2. A separate card is prepared for each of the plate types and arranged to read sequentially from plate Type 1 to plate Type NPL.

*4. ELEMENT DATA - (4I4)

Column 1-4 - I, element number.

Column 4-8 - NPI(I), joint number at element I-edge.

Column 9-12 - NPJ(I), joint number at element J-edge.

Column 13-16 - KPL(I), plate type number of plate type describing element I.

Remarks - Card 4

1. A separate card is prepared for each element and arranged to read sequentially from element 1 to element NEL.

5. TENDON DATA - (10X, 3(F10.0))

Column 11-20 - CFC, friction coefficient, μ.

Column 21-30 - CLC, wobble coefficient, λ.

Column 31-40 - YMS, elastic modulus of tendons.

*6(A) STAGE CONTROL DATA - First Stage - (4I4)

Column 1-4 - NNSG(1), total number of segments in first stage structure.

Column 5-8 - NCBA(1), number of tendons stressed at first stage (may not be zero).

Column 9-12 - NXTL(1), left terminal station for tendons stressed at first stage.

Column 13-16 - NXTR(1), right terminal station for tendons stressed at first stage.

*6(B) STAGE CODE WORDS - First Stage - (2I4)

Column 1-4 - KREF, reference stage code word.

Column 5-8 - KODTS, tendon stress check code word.

Remarks - Cards 6(A) and 6(B)

1. Cards 6 follow Card 5 for the initial stage of construction.
2. KREF is an index indicating whether the stage is a stage of the cantilevering sequence or of the closure sequence. KREF = 0: This stage is a typical stage of the cantilevering sequence. KREF = 1: This stage is either the last stage of the cantilevering sequence (the reference stage) or a typical stage of the closure sequence.
3. KODTS is an index indicating whether tendon stresses are to be checked at this stage.
   KODTS = 0: Skip check of tendon stresses.
   KODTS = 1: Check tendon stresses for all tendons stressed at previous stages.
4. For the initial stage of construction, Cards 7 are omitted and the data deck goes directly from Cards 6 to Cards 8.

*7(A) STAGE CONTROL DATA - Typical Stage - (6I4)

Column 1-4 - NSTG, number of the construction stage. Stages must be numbered in consecutive order.

Column 5-8 - NSAL(NSTG), the number of segments by which the structure has been extended to the left.

Column 9-12 - NR, the number of segments by which the structure has been extended to the right.

Column 13-16 - NCBA(NSTG), the number of tendons stressed at this stage.

Column 17-20 - NXTL(NSTG), left terminal station for tendons stressed at this stage.

Column 21-24 - NXTR(NSTG), right terminal station for tendons stressed at this stage.

*7(B) STAGE CODE WORDS - Typical Stage - (5I4)

Column 1-4 - KODJA, joint actions code word.

Column 5-8 - KODBC, boundary conditions code word.

Column 9-12 - KODSPT, interior support restraint conditions code word.

Column 13-16 - KREF, reference stage code word.

Column 17-20 - KODTS, tendon stress check code word.

Remarks - Cards 7(A) and 7(B)

1. KODJA indicates if prescribed joint actions for any segment have changed (magnitude or location) from those prescribed for the last stage.
   KODJA = 0: All joint actions for every segment prescribed for the last stage remain the same; only INITIAL SEGMENT ACTIONS CARDS, 12(A), are required for those new segments added.
   KODJA = 1: Some, or all, joint actions prescribed for the last stage are modified at this stage. Every segment of the structure requires a segment card, an INITIAL SEGMENT ACTIONS CARD, 12(A), for those segments added at this stage, and a MODIFIED SEGMENT ACTIONS CARD, 12(B), for the remaining segments.

2. KODBC indicates if boundary conditions at the origin and/or the end, for any element of the cross section, have changed from those specified for the last stage.
   KODBC = 0: Boundary conditions at both the origin and the end for all elements of the cross section are the same as those prescribed for the last stage. No BOUNDARY CONDITION CARDS are required.
   KODBC = 1: Boundary conditions at the origin or the end (or both) have been modified from those specified for the last stage. Both ORIGIN and END BOUNDARY CONDITION CARDS (11 and 15) are required in their proper place.

3. KODSPT indicates if some or all the interior support restraint conditions at any of the interior supports have been modified from those specified for the last stage.
   KODSPT = 0: Interior support restraints at all interior supports are unchanged from the last stage. INTERIOR SUPPORT/DIAPHRAGM RESTRAINT CARDS (14) are required only for those supports introduced at this stage.
   KODSPT = 1: Interior support restraints at some/all interior supports are modified from those specified for the last stage. INTERIOR SUPPORT/DIAPHRAGM RESTRAINT CARDS are required for all interior supports in the order in which the supports are encountered from the origin to the end of the structure following the proper segment actions and joint actions cards.

4. KREF is an index indicating whether the stage is a stage of the cantilevering sequence or of the closure sequence.
   KREF = 0: This stage is a typical stage of the cantilevering sequence.
   KREF = 1: This stage is either the last stage of the cantilevering sequence (the reference stage) or a typical stage of the closure sequence.

5. KODTS is an index indicating whether tendon stresses are to be checked at this stage.
   KODTS = 0: Skip check of tendon stresses.
   KODTS = 1: Check tendon stresses for all tendons stressed at previous stages.

*8. SEGMENT LENGTH CARD - (2I4, 2X, F10.0)

Column 1-4 - ISEC, station at which repeating segment length begins.

Column 5-8 - JSEC, station at which repeating segment length terminates.

Column 11-20 - SL, segment length of all segments between ISEC and JSEC.

Remarks - Card 8

1. Each consecutive group of repeating segment lengths requires a new card until JSEC equals the last station in the structure. These new cards are ordered as the segments are encountered from left to right.

2. With the exception of the first stage, these cards are provided only for those segments added in the order in which they are encountered from left to right.

*9(A) TENDON CONTROL DATA - (3I4, F8.0, 2F10.0, I5)

Column 1-4 - KN, tendon number. Tendons are numbered in consecutive ascending order.

Column 5-8 - NCV, number of distinct curves (straight lines or parabolas) in the tendon profile.

Column 9-12 - NELC (KN), element number of the element containing tendon KN.

Column 13-20 - AREA (KN), cross-sectional area of tendon KN.

Column 21-30 - PIP, temporary maximum jacking force. (See remark No. 1.)

Column 31-40 - PIPP, initial prestress force. (See remark No. 1.)

Column 41-45 - KEEP, live end index. (See remark No. 2.)

*9(B) TENDON OUT-OF-PLANE DATA - (F10.0, 2I5)

Column 1-10 - FO, maximum divergence from plane.

Column 11-15 - NXCVGL, left station number at which FO is achieved.

Column 16-20 - NXCVGR, right station number at which convergence into plane begins.

Remarks - Cards 9(A) and 9(B)

1. If the tendon is jacked directly to the initial prestress force (without being overtensioned and slackened) PIP must be specified as that force and PIPP must be specified as zero.
2. KEEP is an index indicating the live ends of the tendon.
   KEEP = -1: Tendon stressed on left end only.
   KEEP = 0: Tendon stressed from both ends simultaneously.
   KEEP = 1: Tendon stressed from right end only.
3. For stressing both PIP and PIPP are input as positive decimal numbers. Temporary tendons may be removed by using negative numbers.
4. If tendon lies in one plane, Card 9(B) is left blank but must be included.
5. Cards 9(A) and 9(B) for a given tendon are immediately followed by Card 10 for that tendon.

*10. TENDON PROFILE DATA - (I10, 3F10.0, I10, F10.0)

Column 1-10 - NXL, left terminal station for the curve.

Column 11-20 - YL, Y coordinate of tendon at NXL.

Column 21-30 - XM, X coordinate of interior point of the curve.

Column 31-40 - YM, Y coordinate of interior point.

Column 41-50 - NXR, right terminal station for the curve.

Column 51-60 - YR, Y coordinate of tendon at NXR.

Remarks - Card 10

1. Each curve in the tendon profile requires one Card 10. The cards must be in the order in which the curves appear in the tendon profile from left to right.
2. The tendon profile must be idealized as a series of distinct curves (straight lines or parabolas) with a continuous tangent slope.
3. For straight line curves the interior point fields (columns 21-40) must be left blank.
4. Y coordinates, YL, YM, and YR, are measured in the plate element (NELC (KN) coordinate system shown in Fig. 2.3. Note that the positive Y axis direction is toward the lower numbered (i) edge of the plate element.

5. For each tendon stressed in the stage, one Card 9(A) and 9(B) immediately followed by its required NCV Cards 10 are provided in sequence.

6. After all tendons are described, the structure must be described from left to right with origin, segment and joint actions, support, segment, and end cards arranged as they occur in the structure.

*11. ORIGIN BOUNDARY CONDITION CARDS - (I10, 3F10.0, 3I2)

Column 1-10 - I, element number.

Column 11-20 - BCORI (1,I), prescribed longitudinal force or displacement.

Column 21-30 - BCORI (2,I), prescribed transverse force or displacement.

Column 31-40 - BCORI (3,I), prescribed moment or rotation.

Column 41-42 - IORI (1,I), longitudinal force/displacement index.

Column 43-44 - IORI (2,I), transverse force/displacement index.

Column 45-46 - IORI (3,I), moment/rotation index.

Remarks - Card 11

1. Each element of the cross section requires one Card 11.

2. IORI (I,J) is an index indicating whether BCORI (I,J) is a force or displacement value.
   IORI (I,J) = 0: BCORI (I,J) is prescribed force.
   IORI (I,J) = 1: BCORI (I,J) is prescribed displacement.

*12(A) INITIAL SEGMENT ACTIONS CARD - (3I4)

Column 1-4 - NN, segment number.

Column 5-8 - IAJA, joint action index.

Column 9-12 - ISTOP (NN), stopover or interior support index.

*12(B) MODIFIED SEGMENT ACTIONS CARD - (2I4)

Column 1-4 - NN, revised segment number.

Column 5-8 - IAJA2, joint actions index.

Remarks - Cards 12(A) and 12(B)

1. For the initial stage, INITIAL SEGMENT ACTIONS CARDS, 12(A) are required for each of the initial segments.

2. If the joint actions applied at the previous stage are not to be modified at the present stage (KODJA = 0), only INITIAL SEGMENT ACTIONS CARDS, 12(A), for those segments added at the present stage are required.

3. If joint actions applied at the previous stage are to be modified at the present stage (KODJA = 1), all segments require a SEGMENT ACTIONS CARD. An INITIAL SEGMENT ACTIONS CARD, 12(A), is provided for those segments added at the present stage, and a MODIFIED SEGMENT ACTIONS CARD, 12(B), is provided for all remaining segments.

4. At each stage there are four possible situations with regard to specification of joint actions for each segment: (a) NSAL (NSTG) + NR = 0. KODJA = 0 indicates that no segments have been added to the structure at this stage, and all joint actions remain unchanged from the previous stage. No SEGMENT ACTIONS CARDS are required in this case. (b) NSAL (NSTG) + NR = 0. KODJA = 1 indicates that no segments have been added to the structure at this stage; however, some existing joint actions are to be changed. MODIFIED SEGMENT ACTION CARDS, 12(B), are required for all segments of the structure. (c) NSAL (NSTG) + NR $\neq$ 0. KODJA = 0 indicates that there have been segments added to the structure; however, joint actions specified for those segments which comprised the structure at the previous stage are not modified. INITIAL SEGMENT ACTIONS CARDS, 12(A), are required for those segments added only. (d) NSAL (NSTG) + NR $\neq$ 0. KODJA = 1 indicates that segments are added to the structure and joint actions applied to those segments comprising the structure at the previous stage are modified. INITIAL SEGMENT ACTIONS CARDS, 12(A), are required for those segments added and MODIFIED SEGMENT ACTIONS CARDS, 12(B), are required for all remaining segments. In any case, all SEGMENT ACTIONS CARDS must be arranged in the order in which segments are encountered from the origin to the end.

5. IAJA is an index for repeating joint actions from Segment NN-1 to Segment NN.
   IAJA = 0: Joint actions applied to Segment NN are the same as those applied to NN-1. No JOINT ACTIONS CARDS are required for this segment.
   IAJA = 1: Joint actions applied to Segment NN are to be specified. JOINT ACTIONS CARDS (13) must follow this card.

6. ISTOP (NN) is an index indicating whether a stopover or interior support follows Segment NN. However, if NN is the last segment of a stage, the index indicates an END BOUNDARY CONDITIONS CARD (15) is required.
   ISTOP (NN) = -1: An interior support occurs at Station NN+1. An INTERIOR SUPPORT/DIAPHRAGM RESTRAINT CONDITION CARD (14) must follow either this INITIAL SEGMENT ACTIONS CARD or the INITIAL SEGMENT ACTIONS CARD and its JOINT ACTIONS CARDS, except when NN is the last segment.
   ISTOP (NN) = 0: Neither an interior support nor a stopover occurs at Station NN+1.
   ISTOP (NN) = 1: A stopover occurs at Station NN+1.

7. The stopover status for each station is specified only on the INITIAL SEGMENT ACTIONS CARD. There is no provision for revising the value of ISTOP initially assigned to a particular station. Therefore, if Station NN+1 is to be supported at some stage of construction after the stage at which it is introduced, it is necessary to specify a fictitious support at Station NN+1 initially, and specify a change in support restraint conditions (KODSPT) at the appropriate stage. If a boundary condition at one stage is to become an interior support at the following stage as illustrated below,

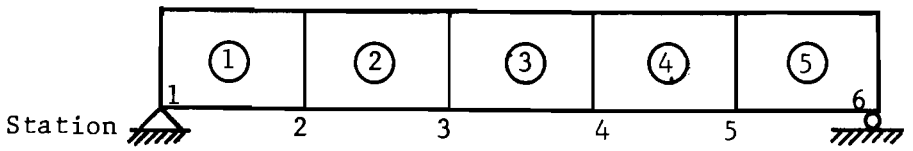

Structure at Stage L (ISTOP (5) = -1)

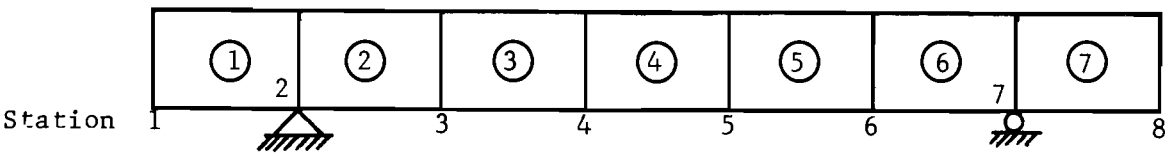

Structure at Stage L+1 (ISTOP (1) = -1; ISTOP (6) = -1)

the approach is as follows. The station designated as No. 6 at Stage L marks the location of an interior support at Stage L+1 and all subsequent stages; therefore, ISTOP (5) = -1. At Stage L, however, Station 6 is the end boundary of the structure. There are no interior supports; thus no INTERIOR SUPPORT/DIAPHRAGM RESTRAINT CONDITIONS CARDS are provided. However, an END BOUNDARY CONDITIONS CARD (15) must be provided. At Stage L+1, the boundary conditions at both boundaries (Station 1 and Station 8) have changed (KODBC = 1). The interior support restraining conditions are also considered changed (KODSPT = 1). Although the physical restraints imposed upon the structure at Stations 2 and 7 (Stage L+1) may be the same as those imposed at Stations 1 and 6 (Stage L), the designation is changed from a boundary condition to interior support; therefore, KODSPT = 1. INTERIOR SUPPORT/DIAPHRAGM RESTRAINT CONDITIONS CARDS are required for both supports at Stage L+1.

8. IAJA2 is an index indicating the modification required for the joint actions applied to Segment NN.
IAJA2 = 0: Joint actions applied to Segment NN are the same as those applied to Segment NN-1. No JOINT ACTIONS CARDS are required for this segment.
IAJA2 = 1: Joint actions applied to Segment NN are the same as those prescribed for this segment at the preceding stage. No JOINT

ACTIONS CARDS are required for this segment. If this stage is the first stage of closure, this option is not available and IAJA2 must be specified as either 0 or 2.
IAJA2 = 2: Joint actions applied to Segment NN are to be respecified. JOINT ACTIONS CARDS must follow this card.

9. The structure is always sequentially described from far left to right. If the cards for boundaries and supports are required, the deck is always assembled as origin, segment action cards up to support with any joint action cards immediately following the segment action cards, support cards, additional segment, joint, and support cards, until the right end of the structure is reached. At that point the end boundary condition is inserted.

*13. JOINT ACTIONS CARD - (I10, 4F10.0, 4I2)

Column 1-10 - L, joint number.

Column 11-20 - AJP (1,L), applied horizontal force or displacement

Column 21-30 - AJP (2,L), applied vertical force or displacement.

Column 31-40 - AJP (3,L), applied moment or rotation.

Column 41-50 - AJP (4,L), applied longitudinal force or displacement.

Column 51-52 - LIND (1,L), horizontal force/displacement indicator.

Column 53-54 - LIND (2,L), vertical force/displacement indicator.

Column 55-56 - LIND (3,L), moment/rotation indicator.

Column 57-58 - LIND (4,L), longitudinal force/displacement indicator.

Remarks - Card 13

1. Each joint requires one card 13. Cards must be arranged with joint numbers in ascending order.

2. LIND (I,J) is an index indicating whether AJP (I,J) is a force or displacement value.
LIND (I,J) = 0: AJP (I,J) is a prescribed force applied to joint J as a uniformly distributed line load over the length of segment NN. Dimensions are force/unit length.
LIND (I,J) = 1: AJP (I,J) is a prescribed displacement enforced at joint J at the longitudinal center of segment NN.

*14. INTERIOR SUPPORT/DIAPHRAGM RESTRAINT CONDITIONS CARD -(4I4,4X,3F15.0)

Column 1-4 - J, element number.

Column 5-8 - IED (1,J), axial indicator.

Column 9-12 - IED (2,J), shear indicator.

Column 13-16 - IED (3,J), rotation indicator.

Column 21-35 - SSC (1,J), axial elastic restraint stiffness coefficient.

Column 36-50 - SSC (2,J), transverse elastic restraint stiffness coefficient.

Column 51-65 - SSC (3,J), rotational elastic restraint stiffness coefficient.

Remarks - Card 14

1. Support for the structure (displacement restraint) may be prescribed by restraining joint displacements (JOINT ACTIONS CARDS) or element displacements (INTERIOR SUPPORT/DIAPHRAGM RESTRAINT CONDITIONS CARD) or a combination of both.
2. The type and degree of restraint imposed by the interior support is specified for each element individually. The interior support restraints are imposed on the plate degrees of freedom at the station of the interior support.
3. IED (I,J) is an index indicating the type of restraint imposed on the associated (Ith) plate degree of freedom of the Jth element.
   IED (I,J) = -1: The associated displacement is partially restrained by the interior support. A non-zero value of the corresponding restraint stiffness, SSC (I,J) must be provided.
   IED (I,J) = 0: The associated displacement is not restrained by the support.
   IED (I,J) = 1: The associated displacement is completely restrained by the support; i.e., the displacement is equal to zero.
4. The nature of restraint imposed upon the structure by a particular support may change from stage to stage. The degree of restraint may range from complete fixity of all elements to no restraint of any element. Therefore, even though interior supports may not be arbitrarily imposed and removed at every stage, the same effect may be accomplished by changing the support restraint conditions as desired. (See remarks Nos. 6 and 7, Cards 12(A) and 12(B).)

*15. END BOUNDARY CONDITIONS CARDS - (I10, 3F10.0, 3I2)

Column 1-10 - I, element number.

Column 11-20 - BCEND (1,I), prescribed longitudinal force or displacement.

Column 21-30 - BCEND (2,I), prescribed transverse force or displacement.

Column 31-40 - BCEND (3,I), prescribed moment or rotation.

Column 41-42 - IEND (1,I), longitudinal force/displacement index.

Column 43-44 - IEND (2,I), transverse force/displacement index.

Column 45-46 - IEND (3,I), moment/rotation index.

Remarks - Card 15

1. Each element of the cross section requires one card 15.
2. IEND (I,J) is an index indicating whether BCEND (I,J) is a force or displacement value.
   IEND (I,J) = 0: BCEND (I,J) is prescribed force.
   IEND (I,J) = 1: BCEND (I,J) is prescribed displacement.

16. SEQUENCING

A. Card Type 7(A) will follow card Type 15 for analysis of the next stage of construction.

B. A blank card follows card Type 15 in order to terminate the run.

B.3 - Flow of Input Data

The following chart is presented in the form of a program flow chart and is intended to indicate graphically the sequence in which the program reads the input data. The numbers associated with READ statements refer to the card numbers defined in B.2, and statement numbers are for purposes of this chart only. All variable names appearing in the chart have been defined in B.2. L is a symbol for a typical stage.

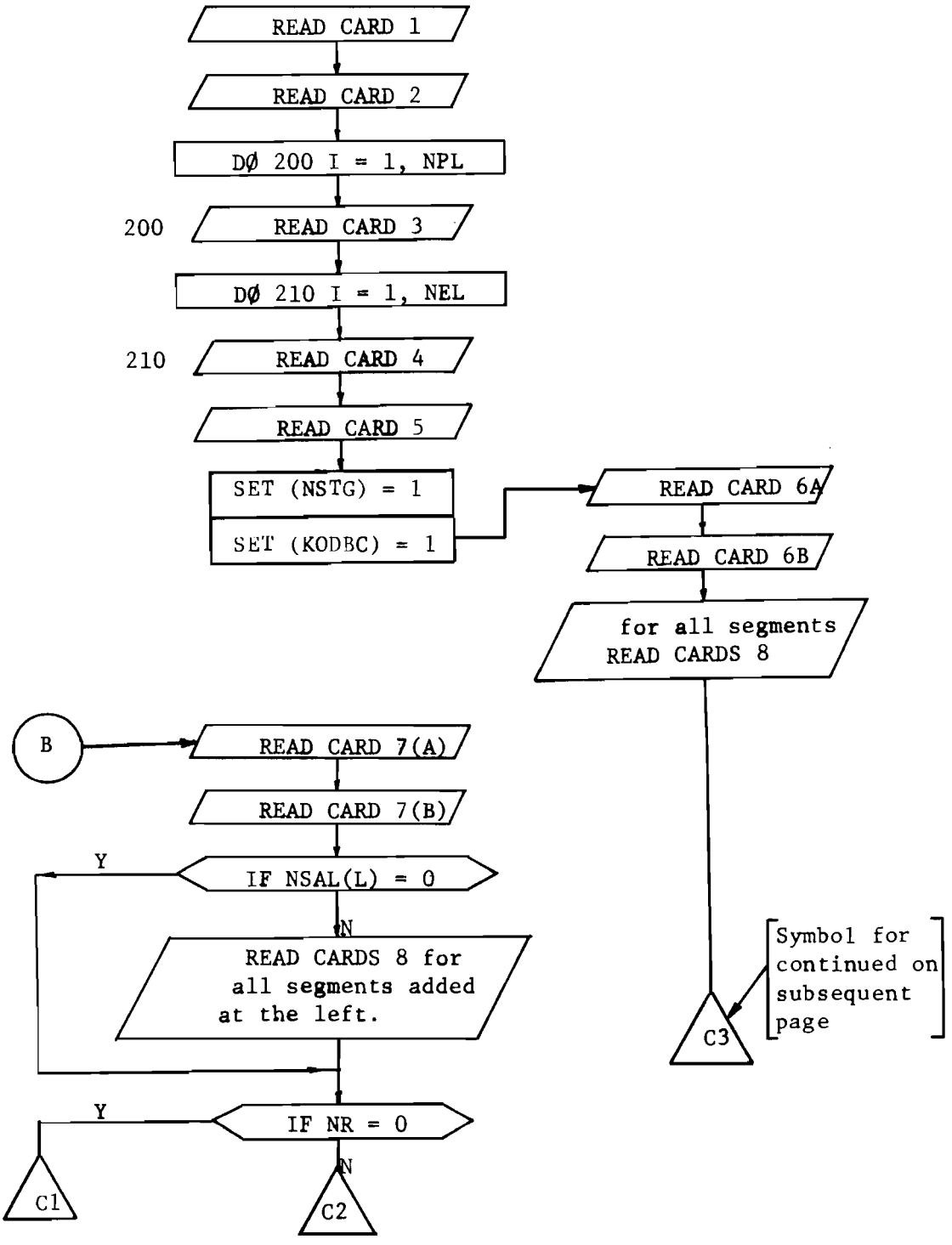

B.3 - Flow of Input Data (con't)

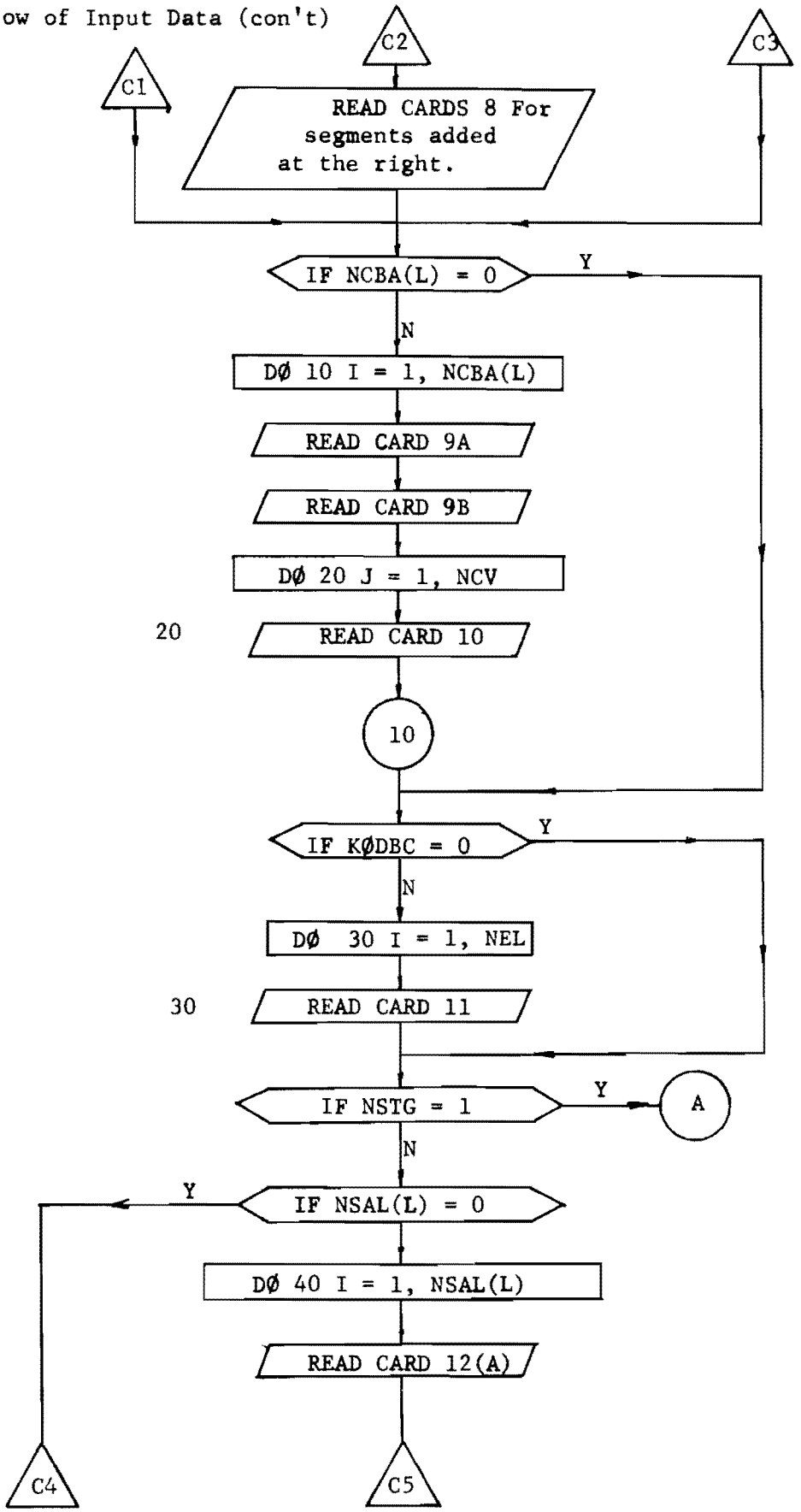

B.3 - Flow of Input Data (con't)

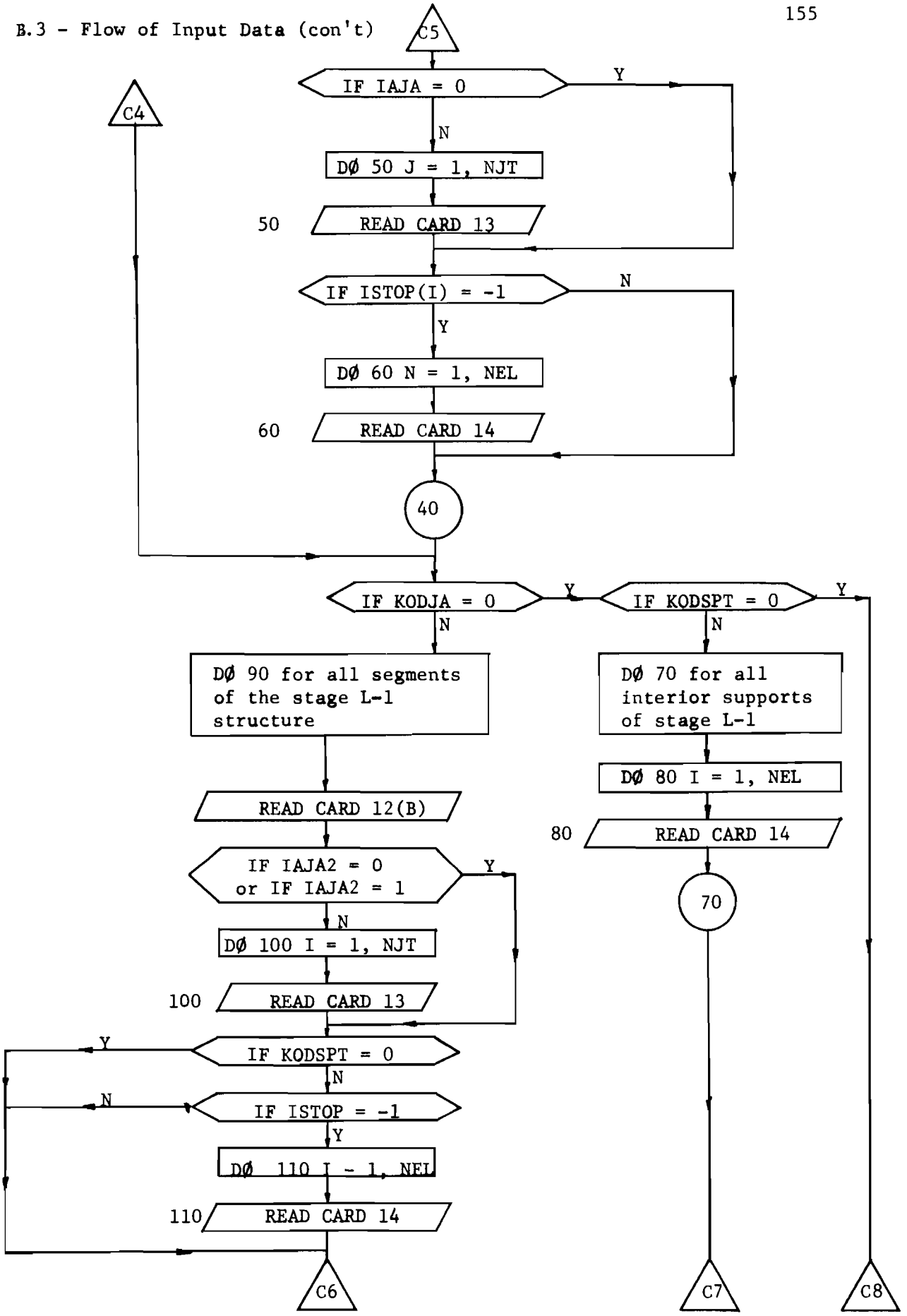

B.3 Flow of Input Data (con't.)

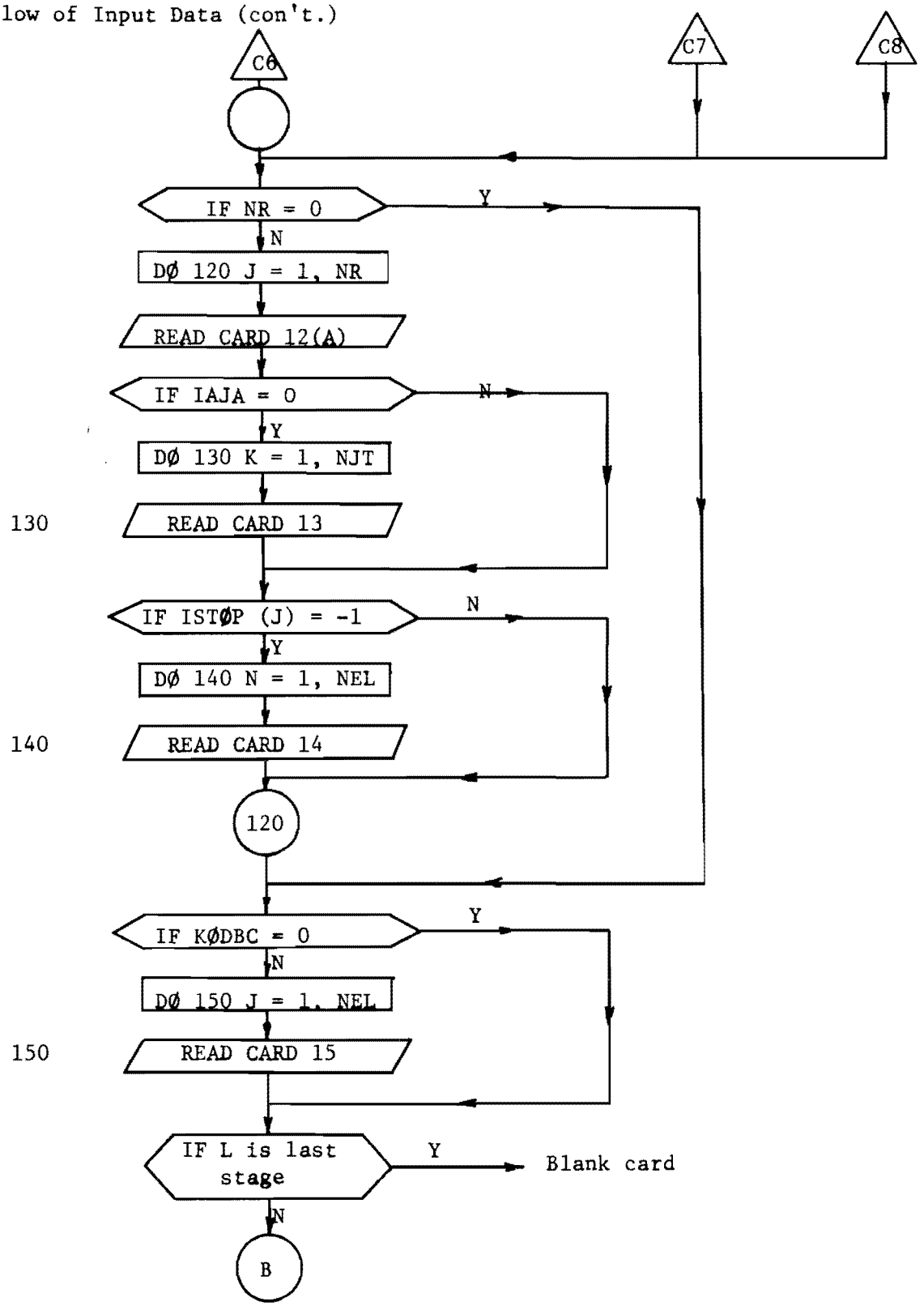

B.3 - Flow of Input Data (con't)

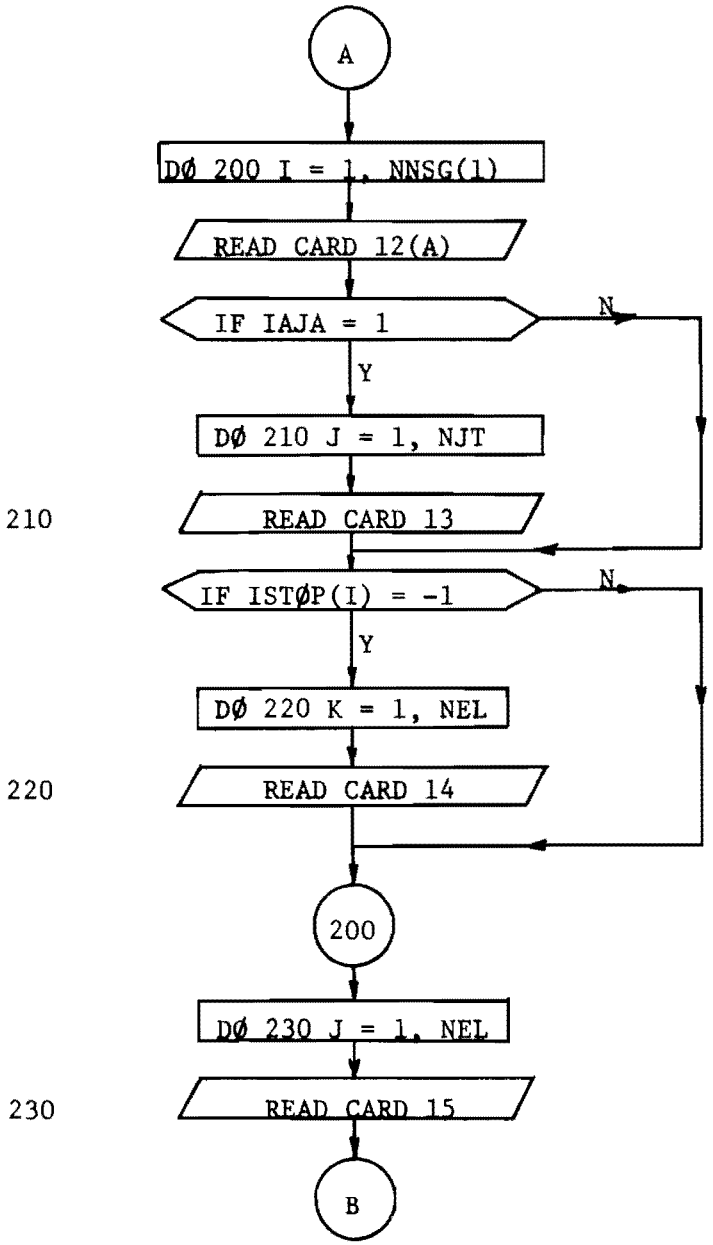

B.4 - Computer Output

SIMPLA2 performs a complete structural analysis for each stage of construction and outputs the results for each stage. The output consists of:

B.4.1 Title and echo print of structure constant data (output for initial stage only).

B.4.2 Echo print of construction stage XX data.

(a) LONGITUDINAL CONFIGURATION OF STRUCTURE AT STAGE XX

(b) INPUT DATA FOR TENDONS STRESSED AT STAGE XX

(c) ORIGIN BOUNDARY CONDITIONS AT STAGE XX

(d) JOINT ACTIONS, SUPPORT AND STOPOVER DATA FOR STAGE XX

(e) END BOUNDARY CONDITIONS AT STAGE XX

B.4.3 Printout of Computed Results

(a) FINAL PLATE FORCES AND DISPLACEMENTS FOR LONGITUDINAL PLATE ELEMENTS AT END - These values are the components of the state vector at the end of the structure. Superposition of reference and continuous solutions is not accomplished automatically at the end stations. (See Figs. 2.3 and B.4 for sign convention.)

PLATE INTERNAL DISPLACEMENTS - The following displacements are given for each element.

Longitudinal displacement

Transverse displacement

Beam rotation

PLATE INTERNAL FORCES - The following forces and stresses are given for each element.

Beam moment

Transverse shear

Axial force

Longitudinal normal force/unit length at element I-edge, NX (I)

Longitudinal normal force/unit length at element J-edge, NX (J)

Longitudinal normal force/unit area at element I-edge, SX (I)

Longitudinal normal force/unit area at element J-edge, SX)J)

(a) Positive Element Forces

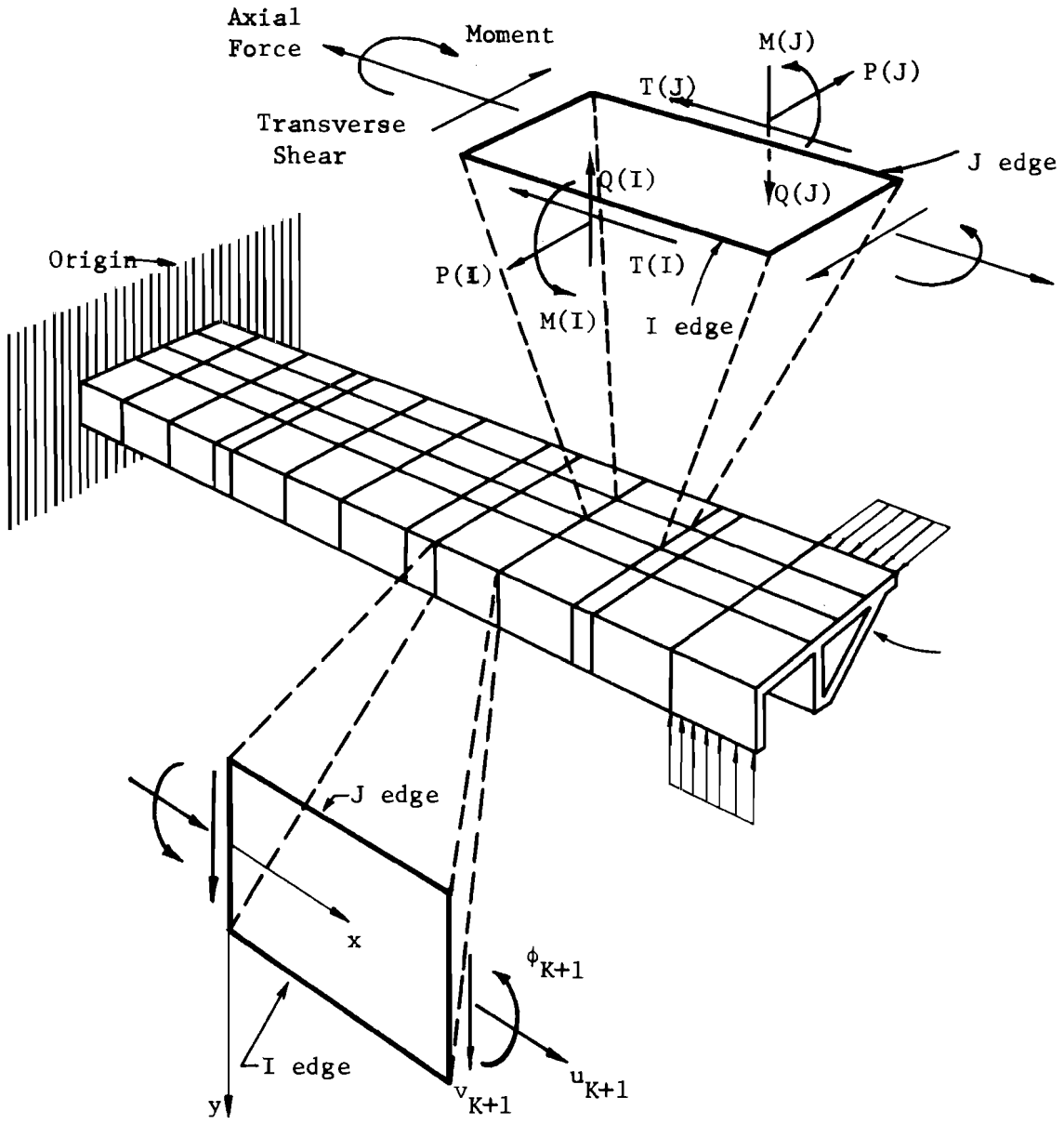

(b) Positive Element Displacements

NOTE: With the exception of the longitudinal element edge displacement, the edge nodal point displacements have the same positive directions as their associated forces.

Fig. B.4. Positive element forces and displacements.

(b) FINAL PLATE FORCES AND DISPLACEMENTS FOR LONGITUDINAL PLATE ELEMENTS AT END OF SEGMENT XX AND AT SUPPORT - These results are provided at each station locating an interior support.
PLATE DISPLACEMENTS AND REACTIONS AT INTERIOR SUPPORT - These results are provided for each element of the cross section. The sign of reaction components is referenced to the element relative coordinate system and indicates the direction of the reaction as it acts on the diaphragm. The plate displacements and reactions at the interior supports for the reference and continuous solutions are not automatically superimposed.
Longitudinal displacement/reaction
Transverse displacement/reaction
Beam rotation/reaction
PLATE INTERNAL DISPLACEMENTS - Same as those listed under B.4.3(a).
PLATE INTERNAL FORCES - Same as those listed under B.4.3(a).

(c) FINAL PLATE FORCES AND DISPLACEMENTS FOR LONGITUDINAL PLATE ELEMENTS AT ORIGIN - These values are the components of the state vector at the origin of the structure. See remark No. 2.
PLATE INTERNAL DISPLACEMENTS - Same as those listed under B.4.3(a).
PLATE INTERNAL FORCES - Same as those listed under B.4.3(a).

(d) FINAL JOINT AND PLATE FORCES AND DISPLACEMENTS FOR SEGMENT XX - The following results are furnished for every segment.
JOINT DISPLACEMENTS - The following displacements are given for every joint. Joint displacements are referred to the longitudinal center of the segment. (See Fig. B.2 for sign convention.)
Horizontal displacement
Vertical displacement
Rotation
Longitudinal displacement
ELEMENT EDGE DISPLACEMENTS - The following displacements are given for each element. (See Fig. B.4 for sign convention.)
Rotation at I-edge.
Rotation at J-edge.

Normal shear displacement at I-edge, W(I).

Normal shear displacement at J-edge, W(J).

Longitudinal shear displacement at I-edge, U(I).

Longitudinal shear displacement at J-edge, U(J).

Transverse membrane displacement at I-edge, V(I).

Transverse membrane displacement at J-edge, V(J).

ELEMENT EDGE FORCES - The following forces are given for each element. (See Fig. B.4 for sign convention.)

Transverse moment per unit length at I-edge, M(I).

Transverse moment per unit length at J-edge, M(J).

Normal shear per unit length at I-edge, Q(I).

Normal shear per unit length at J-edge, Q(J).

Longitudinal shear force per unit length at I-edge, T(I).

Longitudinal shear force per unit length at J-edge, T(J).

Transverse membrane force per unit length at I-edge, P(I).

Transverse membrane force per unit length at J-edge, P(J).

PLATE INTERNAL DISPLACEMENTS - Same as those listed under B.4.3(a). See remarks.

PLATE INTERNAL FORCES - Same as those listed under B.4.3(a). See remarks.

(e) STEEL STRESSES FOR ALL TENDONS AT STAGE XX - These results are provided only at those stages specified by the user.

B.4.4 Remarks

1. Output quantities noted in B.4.3(a), (b), and (c) are the beam-type displacements and stress resultants at the longitudinal end of the respective element.
2. Superposition of solutions is performed automatically only for those quantities associated with a segment (as opposed to those quantities associated with the end of a segment). Therefore, forces and displacements noted in B.4.3(a), (b), and (c) are not automatically superimposed. Should the stage of construction under consideration be a stage of closure, the correct origin and end actions and support reactions would be given by summing corresponding quantities from the reference solution with those printed for this stage.

3. Reaction components are printed when the associated displacement is completely restrained (equal to zero); otherwise, the displacement component is furnished. Reaction components are referred to the respective element relative coordinate system. The sign affixed indicates the direction in which the reaction acts on the diaphragm or support.

4. Results noted in B.4.3(d) pertain to each element at the longitudinal center of the segment. JOINT DISPLACEMENTS AND ELEMENT EDGE DISPLACEMENTS represent the element edge nodal point displacements in the fixed and element relative coordinate system, respectively. PLATE INTERNAL DISPLACEMENTS AND PLATE INTERNAL FORCES are the beam-type displacements and stress resultants at the longitudinal center of the element.

B.5 - Program SIMPLA2

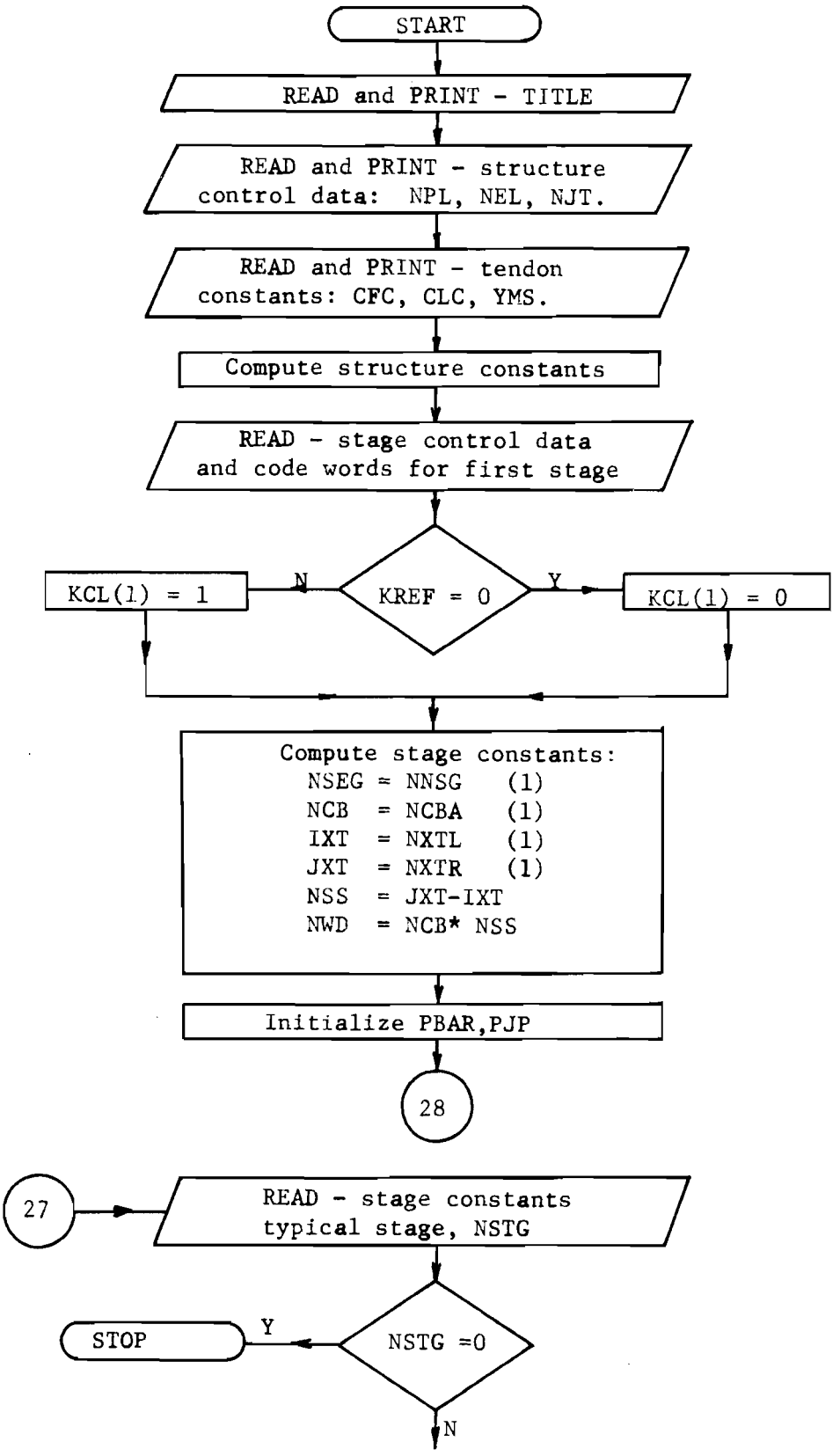

Program SIMPLA2 (con't.)

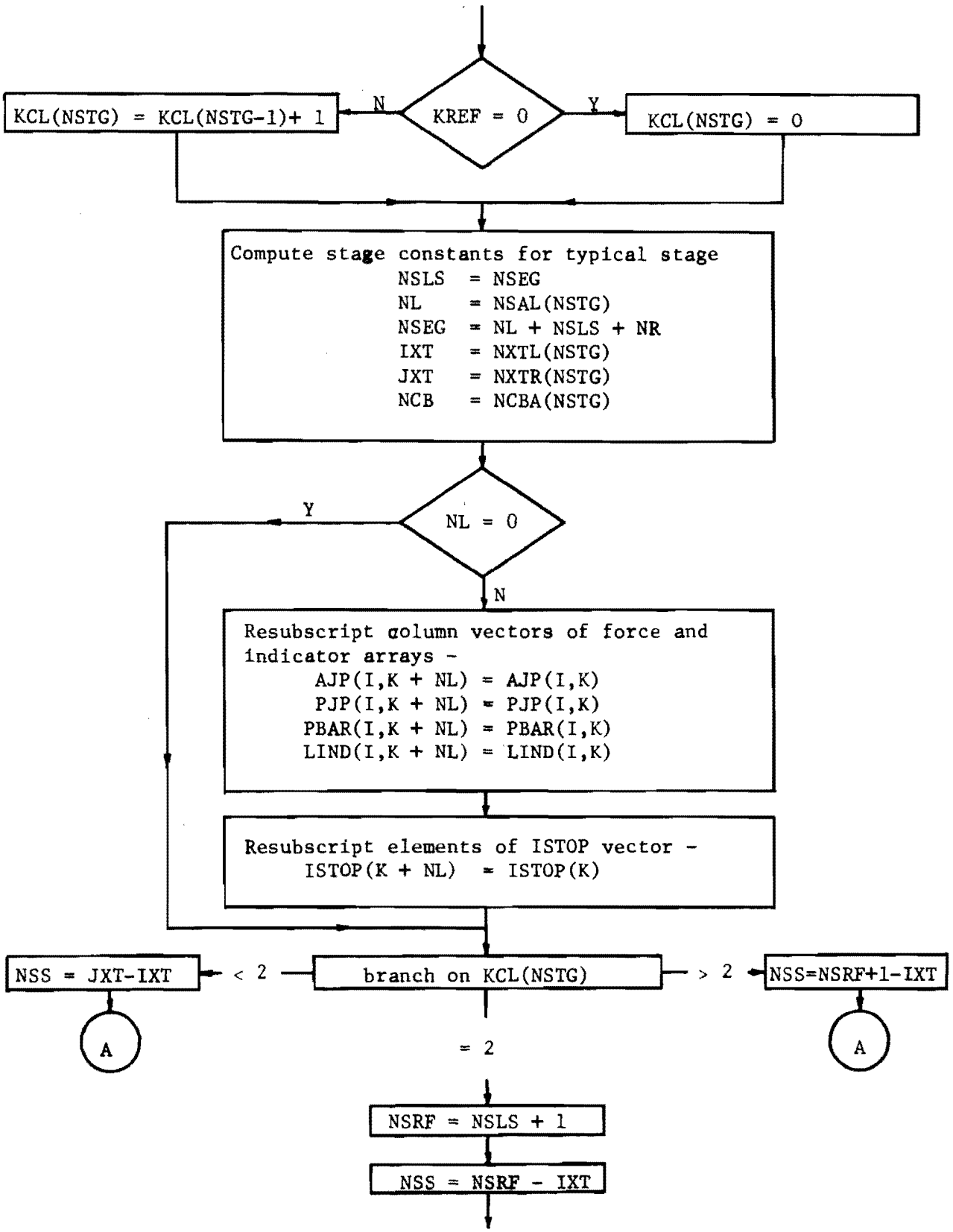

Program SIMPLA2 (con't.)

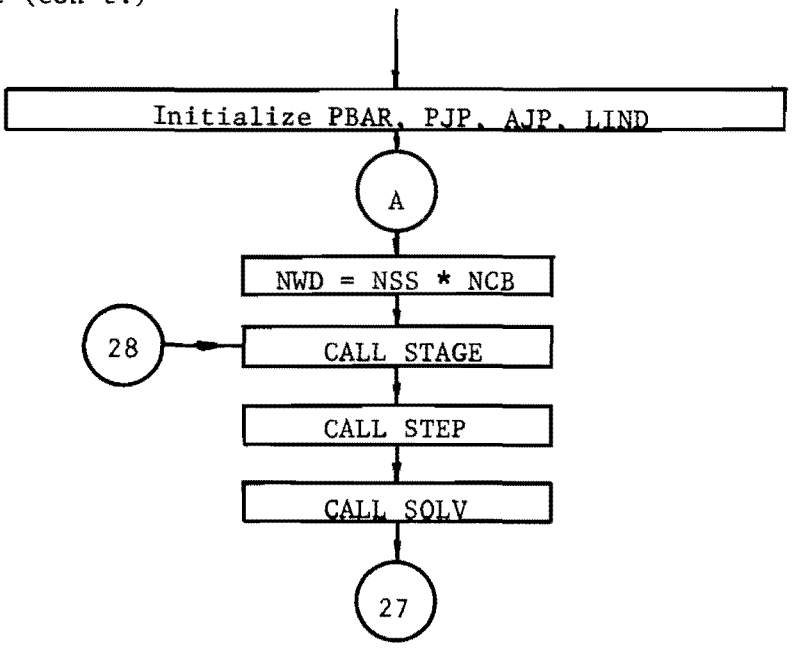

B.5.1 - Subroutine STAGE

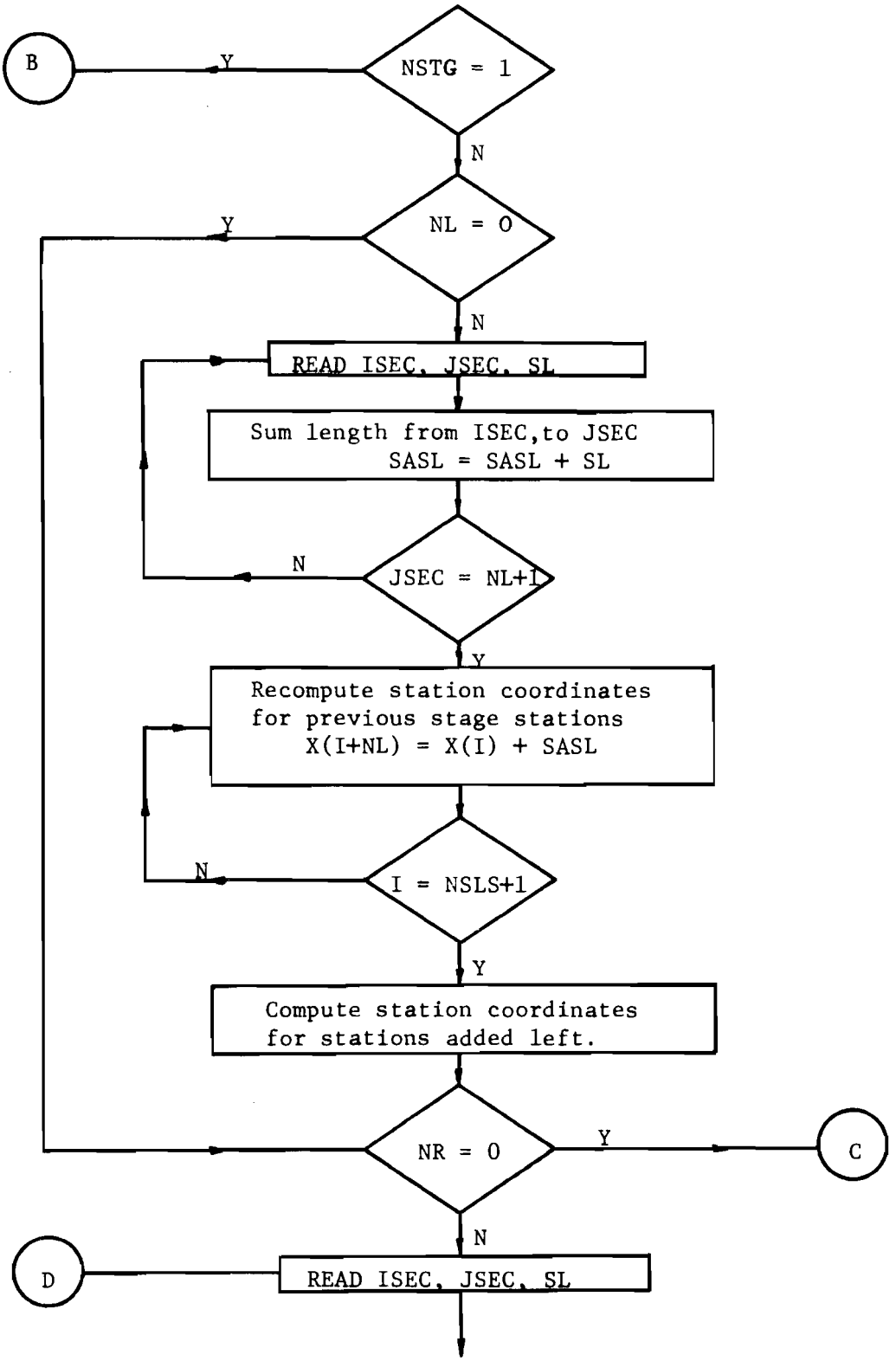

Subroutine STAGE (con't.)

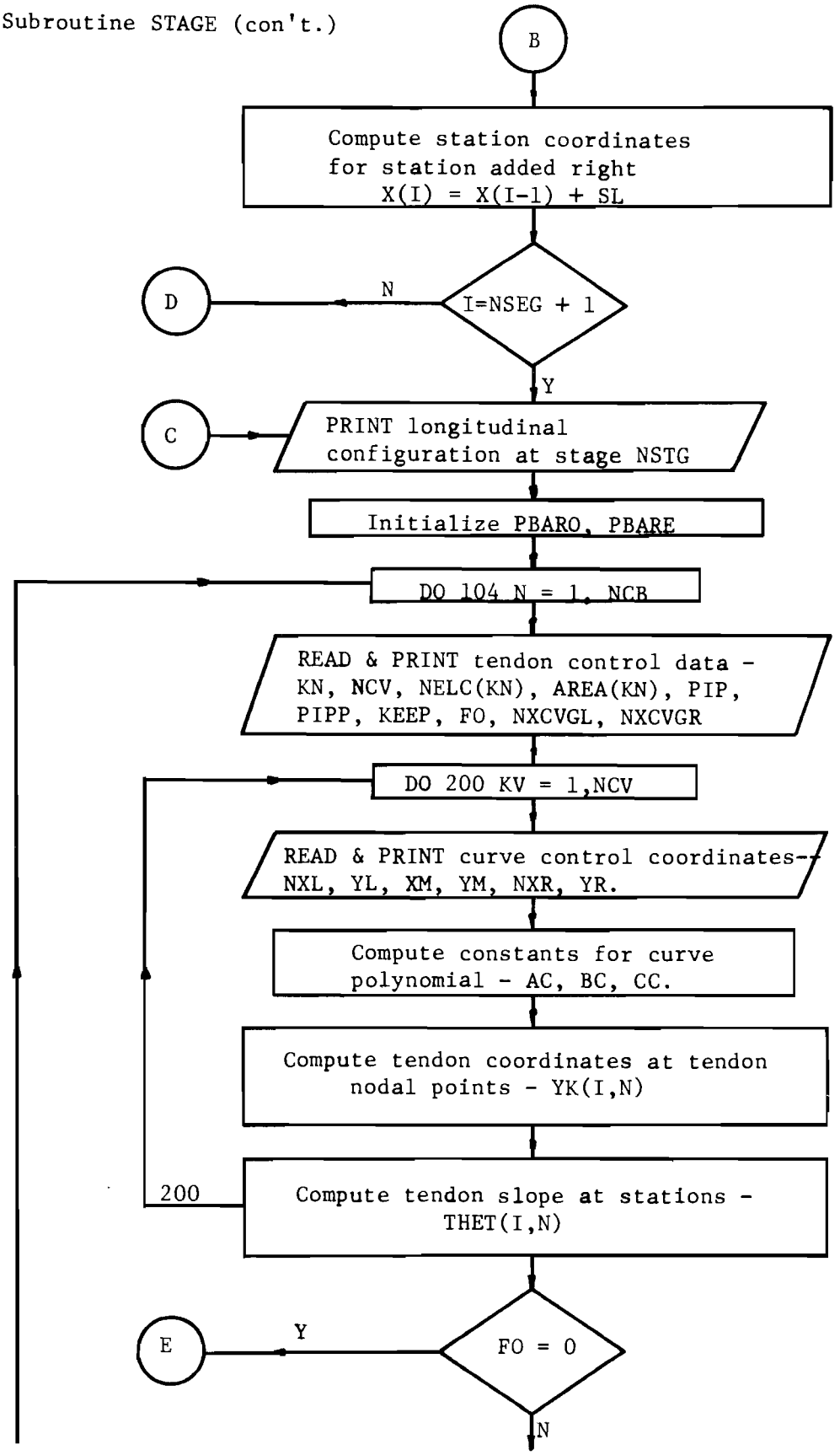

Subroutine STAGE (con't.)

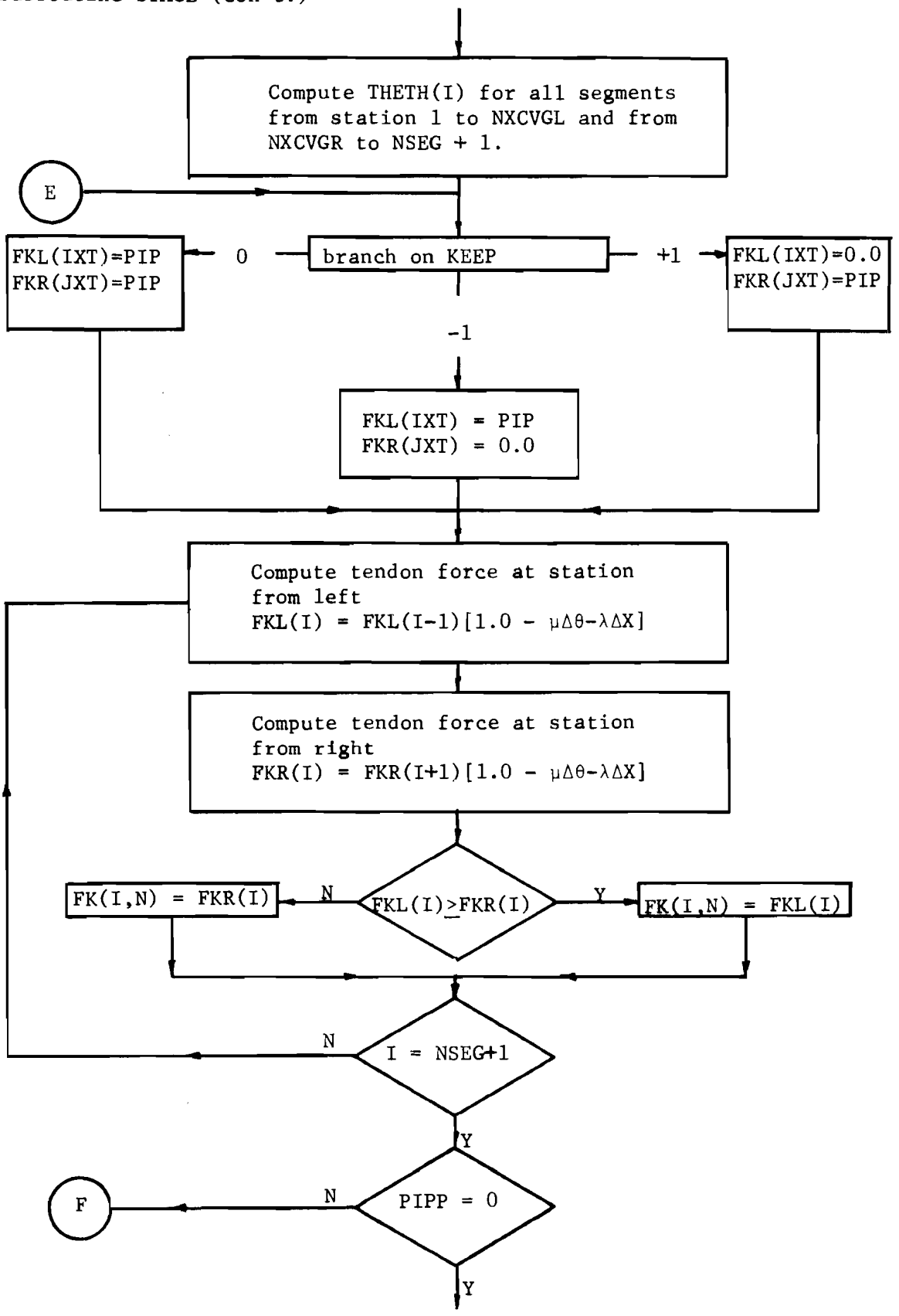

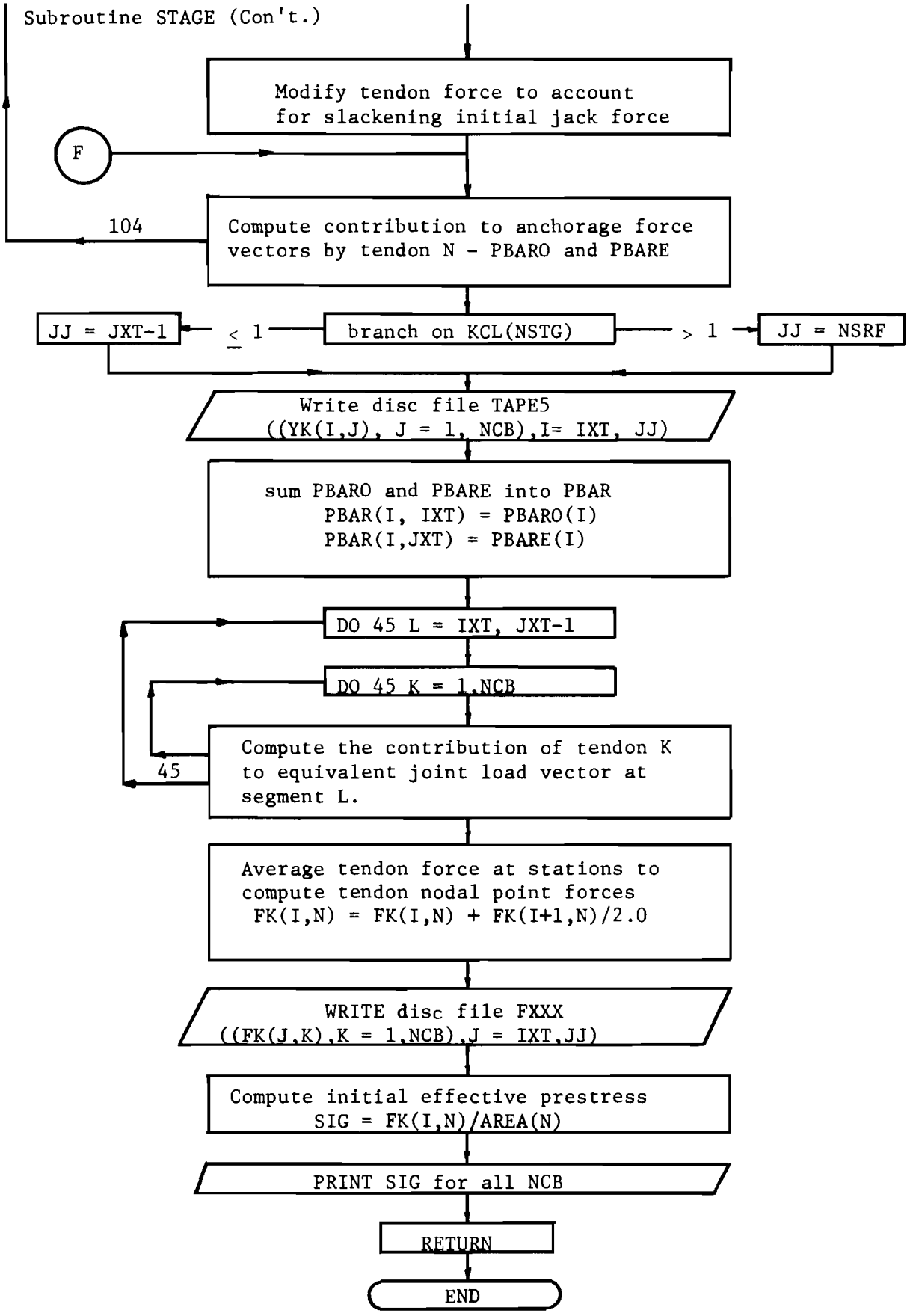
Subroutine STAGE (Con't.)
Modify tendon force to account for slackening initial jack force
F
104
Compute contribution to anchorage force vectors by tendon N - PBARO and PBARE
JJ = JXT-1
≤ 1
branch on KCL(NSTG)
> 1
JJ = NSRF
Write disc file TAPE5 ((YK(I,J), J = 1, NCB),I= IXT, JJ)
sum PBARO and PBARE into PBAR
PBAR(I, IXT) = PBARO(I)
PBAR(I,JXT) = PBARE(I)
DO 45 L = IXT, JXT-1
DO 45 K = 1,NCB
Compute the contribution of tendon K to equivalent joint load vector at segment L.
45
Average tendon force at stations to compute tendon nodal point forces
FK(I,N) = FK(I,N) + FK(I+1,N)/2.0
WRITE disc file FXXX ((FK(J,K),K = 1,NCB),J = IXT,JJ)
Compute initial effective prestress
SIG = FK(I,N)/AREA(N)
PRINT SIG for all NCB
RETURN
END

B.5.2 Subroutine STEP

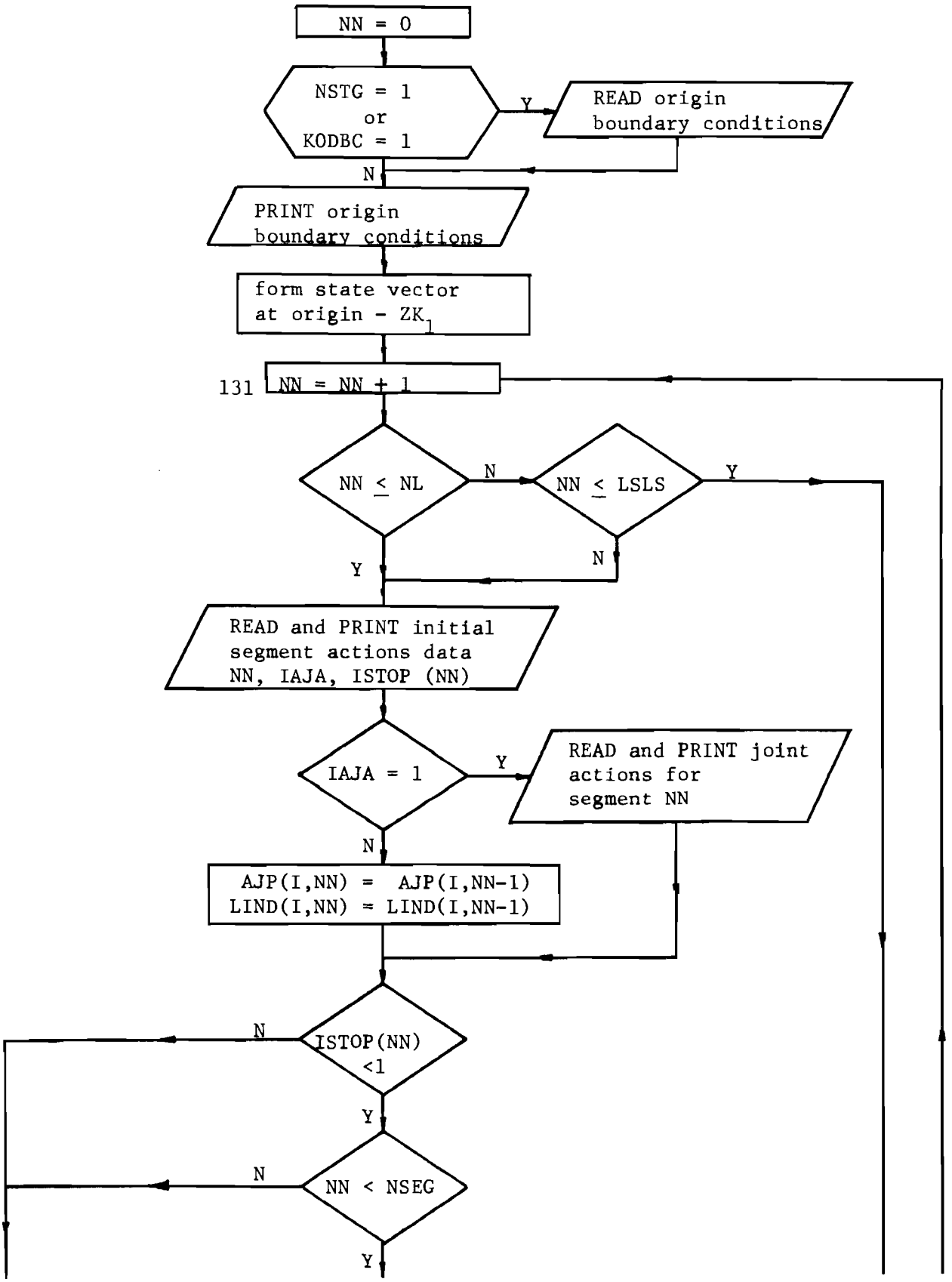

Subroutine STEP (con't.)

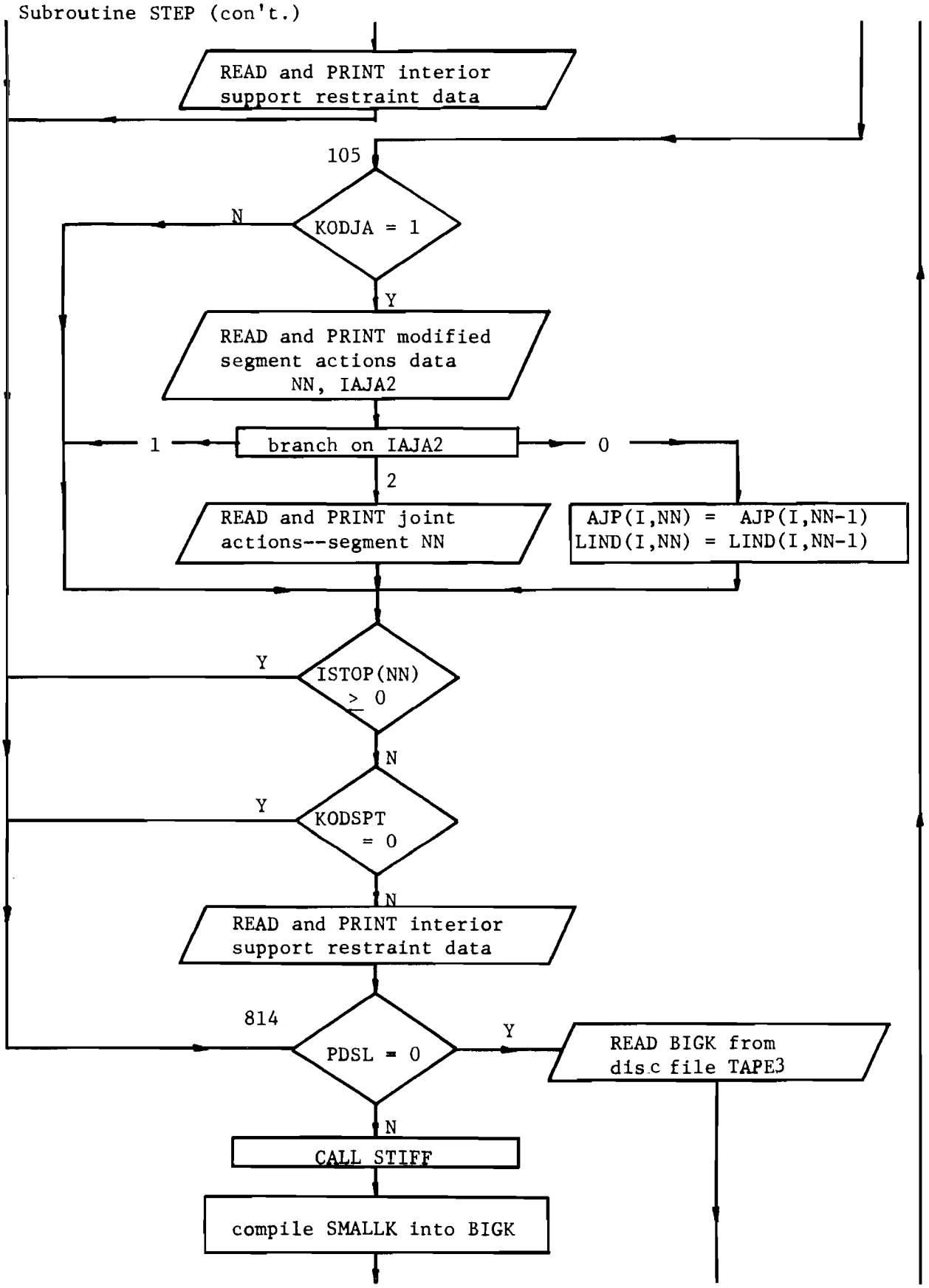

Subroutine STEP (con't.)

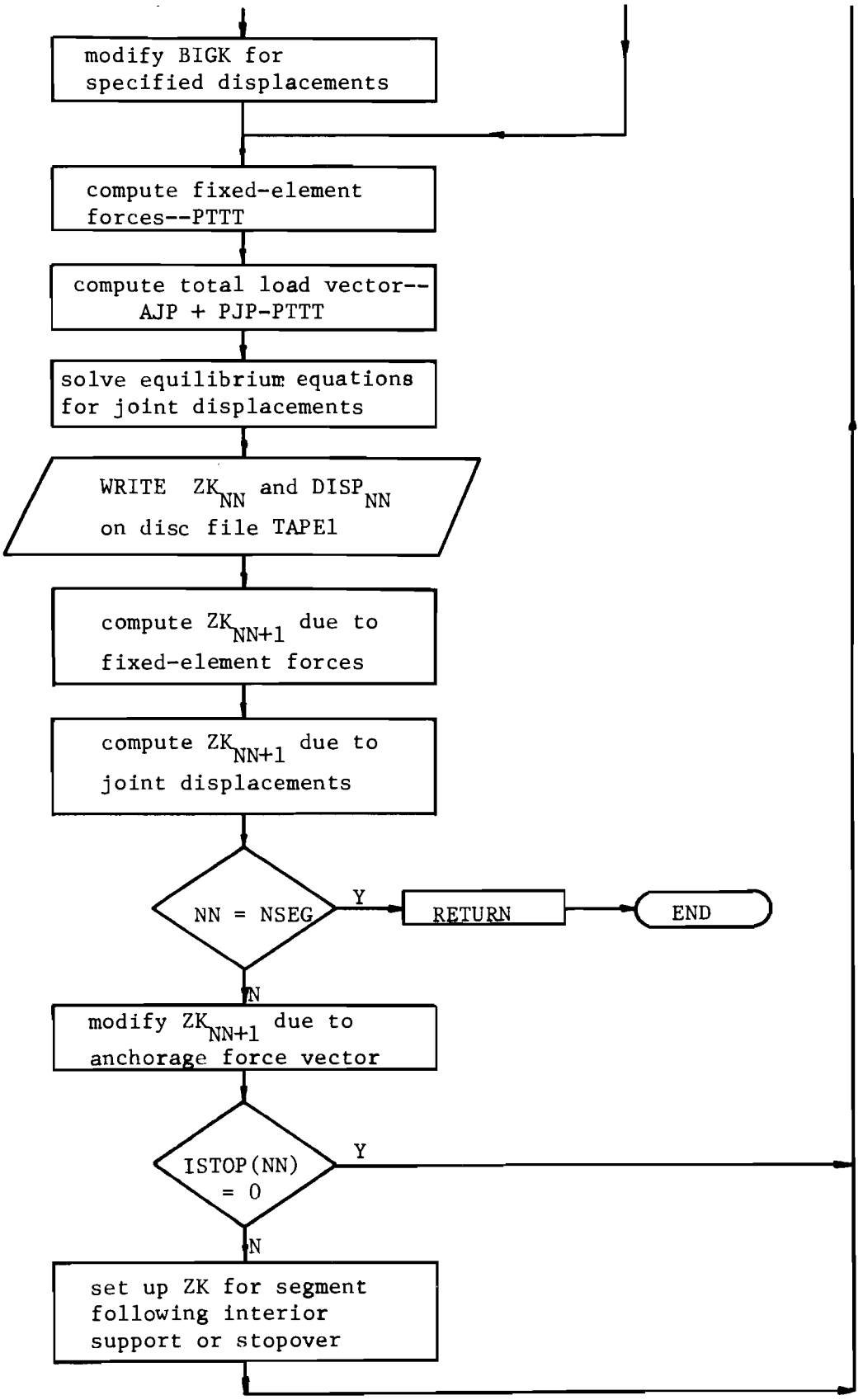

B.5.3 Subroutine SOLV

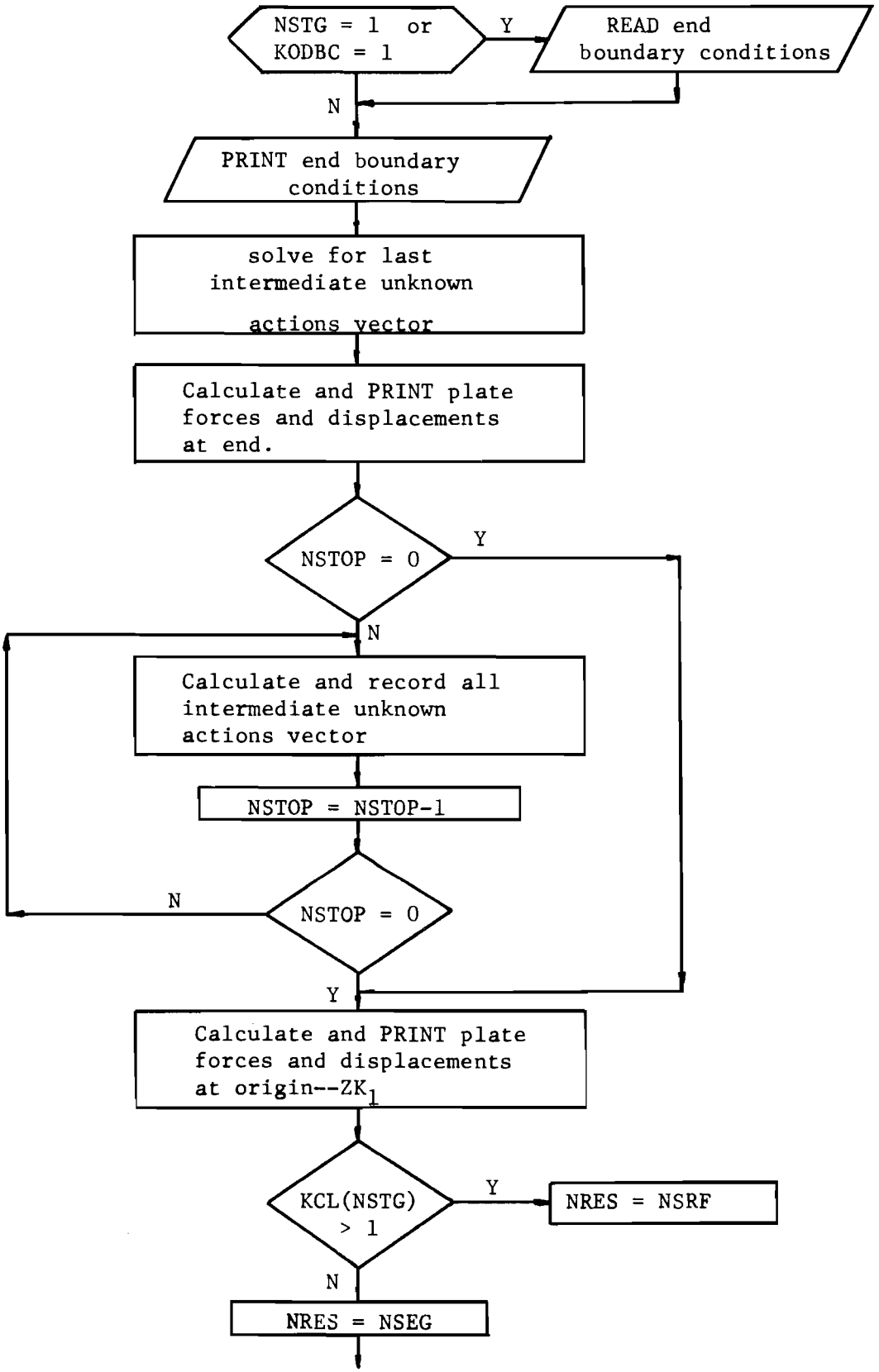

Subroutine SOLV (Con't.)

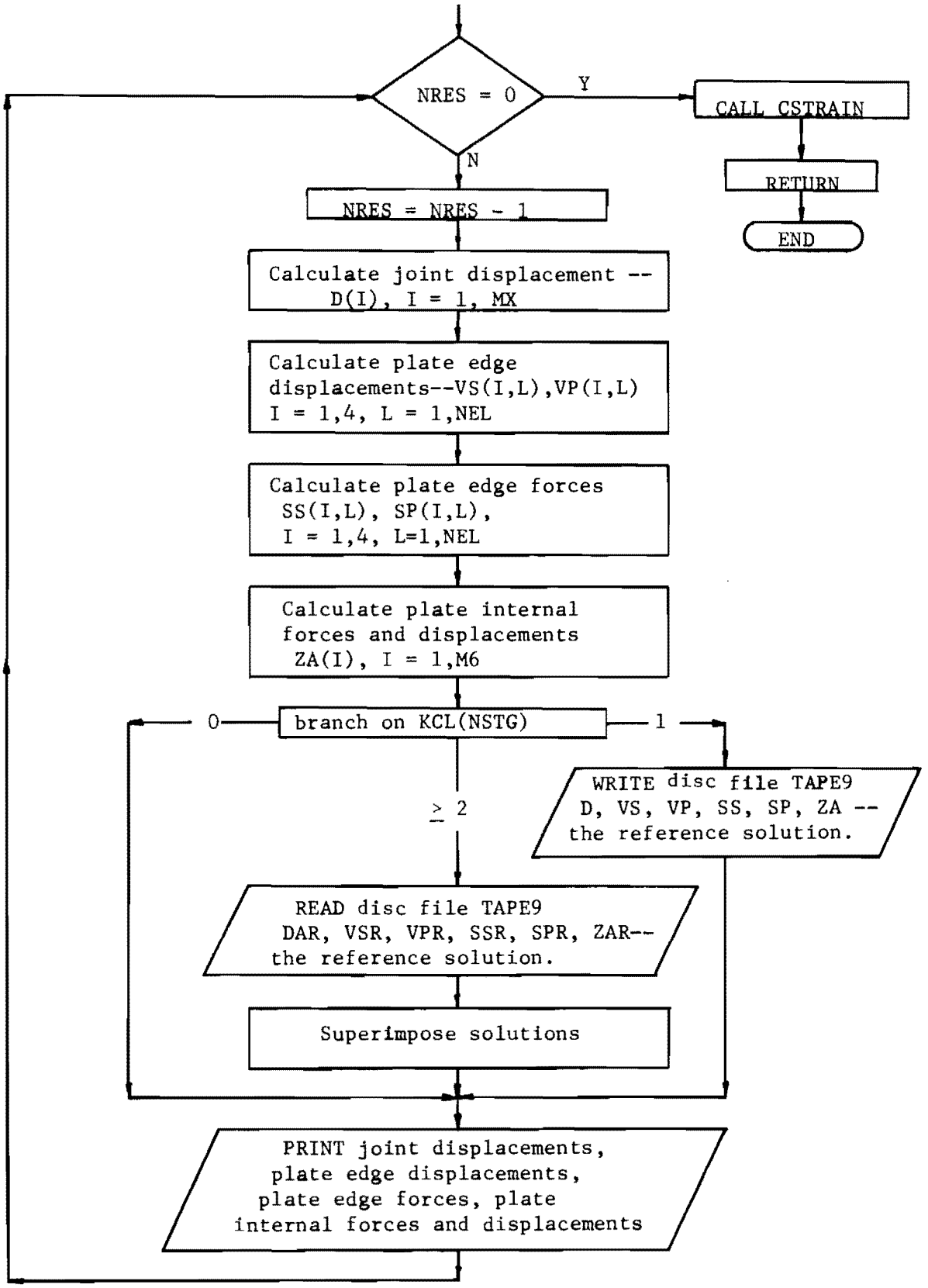

B.5.4 Subroutine CSTRAIN

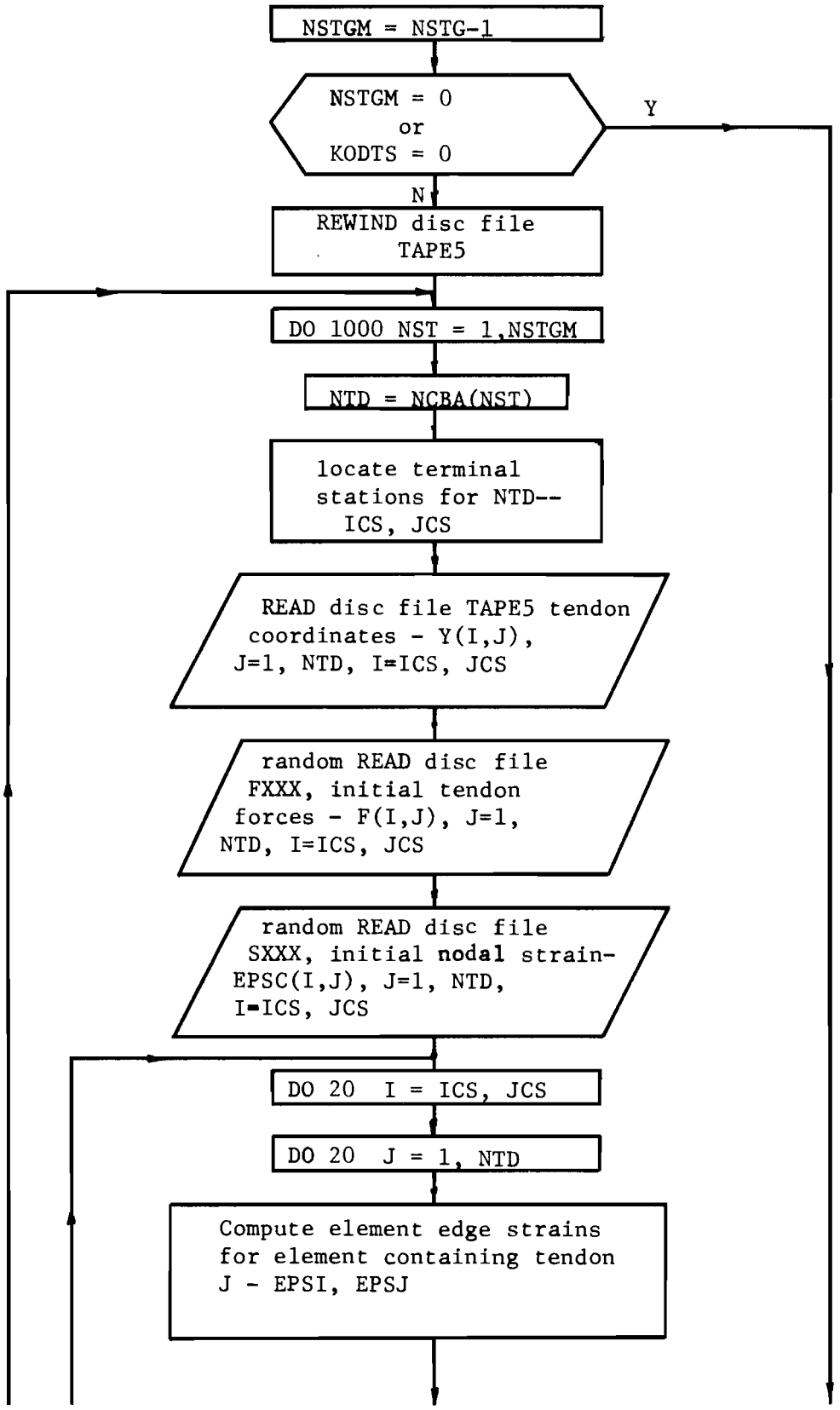

Subroutine CSTRAIN (con't.)

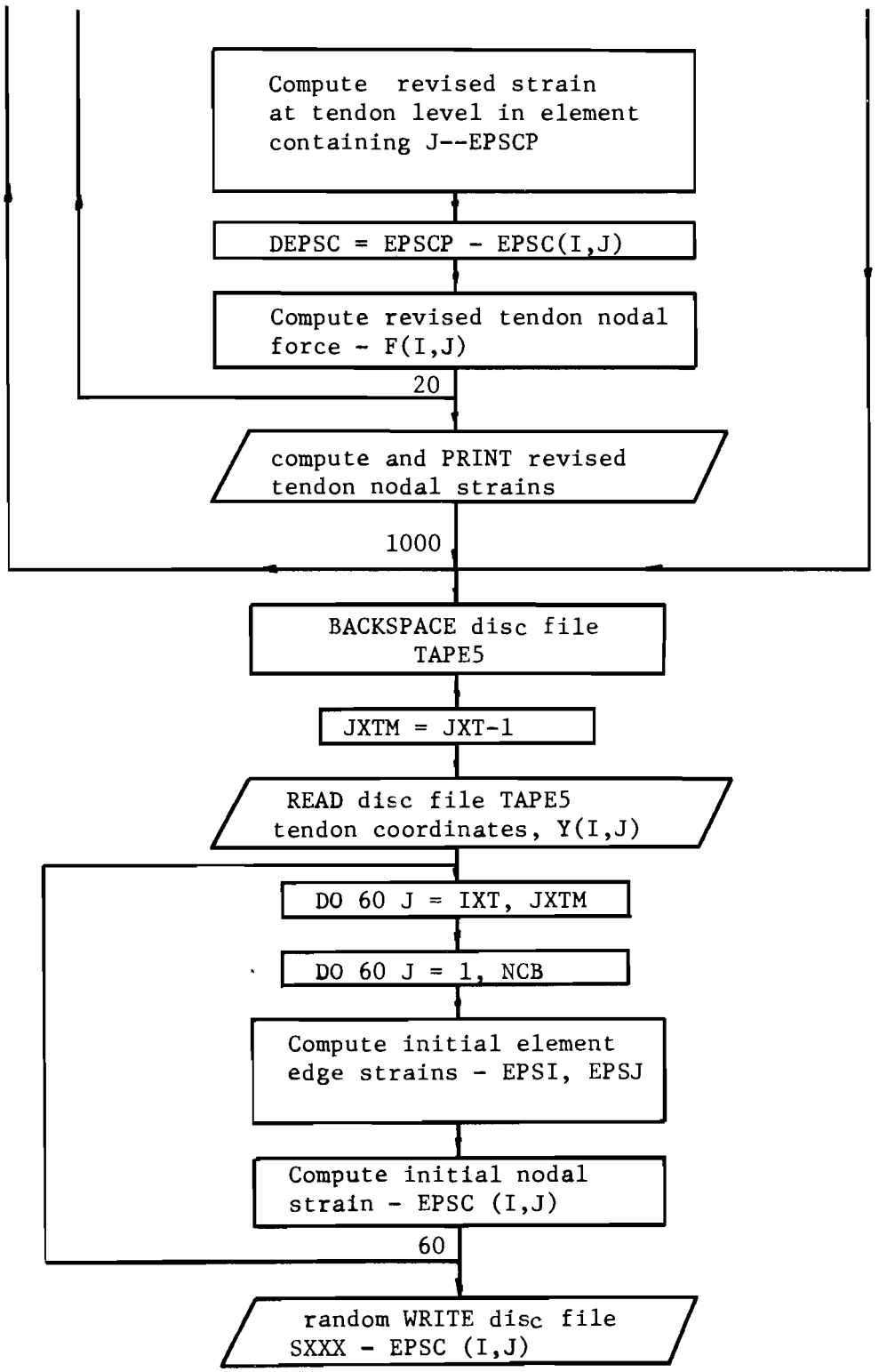

```
      PROGRAM SIMPLA2 (INPUT,OUTPUT,TAPE1,TAPE3,TAPE5,TAPE8,TAPE9,
     1FXXX,SXXX)
C
C
C
   10 FORMAT(//41HO****ERROR-MAX. JOINT DIFFERENCE.GT.4*****)
   20 FORMAT(4I4)
   25 FORMAT(6I4)
    9 FORMAT(I10,4F10.0)
    4 FORMAT(1HO,3X,20HPROBLEM CONTROL DATA)
   17 FORMAT(1HO,3X,16HNO. PL. TYPES = I2/4X,16HNO. ELEMENTS  = I2/4X,16
     1HNO. JOINTS    = I2/)
    5 FORMAT(1H0,3X,32HGEOMETRIC AND ELASTIC PROPERTIES)
   21 FORMAT(1HO,3X,7HPL TYPE,10X,7HH-PROJ.,10X,7HV-PROJ.,10X,9HTHICKNES
     1S,10X,7HMODULUS/)
   22 FORMAT(I8,9X,4(E15.6,3X))
    6 FORMAT(1H0,3X,17HCONNECTIVITY DATA/)
   23 FORMAT(4X,23HELE    I-JT    J-JT    PL/)
   24 FORMAT(4X,4(I2,5X))
    7 FORMAT(1H0,3X,19HTENDON CONTROL DATA/)
    8 FORMAT(4X,16HSTEEL MODULUS = E15.6/4X,20HFRICTION CONSTANT = E15.6
     1/4X,18HWOBBLE CONSTANT = E15.6)
   12 FORMAT(3I4)
   16 FORMAT(1H1,12A6)
   32 FORMAT(10X,3F10.0)
   11 FORMAT (12A6)
C
C     COMMON DIMENSION AND EQUIVALENCE STATEMENTS
C
      COMMON NSTG,NSRF,NSEG,SEGL,NL,NL1,NR,NSLS,NSLS1,NS1,LSLS,NSS,NWD,
     1NCB,IXT,JXT,NPL,NJT,NEL,M3,MX,M6,M31,NXBAND,MAXJTD,YMS,CLC,CFC,
     2NSTOP,KODJA,KODBC,KODSPT,KODTS
      COMMON H(15),V(15),TH(15),E(15),PWTH(15),NPI(15),NPJ(15),KPL(15),
     1NPDIF(15),ZEND(90),BCORI(3,15),IORI(3,15),BCEND(3,15),IEND(3,15),
     2IED(45,4),SSC(45,4),ZK(90,46),IFD(90)
      COMMON NNSG(25),NSAL(25),NCBA(25),KCL(25),NXTL(25),NXTR(25),
     1IDXF(25),IDXS(25),XSEC(51),ISTOP(50),KANCH(50),AJP(64,50),
     2PJP(64,50),LIND(64,50),PBAR(45,51),NELC(25),AREA(25)
      COMMON BIGK(64,20),PTTT(64,46),CM(9,15),HM(17,15),FJ(9,15),
     1A(4,4),BTAV(4),RBAR(4),D(20),ZZ(6)
C
      DIMENSION TITLE(12)
C
  101    READ 11, (TITLE(I),I = 1,12)
      READ 12, NPL,NEL,NJT
         IF(NPL) 999,999,102
  102    PRINT 16, TITLE
      PRINT 4
      PRINT 17, NPL,NEL,NJT
      PRINT 5
         READ 9, (I, H(I), V(I), TH(I), E(I),  J = 1,NPL)
         READ 20, (I,NPI(I), NPJ(I), KPL(I),  J = 1,NEL)
      READ 32, CFC,CLC,YMS
         PRINT 21
         PRINT 22, (I,H(I),V(I),TH(I),E(I),  I = 1,NPL)
      PRINT 6
         PRINT 23
         PRINT 24,(I, NPI(I), NPJ(I), KPL(I), I = 1,NEL)
      PRINT 7
      PRINT 8, YMS,CFC,CLC
C
C     COMPUTE PWTH(I) AND SET H(I) = H(I)/PWTH(I) AND V(I) = V(I)/PWTH(I)
C
         DO 125 I = 1,NPL
         PWTH (I) = SQRT(H(I)*H(I) + V(I)*V(I))
         H(I) = H(I)/PWTH(I)
  125    V(I) = V(I)/PWTH(I)
C
C     COMPUTE PROBLEM CONSTANTS
C
         MX = 4*NJT
         M3 = 3*NEL
         M31 = M3 + 1
         M6 = 6*NEL
         NSTG = 1
C
C     COMPUTE MAX HALF BAND WIDTH AND SET NPI = NPI*4-4 AND NPJ = NPJ*4-4
C
         MX = 4*NJT
         NXBAND = 0
         DO 130 I = 1,NEL
         NPDIF(I) = NPJ(I) - NPI(I)
         K = IABS(NPDIF(I))
         IF(NXBAND - K) 126,127,127
  126    NXBAND = K
  127    NPI(I) = NPI(I)*4-4
  130    NPJ(I) = NPJ(I)*4-4
         MAXJTD = NXBAND
         NXBAND = NXBAND*4+4
         IF(NXBAND - 20) 123,123,72
   72    PRINT 10
         GO TO 999
  123    CONTINUE
C
   26 READ 20, NNSG(1),NCBA(1),NXTL(1),NXTR(1)
      READ 20, KREF,KODTS
      IF(KREF) 31,31,33
   31 KCL(1) = 0
      GO TO 34
   33 KCL(1) = 1
```

```
   34 NL = 0
      NSEG = NNSG(1)
      NR = 0
      NL1 = 0
      NSLS = 0
      NSLS1 = 0
      NS1 = NSEG + 1
      LSLS = 0
      IXT = NXTL(1)
      JXT = NXTR(1)
      NSS = JXT-IXT
      NCB = NCBA(1)
      NWD = NCB*NSS
      REWIND 5
C
      DO 210 I = 1,50
      DO 210 J = 1,MX
      PJP(J,I) = 0.0
  210 CONTINUE
C
      DO 213 J = 1,51
      DO 213 I = 1,M3
      PBAR(I,J) = 0.0
  213 CONTINUE
C
      GO TO 28
C
   27 READ 25, NSTG,NSAL(NSTG),NR,NCBA(NSTG),NXTL(NSTG),NXTR(NSTG)
      READ 25, KODJA,KODBC,KODSPT,KREF,KODTS
      IF(NSTG-1)999,999,44
   44 IF(KREF) 43,43,48
   43 KCL(NSTG) = 0
      GO TO 40
   48 KCL(NSTG) = KCL(NSTG-1)+1
   40 NL = NSAL(NSTG)
      NL1 = NL+1
      NSLS = NSEG
      NSLS1 = NS1
      NSEG = NL+NSLS+NR
      NNSG(NSTG) = NSEG
      NCB = NCBA(NSTG)
      NS1 = NSEG+1
      LSLS = NSLS+NL
      IF(NCB.EQ.0) GO TO 55
      IXT = NXTL(NSTG)
      JXT = NXTR(NSTG)
      NSS = JXT-IXT
      NWD = NSS*NCB
      IF(NL) 999,49,29
C
C     RESUBSCRIPT FORCE AND INDICATOR ARRAYS
C
   29 L = LSLS+1
      DO 45 J = 1,NSLS
      K = L-J
      KK = K+1
      M = L-NL-J
      MM = M+1
      DO 46 I = 1,MX
      PJP(I,K) = PJP(I,M)
      PJP(I,M) = 0.0
      AJP(I,K) = AJP(I,M)
      LIND(I,K) = LIND(I,M)
   46 CONTINUE
      DO 41 I = 1,M3
      PBAR(I,KK) = PBAR(I,MM)
      PBAR(I,MM) = 0.0
   41 CONTINUE
      ISTOP(K) = ISTOP(M)
   45 CONTINUE
      DO 47 I = 1,M3
      PBAR(I,NL1) = PBAR(I,1)
      PBAR(I,1) = 0.0
   47 CONTINUE
   49 IF(KCL(NSTG)-2)28,65,69
   65 NSRF = NSLS1
      NSRF1 = NSRF+1
      DO 66 J = 1,NSLS
      DO 66 I = 1,MX
      AJP(I,J) = 0.0
      LIND(I,J) = 0
   66 PJP(I,J) = 0.0
      DO 67 J = 1,NSRF1
      DO 67 I = 1,M3
   67 PBAR(I,J) = 0.0
   69 IF(JXT-NSRF1) 61,61,62
   61 NWD = (JXT-IXT)*NCB
      GO TO 28
   62 NWD = (NSRF1-IXT)*NCB
C
   28 CALL STAGE
   55 CALL STEP
         CALL SOLV
         GO TO 27
  999    CALL EXIT
         END
      SUBROUTINE STAGE
C
C        FORMATS
C
```

```
  306 FORMAT(13X,I3,14X,F7.3,5X,E15.6,6X,E15.6)
  415 FORMAT(1HO,20X,41HINITIAL TENDON STRESS AFTER FRICTION LOSS//20X,3
     14HTENDON     SEGMENT          STRESS//)
  416 FORMAT(23X,I2,9X,I2,10X,E15.6)
  425 FORMAT(1H1,20X,40HINPUT DATA FOR CABLES STRESSED AT STAGE I2//)
  400 FORMAT(2I4,2X,F10.0)
  405 FORMAT(1H1,20X,42HLONG. CONFIGURATION OF STRUCTURE AT STAGE I3/)
  410 FORMAT(1HO,20X,7HSPAN = F8.3/20X,18HNO. OF SEGMENTS = I3/20X,26HNO
     1. OF TENDONS STRESSED = I2)
  420 FORMAT(1HO,20X,7HSPAN = F8.3/20X,18HNO. OF SEGMENTS = I3/20X,26HNO
     1. OF TENDONS STRESSED = I2/20X,22HNO. SEG. ADDED LEFT = I3/20X,23H
     2NO. SEG. ADDED RIGHT = I3)
  430 FORMAT(1HO,20X,14HSEGMENT NUMBER,5X,14HSEGMENT LENGTH/)
  440 FORMAT(28X,I3,14X,F8.3)
  427 FORMAT(1HO,20X,13HTENDON NO. = I3/20X,7HAREA = E15.6/20X,13HNO. CU
     1RVES = I3/20X,10HELEMENT = I3//20X,21HINITIAL JACK FORCE = E15.6/2
     20X,19HFINAL JACK FORCE = E15.6/20X,17HLIVE END INDEX = I3//20X,13H
     3DIVERGENCE = E15.6/20X,12HSTA. LEFT = I3/20X,13HSTA. RIGHT = I3)
  424 FORMAT(I22,6X,I2,2X,3(F10.3,2X),I2,2X,F10.3)
  428 FORMAT(1HO,20X,19HCONTROL COORDINATES//20X,59HCURVE     NXL      YL
     1          XM          YM       NXR      YR//)
   60 FORMAT(3I4,F8.0,2F10.0,I5)
   70 FORMAT(F10.0,2I5)
   51 FORMAT(I10,3F10.0,I10,F10.0)
C
C      COMMON DIMENSION AND EQUIVALENCE STATEMENTS
C
       COMMON NSTG,NSRF,NS  ,SEGL,NL,NL1,NR,NSLS,NSLS1,NS1,LSLS,NSS,NWD,
      1NCB,IXT,JXT,NPL,NJT,NEL,M3,MX,M6,M31,NXBAND,MAXJTD,YMS,CLC,CFC,
      2NSTOP,KODJA,KODBC,KODSPT,KODTS
       COMMON H(15),V(15),TH(15),E(15),PWTH(15),NPI(15),NPJ(15),KPL(15),
      1NPDIF(15),ZEND(90),BCORI(3,15),IORI(3,15),BCEND(3,15),IEND(3,15),
      2IED(45,4),SSC(45,4),ZK(90,46),IFD(90)
       COMMON NNSG(25),NSAL(25),NC8A(25),KCL(25),NXTL(25),NXTR(25),
      1IDXF(25),IDXS(25),XSEC(51),ISTOP(50),KANCH(50),AJP(64,50),
      2PJP(64,50),LIND(64,50),PBAR(45,51),NELC(25),AREA(25)
       COMMON BIGK(64,20),PTTT(64,46),CM(9,15),HM(17,15),FJ(9,15),
      1A(4,4),BTAV(4),RBAR(4),D(20),ZZ(6)
C
       DIMENSION FK(51,6),FKL(51,6),FKR(51,6),YK(50,6),THET(51,6),
      1THETH(50),YLE(6),YRE(6),ASL(10),PBARO(45),PBARE(45),VFK(300)
C
       EQUIVALENCE (ZK,FK),(ZK(307),FKL),(ZK(614),FKR),(ZK(920),YK),
      1(ZK(1221),THET),(ZK(1528),THETH),(ZK(1579),YLE),(ZK(1586),YRE),
      2(ZK(1593),ASL),(ZK(1604),PBARO),(ZK(1651),PBARE),(ZK(1698),VFK)
C
       IXTP = IXT+1
       JXTM = JXT-1
       IF(NSTG-1)20,20,10
C
   10 KC = KC+NCBA(NSTG-1)
C
C
C      RECOMPUTE STATION COORDINATES FOR LAST STAGE STRUCTURE.
C
       IF(NL) 7,100,7
    7  SASL = 0.0
   17  READ 400, ISEC, JSEC, SL
       JSECM = JSEC-1
       DO 8 I = ISEC,JSECM
       ASL(I) = SL
       SASL = SASL+ASL(I)
    8  CONTINUE
       IF(JSEC-NL1) 17,9,9
    9  I = NSLS1+NL1
       K = NSLS1+1
       DO 14 J = 1,NSLS1
       XSEC(I-J) = XSEC(K-J)+SASL
   14  CONTINUE
C
C      COMPUTE STATION COORDINATES FOR ADDED SEGMENTS.
C
       XSEC(1) = 0.0
       DO 15 L = 2,NL
       XSEC(L) = XSEC(L-1)+ASL(L-1)
   15  CONTINUE
  100  IF(NR)11,110,11
   11  READ 400, ISEC, JSEC, SL
       JSECM = JSEC-1
       DO 16 I = ISEC,JSECM
       XSEC(I+1) = XSEC(I)+SL
   16  CONTINUE
       IF(JSEC-NS1)11,110,110
   20  KC = 0
C
C      COMPUTE STATION COORDINATES FOR FIRST STAGE STRUCTURE
C
       XSEC(1) = 0.0
   21  READ 400, ISEC, JSEC, SL
       JSECM = JSEC-1
       DO 22 L = ISEC,JSECM
       XSEC(L+1) = XSEC(L)+SL
   22  CONTINUE
       IF(JSEC-NS1)21,110,110
  110  PRINT 405, NSTG
       IF(NSTG-1)115,115,120
  115  PRINT 410, XSEC(NS1),NS,NCB
       GO TO 204
  120  PRINT 420, XSEC(NS1),NS,NCB,NL,NR
  204  PRINT 430
```

```
      DO 206 J = 1,NS
      SL = XSEC(J+1)-XSEC(J)
      PRINT 440, J,SL
  206 CONTINUE
      PRINT 425, NSTG
C
C     INITIALIZE THE PBARD AND PBARE VECTORS
C
      DO 23 J = 1,M3
      PBARD(J) = 0.0
      PBARE(J) = 0.0
   23 CONTINUE
C
C     COMPUTATION OF CABLE Y-COORDINATES AND FORCES AFTER LOSS FOR ALL SEGMENT
C
      DO 104 N = 1,NCB
      READ 60, KN,NCV,NELC(KN),AREA(KN),PIP,PIPP,KEEP
      READ 70, FO,NXCVGL,NXCVGR
      IF(PIPP) 29,29,30
   29 PIP2 = PIP
      GO TO 28
   30 PIP2 = PIPP
   28 PRINT 427, KN,AREA(KN),NCV,NELC(KN),PIP,PIP2,KEEP,FO,NXCVGL,NXCVGR
      PRINT 428
      DO 200 KV = 1,NCV
      READ 51, NXL,YL,XM,YM,NXR,YR
      PRINT 424, KV,NXL,YL,XM,YM,NXR,YR
      IF(KV.EQ.1)YLE(N) = YL
      IF(KV.EQ.NCV)YRE(N) = YR
      XL = XSEC(NXL)
      XR = XSEC(NXR)
      IF(XM) 50,50,37
   37 XL2 = XL*XL
      XM2 = XM*XM
      XR2 = XR*XR
C
      DET = XM*XR2 + XL*XM2 + XR*XL2 - XM*XL2 - XR*XM2 - XL*XR2
      DETX = YL*XM*XR2 + XL*XM2*YR + XL2*YM*XR -
     1       YR*XM*XL2 - XR*XM2*YL - XR2*YM*XL
      AC = DETX/DET
      DETX = YM*XR2 + YL*XM2 + XL2*YR - YM*XL2 - YR*XM2 - XR2*YL
      BC = DETX/DET
      DETX = XM*YR + XL*YM + YL*XR - XM*YL - XR*YM - YR*XL
      CC = DETX/DET
      GO TO 52
   50 BC = (YR-YL)/(XR-XL)
      AC = YL-(BC*XL)
      CC = 0.0
C
C     CALC. YK AT CABLE NODES-THETA AT CABLE STATIONS.
C
   52 NXRM = NXR-1
      IF(KV-1) 200,46,47
   46 XX = XSEC(NXL)
      THET2 = ATAN(BC+2.0*CC*XX)
   47 CONTINUE
      DO 200 L = NXL,NXRM
      K = L+1
      XX = (XSEC(L)+XSEC(K))/2.0
      YK(L,N) = AC+BC*XX+CC*XX*XX
      IF(L-NXL) 200,48,49
   48 THET1 = ATAN(BC+2.0*CC*XSEC(L))
      THET(L,N) = (THET1 + THET2)/2.0
      IF(L-NXRM) 200,55,200
   55 THET2 = ATAN(BC+2.0*CC*XSEC(K))
      IF(NXR.EQ.JXT)THET(K,N) = THET2
      GO TO 200
   49 THET(L,N) = ATAN(BC+2.0*CC*XSEC(L))
      IF(L-NXRM) 200,61,200
   61 THET2 = ATAN(BC+2.0*CC*XSEC(K))
      IF(NXR.EQ.JXT)THET(K,N) = THET2
  200 CONTINUE
C
      DO 71 I = IXT,JXTM
      THETH(I) = 0.0
   71 CONTINUE
C
C     TEST FOR CABLE DIVERGENCE FROM SINGLE PLANE.
C
      IF(FO)69,69,54
C
C     ASSUMING CONVERGENCE LENGTH AT BOTH ENDS TO BE THE SAME.
C
   54 CX = XSEC(NXCVGL)
      G = (6.0*FO)/CX
      DO 59 L = IXT,JXTM
      K = L+1
      IF(L-NXCVGL) 56,63,63
   63 IF(L-NXCVGR)59,58,58
   56 XL1 = XSEC(K)/CX
      XL = XSEC(L)/CX
      GO TO 66
   58 XL1 = (XSEC(K)-XSEC(NXCVGR))/CX
      XL = (XSEC(L)-XSEC(NXCVGR))/CX
   66 THETH(L) = ABS(G*(XL1*XL1-XL*XL-XL1+XL))
   59 CONTINUE
C
C     CALC OF CABLE FORCE FOR EACH STA POINT FOR CABLE N
C
   69 IF(KEEP)153,154,155
```

```
153 FKL(IXT,N) = PIP
    FKR(JXT,N) = 0.0
    GO TO 157
155 FKL(IXT,N) = 0.0
    FKR(JXT,N) = PIP
    GO TO 157
154 FKL(IXT,N) = PIP
    FKR(JXT,N) = PIP
157 MM = 0
    DO 162 J = IXTP,JXT
    MM = MM+1
    K = J-1
    M = JXT-MM
    L = M+1
    DTHL = ABS(THET(J,N)-THET(K,N))+THETH(K)
    DTHR = ABS(THET(M,N)-THET(L,N))+THETH(M)
    CLL = XSEC(J)-XSEC(K)
    CLR = XSEC(L)-XSEC(M)
    FKL(J,N) = FKL(K,N)*(1.0-(CFC*DTHL)-(CLC*CLL))
    FKR(M,N) = FKR(L,N)*(1.0-(CFC*DTHR)-(CLC*CLR))
162 CONTINUE
    DO 164 J = IXT,JXT
    IF(FKL(J,N)-FKR(J,N))163,163,167
163 FK(J,N) = FKR(J,N)
    GO TO 164
167 FK(J,N) = FKL(J,N)
164 CONTINUE
    IF(PIPP)101,101,170
170 IF(KEEP)31,31,39
 31 FK(IXT,N) = PIPP
    L = IXT
 76 K = L+1
    CLL = XSEC(K)-XSEC(L)
    DTHL = ABS(THET(K,N)-THET(L,N))+THETH(L)
    FKP = FK(L,N)*(1.0+(CFC*DTHL)+(CLC*CLL))
    IF(FKP-FK(K,N))33,33,34
 33 FK(K,N) = FKP
    L = L+1
    IF(L-JXT)76,34,34
 34 IF(KEEP)101,39,39
 39 FK(JXT,N) = PIPP
    L = JXTM
 79 K = L+1
    CLR = XSEC(K)-XSEC(L)
    DTHR = ABS(THET(K,N)-THET(L,N))+THETH(L)
    FKP = FK(K,N)*(1.0+(CFC*DTHR)+(CLC*CLR))
    IF(FKP-FK(L,N))36,36,101
 36 FK(L,N) = FKP
    L = L-1
    IF(L-IXT)101,79,79

101 CONTINUE
C
C     FORMATION OF PBARO AND PBARE VECTORS
C
      KKC = KC+ N
      NF = NELC(KKC)*3-3
      I = NF+1
      J = I+1
      K = J+1
      PBARO(I) = PBARO(I)-(FK(IXT,N)*COS(THET(IXT,N))*YLE(N))
      PBARO(J) = PBARO(J)-(FK(IXT,N)*SIN(THET(IXT,N)))
      PBARO(K) = PBARO(K)-(FK(IXT,N)*COS(THET(IXT,N)))
      PBARE(I) = PBARE(I)+(FK(JXT,N)*COS(THET(JXT,N))*YRE(N))
      PBARE(J) = PBARE(J)+(FK(JXT,N)*SIN(THET(JXT,N)))
      PBARE(K) = PBARE(K)+(FK(JXT,N)*COS(THET(JXT,N)))
104     CONTINUE
      IF(KCL(NSTG)-1)105,105,106
105 JJ = JXTM
      GO TO 107
106 JJ = NSRF
107 WRITE(5) ((YK(I,J),J = 1,NCB),I = IXT,JJ)
C
C     SUMMATION OF PARO AND PBARE VECTORS INTO PBAR ARRAY.
C
308 DO 99 J = 1,M3
      PBAR(J,IXT) = PBAR(J,IXT) + PBARO(J)
      PBAR(J,JXT) = PBAR(J,JXT) + PBARE(J)
 99 CONTINUE
C
C        COMPUTATION AND SUMATION OF EQUIVALENT PRESTRESS FORCES
C
 42 DO 45 L = IXT,JXTM
      M = L+1
      HL = XSEC(M)-XSEC(L)
      DO 45 K = 1,NCB
      KKC = KC+K
      LC = NELC(KKC)
      KP = KPL(LC)
      IDF = NPI(LC)+1
      DTHT = THET(M,K)-THET(L,K)
      FVL = FK(L,K)*SIN(THET(L,K))
      FVR = FK(M,K)*SIN(THET(M,K))
      IF(DTHT) 43,40,44
 43 PI = (-1.0*(ABS(FVL-FVR)))/HL
      GO TO 62
 44 PI = (ABS(FVL-FVR))/HL
      GO TO 62
 40 PI = 0.0
 62 PJP(IDF,L) = PJP(IDF,L)-PI*H(KP)
      PJP(IDF+1,L) = PJP(IDF+1,L)+PI*V(KP)
```

```
   45 CONTINUE
C
      IF(KCL(NSTG)-1)80,80,81
   80 JJ = JXTM
      GO TO 83
   81 JJ = NSRF
C
C     AVERAGING THE CABLE FORCES AT STA POINTS TO OBATIN CABLE FORCE
C     AT THE CABLE NODAL POINTS AT THE CENTER OF EACH SEGMENT
C
   83 PRINT 415
      LM = 0
      DO 78 N = 1,MCB
      KKC = KC+N
      DO 78 L = IXT,JJ
      LM = LM+1
      VFK(LM) = (FK(L,N)+FK(L+1,N))/2.0
      SIG = VFK(LM)/AREA(KKC)
      PRINT 416, KKC,L,SIG
   78 CONTINUE
C
      CALL IOBIN(6HWRITER,4LFXXX,VFK(1),NWO,IDXF(NSTG))
C
      RETURN
         END
      SUBROUTINE STEP
C
C     FORMAT STATEMENTS FOR SUBROUTINE STEP
C
    2 FORMAT(1H08X,26H INDEX = 0 FOR GIVEN FORCE/17X,25H 1 FOR GIVEN DIS
     1PLACEMENT//)
   10 FORMAT(I10,3F10.0,3I2)
   11 FORMAT(37H1ORIGIN BOUNDARY CONDITIONS AT STAGE I3)
   27 FORMAT(I10,4F10.0,4I2)
   41 FORMAT(3I4)
   45 FORMAT(4I4,4X,3F15.0)
  112 FORMAT (85HOELE      AXIAL FOR/DISP  INDEX      SHEAR FOR/DISP  IN
     1DEX       MOMENT OR ROT  INDEX/(I4,3(E20.8,I5,2X)))
  862 FORMAT(2I4)
  850 FORMAT(1H1,3X,51HJOINT ACTIONS, SUPPORT AND STOPOVER DATA FOR STAG
     1E I3//10X,44HIAJA = 0, JOINT ACTIONS SAME AS LAST SEGMENT/16X,44H1
     2, JOINT ACTIONS DIFFERENT FROM LAST SEGMENT//9X,45HIAJA2 = 0, JOIN
     3T ACTIONS SAME AS LAST SEGMENT/16X,35H1, JOINT ACTIONS SAME AS LAS
     4T STAGE/16X,29H2, JOINT ACTIONS RE-SPECIFIED//9X,37HISTOP =-1, SUP
     5PORT AFTER THIS SEGMENT/16X,25H0, NO SUPPORT OR STOPOVER/16X,30H1,
     6 STOPOVER AFTER THIS SEGMENT///)
   42 FORMAT(14X,4HSEG I2,4X,7HIAJA = I2,4X,8HISTOP = I2)
  847 FORMAT(    16X,21HAPPLIED JOINT ACTIONS//2X,3HJT.,5X,6HHORIZ.,6X,3
     1HF/D,6X,5HVERT.,5X,3HF/D,6X,4HROT.,6X,3HM/R,5X,5HLONG.,6X,3HF/D/)
  851 FORMAT(I4,3X,4(F14.7,1X,I2,2X)/)
  860 FORMAT(1HO,85H**********************************************************
     1**********************************//)
  848 FORMAT(16X,27HINTERIOR SUPPORT RESTRAINTS//10X,70HELE.   AXIAL   C
     1OEFFICIENT   SHEAR    COEFFICIENT   ROT.   COEFFICIENT)
   43 FORMAT(14X,4HSEG I2,3X,8HIAJA2 = I2,4X,8HISTOP = I2)
  890 FORMAT(14X,21HJT. ACTIONS FOR SEG. I3,6H THRU I3,26H UNCHANGED FRO
     1M LAST STAGE)
  866 FORMAT(I12,6X,3(I2,3X,E15.6,3X))
C
C     COMMON, DIMENSION AND EQUIVALENCE STATEMENTS
C
      COMMON NSTG,NSRF,NSEG,SEGL,NL,NL1,NR,NSLS,NSLS1,NS1,LSLS,NSS,NWD,
     1NCB,IXT,JXT,NPL,NJT,NEL,M3,MX,M6,M31,NXBAND,MAXJTD,YMS,CLC,CFC,
     2NSTOP,KODJA,KODBC,KODSPT,KODTS
      COMMON H(15),V(15),TH(15),E(15),PWTH(15),NPI(15),NPJ(15),KPL(15),
     1NPDIF(15),ZEND(90),BCORI(3,15),IORI(3,15),BCEND(3,15),IEND(3,15),
     2IED(45,4),SSC(45,4),ZK(90,46),IFD(90)
      COMMON NNSG(25),NSAL(25),NCBA(25),KCL(25),NXTL(25),NXTR(25),
     1IDXF(25),IDXS(25),XSEC(51),ISTOP(50),KANCH(50),AJP(64,50),
     2PJP(64,50),LIND(64,50),PBAR(45,51),NELC(25),AREA(25)
      COMMON BIGK(64,20),PTTT(64,46),CM(9,15),HM(17,15),FJ(9,15),
     1A(4,4),BTAV(4),RBAR(4),D(20),ZZ(6)
C
      DIMENSION DISP(64,46),SMALLK(8,8,15),ZSTOP(45,91), IDU(45)
C
      EQUIVALENCE (BIGK,ZSTOP),(PTTT,DISP,SMALLK)
C
C     SET UP BOUNDARY ACTION, INDICATOR ARRAYS AT ORIGIN
C
      IF(NSTG.EQ.1.OR.KODBC.EQ.1)READ10,(I,(BCORI(J,I),J=1,3),
     1(IORI(K,I),K=1,3),L=1,NEL)
      PRINT 11,NSTG
      PRINT 112, (I,(BCORI(J,I),IORI(J,I),J=1,3),I=1,NEL)
      PRINT 2
      DO 104 I=1,M31
      DO 104 J=1,M6
  104 ZK(J,I)=0.
      L=0
      DO 108 I=1,NEL
      M=6*I+1
      MM = I*3+1
      N=M-7
      DO 108 J=1,3
      L=L+1
      M=M-1
      N=N+1
      MM = MM-1
      IFD(M)=0
      IFD(N)=1
      IF (IORI(J,I)) 107,106,107
```

```
  106 ZK(N,L)=1.
      ZK(M,M31)=BCORI(J,I)+PBAR(MM,1)
      GO TO 108
  107 ZK(M,L)=1.
      ZK(N,M31)=BCORI(J,I)
  108 CONTINUE
C
C     INITATION OF FORWARD PROGRESSION
C
      NN = 0
      NSTOP = 0
      SEGL = 0.0
      KSPT = 0
      IF(NSTG.EQ.1)NSPT = 0
      REWIND 1
      REWIND 8
      PRINT 850, NSTG
C
  131 NN = NN + 1
C
      IF(NN-1)930,930,940
  930 SEGL = XSEC(2)
      FSEGL = XSEC(3)-XSEC(2)
      FDSL = FSEGL-SEGL
      PDSL = 1.0
      GO TO 100
  940 IF(NSEG-NN)935,935,945
  935 PSEGL = SEGL
      SEGL = FSEGL
      PDSL = PSEGL-SEGL
      FDSL = 1.0
      GO TO 100
  945 PSEGL = SEGL
      SEGL = FSEGL
      FSEGL = XSEC(NN+2)-XSEC(NN+1)
      PDSL = PSEGL-SEGL
      FDSL = FSEGL-SEGL
C
  100 IF(NN-NL)102,102,101
  101 IF(NN-LSLS)105,105,102
C
  102 READ 41, NN,IAJA,ISTOP(NN)
      PRINT 42, NN,IAJA,ISTOP(NN)
C
      IF(IAJA)3,4,3
C
    4 L = NN-1
      DO 7 J = 1,MX
      AJP(J,NN) = AJP(J,L)
      LIND(J,NN) = LIND(J,L)
    7 CONTINUE
      GO TO 9
C
    3 PRINT 860
      PRINT 847
      KDF = 0
      DO 5 L = 1,NJT
      READ 27, JT,(AJP(KDF+I,NN),I=1,4),(LIND(KDF+I,NN),I=1,4)
      PRINT 851, L,(AJP(KDF+I,NN),LIND(KDF+I,NN),I=1,4)
      KDF = KDF+4
    5 CONTINUE
      PRINT 2
      PRINT 860
C
    9 IF(ISTOP(NN))8,814,814
    8 IF(NN-NL)910,910,905
  905 IF(NN-NSEG)907,920,920
  907 KSPT = KSPT+1
      GO TO 71
C
  920 NSPT = KSPT
      GO TO 814
C
  910 KSPT = KSPT + 1
      K = NSPT + 1
   24 CONTINUE
      L = K-1
      IF(L)71,71,73
   73 DO 48 J = 1,M3
      IED(J,K) = IED(J,L)
      SSC(J,K) = SSC(J,L)
   48 CONTINUE
      K = K-1
      GO TO 24
C
   71 CONTINUE
C
      DO 13 I = 1,NEL
      KDF = I*3-3
      READ 45, L,(IED(KDF+L,KSPT),L = 1,3),(SSC(KDF+L,KSPT),L = 1,3)
   13 CONTINUE
      PRINT 860
      PRINT 848
      DO 14 I = 1,NEL
      KDF = I*3-3
      PRINT 866, I,(IED(KDF+L,KSPT),SSC(KDF+L,KSPT),L = 1,3)
   14 CONTINUE
      PRINT 860
      GO TO 814
C
```

```
  105 IF(KODJA)806,874,806
C
  874 IF(NN-NL1)820,820,810
  820 PRINT 860
      PRINT 890, NL1,LSLS
      PRINT 860
      GO TO 810
C
  806 READ 862, NN,IAJA2
      PRINT 43, NN,IAJA2,ISTOP(NN)
      IF(IAJA2-1)830,810,802
  830 L = NN-1
      DO 831 J = 1,MX
      AJP(J,NN) = AJP(J,L)
  831 LIND(J,NN) = LIND(J,L)
      GO TO 810
  802 PRINT 860
      PRINT 847
      KDF = 0
      DO 805 L = 1,NJT
      READ 27, JL,(AJP(KDF+I,NN),I = 1,4),(LIND(KDF+I,NN),I = 1,4)
      PRINT 851, L,(AJP(KDF+I,NN),LIND(KDF+I,NN),I = 1,4)
      KDF = KDF+4
  805 CONTINUE
      PRINT 2
      PRINT 860
C
  810 IF(ISTOP(NN))808,814,814
  808 KSPT = KSPT+1
      IF(KODSPT)74,814,74
   74 PRINT 860
      PRINT 848
      DO 812 I = 1,NEL
      KDF = I*3-3
      READ 45, L,(IED(KDF+L,KSPT),L = 1,3),(SSC(KDF+L,KSPT),L = 1,3)
      PRINT 866, I,(IED(KDF+L,KSPT),SSC(KDF+L,KSPT),L = 1,3)
  812 CONTINUE
      PRINT 860
C
  814 IF(PDSL) 144,215,144
C
C         FORMATION OF BIGK MATRIX FOR SEGMENT NN
C
  144 DO 145 J=1,NXBAND
      DO 145 I=1,MX
  145 BIGK(I,J)=0.
C
      CALL STIF
C
      DO 210 L=1,NEL
      K=KPL(L)
      M=NPI(L)
      N=NPJ(L)
      DO 201 I=1,4
      II=M+I
      IJ=N+I
      IK=I+4
      DO 201 J=1,4
      BIGK(II,J)=BIGK(II,J)+SMALLK(I,J,K)
  201 BIGK(IJ,J)=BIGK(IJ,J)+SMALLK(IK,J+4,K)
      IF (NPDIF(L)) 205,202,202
  202 IK=N-M-4
      DO 203 I=1,4
      II=M+I
      DO 203 J=5,8
      IJ=IK+J
  203 BIGK(II,IJ)=BIGK(II,IJ)+SMALLK(I,J,K)
      GO TO 210
  205 IK=M-N
      N=N-4
      DO 206 I=5,8
      II=N+I
      DO 206 J=1,4
      IJ=IK+J
  206 BIGK(II,IJ)=BIGK(II,IJ)+SMALLK(I,J,K)
  210 CONTINUE
  211    IF(PDSL) 220,212,220
  212 REWIND 3
      WRITE (3) ((BIGK(I,J),I=1,MX),J=1,NXBAND)
      END FILE 3
      GO TO 220
C
  215 REWIND 3
      READ (3) ((BIGK(I,J),I=1,MX),J=1,NXBAND)
C
C     CALCULATE  -(FIXED JOINT FORCES)
C
  220 DO 221 J=1,M31
      DO 221 I=1,MX
  221 PTTT(I,J)=0.
      U1=2./SEGL
      DO 240 L=1,NEL
      M=KPL(L)
      DO 225 I=1,9
  225 D(I)=CM(I,M)
      HD=H(M)
      VD=V(M)
      I1=NPI(L)+1
      I2=I1+1
      I4=I1+3
```

```
      J1=NPJ(L)+1
      J2=J1+1
      J4=J1+3
      N=6*L-6
      DO 240 I=1,M31
      DO 230 J=1,6
      K=J+N
  230 ZZ(J)=ZK(K,I)
      C1=D(1)*ZZ(1)+U1*ZZ(6)
      C2=D(2)*ZZ(2)+D(3)*ZZ(3)+D(4)*ZZ(4)+D(5)*ZZ(5)
      C=C1+C2
      C1=C1-C2
      PTTT(I4,I)=PTTT(I4,I)+C
      PTTT(J4,I)=PTTT(J4,I)+C1
      C1=D(7)*ZZ(2)+D(8)*ZZ(3)+D(9)*ZZ(4)+D(6)*ZZ(5)
      C2=-C1
      PTTT(I1,I)=PTTT(I1,I)-HD*C1
      PTTT(I2,I)=PTTT(I2,I)+VD*C1
      PTTT(J1,I)=PTTT(J1,I)+HD*C2
      PTTT(J2,I)=PTTT(J2,I)-VD*C2
  240 CONTINUE
         DO 241 I = 1,MX
  241    PTTT(I,M31) = PTTT(I,M31)+PJP(I,NN)
         DO 243 I = 1,MX
         IF(LIND(I,NN))243,242,243
  242    PTTT(I,M31) = PTTT(I,M31) + AJP(I,NN)
  243    CONTINUE
C
C     CHECK FOR SPECIFIED DISPLACEMENT - MODIFY BIGK MATRIX
C
         DO 260 J = 1,NJT
         DO 260 I = 1,4
         IL = (J-1)*4+1
      IF(LIND(IL,NN))245,260,245
  245    C = AJP(IL,NN)
         IF(C)246,252,246
  246    II = IL-I
         DO 248 K = 5,NXBAND
         L = K+II
         IF(LIND(L,NN))248,247,248
  247    PTTT(L,M31) = PTTT(L,M31) - BIGK(IL,K)*C
  248 CONTINUE
  252 DO 253 L=1,NXBAND
  253 BIGK(IL,L)=0.0
      DO 254 L=1,M31
  254 PTTT(IL,L)=0.
      PTTT(IL,M31)=C
      K=J-MAXJTD
      L=MAXO(K,1)
      DO 255 M=L,J
      N=(J-M)*4+I
      II=(M-1)*4
      DO 255 IJ=1,4
      IK=II+IJ
         IF(LIND(IK,NN))255,256,255
  256 PTTT(IK,M31)=PTTT(IK,M31)-BIGK(IK,N)*C
  255 BIGK(IK,N)=0.0
      BIGK(IL,I)=1.0
  260    CONTINUE
C
C     INVERT DIAGONAL K AND MODIFY BIGK AND PTTT FOR BACKSUBSTITUTION
C
      N=0
  300 N=N+1
      IL=N*4
      L=IL-4
      DO 301 I=1,4
      K=I+L
      DO 301 J=1,4
  301 A(I,J)=BIGK(K,J)
      CALL DSYINV (A)
      K=NJT-N
      IF (K) 400,400,302
C
  302 M=MINO(K,MAXJTD)
      IK=M*4
      DO 305 I=1,4
      II=I+L
      DO 305 J=1,4
  305 BIGK(II,J)=A(I,J)
C
      J=0
      DO 340 IM=1,M
      DO 340 IN=1,4
      J=J+1
      IJ=J+4
C
      DO 320 I=1,4
  320 BTAV(I)=BIGK(L+1,IJ)*A(1,I)+BIGK(L+2,IJ)*A(2,I)+BIGK(L+3,IJ)*
     1A(3,I)+BIGK(L+4,IJ)*A(4,I)
C
      K=J+IL
      DO 330 I=1,M31
  330 PTTT(K,I)=PTTT(K,I)-(BTAV(1)*PTTT(L+1,I)+BTAV(2)*PTTT(L+2,I)
     1+BTAV(3)*PTTT(L+3,I)+BTAV(4)*PTTT(L+4,I))
C
      IS=0
      IU=IM*4-3
      DO 340 I=IU,IK
      IT=I+4
```

```
      IS=IS+1
      BIGK(K,IS)=BIGK(K,IS)-(BTAV(1)*BIGK(L+1,IT)+BTAV(2)*BIGK(L+2,IT)
     1+BTAV(3)*BIGK(L+3,IT)+BTAV(4)*BIGK(L+4,IT))
  340 CONTINUE
      GO TO 300
C
C     START BACKSUBSTITUTION AND SOLVE FOR UNKNOWN JOINT DISPLACEMENTS
C
C     L=IL-4      SEE AFTER STATEMENT 300
  400 DO 403 K=1,M31
      RBAR(1)=PTTT(L+1,K)
      RBAR(2)=PTTT(L+2,K)
      RBAR(3)=PTTT(L+3,K)
      RBAR(4)=PTTT(L+4,K)
      DO 403 I=1,4
      J=I+L
  403 DISP(J,K)=A(I,1)*RBAR(1)+A(I,2)*RBAR(2)+A(I,3)*RBAR(3)+A(I,4)*
     1 RBAR(4)
C     N=NJT        FROM STATEMENT 300
  410 N=N-1
      IF(N) 465,465,411
  411 M=MIN0((NJT-N),MAXJTD)*4+4
      IN=N*4
      IL=IN-4
      IM=IL+1
      DO 425 K=1,M31
      DO 415 I=5,M
      J=I+IL
  415 D(I)=DISP(J,K)
      DO 420 I=1,4
      II=IL+I
      C=0.0
      DO 418 J=5,M
  418 C=C+BIGK(II,J)*D(J)
  420 RBAR(I)=PTTT(I1,K)-C
      DO 425 I=IM,IN
  425 DISP(I,K)=BIGK(I,1)*RBAR(1)+BIGK(I,2)*RBAR(2)+BIGK(I,3)*RBAR(3)
     1 +BIGK(I,4)*RBAR(4)
      GO TO 410
C
C     WRITE ZK, DISP ON TAPE 1
C
  465 IF(KCL(NSTG)-1)440,440,455
  455 IF(NN-NSRF)440,440,450
  440 WRITE (1)  NN,SEGL,((ZK(I,J),I=1,M6),J=1,M31),((DISP(I,J),I=1,MX),
     1 J=1,M31)
C
C     ZK DUE TO FIXED JOINT
C
  450 DO 500 L = 1,NEL
      M=KPL(L)
      DO 460 I=1,17
  460 D(I)=HM(I,M)
      N=6*L-6
      DO 500 I=1,M31
      DO 470 J=1,6
      K=J+N
  470 ZZ(J)=ZK(K,I)
      ZK(N+1,I)=-3.*ZZ(1)+D(1)*ZZ(6)
      ZK(N+2,I)=ZZ(2)*D(3)+ZZ(3)*D(4)+ZZ(4)*D(5)+ZZ(5)*D(6)
      ZK(N+3,I)=ZZ(2)*D(7)+ZZ(3)*D(8)+ZZ(4)*D(9)+ZZ(5)*D(10)
      ZK(N+4,I)=ZZ(2)*D(11)+ZZ(3)*D(12)+ZZ(4)*D(13)+ZZ(5)*D(14)
      ZK(N+5,I)=ZZ(2)*D(15)-ZZ(3)*D(11)+ZZ(4)*D(16)+ZZ(5)*D(17)
      ZK(N+6,I)=D(2)*ZZ(1)-3.*ZZ(6)
  500 CONTINUE
C
C     MODIFY ZK DUE TO JOINT DISPLACEMENT
C
      DO 600 L=1,NEL
      I1=NPI(L)+1
      I2=I1+1
      I4=I1+3
      J1=NPJ(L)+1
      J2=J1+1
      J4=J1+3
      M=KPL(L)
      HD=H(M)
      VD=V(M)
      N=6*L-6
      DO 550 I=1,9
  550 D(I)=FJ(I,M)
      DO 600 I=1,M31
      U1=DISP(I4,I)
      U2=DISP(J4,I)
      V1=-HD*DISP(I1,I)+VD*DISP(I2,I)
      V2=HD*DISP(J1,I)-VD*DISP(J2,I)
      C1=U1+U2
      ZK(N+1,I)=ZK(N+1,I)+2.*C1
      ZK(N+6,I)=ZK(N+6,I)+D(5)*C1
      C1=U1-U2
      C2=V1-V2
      ZK(N+2,I)=ZK(N+2,I)+D(1)*C1+D(6)*C2
      ZK(N+3,I)=ZK(N+3,I)+D(2)*C1+D(7)*C2
      ZK(N+4,I)=ZK(N+4,I)+D(3)*C1+D(8)*C2
      ZK(N+5,I)=ZK(N+5,I)+D(4)*C1+D(9)*C2
  600 CONTINUE
      IF(NSEG-NN) 720,720,555
  555 L = NN+1
C
C     MODIFY ZK VECTOR DUE TO THE ANCHORAGE FORCE VECTOR
```

```
C
      DO 565 I = 1,NEL
      M = I*6-3
      N = I*3-3
      DO 565 J = 1,3
      MJ = M+J
      NJ = N+J
  565 ZK(MJ,M31) = ZK(MJ,M31) + PBAR(NJ,L)
  601    IF(ISTOP(NN)) 605,131,605
C
C     SET UP ZK FOR NEXT SEGMENT AFTER A STOPOVER OR AN INTERIOR SUPPORT
C
  605 NSTOP=NSTOP+1
      L=0
      DO 610 M=1,M6
      IF (IFD(M)) 607,610,607
  607 L=L+1
      ZSTOP(L,M31)=-ZK(M,M31)
      DO 609 N=1,M3
  609 ZSTOP(L,N)=ZK(M,N)
  610 CONTINUE
C
        IF(ISTOP(NN)) 650,131,620
C
  620 M=M31+1
      N=M31+M3
      DO 630 I=M,N
      L=I-M31
      DO 625 J=1,M3
  625 ZSTOP(J,I)=0.
  630 ZSTOP(L,I)=1.
      CALL OSIMEQ (ZSTOP,M3,M31)
      WRITE (8)NN,ISTOP(NN),M3,((ZK(I,J),I=1,M6),J=1,M31),(ZSTOP(I,M31),
     1I=1,M3),((ZSTOP(I,J),I=1,M3),J=M,N),(IED(I),I=1,M3)
C       IED IS A DUMMY HERE
      L=0
      DO 640 I=1,M6
      IF (IFD(I)) 637,632,637
  632 DO 633 J=1,M3
  633 ZEND(J)=ZK(I,J)
      DO 635 J=1,M3
      M=M31+J
      C=0.
      DO 634 K=1,M3
  634 C=C+ZEND(K)*ZSTOP(K,M)
  635 ZK(I,J)=C
      C=0.
      DO 636 K=1,M3
  636 C=C+ZEND(K)*ZSTOP(K,M31)
      ZK(I,M31)=ZK(I,M31)+C
      GO TO 640
  637 L=L+1
      DO 638 J=1,M31
  638 ZK(I,J)=0.
      ZK(I,L)=1.
  640 CONTINUE
      GO TO 131
C
  650 I=M31
      IU = 0
      DO 660 L=1,M3
      IF(IED(L,KSPT))654,654,660
  654 I=I+1
      IU = IU + 1
      IDU(IU) = L
      DO 655 J=1,M3
  655 ZSTOP(J,I)=0.
      ZSTOP(L,I)=1.
  660 CONTINUE
      N=I
      M=M31+1
      K=N-M31
      L=K+1
      CALL DSIMEQ (ZSTOP,M3,L)
      WRITE (8)NN,ISTOP(NN), K,((ZK(I,J),I=1,M6),J=1,M31),(ZSTOP(I,M31),
     1I=1,M3),((ZSTOP(I,J),I=1,M3),J=M,N),(IED(I,KSPT),I=1,M3)
      IJ=0
      K1=K+1
      L=0
      LL = 0
      DO 710 I = 1,M6
      IF(I.LE.3)GO TO 695
      IF(IFD(I)-IFD(I-1))668,669,695
  668 LL = LL+1
      LM = 0
      GO TO 671
  669 IF(IFD(I))695,670,695
  670 LM = LM+1
  671 IS = 3*LL-LM
      DO 675 J = 1,M3
  675 ZEND(J)=ZK(I,J)
      DO 685 J=1,K
      M=M31+J
      C=0.
      DO 680 N=1,M3
  680 C=C+ZEND(N)*ZSTOP(N,M)
      IF(IDU(J)-IS)682,683,682
  682 ZK(I,J) = C
      GO TO 685
  683 ZK(I,J) = C + SSC(IS,KSPT)
```

```
  685 CONTINUE
      C=0.
      DO 690 N=1,M3
  690 C=C+ZEND(N)*ZSTOP(N,M31)
      ZK(I,M31)=ZK(I,M31)+C
      IF(K1-M3)691,691,710
  691 DO 692 N=K1,M3
  692 ZK(I,N)=0.
      GO TO 710
  695 L=L+1
      DO 700 J=1,M31
  700 ZK(I,J)=0.
      IF(IED(L,KSPT))705,705,710
  705 IJ=IJ+1
      ZK(I,IJ)=1.
  710 CONTINUE
      L=0
      DO 715 I=1,NEL
      DO 715 J=1,3
      L=L+1
      IF(IED(L,KSPT))715,715,712
  712 K=6*I-J+1
      ZK(K,K1)=1.
      K1=K1+1
  715 CONTINUE
      GO TO 131
C
  720 END FILE 1
C
  760 RETURN
      END
      SUBROUTINE SOLV
C
C     COMMON, DIMENSION AND EQUIVALENCE STATEMENTS
C
      COMMON NSTG,NSRF,NSEG,SEGL,NL,NL1,NR,NSLS,NSLS1,NS1,LSLS,NSS,NWD,
     1NCB,IXT,JXT,NPL,NJT,NEL,M3,MX,M6,M31,NXBAND,MAXJTD,YMS,CLC,CFC,
     2NSTOP,KODJA,KODBC,KODSPT,KODTS
      COMMON H(15),V(15),TH(15),E(15),PWTH(15),NPI(15),NPJ(15),KPL(15),
     1NPDIF(15),ZEND(90),BCORI(3,15),IORI(3,15),BCEND(3,15),IEND(3,15),
     21ED(45,4),SSC(45,4),ZK(90,46),IFD(90)
      COMMON NNSG(25),NSAL(25),NCBA(25),KCL(25),NXTL(25),NXTR(25),
     1IDXF(25),IDXS(25),XSEC(51),ISTOP(50),KANCH(50),AJP(64,50),
     2PJP(64,50),LIND(64,50),PBAR(45,51),NELC(25),AREA(25)
      COMMON NI(15),NJ(15),AE(15),E1P(15),EIS(3,15),PP(15),Z(90),
     1ZORI(45),DISP(64,46),D(64),VS(4,15),VP(4,15),SS(4,15),
     2SP(4,15),NN
C
      DIMENSION DA(4,16),ZA(6,15),ZKEND(45,91),ZOR(3,15),IEN(3,15)
      DIMENSION DAR(4,16),VPR(4,15),VSR(4,15),SPR(4,15),SSR(4,15),
     1ZAR(6,15)
C
      EQUIVALENCE (D,DA),(Z,ZA),(DISP,ZKEND),(ZORI,ZOR)
      EQUIVALENCE (DISP,DAR),(DISP(65),VPR),(DISP(126),VSR),(DISP(187),
     1SPR),(DISP(248),SSR),(DISP(309),ZAR)
C
C
C     FORMAT STATEMENTS
C
    2 FORMAT (1H08X,26H INDEX = 0 FOR GIVEN FORCE/17X,25H 1 FOR GIVEN DI
     1SPLACEMENT)
   10 FORMAT(I10,3F10.0,3I2)
  112 FORMAT (85H0ELE      AXIAL FOR/DISP  INDEX      SHEAR FOR/DISP  IN
     1DEX       MOMENT OR ROT  INDEX/(I4,3(E20.8,I5,2X)))
  114 FORMAT(33H1END BOUNDARY CONDITIONS AT STAGE I3)
   11 FORMAT (79H1FINAL PLATE FORCES AND DISPLACEMENTS FOR LONGITUDINAL
     1PLATE ELEMENTS AT ORIGIN)
   12 FORMAT (76H1FINAL PLATE FORCES AND DISPLACEMENTS FOR LONGITUDINAL
     1PLATE ELEMENTS AT END)
   15 FORMAT(1H0,54H PLATE DISPLACEMENTS AND REACTIONS AT INTERIOR SUPPO
     1RT//96H   ELE     I      J   LONG. DISP/REACT. INDEX   TRAN. DISP/R
     2EACT. INDEX    BEAM ROT./REACT. INDEX/(3I6,3(E20.8,I4,2X)))
   13 FORMAT (87H1FINAL PLATE FORCES AND DISPLACEMENTS FOR LONGITUDINAL
     1PLATE ELEMENTS AT END OF SEGMENT I4,15H AND AT SUPPORT)
   16 FORMAT(56H0  INDEX IS -1 OR 0 FOR DISPLACEMENT, AND 1 FOR REACTION
     1)
   20 FORMAT(63H1FINAL JOINT AND PLATE FORCES AND DISPLACEMENTS FOR SEGM
     1ENT NO. I4)
   21 FORMAT (///20H JOINT DISPLACEMENTS//86H JOINT      HORIZONTAL DISP
     1      VERTICAL DISP              ROTATION           LONG. DISP)
   22 FORMAT (I6,4E20.8)
   30 FORMAT (///25H PLATE EDGE DISPLACEMENTS//116H   ELE    I    J     ROT
     1ATION(I)  ROTATION(J)      N(I)          N(J)          U(I)          U
     2(J)          V(I)          V(J))
   31 FORMAT (I6,2I4,2X,1P8E13.5)
   40 FORMAT (///18H PLATE EDGE FORCES//116H    ELE    I    J        M(I)
     1      M(J)          Q(I)          Q(J)          T(I)          T(J)
     2      P(I)          P(J))
C
      SHEAR = 1.0
C     SET UP BOUNDARY CONDITIONS AT END
      IF(NSTG.EQ.1.OR.KODBC.EQ.1)READ 10,(I,(BCEND(J,I),J=1,3),
     1(IEND(K,I),K=1,3),L=1,NEL)
      PRINT 114, NSTG
      PRINT 112,(I,(BCEND(J,I),IEND(J,I),J=1,3),I=1,NEL)
      PRINT 2
      L=0
      DO 750 I = 1,NEL
      M = 6*I+1
      MM = 3*I+1
```

```
      N = M-7
      DO 750 J = 1,3
      M = M-1
      N = N+1
      MM = MM-1
      IF(IEND(J,I))740,730,740
  730 ZEND(M) = BCEND(J,I)-PBAR(MM,NS1)
      L = L+1
      ZKEND(L,M31) = ZEND(M)-ZK(M,M31)
      DO 731 K = 1,M3
  731 ZKEND(L,K) = ZK(M,K)
      GO TO 750
  740 ZEND(N) = BCEND(J,I)
      L = L+1
      ZKEND(L,M31) = BCEND(J,I)-ZK(N,M31)
      DO 741 K = 1,M3
  741 ZKEND(L,K) = ZK(N,K)
  750 CONTINUE
C
      CALL BSIMEQ (ZKEND,M3,1)
C
      DO 800 I=1,M3
  800 ZORI(I)=ZKEND(I,M31)
C
C     INITIATION
C
   50 DO 51 I=1,NEL
      NI(I)=NPI(I)/4+1
   51 NJ(I)=NPJ(I)/4+1
      DO 60 I=1,NPL
      C=PWTH(I)
      C1=C*C
      AE(I)=E(I)*TH(I)*C
      EIP(I)=AE(I)*C1/12.
      C2=E(I)*(TH(I)**3)/C
      EIS(1,I)=C2/6.
      EIS(2,I)=C2/(2.*C)
      EIS(3,I)=C2/C1
   60 PP(I)=6./C1
C
C     CALCULATE AND PRINT PLATE FORCES AND DISPLACEMENTS AT END
C
      DO 80 I=1,M6
      C=0.
      DO 75 J=1,M3
   75 C=C+ZK(I,J)*ZORI(J)
   80 Z(I)=C+ZK(I,M31)
      PRINT 12
      CALL PLFDS
C
C     CALCULATE AND PRINT PLATE FORCES AND DISPLACEMENTS AT STOPOVER OR
C     INTERIOR SUPPORT
C
      NN = NSEG
      IF(NSTOP) 61,61,300
  300 REWIND 3
  301 WRITE (3) NN,(ZORI(I),I=1,M3)
      BACKSPACE 8
      READ(8) NN,ISTOP(NN),MM,((ZK(I,J),I=1,M6),J=1,M31),(ZKEND(I,M31),
     1I=1,M3),((ZKEND(I,J),I=1,M3),J=1,MM),((IEN(J,I),J=1,3),I=1,NEL)
      IF(ISTOP(NN))320,200,340
  320 PRINT 13, NN
      N = 0
      M=MM
      DO 330 I=1,NEL
      DO 330 J=1,3
      IF(IEN(J,I))323,323,325
  323 N=N+1
      ZA(J,I)=ZORI(N)
      GO TO 330
  325 M=M+1
      ZA(J,I)=ZORI(M)
  330 CONTINUE
      PRINT 15, (I,NI(I),NJ(I),(ZA(J,I),IEN(J,I),J=1,3),I=1,NEL)
      PRINT 16
C
  340 DO 345 I=1,MM
  345 Z(I)=ZORI(I)
      DO 350 I=1,M3
      C=0.
      DO 347 J=1,MM
  347 C=C+Z(J)*ZKEND(I,J)
  350 ZORI(I)=C+ZKEND(I,M31)
      DO 360 I=1,M6
      C=0.
      DO 355 J=1,M3
  355 C=C+ZORI(J)*ZK(I,J)
  360 Z(I)=C+ZK(I,M31)
      IF(ISTOP(NN))361,362,362
  361 CALL PLFDS
  362 NSTOP = NSTOP-1
      IF (NSTOP) 61,61,370
  370 BACKSPACE 8
      GO TO 301
C
C     CALCULATE AND PRINT PLATE FORCES AND DISPLACEMENTS AT ORIGIN
C
   61 L=0
      DO 70 I=1,NEL
      M=6*I+1
```

```
      MM = I*3+1
      N=M-7
      DO 70 J=1,3
      L=L+1
      M=M-1
      MM = MM-1
      N=N+1
      IF (IORI(J,I)) 67,65,67
   65 Z(N)=ZORI(L)
      Z(M) = BCORI(J,I) + PBAR(MM,1)
      GO TO 70
   67 Z(M) = ZORI(L)
      Z(N) = BCORI(J,I)
   70 CONTINUE
      PRINT 11
      CALL PLFDS
      NSTOP = NSTOP-1
C
C  READ ZK, DISP FROM TAPE 1 AND FIND STATE VECTORS AT SEGMENT K
C
      MM=MM
      IF(KCL(NSTG)-1)72,73,74
   73 REWIND 9
   72 NRES = NSEG
      GO TO 76
   74 NRES = NSRF
   76 REWIND 1
   90 IF (NRES) 200,200,91
   91 NRES=NRES-1
      READ (1)  MM,SEGL,((ZK(I,J),I=1,M6),J=1,M31),((DISP(I,J),I=1,MX),J
     1=1,M31)
C
  400 IF (NN-MM) 93,93,410
  410 BACKSPACE 3
      READ (3) MM,(ZORI(I),I=1,M3)
      BACKSPACE 3
      GO TO 400
C
   93 SE=SEGL*0.5
      SE2=SE*SE
      DO 95 I=1,M6
      C=0.
      DO 94 J=1,M3
   94 C=C+ZK(I,J)*ZORI(J)
   95 Z(I)=C+ZK(I,M31)
      DO 98 I=1,MX
      C=0.
      DO 97 J=1,M3
   97 C=C+DISP(I,J)*ZORI(J)
   98 D(I)=C+DISP(I,M31)
C
C      CALCULATE AND PRINT PLATE EDGE DISPLACEMENTS
C
      DO 105 L=1,NEL
      II=NPI(L)
      JJ=NPJ(L)
      M=KPL(L)
      HD=H(M)
      VD=V(M)
      VS(1,L)=D(II+3)
      VS(2,L)=D(JJ+3)
      VS(3,L)=-VD*D(II+1)-HD*D(II+2)
      VS(4,L)=VD*D(JJ+1)+HD*D(JJ+2)
      VP(1,L)=D(II+4)
      VP(2,L)=D(JJ+4)
      VP(3,L)=-HD*D(II+1)+VD*D(II+2)
  105 VP(4,L)=HD*D(JJ+1)-VD*D(JJ+2)
C
C      CALCUALTE AND PRINT PLATE EDGE FORCES, PLATE INTERNAL FORCES AND DISPL.
C
      DO 115 L=1,NEL
      M=KPL(L)
      BET=1.2*(PWTH(M)/SE)**2*SHEAR
      BET1=1./(1.+6.*BET)
      C=VS(3,L)+VS(4,L)
      C1=EIS(2,M)*(VS(1,L)+VS(2,L))+EIS(3,M)*C
      SS(3,L)=C1
      SS(4,L)=C1
      C=C*EIS(2,M)
      C1=EIS(1,M)*VS(1,L)
      C2=EIS(1,M)*VS(2,L)
      SS(1,L)=2.*C1+C2+C
      SS(2,L)=C1+2.*C2+C
      CC1=0.5*(VP(1,L)+VP(2,L))
      CC2=0.5*(VP(3,L)-VP(4,L))
      CC3=(VP(1,L)-VP(2,L))/PWTH(M)
      C=0.5*(VP(3,L)+VP(4,L))
      C1=CC1-ZA(1,L)-SE/AE(M)*ZA(6,L)
      C2=CC2-ZA(2,L)+SE*ZA(3,L)+SE2/(2.*EIP(M))*(ZA(4,L)+SE*ZA(5,L)/3.*
     1 (1.-BET))
      C3=CC3-ZA(3,L)-SE/EIP(M)*(ZA(4,L)+SE*ZA(5,L)/2.)
      C4=C1*AE(M)/SE2
      C5=6.*EIP(M)/(PWTH(M)*SE2)*(4.*C2/SE+C3*(1.-2.*BET))*BET1
      SP(1,L)=C4-C5
      SP(2,L)=C4+C5
      C4=C*2.*E(M)*TH(M)/PWTH(M)
      C5=12.*EIP(M)/(SE*SE2)*(3.*C2/SE+C3)*BET1
      SP(3,L)=C4-C5
      SP(4,L)=C4+C5
      ZA(1,L)=CC1
```

```
      ZA(2,L)=CC2
      ZA(3,L)=CC3
      C=6.*EIP(M)/SE*BET1
      ZA(4,L)=ZA(4,L)+SE*ZA(5,L)+C*(C2*2./SE+C3*(1.+2.*BET))
      ZA(5,L)=ZA(5,L)+4.*C/SE*(C2*3./SE+C3)
      ZA(6,L)=ZA(6,L)+2.*AE(M)*C1/SE
  115 CONTINUE
      IF(KCL(NSTG)-1)81,82,83
   82 WRITE(9) ((OA(J,I),J = 1,4),I = 1,NJT),((VS(J,I),VP(J,I),SS(J,I),
     1SP(J,I),J = 1,4),I = 1,NEL),((ZA(J,I),J = 1,6),I = 1,NEL)
      GO TO 81
   83 IF(NN-1)84,84,85
   85 IF(NRES)81,81,86
   84 REWIND 9
   86 READ(9) ((DAR(J,I),J=1,4),I=1,NJT),((VSR(J,I),VPR(J,I),SSR(J,I),
     1SPR(J,I),J = 1,4),I = 1,NEL),((ZAR(J,I),J = 1,6),I = 1,NEL)
      DO 87 I = 1,NJT
      DO 87 J = 1,4
   87 DA(J,I) = DA(J,I)+DAR(J,I)
      DO 88 I = 1,NEL
      DO 88 J = 1,4
      VS(J,I) = VS(J,I)+VSR(J,I)
      VP(J,I) = VP(J,I)+VPR(J,I)
      SS(J,I) = SS(J,I)+SSR(J,I)
   88 SP(J,I) = SP(J,I)+SPR(J,I)
      DO 89 I = 1,NEL
      DO 89 J = 1,6
   89 ZA(J,I) = ZA(J,I)+ZAR(J,I)
   81 PRINT 20, NN
      PRINT 21
      PRINT 22, (I,(DA(J,I),J=1,4),I=1,NJT)
      PRINT 30
      PRINT 31, (I,NI(I),NJ(I),(VS(J,I),J=1,4),(VP(J,I),J=1,4),I=1,NEL)
      PRINT 40
      PRINT 31, (I,NI(I),NJ(I),(SS(J,I),J=1,4),(SP(J,I),J=1,4),I=1,NEL)
      CALL PLFDS
      GO TO 90
  200 CALL CSTRAIN
      RETURN
      END
      SUBROUTINE PLFDS
C
C     TO PRINT FINAL PLATE FORCES AND DISPLACEMENTS
C
C     COMMON, DIMENSION AND EQUIVALENCE STATEMENTS
C
      COMMON NSTG,NSRF,NSEG,SEGL,NL,NL1,NR,NSLS,NSLS1,NS1,LSLS,NSS,NWD,
     1NCB,IXT,JXT,NPL,NJT,NEL,M3,MX,M6,M31,NXBAND,MAXJTD,YMS,CLC,CFC,
     2NSTOP,KODJA,KODBC,KODSPT,KODTS
      COMMON H(15),V(15),TH(15),E(15),PWTH(15),NPI(15),NPJ(15),KPL(15),
     1NPDIF(15),ZEND(90),BCORI(3,15),IORI(3,15),BCEND(3,15),IEND(3,15),
     2IED(45,4),SSC(45,4),ZK(90,46),IFD(90)
      COMMON NNSG(25),NSAL(25),NCBA(25),KCL(25),NXTL(25),NXTR(25),
     1IDXF(25),IDXS(25),XSEC(51),ISTOP(50),KANCH(50),AJP(64,50),
     2PJP(64,50),LIND(64,50),PBAR(45,51),NELC(25),AREA(25)
      COMMON NI(15),NJ(15),AE(15),EIP(15),EIS(3,15),PP(15),Z(90),
     1ZORI(45),DISP(64,46),D(64),VS(4,15),VP(4,15),SS(4,15),
     2SP(4,15),NN,S(2,15,50)
C
      DIMENSION ZA(6,15),SI(15),SJ(15)
C
      EQUIVALENCE (Z,ZA)
C
C
   10 FORMAT (///29H PLATE INTERNAL DISPLACEMENTS//78H   ELE     I      J
     I          LONG. DISP      TRANSVERSE DISP        BEAM ROTATION)
   11 FORMAT (3I6,3E20.8)
   12 FORMAT (///22H PLATE INTERNAL FORCES//115H   ELE    I    J    BEAM M
     1OMENT    TRAN. SHEAR    AXIAL FORCE      NX(I)          NX(J)
     2     SX(I)          SX(J))
   13 FORMAT (I6,2I4,3E15.6,4E15.6)
C
      PRINT 10
      PRINT 11, (I,NI(I),NJ(I),(ZA(J,I),J=1,3),I=1,NEL)
      PRINT 12
      DO 20 I=1,NEL
      J=KPL(I)
      C1=ZA(6,I)/PWTH(J)
      C2=ZA(4,I)*PP(J)
      FI=C1+C2
      FJ=C1-C2
      SI(I) = FI/TH(J)
      SJ(I) = FJ/TH(J)
      PRINT 13, I,NI(I),NJ(I),(ZA(K,I),K=4,6),FI,FJ,SI(I),SJ(I)
      IF(NSTOP) 21,20,20
   21 S(1,I,NN) = SI(I)
      S(2,I,NN) = SJ(I)
   20 CONTINUE
      RETURN
      END
      SUBROUTINE CSTRAIN
C
C     FORMAT STATEMENTS   SUBROUTINE CSTRAIN
C
  450 FORMAT(1H1,19X,39HSTEEL STRESSES FOR ALL CABLES AT STAGE I2/20X,40
     1HNOTE   SEG.NOS. REFERED TO PRESENT STAGE//)
   74 FORMAT(25X,9HCABLE NO.,2X,7HSEG.NO.,2X,14HREVISED STRESS)
   75 FORMAT(27X,I2,10X,I2,4X,E15.6)
   76 FORMAT(1HO,I3,13H STAGE CABLES)
C
```

```
C      COMMON DIMENSION AND EQUIVALENCE STATEMENTS
C
       COMMON NSTG,NSRF,NSEG,SEGL,NL,NL1,NR,NSLS,NSLS1,NS1,LSLS,NSS,NWD,
      1NCB,IXT,JXT,NPL,NJT,NEL,M3,MX,M6,M31,NXBAND,MAXJTD,YMS,CLC,CFC,
      2NSTOP,KODJA,KODBC,KODSPT,KODTS
       COMMON H(15),V(15),TH(15),E(15),PWTH(15),NPI(15),NPJ(15),KPL(15),
      1NPDIF(15),ZEND(90),BCORI(3,15),IORI(3,15),BCEND(3,15),IEND(3,15),
      2IED(45,4),SSC(45,4),ZK(90,46),IFD(90)
       COMMON NNSG(25),NSAL(25),NCBA(25),KCL(25),NXTL(25),NXTR(25),
      1IDXF(25),IDXS(25),XSEC(51),ISTOP(50),KANCH(50),AJP(64,50),
      2PJP(64,50),LIND(64,50),PBAR(45,51),NELC(25),AREA(25)
       COMMON NI(15),NJ(15),AE(15),EIP(15),EIS(3,15),PP(15),Z(90),
      1ZORI(45),DISP(64,46),D(64),VS(4,15),VP(4,15),SS(4,15),
      2SP(4,15),NN,S(2,15,50)
C
       DIMENSION Y(50,6),F(50,6),EPSC(50,6),TEMPF(300),TEMPE(300)
C
       EQUIVALENCE (ZK,Y),(ZK(301),F),(ZK(602),EPSC),(ZK(903),TEMPF),
      1(ZK(1204),TEMPE)
C
       LFC = 0
       NSTGM = NSTG-1
       IF(NSTGM)86,86,80
   80  IF(KODTS-1)85,90,90
   85  CONTINUE
       DO 91 J = 1,NSTGM
   91  LFC = LFC+NCBA(J)
   86  BACKSPACE 5
       GO TO 500
   90  REWIND 5
       PRINT 450, NSTG
       PRINT 74
       DO 1000 NST = 1,NSTGM
       NTD = NCBA(NST)
       IF(NTD.EQ.0) GO TO 1000
       NSG = NNSG(NST)
       IXE = NXTL(NST)
       JXE = NXTR(NST)
       IF(KCL(NST)-1)40,40,41
   40  LCS = JXE-1
       GO TO 42
   41  LCS = NSRF
   42  NCS = (LCS+1)-IXE
       NTRM = NTD*NCS
C
       K = NST+1
       KSAL = 0
       DO 10 I = K,NSTG
       KSAL = KSAL+NSAL(I)
   10  CONTINUE
C
       ICS = IXE+KSAL
       JCS = LCS+KSAL
C
       READ (5) ((Y(I,J),J = 1,NTD),I = IXE,LCS)
C
       CALL IOBIN (4HREAD,4LFXXX,TEMPF(1),NTRM,IDXF(NST))
C
       LM = 0
       DO 5 M = 1,NTD
       DO 5 L = IXE,LCS
       LM = LM + 1
       F(L,M) = TEMPF(LM)
    5  CONTINUE
C
       CALL IOBIN (4HREAD,4LSXXX,TEMPE(1),NTRM,IDXS(NST))
C
       LM = 0
       DO 6 M = 1,NTD
       DO 6 L = IXE,LCS
       LM = LM + 1
       EPSC(L,M) = TEMPE(LM)
    6  CONTINUE
C
       K = ICS-1
       DO 20 I = IXE,LCS
       K = K+1
       DO 20 J = 1,NTD
       KC = LFC+J
       NL = NELC(KC)
       KP = KPL(NL)
       EPSI = S(1,NL,K)/E(KP)
       EPSJ = S(2,NL,K)/E(KP)
       EPSCP = (((EPSI-EPSJ)/PWTH(KP))*Y(I,J))+(EPSI+EPSJ)/2.0
       DEPSC = EPSCP-EPSC(I,J)
       F(I,J) = F(I,J) + (DEPSC*YMS*AREA(KC))
   20  CONTINUE
       PRINT 76, NST
       DO 35 I = 1,NTD
       KC = LFC+I
       DO 35 J = IXE,LCS
       L = KSAL+J
       SIG = F(J,I)/AREA(KC)
       PRINT 75, KC,L,SIG
   35  CONTINUE
       LFC = LFC+NTD
 1000  CONTINUE
C
C
  500  IF(NCBA(NSTG))14,14,501
```

```
  501 IF(KCL(NSTG)-1)50,50,51
   50 JXTM = JXT-1
      GO TO 52
   51 JXTM = NSRF
   52 READ (5) ((Y(I,J),J = 1,NCB),I = IXT,JXTM)
C
      DO 60 J = IXT,JXTM
      DO 60 I = 1,NCB
      KC = LFC+I
      NL = NELC(KC)
      KP = KPL(NL)
      EPSI = S(1,NL,J)/E(KP)
      EPSJ = S(2,NL,J)/E(KP)
      EPSC(J,I) = (((EPSI-EPSJ)/PWTH(KP))*Y(J,I))+(EPSI+EPSJ)/2.0
   60 CONTINUE
C
      LM = 0
      DO 25 M = 1,NCB
      DO 25 L = IXT,JXTM
      LM = LM+1
      TEMPE(LM) = EPSC(L,M)
   25 CONTINUE
C
      CALL IO8IN (6HWRITER,4LSXXX,TEMPE(1),NWD,IDXS(NSTG))
   13 IF(IO8IN(4HTEST,4LSXXX))13,14,14
   14 RETURN
      END
      SUBROUTINE STIF
C
C     TO CALCULATE STIFFNESS AND COEFFICIENT MATRICES FOR EACH TYPE OF PLATE
C
C     COMMON, DIMENSION AND EQUIVALENCE STATEMENTS
C
      COMMON NSTG,NSRF,NSEG,SEGL,NL,NL1,NR,NSLS,NSLS1,NS1,LSLS,NSS,NWD,
     1NCB,IXT,JXT,NPL,NJT,NEL,M3,MX,M6,M31,NXBAND,MAXJTD,YMS,CLC,CFC,
     2NSTOP,KODJA,KODBC,KODSPT,KODTS
      COMMON H(15),V(15),TH(15),E(15),PWTH(15),NPI(15),NPJ(15),KPL(15),
     1NPDIF(15),ZEND(90),BCORI(3,15),IORI(3,15),BCEND(3,15),IEND(3,15),
     2IED(45,4),SSC(45,4),ZK(90,46),IFD(90)
      COMMON NNSG(25),NSAL(25),NCBA(25),KCL(25),NXTL(25),NXTR(25),
     1IDXF(25),IDXS(25),XSEC(51),ISTOP(50),KANCH(50),AJP(64,50),
     2PJP(64,50),LIND(64,50),PBAR(45,51),NELC(25),AREA(25)
      COMMON BIGK(64,20),PTTT(64,46),CM(9,15),HM(17,15),FJ(9,15),
     1A(4,4),BTAV(4),RBAR(4),D(20),ZZ(6)
C
      DIMENSION SK(8,8),SKA(8,8),B(15),SM(8,8,15)
C
      EQUIVALENCE (B,TH),(PTTT,SM),(PTTT(1001),SK),(PTTT(1101),SKA)
C
C     FOR NEGLECTING SHEAR DEFORMATION SET SHEAR = 0
C
      SHEAR = 1.0
      DO 100 L=1,NPL
      HD=H(L)
      VD=V(L)
C
C      COMPUTATION CONSTANTS ARE FORMED
C
      G=PWTH(L)
      EG=SEGL/2.
      BET=1.2*(G/EG)**2*SHEAR
      BET1=1./(1.+6.*BET)
      EG2=EG*EG
      G1=E(L)*B(L)*G
      CC=1.5*G1*G*G
      G2=G1/(G*G)
      G1=G1/EG2
      G3=G1*G/EG*BET1
      G4=CC/(EG2*EG2)*BET1
C
C     STIFFNESS MATRIX FOR SINGLE PLATE IS LOADED
C
      D1=E(L)*B(L)**3/(6.*G)
      SK(1,2)=D1
      SK(2,1)=D1
      SK(1,1)=2.*D1
      SK(2,2)=SK(1,1)
      C=D1*3./G
      SK(1,3)=C
      SK(1,4)=C
      SK(2,3) = C
      SK(2,4)=C
      SK(3,1)=C
      SK(3,2)=C
      SK(4,1)=C
      SK(4,2)=C
      C=C*2./G
      SK(3,3)=C
      SK(3,4)=C
      SK(4,3)=C
      SK(4,4)=C
      C=4.*BET*BET1*G1
      SK(5,5)=C
      SK(6,6)=C
      C=(1.+2.*BET)*BET1*G1
      SK(5,6)=C
      SK(6,5)=C
      SK(5,7)=-G3
      SK(5,8)=G3
      SK(6,7)=G3
```

```
      SK(6,8)=-G3
      SK(7,5)=-G3
      SK(7,6)=G3
      SK(8,5)=G3
      SK(8,6)=-G3
      SK(7,7)=G2-G4
      SK(7,8)=G2+G4
      SK(8,7)=SK(7,8)
      SK(8,8)=SK(7,7)
C
C     STIFFNESS MATRIX * TRANSFORMATION MATRIX
C
      DO 10 I=1,4
      J=I+4
      SKA(I,1)=-SK(I,3)*VD
      SKA(I,2)=-SK(I,3)*HD
      SKA(I,3)= SK(I,1)
      SKA(I,4)= 0.0
      SKA(I,5)= SK(I,4)*VD
      SKA(I,6)= SK(I,4)*HD
      SKA(I,7)= SK(I,2)
      SKA(I,8)= 0.0
      SKA(J,1)=-SK(J,7)*HD
      SKA(J,2)= SK(J,7)*VD
      SKA(J,3)= 0.0
      SKA(J,4)= SK(J,5)
      SKA(J,5)= SK(J,8)*HD
      SKA(J,6)=-SK(J,8)*VD
      SKA(J,7)= 0.0
   10 SKA(J,8)= SK(J,6)
C
C     TRANSPOSED TRANSFORMATION MATRIX*STIFFNESS*TRANSFORMATION MATRIX
C
      DO 20 I=1,8
      SM(1,I,L)=-SKA(3,I)*VD-SKA(7,I)*HD
      SM(2,I,L)=-SKA(3,I)*HD+SKA(7,I)*VD
      SM(3,I,L)= SKA(1,I)
      SM(4,I,L)= SKA(5,I)
      SM(5,I,L)= SKA(4,I)*VD+SKA(8,I)*HD
      SM(6,I,L)= SKA(4,I)*HD-SKA(8,I)*VD
      SM(7,I,L)= SKA(2,I)
   20 SM(8,I,L)= SKA(6,I)
C
C     CALCULATE CM MATRIX,  -(FIXED JOINT FORCES) DUE TO ACTIONS AT PREVIOUS
C     SECTION
C
      G2=(3.+2.*BET)*EG*G3/2.
      G3=2.*G3
      G4=2.*G4
      C=G3*G
      CM(1,L)=G1
      CM(2,L)=-G3
      CM(3,L)=G2
      CM(5,L)=(1.+2.*BET)*BET1/G
      CM(4,L)=CM(5,L)*6./EG
      CM(7,L)=-G4
      CM(8,L)=C
      D1=6.*BET1/EG
      CM(9,L)=D1/EG
      CM(6,L)=-D1*BET
C
C     CALCULATE HM MATRIX (ZK DUE TO FIXED JOINT)
C
      G1=E(L)*B(L)*G/SEGL
      HM(1,L)=-1./G1
      HM(2,L)=-8.*G1
      CC=18.*SEGL/CC
      C=CC*SEGL*BET1
      HM(3,L)=BET1*(17.-18.*BET)
      HM(4,L)=BET1*SEGL*(10.*BET-5.)
      HM(5,L)=C*(4.*BET-1.)/2.
      HM(6,L)=C*SEGL*BET*(3.-2.*BET)/8.
      HM(7,L)=-96.*BET1/SEGL
      HM(8,L)=BET1*(29.-18.*BET)
      HM(9,L)=BET1*CC*(3.-6.*BET)
      HM(10,L)=-2.*BET*C
      C=BET1/(CC*SEGL)
      HM(11,L)=-384.*C
      HM(12,L)=BET1*(120.-48.*BET)/CC
      HM(13,L)=BET1*(13.-18.*BET)
      HM(14,L)=-8.*BET1*SEGL*BET
      HM(15,L)=-6.*CM(8,L)
      HM(16,L)=48.*BET1/SEGL
      HM(17,L)=BET1*(1.-18.*BET)
C
C     CALCULATE FJ MATRIX (ZK DUE TO JOINT DISPLACEMENTS)
C
      CC=SEGL/G
      FJ(1,L)=-4.*(1.+BET)*BET1*CC
      FJ(2,L)=BET1*(20.+24.*BET)/G
      FJ(3,L)=C*CC*(72.+48.*BET)
      C=192.*C
      FJ(4,L)=C/G
      FJ(5,L)=4.*G1
      FJ(6,L)=BET1*(12.*BET-8.)
      FJ(7,L)=HM(16,L)
      FJ(8,L)=C
      FJ(9,L)=3.*C/SEGL
C
  100 CONTINUE
```

```
      RETURN
      END
      SUBROUTINE DSYINV (A)
C
      DIMENSION A(4,4)
C
      A(2,1)=A(1,2)
      A(3,1)=A(1,3)
      A(4,1)=A(1,4)
C
   20 DO 160 N=1,4
   30 PIVOT=A(N,N)
      IF(PIVOT.EQ.0.0) CALL ERROR
   40 A(N,N)=-1.
   50 DO 60 J=1,4
   60 A(N,J)=A(N,J)/PIVOT
   80 DO 145 I=1,4
   90 IF(N-I) 95,145,95
   95 IF(A(I,N)) 100,145,100
  100 DO 140 J=1,4
  110 IF(N-J) 120,140,120
  120 A(I,J)=A(I,J)-A(I,N)*A(N,J)
  130 A(J,I)=A(I,J)
  140 CONTINUE
  145 CONTINUE
  150 DO 160 I=1,4
  160 A(I,N)=A(N,I)
C
  163 DO 165 I=1,4
  164 DO 165 J=1,4
  165 A(I,J)=-A(I,J)
  250 RETURN
      END
      SUBROUTINE DSIMEQ (A,NN,ML)
C
      DIMENSION A(45,1), ID(45)
C
C     SET I.D. ARRAY
C
      LL=NN+ML
      MM=NN+1
      DO 50 N=1,NN
   50 ID(N)=N
C
      DO 475 N=1,NN
      N1=N+1
C
C     LOCATE LARGEST ELEMENT
C
      D=0.0
      DO 100 I=N,NN
      DO 100 J=N,NN
      IF (ABS(A(I,J))-D) 100,90,90
   90 D=ABS(A(I,J))
      II=I
      JJ=J
  100 CONTINUE
C
C     INTERCHANGE COLUMNS
C
      DO 110 I=1,NN
      D=A(I,N)
      A(I,N)=A(I,JJ)
  110 A(I,JJ)=D
C
C     RECORD COLUMN INTERCHANGE
C
      I=ID(N)
      ID(N)=ID(JJ)
      ID(JJ)=I
C
C     INTERCHANGE ROWS
C
      DO 120 J=N,NN
      D=A(N,J)
      A(N,J)=A(II,J)
  120 A(II,J)=D
C
      DO 130 L=MM,LL
      D=A(N,L)
      A(N,L)=A(II,L)
  130 A(II,L)=D
C
C     FORM D(N,L)
C
      IF(A(N,N).EQ.0.0) CALL ERROR
      DO 150 L=MM,LL
  150 A(N,L)=A(N,L)/A(N,N)
C
C     CHECK FOR LAST EQUATION
C
      IF (N-NN) 200,500,200
C
  200 DO 450 J=N1,NN
C
C     FORM H(N,J)
C
      IF (A(N,J)) 250,350,250
  250 A(N,J)=A(N,J)/A(N,N)
C
```

```
C      MODIFY A(I,J)
C
       DO 300 I=N1,NN
  300  A(I,J)=A(I,J)-A(I,N)*A(N,J)
C
C      MODIFY B(I,L)
C
  350  DO 400 L=MM,LL
  400  A(J,L)=A(J,L)-A(J,N)*A(N,L)
  450  CONTINUE
  475  CONTINUE
C
C      BACK-SUBSTITUTION
C
  500  N1=N
       N=N-1
       IF (N) 700,700,550
C
  550  DO 600 L=MM,LL
       DO 600 J=N1,NN
  600  A(N,L)=A(N,L)-A(N,J)*A(J,L)
C
       GO TO 500
C
C      REORDER UNKNOWNS
C
  700  DO 950 N=1,NN
       DO 900 I=N,NN
       IF (ID(I)-N) 900,750,900
  750  DO 800 L=MM,LL
       D=A(N,L)
       A(N,L)=A(I,L)
  800  A(I,L)=D
       GO TO 950
  900  CONTINUE
  950  ID(I)=ID(N)
C
C
       RETURN
C
       END
       SUBROUTINE ERROR
     1 FORMAT (16HOSINGULAR MATRIX)
       PRINT 1
       STOP
       END
```

A P P E N D I X C

EXAMPLE PROBLEMS

C.1 Input Data for Example Problem 1

No. Card	Type Card	Data
1	1	EXAMPLE PROB. 1 THREE SPAN CONTINUOUS GIRDER.
2	2	1 1 2
3	3-1	1 0. -3.0 1.0 432000.
4	4-1	1 1 2 1
5	5	0. 0. 4175000.
6	6A	7 1 1 8
7	6B	0 0
8	8-1	1 6 10.
9	8-2	6 8 5.
10	9A	1 1 1 .00635 135. 0. 0
11	9B	0. 0 0
12	10	1 0. 30. -1. 8 0.5
13	11	1 0. 0. 0. 1 1 0
14	12A-1	1 1 0
15	13-1	1 0. .225 0. 0. 0 0 0 0
16	13-2	2 0. .225 0. 0. 0 0 0 0
17	12A-2	2 0 0
18	12A-3	3 0 1
19	12A-4	4 0 0
20	12A-5	5 0 0
21	12A-6	6 0 0
22	12A-7	7 0 -1
23	15	1 0. 0. 0. 0 1 0
24	7A	2 0 6 1 1 14
25	7B	0 1 1 1 0
26	8-3	8 10 5.
27	8-4	10 14 10.
28	9A	2 3 1 .0191 435. 0. 0
29	9B	0. 0 0
30	10	1 -.25 7 1.2
31	10	7 1.2 60. 1.25 9 1.1
32	10	9 1.1 14 0.
33	11	1 0. 0. 0. 1 1 0
34	14	1 0 1 0 0. 0. 0.
35	12A-8	8 0 0
36	12A-9	9 0 0
37	12A-10	10 0 1
38	12A-11	11 0 0
39	12A-12	12 0 0
40	12A-13	13 0 0
41	15	1 0. -1.125 0. 0 0 0
42	7A	3 0 14 1 10 19
43	7B	0 1 0 1 0
44	8-5	14 15 5.
45	8-6	15 19 10.
46	8-7	19 23 5.
47	8-8	23 28 10.
48	9A	3 3 1 .00955 225. 0. 0
49	9B	0. 0 0
50	10	10 1.5 77. -.645 11 -.85
51	10	11 -.85 18 -.85
52	10	18 -.85 148. -.645 19 1.5
53	11	1 0. 0. 0. 1 1 0

STAGE 1

STAGE 2

STAGE 3

No. Card	Type Card	Data																			
54	12A-14	14	0	1																	
55	12A-15	15	0	0																	
56	12A-16	16	0	0																	
57	12A-17	17	0	1																	
58	12A-18	18	0	0																	
59	12A-19	19	0	0																	
60	12A-20	20	0	-1																	
61	14	1	0	1	0							0.					0.				0.
62	12A-21	21	0	0																	
63	12A-22	22	0	0																	
64	12A-23	23	0	1																	
65	12A-24	24	0	0																	
66	12A-25	25	0	0																	
67	12A-26	26	0	0																	
68	12A-27	27	0	0																	
69	15			1			0.			0.			0.	0	1	0					
70	7A	4	0	0	0																
71	7B	1	0	0	1	1															
72	12B-1	1	2																		
73	13-1			1			0.			.3			0.				0.	0	0	0	0
74	13-2			2			0.			0.			0.				0.	0	0	0	0
75	12B-2	2	0																		
76	12B-3	3	0																		
77	12B-4	4	0																		
78	12B-5	5	0																		
79	12B-6	6	0																		
80	12B-7	7	0																		
81	12B-8	8	0																		
82	12B-9	9	0																		
83	12B-10	10	0																		
84	12B-11	11	0																		
85	12B-12	12	0																		
86	12B-13	13	0																		
87	12B-14	14	0																		
88	12B-15	15	0																		
89	12B-16	16	0																		
90	12B-17	17	0																		
91	12B-18	18	0																		
92	12B-19	19	0																		
93	12B-20	20	0																		
94	12B-21	21	0																		
95	12B-22	22	0																		
96	12B-23	23	0																		
97	12B-24	24	0																		
98	12B-25	25	0																		
99	12B-26	26	0																		
100	12B-27	27	0																		
101		BLANK CARD TERMINATES RUN																			

STAGE 3

STAGE 4

C.2 Explanatory Remarks for Data Input for Example 1

Card No.	Card Type	Remarks
1	1	Title
2	2	Cross section data
3	3	Plate data--one card for each plate type. This example, 1 card.
4	4	Element data--one card for each element. This example, 1 card.
5	5	Tendon data
6	6A	Stage data for initial stage
7	6B	Stage data word for initial stage
8	8	In the initial stage, cards 7 are omitted and data input goes directly to cards 8, segment data. In this example segments between stations 1-6 are identical so they are included in one card.
9	8	Remainder of segment data for segments between stations 6-8.
10	9A	Initial stage tendon data
11	9B	Initial stage tendon out of plane data
12	10	Tendon profile data. All tendons stressed in a stage must have their type 9A, 9B, and 10 cards arranged in sequence here.
13	11	Boundary condition for each element at origin. In example, provides for no longitudinal or transverse displacement and no moment at the origin.
14	12A	For the initial stage, type 12 initial segment cards are required for each of the initial segments. This card shows IAJA = 1, since joint actions are to be specified so that dead load acting on joints can be applied.
15	13	This joint action card specifies that one-half the dead load (0.225 k/ft.) be applied as a transverse load along joint 1.
16	13	Remainder of dead load is applied along joint 2.
17-21	12A	Initial segment cards for segments 2 through 6. IAJA = 0 means same joint loads as previous segment, so that dead load is applied to all segments uniformly.
22	12A	Initial segment card for segment 7. ISTOP = -1 indicates that either an interior support or stopover will follow segment 7 at this stage or some future stage. In this case station 8 will locate the interior support at stage 2, 3, and 4.

23	15	Gives boundary condition at station 8 as a roller with transverse displacement prevented.
END STAGE 1 - BEGIN STAGE 2		
24	7A	Information on number of segments and tendons added in the second stage.
25	7B	Second stage code words - KODJA = 0 indicates no change in joint actions for segments of stage 1. Only type 12A cards needed for new segments. KODBC indicates a change in origin or end boundary conditions due to change at station 8 from end to interior station. Both card type 11 and 15 required. KODSPT = 1 indicates interior support condition (at station 8) has changed. Type 14 card required. KREF = 1 indicates this is last stage of cantilevering sequence.
26	8	Segment data for segments between stations 8-10
27	8	Segment data for segments between stations 10-14
28	9A	Second stage tendon data
29	9B	Second stage tendon out of plane data
30	10	Tendon profile data--linear--stations 1-7
31	10	Tendon profile data--parabolic--stations 7-9
32	10	Tendon profile data--linear--stations 9-14
33	11	Origin boundary - same as #13
34	14	Interior support designation at station 8, which has changed from end boundary to interior support--follows card 33, since no card 12A, or 12B, or 13 is needed for segments 1-7, this stage. Whenever card 14 is used, it must come right after applicable card 12A or 12B and 13.
35-40	12A	Initial segment cards for new segments 8-13
41	15	End boundary card for station 14 with dead load of 1/2 the closure segment imposed as a prescribed transverse force.
END STAGE 2 - BEGIN STAGE 3		
42	7A	Adds 3rd stage structure and closure tendon
43	7B	Third stage code words - same as #25 except KODSPT = 0, since no change in interior support from stage 2.
44-47	8	Segment data for segments between stations 14-28
48-52	9A-9B-10	Tendon data for tendon 3
53	11	Origin boundary - same as #13 and #33
54-60	12A	Initial segment cards for new segments 14-20
61	14	Interior support card for station 21

202

62-68	12A	Initial segment cards for new segments 21-27
69	15	End boundary card for vertical reaction at station 28

END STAGE 3 - BEGIN STAGE 4

70	7A	No new segments or tendons added for fourth stage
71	7B	To analyze for live load, joint actions must be changed, hence KODJA = 1. All boundary conditions remain same, so KODBC and KODSPT = 0. Therefore, modified segment cards required for all segments but no boundary or support cards.
72	12B	Modified segment card for segment 1
73-74	13	Joint load card with live load at 0.3 k/ft.
75-100	12B	Modified segment cards for other segments. IAJA2 = 0 indicates uniform load on all segments
101	BLANK CARD TERMINATES RUN	

C.3 Selected Data Output - Example Problem 1

B.4.1

```
EXAMPLE PROB. NO. 1 - 3 SPAN CONTINUOUS GIRDER CONSTRUCTED IN 3 STAGES.

 PROBLEM CONTROL DATA

 NO. PL. TYPES =  1
 NO. ELEMENTS  =  1
 NO. JOINTS    =  2

 GEOMETRIC AND ELASTIC PROPERTIES

 PL TYPE        H=PROJ.        V=PROJ.        THICKNESS        MODULUS
    1            0.          -3.000000E+00     1.000000E+00     4.320000E+05

 CONNECTIVITY DATA

 ELE   I-JT   J-JT   PL
  1      1      2     1

 TENDON CONTROL DATA

 STEEL MODULUS =    4.175000E+06
 FRICTION CONSTANT =    0.
 WOBBLE CONSTANT =      0.
```

B.4.2a Stage 1

```
 LONG. CONFIGURATION OF STRUCTURE AT STAGE   1

 SPAN =   60.000
 NO. OF SEGMENTS =   7
 NO. OF TENDONS STRESSED =  1

 SEGMENT NUMBER     SEGMENT LENGTH

        1              10.000
        2              10.000
        3              10.000
        4              10.000
        5              10.000
        6               5.000
        7               5.000
```

B.4.2b Stage 1

```
 INPUT DATA FOR CABLES STRESSED AT STAGE  1

 TENDON NO. =   1
 AREA =    4.350000E-03
 NO. CURVES =   1
 ELEMENT =   1

 INITIAL JACK FORCE =    1.350000E+02
 FINAL JACK FORCE =    1.350000E+02
 LIVE END INDEX =   0

 DIVERGENCE =    0.
 STA. LEFT =   0
 STA. RIGHT =   0

 CONTROL COORDINATES

 CURVE    NXL     YL          XM          YM        NXR      YR

  1       1      0.000       30.000      -1.000     0        .900

 INITIAL TENDON STRESS AFTER FRICTION LOSS

 TENDON     SEGMENT          STRESS

    1          1          2.125984E+04
    1          2          2.125984E+04
    1          3          2.125984E+04
    1          4          2.125984E+04
    1          5          2.125984E+04
    1          6          2.125984E+04
    1          7          2.125984E+04
```

ORIGIN BOUNDARY CONDITIONS AT STAGE 1

ELE	AXIAL FOR/DISP	INDEX	SHEAR FOR/DISP	INDEX	MOMENT OR ROT	INDEX
1	0.	1	0.	1	0.	0

B.4.2(c) INDEX = 0 FOR GIVEN FORCE
1 FOR GIVEN DISPLACEMENT

Stage 1

JOINT ACTIONS, SUPPORT AND STOPOVER DATA FOR STAGE 1

IAJA = 0, JOINT ACTIONS SAME AS LAST SEGMENT
1, JOINT ACTIONS DIFFERENT FROM LAST SEGMENT

IAJA2 = 0, JOINT ACTIONS SAME AS LAST SEGMENT
1, JOINT ACTIONS SAME AS LAST STAGE
2, JOINT ACTIONS RE-SPECIFIED

ISTOP = -1, SUPPORT AFTER THIS SEGMENT
0, NO SUPPORT OR STOPOVER
1, STOPOVER AFTER THIS SEGMENT

B.4.2(d)
Stage 1

SEG 1 IAJA = 1 ISTOP = 0

****

APPLIED JOINT ACTIONS

JT.	HORIZ.	F/D	VERT.	F/D	ROT.	M/R	LONG.	F/D
1	0.0000000	0	.2250000	0	0.0000000	0	0.0000000	0
2	0.0000000	0	.2250000	0	0.0000000	0	0.0000000	0

INDEX = 0 FOR GIVEN FORCE
1 FOR GIVEN DISPLACEMENT

****

SEG 2 IAJA = 0 ISTOP = 0
SEG 3 IAJA = 0 ISTOP = 1
SEG 4 IAJA = 0 ISTOP = 0
SEG 5 IAJA = 0 ISTOP = 0
SEG 6 IAJA = 0 ISTOP = 0
SEG 7 IAJA = 0 ISTOP = -1

END BOUNDARY CONDITIONS AT STAGE 1

ELE	AXIAL FOR/DISP	INDEX	SHEAR FOR/DISP	INDEX	MOMENT OR ROT	INDEX
1	0.	0	0.	1	0.	0

INDEX = 0 FOR GIVEN FORCE
1 FOR GIVEN DISPLACEMENT

B.4.2(e)
Stage 1

FINAL PLATE FORCES AND DISPLACEMENTS FOR LONGITUDINAL PLATE ELEMENTS AT END

PLATE INTERNAL DISPLACEMENTS

ELE	I	J	LONG. DISP	TRANSVERSE DISP	BEAM ROTATION
1	1	2	-6.22390565E-03	0.	-2.08806942E-03

B.4.3(a)

PLATE INTERNAL FORCES

ELE	I	J	BEAM MOMENT	TRAN. SHEAR	AXIAL FORCE	NX(I)	NX(J)	SX(I)	SX(J)
1	1	2	-6.721818E+01	1.177475E+00	-1.344364E+02	-8.962424E+01	-6.821210E-13	-8.962424E+01	-6.821210E-13

FINAL PLATE FORCES AND DISPLACEMENTS FOR LONGITUDINAL PLATE ELEMENTS AT ORIGIN

PLATE INTERNAL DISPLACEMENTS

ELE	I	J	LONG. DISP	TRANSVERSE DISP	BEAM ROTATION
1	1	2	0.	0.	1.39149984E-03

B.4.3(c)

Stage 1

PLATE INTERNAL FORCES

ELE	I	J	BEAM MOMENT	TRAN. SHEAR	AXIAL FORCE	NX(I)	NX(J)	SX(I)	SX(J)
1	1	2	0.	-3.402548E+00	-1.344364E+02	-4.481212E+01	-4.481212E+01	-4.481212E+01	-4.481212E+01

FINAL JOINT AND PLATE FORCES AND DISPLACEMENTS FOR SEGMENT NO. 1

JOINT DISPLACEMENTS

JOINT	HORIZONTAL DISP	VERTICAL DISP	ROTATION	LONG. DISP
1	0.	6.91570955E-03	0.	1.50543500E-03
2	0.	6.91700476E-03	0.	-2.54275261E-03

PLATE EDGE DISPLACEMENTS

ELE	I	J	ROTATION(I)	ROTATION(J)	W(I)	W(J)	U(I)	U(J)	V(I)	V(J)
1	1	2	0.	0.	0.	0.	15.05475E-04	-25.42753E-04	-69.15710E-04	69.17004E-04

PLATE EDGE FORCES

ELE	I	J	M(I)	M(J)	Q(I)	Q(J)	T(I)	T(J)	P(I)	P(J)
1	1	2	0.	0.	0.	0.	-13.99450E-13	-39.91116E-14	14.78739E-02	22.50000E-02

B.4.3(d)

Stage 1

PLATE INTERNAL DISPLACEMENTS

ELE	I	J	LONG. DISP	TRANSVERSE DISP	BEAM ROTATION
1	1	2	-5.186588804E-04	-6.916356691E-03	1.34939587E-03

PLATE INTERNAL FORCES

ELE	I	J	BEAM MOMENT	TRAN. SHEAR	AXIAL FORCE	NX(I)	NX(J)	SX(I)	SX(J)
1	1	2	-1.804867E+01	-3.016918E+00	-1.344364E+02	-5.551123E+01	-3.411301E+01	-5.551123E+01	-3.411301E+01

FINAL JOINT AND PLATE FORCES AND DISPLACEMENTS FOR SEGMENT NO. 2

JOINT DISPLACEMENTS

JOINT	HORIZONTAL DISP	VERTICAL DISP	ROTATION	LONG. DISP
1	0.	1.91485967E-02	0.	7.45574738E-04
2	0.	1.91498969E-02	0.	-3.11940857E-03

PLATE EDGE DISPLACEMENTS

ELE	I	J	ROTATION(I)	ROTATION(J)	W(I)	W(J)	U(I)	U(J)	V(I)	V(J)
1	1	2	0.	0.	0.	0.	74.55747E-07	-31.19409E-04	-19.14860E-03	19.14990E-03

PLATE EDGE FORCES

ELE	I	J	M(I)	M(J)	Q(I)	Q(J)	T(I)	T(J)	P(I)	P(J)
1	1	2	0.	0.	0.	0.	-38.68848E-13	78.25703E-13	14.93400E-02	22.50000E-02

PLATE INTERNAL DISPLACEMENTS

ELE	I	J	LONG. DISP	TRANSVERSE DISP	BEAM ROTATION
1	1	2	-1.555976461E-03	-1.91492466E-02	1.04228811E-03

PLATE INTERNAL FORCES

ELE	I	J	BEAM MOMENT	TRAN. SHEAR	AXIAL FORCE	NX(I)	NX(J)	SX(I)	SX(J)
1	1	2	-4.237987E+01	-2.255987E+00	-1.344364E+02	-7.306537E+01	-1.655888E+01	-7.306537E+01	-1.655888E+01

FINAL JOINT AND PLATE FORCES AND DISPLACEMENTS FOR SEGMENT NO. 3

JOINT DISPLACEMENTS

JOINT	HORIZONTAL DISP	VERTICAL DISP	ROTATION	LONG. DISP
1	0.	2.70727751E-02	0.	-1.83827339E-03
2	0.	2.70735770E-02	0.	-3.34831465E-03

PLATE EDGE DISPLACEMENTS

ELE	I	J	ROTATION(I)	ROTATION(J)	W(I)	W(J)	U(I)	U(J)	V(I)	V(J)
1	1	2	0.	0.	0.	0.	-18.38273E-04	-33.48315E-04	-27.07228E-03	27.07358E-03

PLATE EDGE FORCES

ELE	I	J	M(I)	M(J)	Q(I)	Q(J)	T(I)	T(J)	P(I)	P(J)
1	1	2	0.	0.	0.	0.	-33.50244E-13	37.09957E-13	14.95465E-02	22.50000E-02

PLATE INTERNAL DISPLACEMENTS

ELE	I	J	LONG. DISP	TRANSVERSE DISP	BEAM ROTATION
1	1	2	-2.59329402E-03	-2.70729260E-02	5.03347085E-04

PLATE INTERNAL FORCES

ELE	I	J	BEAM MOMENT	TRAN. SHEAR	AXIAL FORCE	NX(I)	NX(J)	SX(I)	SX(J)
1	1	2	-6.11343?E+01	-1.49942?E+00	-1.?44364E+02	-8.556834E+01	-4.055906E+00	-8.556834E+01	-4.055906E+00

B.4.3(d)
Stage 1

FINAL JOINT AND PLATE FORCES AND DISPLACEMENTS FOR SEGMENT NO. 7

JOINT DISPLACEMENTS

JOINT	HORIZONTAL DISP	VERTICAL DISP	ROTATION	LONG. DISP
1	0.	5.00538330E-03	0.	-8.81198409E-03
2	0.	5.00667140E-03	0.	-3.09716842E-03

PLATE EDGE DISPLACEMENTS

ELE	I	J	ROTATION(I)	ROTATION(J)	W(I)	W(J)	U(I)	U(J)	V(I)	V(J)
1	1	2	0.	0.	0.	0.	-88.31984E-04	-30.97168E-04	-50.05383E-04	50.06671E-04

PLATE EDGE FORCES

ELE	I	J	M(I)	M(J)	Q(I)	Q(J)	T(I)	T(J)	P(I)	P(J)
1	1	2	0.	0.	0.	0.	83.49842E-13	-10.50812E-12	14.99894E-02	22.50000E-02

PLATE INTERNAL DISPLACEMENTS

ELE	I	J	LONG. DISP	TRANSVERSE DISP	BEAM ROTATION
1	1	2	-5.96457625E-03	-5.00602738E-03	-1.91160522E-03

PLATE INTERNAL FORCES

ELE	I	J	BEAM MOMENT	TRAN. SHEAR	AXIAL FORCE	NX(I)	NX(J)	SX(I)	SX(J)
1	1	2	-6.991496E+01	9.799500E-01	-1.344364E+02	-9.142210E+01	1.797854E+00	-9.142210E+01	1.797854E+00

Begin
Stage 2
B.4.2

LONG. CONFIGURATION OF STRUCTURE AT STAGE 2

SPAN = 110.000
NO. OF SEGMENTS = 13
NO. OF TENDONS STRESSED = 1
NO. SEG. ADDED LEFT = 0
NO. SEG. ADDED RIGHT = 0

SEGMENT NUMBER	SEGMENT LENGTH
1	10.000
2	10.000
3	10.000
4	10.000
5	10.000
6	5.000
7	5.000
8	5.000
9	5.000
10	10.000
11	10.000
12	10.000
13	10.000

INPUT DATA FOR CABLES STRESSED AT STAGE 2

TENDON NO. = 2
AREA = 1.910000E-02
NO. CURVES = 3
ELEMENT = 1

INITIAL JACK FORCE = 4.350000E+02
FINAL JACK FORCE = 4.350000E+02
LIVE END INDEX = 0

ECCENTRICITY = 0.
STR. LEFT = 0
STR. RIGHT = 0

CONTROL COORDINATES

CURVE	NXL	YL	XM	YM	NXR	YR
1	1	-.250	-0.000	-0.000	7	1.200
2	7	1.200	60.000	1.250	9	1.100
3	9	1.100	-0.000	-0.000	14	0.000

INITIAL TENDON STRESS AFTER FRICTION LOSS

TENDON	SEGMENT	STRESS
2	1	2.277487E+04
2	2	2.277487E+04
2	3	2.277487E+04
2	4	2.277487E+04
2	5	2.277487E+04
2	6	2.277487E+04
2	7	2.277487E+04
2	8	2.277487E+04
2	9	2.277487E+04
2	10	2.277487E+04
2	11	2.277487E+04
2	12	2.277487E+04
2	13	2.277487E+04

ORIGIN BOUNDARY CONDITIONS AT STAGE 2

ELE	AXIAL FOR/DISP	INDEX	SHEAR FOR/DISP	INDEX	MOMENT OR ROT	INDEX
1	0.	1	0.	1	0.	0

INDEX = 0 FOR GIVEN FORCE
1 FOR GIVEN DISPLACEMENT

JOINT ACTIONS, SUPPORT AND STOPOVER DATA FOR STAGE 2

IAJA = 0, JOINT ACTIONS SAME AS LAST SEGMENT
1, JOINT ACTIONS DIFFERENT FROM LAST SEGMENT

IAJA2 = 0, JOINT ACTIONS SAME AS LAST SEGMENT
1, JOINT ACTIONS SAME AS LAST STAGE
2, JOINT ACTIONS RE-SPECIFIED

ISTOP =-1, SUPPORT AFTER THIS SEGMENT
0, NO SUPPORT OR STOPOVER
1, STOPOVER AFTER THIS SEGMENT

****

JT, ACTIONS FOR SEG, 1 THRU 7 UNCHANGED FROM LAST STAGE

****

****

INTERIOR SUPPORT RESTRAINTS

ELE,	AXIAL	COEFFICIENT	SHEAR	COEFFICIENT	ROT,	COEFFICIENT
1	0	-0,	1	-0,	0	-0,

****

SEG 8 IAJA = 0 ISTOP = 0
SEG 9 IAJA = 0 ISTOP = 0
SEG 10 IAJA = 0 ISTOP = 1
SEG 11 IAJA = 0 ISTOP = 0
SEG 12 IAJA = 0 ISTOP = 0
SEG 13 IAJA = 0 ISTOP = 0

END BOUNDARY CONDITIONS AT STAGE 2

ELE	AXIAL FOR/DISP	INDEX	SHEAR FOR/DISP	INDEX	MOMENT OR ROT	INDEX
1	0,	0	-1.12500000E+00	0	0,	0

INDEX = 0 FOR GIVEN FORCE
1 FOR GIVEN DISPLACEMENT

FINAL PLATE FORCES AND DISPLACEMENTS FOR LONGITUDINAL PLATE ELEMENTS AT END

PLATE INTERNAL DISPLACEMENTS

ELE	I	J	LONG, DISP	TRANSVERSE DISP	BEAM ROTATION
1	1	2	-4.31341761E-02	5.64534291E-02	-2.80280929E-03

PLATE INTERNAL FORCES

ELE	I	J	BEAM MOMENT	TRAN, SHEAR	AXIAL FORCE	NX(I)	NX(J)	SX(I)	SX(J)
1	1	2	1.81899B9E-12	9.50515BE+00	-4.34B701F+02	-1.449567E+02	-1.449567E+02	-1.449567E+02	-1.449567E+02

FINAL PLATE FORCES AND DISPLACEMENTS FOR LONGITUDINAL PLATE ELEMENTS AT END OF SEGMENT 7 AND AT SUPPORT

PLATE DISPLACEMENTS AND REACTIONS AT INTERIOR SUPPORT

ELE	I	J	LONG. DISP/REACT.	INDEX	TRAN. DISP/REACT.	INDEX	BEAM ROT./REACT.	INDEX
1	1	2	-2.63567804E-02	0	-4.74384646E+01	1	-1.08394821E-04	0

INDEX IS -1 OR 0 FOR DISPLACEMENT, AND 1 FOR REACTION

PLATE INTERNAL DISPLACEMENTS

ELE	I	J	LONG. DISP	TRANSVERSE DISP	BEAM ROTATION
1	1	2	-2.63567804E-02	4.44089210E-16	-1.08394821E-04

PLATE INTERNAL FORCES

ELE	I	J	BEAM MOMENT	TRAN. SHEAR	AXIAL FORCE	NX(I)	NX(J)	SX(I)	SX(J)
1	1	2	7.52047[illegible]E+01	2.816325E+01	-4.348701E+02	-9.482023E+01	-1.950932E+02	-9.482023E+01	-1.950932E+02

FINAL PLATE FORCES AND DISPLACEMENTS FOR LONGITUDINAL PLATE ELEMENTS AT ORIGIN

PLATE INTERNAL DISPLACEMENTS

ELE	I	J	LONG. DISP	TRANSVERSE DISP	BEAM ROTATION
1	1	2	0.	0.	-1.25444586E-03

PLATE INTERNAL FORCES

ELE	I	J	BEAM MOMENT	TRAN. SHEAR	AXIAL FORCE	NX(I)	NX(J)	SX(I)	SX(J)
1	1	2	1.[illegible]E+02	-4.554091E+00	-5.693065E+02	-1.172940E+02	-2.622436E+02	-1.172940E+02	-2.622436E+02

FINAL JOINT AND PLATE FORCES AND DISPLACEMENTS FOR SEGMENT NO. 1

JOINT DISPLACEMENTS

JOINT	HORIZONTAL DISP	VERTICAL DISP	ROTATION	LONG. DISP
1	0.	-4.92996990E-03	0.	-3.32460740E-03
2	0.	-4.92869520E-03	0.	-1.06818914E-03

PLATE EDGE DISPLACEMENTS

ELE	I	J	ROTATION(I)	ROTATION(J)	W(I)	W(J)	U(I)	U(J)	V(I)	V(J)
1	1	2	0.	0.	0.	0.	-33.24608E-04	-10.68189E-04	49.29990E-04	-49.28695E-04

PLATE EDGE FORCES

ELE	I	J	M(I)	M(J)	Q(I)	Q(J)	T(I)	T(J)	P(I)	P(J)
1	1	2	0.	0.	0.	0.	26.01342E-13	17.15205E-13	14.78739E-02	22.50000E-02

PLATE INTERNAL DISPLACEMENTS

ELE	I	J	LONG. DISP	TRANSVERSE DISP	BEAM ROTATION
1	1	2	-2.19639837E-03	4.92934259E-03	-7.52139488E-04

PLATE INTERNAL FORCES

ELE	I	J	BEAM MOMENT	TRAN. SHEAR	AXIAL FORCE	NX(I)	NX(J)	SX(I)	SX(J)
1	1	2	8.[illegible]E+01	-4.168460E+00	-5.693065E+02	-1.318316E+02	-2.477061E+02	-1.318316E+02	-2.477061E+02

FINAL JOINT AND PLATE FORCES AND DISPLACEMENTS FOR SEGMENT NO. 2

JOINT DISPLACEMENTS

JOINT	HORIZONTAL DISP	VERTICAL DISP	ROTATION	LONG. DISP
1	0.	-8.49256978E-03	0.	-6.67811534E-03
2	0.	-8.59126999E-03	0.	-6.56027488E-03

PLATE EDGE DISPLACEMENTS

ELE	I	J	ROTATION(I)	ROTATION(J)	W(I)	W(J)	U(I)	U(J)	V(I)	V(J)
1	1	2	0.	0.	0.	0.	-66.78115E-04	-65.00275E-04	85.92570E-04	-85.91270E-04

PLATE EDGE FORCES

ELE	I	J	M(I)	M(J)	Q(I)	Q(J)	T(I)	T(J)	P(I)	P(J)
1	1	2	0.	0.	0.	0.	-23.13664E-13	-10.63598E-12	14.93400E-02	22.50000E-02

PLATE INTERNAL DISPLACEMENTS

ELE	I	J	LONG. DISP	TRANSVERSE DISP	BEAM ROTATION
1	1	2	-6.58919511E-03	8.59191949E-03	-5.92801556E-05

PLATE INTERNAL FORCES

ELE	I	J	BEAM MOMENT	TRAN. SHEAR	AXIAL FORCE	NX(I)	NX(J)	SX(I)	SX(J)
1	1	2	4.[illegible]922E+01	-3.404530E+00	-5.493065E+02	-1.570627E+02	-2.224750E+02	-1.570627E+02	-2.224750E+02

FINAL JOINT AND PLATE FORCES AND DISPLACEMENTS FOR SEGMENT NO. 13

JOINT DISPLACEMENTS

JOINT	HORIZONTAL DISP	VERTICAL DISP	ROTATION	LONG. DISP
1	0.	-4.25534608E-02	0.	-4.54917624E-02
2	0.	-4.25534608E-02	0.	-3.74211107E-02

PLATE EDGE DISPLACEMENTS

ELE	I	J	ROTATION(I)	ROTATION(J)	W(I)	W(J)	U(I)	U(J)	V(I)	V(J)
1	1	2	0.	0.	0.	0.	-45.49176E-03	-37.42111E-03	42.55346E-03	-42.55346E-03

PLATE EDGE FORCES

ELE	I	J	M(I)	M(J)	Q(I)	Q(J)	T(I)	T(J)	P(I)	P(J)
1	1	2	0.	0.	0.	0.	35.66311E-12	29.08509E-12	-22.50000E-02	22.50000E-02

PLATE INTERNAL DISPLACEMENTS

ELE	I	J	LONG. DISP	TRANSVERSE DISP	BEAM ROTATION
1	1	2	-4.14564365E-02	4.25534608E-02	-2.69021724E-03

PLATE INTERNAL FORCES

ELE	I	J	BEAM MOMENT	TRAN. SHEAR	AXIAL FORCE	NX(I)	NX(J)	SX(I)	SX(J)
1	1	2	-4.[illegible]90079E+01	7.955158E+00	-4.348701F+02	-1.728906E+02	-1.170228E+02	-1.728906E+02	-1.170228E+02

LONG. CONFIGURATION OF STRUCTURE AT STAGE 3

SPAN = 225.000
NO. OF SEGMENTS = 27
NO. OF TENDONS STRESSED = 1
NO. SEG. ADDED LEFT = 0
NO. SEG. ADDED RIGHT = 14

SEGMENT NUMBER	SEGMENT LENGTH
1	10.000
2	10.000
3	10.000
4	10.000
5	10.000
6	5.000
7	5.000
8	5.000
9	5.000
10	10.000
11	10.000
12	10.000
13	10.000
14	5.000
15	10.000
16	10.000
17	10.000
18	10.000
19	5.000
20	5.000
21	5.000
22	5.000
23	10.000
24	10.000
25	10.000
26	10.000
27	10.000

INPUT DATA FOR CABLES STRESSED AT STAGE 3

TENDON NO. = 3
AREA = 9.550000E-03
NO. CURVES = 3
ELEMENT = 1

INITIAL JACK FORCE = 2.250000E+02
FINAL JACK FORCE = 2.250000E+02
LIVE END INDEX = 0

DIVERGENCE = 0.
STA. LEFT = 0
STA. RIGHT = 0

CONTROL COORDINATES

CURVE	NXL	YL	XM	YM	NXR	YR
1	10	1.500	77.000	-.645	11	-.850
2	11	-.850	-0.000	-0.000	18	-.850
3	18	-.850	148.000	-.645	19	1.500

INITIAL TENDON STRESS AFTER FRICTION LOSS

TENDON	SEGMENT	STRESS
3	10	2.356021E+04
3	11	2.356021E+04
3	12	2.356021E+04
3	13	2.356021E+04
3	14	2.356021E+04

ORIGIN BOUNDARY CONDITIONS AT STAGE 3

ELE	AXIAL FOR/DISP	INDEX	SHEAR FOR/DISP	INDEX	MOMENT OR ROT	INDEX
1	0.	1	0.	1	0.	0

INDEX = 0 FOR GIVEN FORCE
1 FOR GIVEN DISPLACEMENT

JOINT ACTIONS, SUPPORT AND STOPOVER DATA FOR STAGE 3

IAJA = 0, JOINT ACTIONS SAME AS LAST SEGMENT
1, JOINT ACTIONS DIFFERENT FROM LAST SEGMENT

IAJA2 = 0, JOINT ACTIONS SAME AS LAST SEGMENT
1, JOINT ACTIONS SAME AS LAST STAGE
2, JOINT ACTIONS RE-SPECIFIED

ISTOP =-1, SUPPORT AFTER THIS SEGMENT
0, NO SUPPORT OR STOPOVER
1, STOPOVER AFTER THIS SEGMENT

****

JT, ACTIONS FOR SEG. 1 THRU 13 UNCHANGED FROM LAST STAGE

****

SEG 14 IAJA = 0 ISTOP = 1
SEG 15 IAJA = 0 ISTOP = 0
SEG 16 IAJA = 0 ISTOP = 0
SEG 17 IAJA = 0 ISTOP = 1
SEG 18 IAJA = 0 ISTOP = 0
SEG 19 IAJA = 0 ISTOP = 0
SEG 20 IAJA = 0 ISTOP = -1

****

INTERIOR SUPPORT RESTRAINTS

ELE.	AXIAL	COEFFICIENT	SHEAR	COEFFICIENT	ROT.	COEFFICIENT
1	0	-0.	1	-0.	0	-0.

****

SEG 21 IAJA = 0 ISTOP = 0
SEG 22 IAJA = 0 ISTOP = 0
SEG 23 IAJA = 0 ISTOP = 1
SEG 24 IAJA = 0 ISTOP = 0
SEG 25 IAJA = 0 ISTOP = 0
SEG 26 IAJA = 0 ISTOP = 0
SEG 27 IAJA = 0 ISTOP = 0

END BOUNDARY CONDITIONS AT STAGE 3

ELE	AXIAL FOR/DISP	INDEX	SHEAR FOR/DISP	INDEX	MOMENT OR ROT	INDEX
I	0.	0	0.	1	0.	0

INDEX = 0 FOR GIVEN FORCE
1 FOR GIVEN DISPLACEMENT

FINAL PLATE FORCES AND DISPLACEMENTS FOR LONGITUDINAL PLATE ELEMENTS AT END

PLATE INTERNAL DISPLACEMENTS

ELE	I	J	LONG. DISP	TRANSVERSE DISP	BEAM ROTATION
1	1	2	-1.33394471F-02	-8.8817842E-16	-8.15185311E-04

PLATE INTERNAL FORCES

ELE	I	J	BEAM MOMENT	TRAN. SHEAR	AXIAL FORCE	NX(I)	NX(J)	SX(I)	SX(J)
1	1	2	7.275958E-12	1.324574E+00	1.364242F-12	5.305386E-12	-4.395091E-12	5.305386E-12	-4.395091E-12

FINAL PLATE FORCES AND DISPLACEMENTS FOR LONGITUDINAL PLATE ELEMENTS AT END OF SEGMENT 20 AND AT SUPPORT

PLATE DISPLACEMENTS AND REACTIONS AT INTERIOR SUPPORT

ELE	I	J	LONG. DISP/REACT.	INDEX	TRAN. DISP/REACT.	INDEX	BEAM ROT./REACT.	INDEX
1	1	2	-1.33394471E-02	0	1.32457392E+00	1	1.63772937E-03	0

INDEX IS -1 OR 0 FOR DISPLACEMENT, AND 1 FOR REACTION

PLATE INTERNAL DISPLACEMENTS

ELE	I	J	LONG. DISP	TRANSVERSE DISP	BEAM ROTATION
1	1	2	-1.33394471E-02	8.88178420E-16	1.63772937E-03

PLATE INTERNAL FORCES

ELE	I	J	BEAM MOMENT	TRAN. SHEAR	AXIAL FORCE	NX(I)	NX(J)	SX(I)	SX(J)
1	1	2	-7.947444E+01	8.252357E-09	-1.568878E-10	-5.298296E+01	5.298296E+01	-5.298296E+01	5.298296E+01

FINAL PLATE FORCES AND DISPLACEMENTS FOR LONGITUDINAL PLATE ELEMENTS AT END OF SEGMENT 7 AND AT SUPPORT

PLATE DISPLACEMENTS AND REACTIONS AT INTERIOR SUPPORT

ELE	I	J	LONG. DISP/REACT.	INDEX	TRAN. DISP/REACT.	INDEX	BEAM ROT./REACT.	INDEX
1	1	2	2.86368151E-14	0	1.32457392E+00	1	-1.63772937E-03	0

INDEX IS -1 OR 0 FOR DISPLACEMENT, AND 1 FOR REACTION

PLATE INTERNAL DISPLACEMENTS

ELE	I	J	LONG. DISP	TRANSVERSE DISP	BEAM ROTATION
1	1	2	2.86368151E-14	0.	-1.63772937E-03

PLATE INTERNAL FORCES

ELE	I	J	BEAM MOMENT	TRAN. SHEAR	AXIAL FORCE	NX(I)	NX(J)	SX(I)	SX(J)
1	1	2	-7.947444E+01	-1.324574E+00	6.894148E-10	-5.298296E+01	5.298296E+01	-5.298296E+01	5.298296E+01

FINAL PLATE FORCES AND DISPLACEMENTS FOR LONGITUDINAL PLATE ELEMENTS AT ORIGIN

PLATE INTERNAL DISPLACEMENTS

ELE	I	J	LONG. DISP	TRANSVERSE DISP	BEAM ROTATION
1	1	2	0.	0.	8.15185311E-04

PLATE INTERNAL FORCES

ELE	I	J	BEAM MOMENT	TRAN. SHEAR	AXIAL FORCE	NX(I)	NX(J)	SX(I)	SX(J)
1	1	2	0.	-1.324574E+00	5.639414E-10	1.879805E-10	1.879805E-10	1.879805E-10	1.879805E-10

FINAL JOINT AND PLATE FORCES AND DISPLACEMENTS FOR SEGMENT NO. 1

JOINT DISPLACEMENTS

JOINT	HORIZONTAL DISP	VERTICAL DISP	ROTATION	LONG. DISP
1	0.	-8.70188986E-04	0.	-2.12738083E-03
2	0.	-6.48894285E-04	0.	-2.26541591E-03

PLATE EDGE DISPLACEMENTS

ELE	I	J	ROTATION(I)	ROTATION(J)	M(I)	M(J)	U(I)	U(J)	V(I)	V(J)
1	1	2	0.	0.	0.	0.	-21.27381E-04	-22.65416E-04	87.01890E-05	-86.88943E-05

PLATE EDGE FORCES

ELE	I	J	M(I)	M(J)	Q(I)	Q(J)	T(I)	T(J)	P(I)	P(J)
1	1	2	0.	0.	0.	0.	11.60313E-13	20.40127E-13	14.78739E-02	22.50000E-02

PLATE INTERNAL DISPLACEMENTS

ELE	I	J	LONG. DISP	TRANSVERSE DISP	BEAM ROTATION
1	1	2	-2.19639837E-03	8.69541636E-04	4.60116932E-05

PLATE INTERNAL FORCES

ELE	I	J	BEAM MOMENT	TRAN. SHEAR	AXIAL FORCE	NX(I)	NX(J)	SX(I)	SX(J)
1	1	2	9.07298E+01	-8.49[illegible]034E+00	-8.69306B5E+02	-1.362468E+02	-2.432908E+02	-1.362468E+02	-2.432908E+02

FINAL JOINT AND PLATE FORCES AND DISPLACEMENTS FOR SEGMENT NO. 14

JOINT DISPLACEMENTS

JOINT	HORIZONTAL DISP	VERTICAL DISP	ROTATION	LONG. DISP
1	0.	-1.03909681E-01	0.	-6.66972353E-03
2	0.	-1.03909681E-01	0.	-6.66972353E-03

PLATE EDGE DISPLACEMENTS

ELE	I	J	ROTATION(I)	ROTATION(J)	M(I)	M(J)	U(I)	U(J)	V(I)	V(J)
1	1	2	0.	0.	0.	0.	-66.69724E-04	-66.69724E-04	10.39097E-02	-10.39097E-02

PLATE EDGE FORCES

ELE	I	J	M(I)	M(J)	Q(I)	Q(J)	T(I)	T(J)	P(I)	P(J)
1	1	2	0.	0.	0.	0.	37.82261E-11	-43.43412E-11	19.41841E-11	-70.57749E-11

PLATE INTERNAL DISPLACEMENTS

ELE	I	J	LONG. DISP	TRANSVERSE DISP	BEAM ROTATION
1	1	2	-6.66972353E-03	1.03909681E-01	-7.59762623E-14

PLATE INTERNAL FORCES

ELE	I	J	BEAM MOMENT	TRAN. SHEAR	AXIAL FORCE	NX(I)	NX(J)	SX(I)	SX(J)
1	1	2	9.30703E+01	-5.92570E-10	-2.03387E+02	-5.74889E+00	-1.29842E+02	-5.74889E+00	-1.29842E+02

ORIGIN BOUNDARY CONDITIONS AT STAGE 4

ELE	AXIAL FOR/DISP	INDEX	SHEAR FOR/DISP	INDEX	MOMENT OR ROT	INDEX
1	0.	1	0.	1	0.	0

INDEX = 0 FOR GIVEN FORCE
1 FOR GIVEN DISPLACEMENT

JOINT ACTIONS, SUPPORT AND STOPOVER DATA FOR STAGE 4

IAJA = 0, JOINT ACTIONS SAME AS LAST SEGMENT
1, JOINT ACTIONS DIFFERENT FROM LAST SEGMENT

IAJA2 = 0, JOINT ACTIONS SAME AS LAST SEGMENT
1, JOINT ACTIONS SAME AS LAST STAGE
2, JOINT ACTIONS RE-SPECIFIED

ISTOP =-1, SUPPORT AFTER THIS SEGMENT
0, NO SUPPORT OR STOPOVER
1, STOPOVER AFTER THIS SEGMENT

SEG 1 IAJA2 = 2 ISTOP = 0

****

APPLIED JOINT ACTIONS

JT.	HORIZ.	F/D	VERT.	F/D	ROT.	M/R	LONG.	F/D
1	0.0000000	0	.3000000	0	0.0000000	0	0.0000000	0
2	0.0000000	0	0.0000000	0	0.0000000	0	0.0000000	0

INDEX = 0 FOR GIVEN FORCE
1 FOR GIVEN DISPLACEMENT

****

SEG 2 IAJA2 = 0 ISTOP = 0
SEG 3 IAJA2 = 0 ISTOP = 1
SEG 4 IAJA2 = 0 ISTOP = 0
SEG 5 IAJA2 = 0 ISTOP = 0
SEG 6 IAJA2 = 0 ISTOP = 0
SEG 7 IAJA2 = 0 ISTOP = -1
SEG 8 IAJA2 = 0 ISTOP = 0
SEG 9 IAJA2 = 0 ISTOP = 0
SEG 10 IAJA2 = 0 ISTOP = 1
SEG 11 IAJA2 = 0 ISTOP = 0
SEG 12 IAJA2 = 0 ISTOP = 0
SEG 13 IAJA2 = 0 ISTOP = 0
SEG 14 IAJA2 = 0 ISTOP = 1
SEG 15 IAJA2 = 0 ISTOP = 0
SEG 16 IAJA2 = 0 ISTOP = 0
SEG 17 IAJA2 = 0 ISTOP = 1
SEG 18 IAJA2 = 0 ISTOP = 0
SEG 19 IAJA2 = 0 ISTOP = 0
SEG 20 IAJA2 = 0 ISTOP = -1
SEG 21 IAJA2 = 0 ISTOP = 0
SEG 22 IAJA2 = 0 ISTOP = 0
SEG 23 IAJA2 = 0 ISTOP = 1
SEG 24 IAJA2 = 0 ISTOP = 0
SEG 25 IAJA2 = 0 ISTOP = 0
SEG 26 IAJA2 = 0 ISTOP = 0

SEG 27 IAJA2 = 0 ISTOP = 0

END BOUNDARY CONDITIONS AT STAGE 4

ELE	AXIAL FOR/DISP	INDEX	SHEAR FOR/DISP	INDEX	MOMENT OR ROT	INDEX
1	0.	0	0.	1	0.	0

INDEX = 0 FOR GIVEN FORCE
1 FOR GIVEN DISPLACEMENT

FINAL PLATE FORCES AND DISPLACEMENTS FOR LONGITUDINAL PLATE ELEMENTS AT END

PLATE INTERNAL DISPLACEMENTS

ELE	I	J	LONG. DISP	TRANSVERSE DISP	BEAM ROTATION
1	1	2	-1.33394471E-02	0.	-1.16473536E-03

PLATE INTERNAL FORCES

ELE	I	J	BEAM MOMENT	TRAN. SHEAR	AXIAL FORCE	NX(I)	NX(J)	SX(I)	SX(J)
1	1	2	0.	6.37900BE+00	9.094947E-13	3.031649E-13	3.031649E-13	3.031649E-13	3.031649E-13

FINAL PLATE FORCES AND DISPLACEMENTS FOR LONGITUDINAL PLATE ELEMENTS AT END OF SEGMENT 20 AND AT SUPPORT

PLATE DISPLACEMENTS AND REACTIONS AT INTERIOR SUPPORT

ELE	I	J	LONG. DISP/REACT.	INDEX	TRAN. DISP/REACT.	INDEX	BEAM ROT./REACT.	INDEX
1	1	2	-1.33394471E-02	0	-2.73709917E+01	1	-4.62868132E-04	0

INDEX IS -1 OR 0 FOR DISPLACEMENT, AND 1 FOR REACTION

PLATE INTERNAL DISPLACEMENTS

ELE	I	J	LONG. DISP	TRANSVERSE DISP	BEAM ROTATION
1	1	2	-1.33394471E-02	-2.22044605E-16	-4.62868132E-04

PLATE INTERNAL FORCES

ELE	I	J	BEAM MOMENT	TRAN. SHEAR	AXIAL FORCE	NX(I)	NX(J)	SX(I)	SX(J)
1	1	2	1.572595E+02	1.575000E+01	-2.173692E-10	1.048397E+02	-1.048397E+02	1.048397E+02	-1.048397E+02

FINAL PLATE FORCES AND DISPLACEMENTS FOR LONGITUDINAL PLATE ELEMENTS AT END OF SEGMENT 7 AND AT SUPPORT

PLATE DISPLACEMENTS AND REACTIONS AT INTERIOR SUPPORT

ELE	I	J	LONG. DISP/REACT.	INDEX	TRAN. DISP/REACT.	INDEX	BEAM ROT./REACT.	INDEX
1	1	2	-3.42156858E-14	0	-2.73709917E+01	1	4.62868132E-04	0

INDEX IS -1 OR 0 FOR DISPLACEMENT, AND 1 FOR REACTION

PLATE INTERNAL DISPLACEMENTS

ELE	I	J	LONG. DISP	TRANSVERSE DISP	BEAM ROTATION
1	1	2	-3.42156858E-14	-1.11022302E-15	4.62868132E-04

PLATE INTERNAL FORCES

ELE	I	J	BEAM MOMENT	TRAN. SHEAR	AXIAL FORCE	NX(I)	NX(J)	SX(I)	SX(J)
1	1	2	1.572595E+02	1.169099E+01	-5.414286E-10	1.048397E+02	-1.048397E+02	1.048397E+02	-1.048397E+02

FINAL PLATE FORCES AND DISPLACEMENTS FOR LONGITUDINAL PLATE ELEMENTS AT ORIGIN

PLATE INTERNAL DISPLACEMENTS

ELE	I	J	LONG. DISP	TRANSVERSE DISP	BEAM ROTATION
1	1	2	0.	0.	1.16473536E-03

PLATE INTERNAL FORCES

ELE	I	J	BEAM MOMENT	TRAN. SHEAR	AXIAL FORCE	NX(I)	NX(J)	SX(I)	SX(J)
1	1	2	0.	-6.379008E+00	-7.821027E-10	-2.607009E-10	-2.607009E-10	-2.607009E-10	-2.607009E-10

FINAL JOINT AND PLATE FORCES AND DISPLACEMENTS FOR SEGMENT NO. 1

JOINT DISPLACEMENTS

JOINT	HORIZONTAL DISP	VERTICAL DISP	ROTATION	LONG. DISP
1	0.	8.17641424E-04	0.	-1.69091136E-03
2	0.	8.17894459E-04	0.	-2.70188537E-03

PLATE EDGE DISPLACEMENTS

ELE	I	J	ROTATION(I)	ROTATION(J)	W(I)	W(J)	U(I)	U(J)	V(I)	V(J)
1	1	2	0.	0.	0.	0.	-16.90911E-04	-27.01885E-04	-81.76414E-05	81.78945E-05

PLATE EDGE FORCES

ELE	I	J	M(I)	M(J)	Q(I)	Q(J)	T(I)	T(J)	P(I)	P(J)
1	1	2	0.	0.	0.	0.	84.14782E-14	15.47940E-13	-15.21861E-02	22.50000E-02

PLATE INTERNAL DISPLACEMENTS

ELE	I	J	LONG. DISP	TRANSVERSE DISP	BEAM ROTATION
1	1	2	-2.19639837E-03	-8.17747942E-04	3.36991337E-04

PLATE INTERNAL FORCES

ELE	I	J	BEAM MOMENT	TRAN. SHEAR	AXIAL FORCE	NX(I)	NX(J)	SX(I)	SX(J)
1	1	2	5.87A061E+01	-9.047469E+00	-5.693065E+02	-1.505949E+02	-2.289427E+02	-1.505949E+02	-2.289427E+02

FINAL JOINT AND PLATE FORCES AND DISPLACEMENTS FOR SEGMENT NO. 14

JOINT DISPLACEMENTS

JOINT	HORIZONTAL DISP	VERTICAL DISP	ROTATION	LONG. DISP
1	0.	4.96940888E-02	0.	-6.66972353E-03
2	0.	4.96930472E-02	0.	-6.66972953E-03

PLATE EDGE DISPLACEMENTS

ELE	I	J	ROTATION(I)	ROTATION(J)	W(I)	W(J)	U(I)	U(J)	V(I)	V(J)
1	1	2	0.	0.	0.	0.	-66.69724E-04	-66.69724E-04	-49.89409E-03	49.69305E-03

PLATE EDGE FORCES

ELE	I	J	M(I)	M(J)	Q(I)	Q(J)	T(I)	T(J)	P(I)	P(J)
1	1	2	0.	0.	0.	0.	-11.03709E-12	44.85004E-12	-38.00000E-02	38.11342E-11

PLATE INTERNAL DISPLACEMENTS

ELE	I	J	LONG. DISP	TRANSVERSE DISP	BEAM ROTATION
1	1	2	-6.66972353E-03	-4.96935680E-02	2.91433544E-14

PLATE INTERNAL FORCES

ELE	I	J	BEAM MOMENT	TRAN. SHEAR	AXIAL FORCE	NX(I)	NX(J)	SX(I)	SX(J)
1	1	2	-8.363323E+01	-7.810641E-10	-2.033873E+02	-1.235513E+02	-1.204029E+01	-1.835513E+02	-1.204029E+01

STEEL STRESSES FOR ALL CABLES AT STAGE 4
NOTE SEG.NOS. REFERED TO PRESENT STAGE

	CABLE NO.	SEG.NO.	REVISED STRESS
1 STAGE CABLES			
	1	1	1.974959E+04
	1	2	1.975596E+04
	1	3	1.979752E+04
	1	4	1.974431E+04
	1	5	1.968114E+04
	1	6	1.979959E+04
	1	7	2.007272E+04
2 STAGE CABLES			
	2	1	2.278916E+04
	2	2	2.273617E+04
	2	3	2.265938E+04
	2	4	2.266069E+04
	2	5	2.284201E+04
	2	6	2.315745E+04
	2	7	2.346826E+04
	2	8	2.338732E+04
	2	9	2.298715E+04
	2	10	2.215669E+04
	2	11	2.219904E+04
	2	12	2.206030E+04
	2	13	2.208019E+04
3 STAGE CABLES			
	3	10	2.352047E+04
	3	11	2.379119E+04
	3	12	2.403763E+04
	3	13	2.417455E+04
	3	14	2.420535E+04

C.4 Listing of Input Data - Example 3

Stage	Card Type	Listing - Page 1
0	1	INTRACOASTAL CANAL BRIDGE CHANGING LAST STAGE TO 0 DISPL.
	2	4 4 5
	3	1 5.833 0.584 634000.
	3	2 7.667 0.584 634000.
	3	3 1.667 -7.375 1.000 634000.
	3	4 6.000 .6667 634000.
	4	1 1 2 1
	4	2 2 3 2
	4	3 2 4 3
	4	4 4 5 4
	5	.25 .0002 4180000.
1	6A	6 1 1 7
	6B	
	8	1 7 5.
	9A	1 3 3 .02554 744. 595.
	9B	
	10	1 -.136 4.69 2.480 3 3.518
	10	3 3.518 5 3.518
	10	5 3.518 25.31 2.480 7 -.136
	11	1
	11	2
	11	3
	11	4
	12A	1 1 1
	13	1
	13	2 1.410 0.898
	13	3 0.336 1 1
	13	4 0.938 -0.217
	13	5 0.375 1 1
	12A	2 0 0
	12A	3 1 -1
	13	1
	13	2 1 1 1 0
	13	3 1 1 1 0
	13	4 1 1 1 0
	13	5 1 1 1 0
	14	1 0 0 0
	14	2 0 1 0
	14	3 0 1 -1 1480000.
	14	4 -1 1 1 655.
	12A	4 0 0
	12A	5 1 0
	13	1
	13	2 1.410 0.898
	13	3 0.336 1 1
	13	4 0.938 -0.217
	13	5 0.375 1 1
	12A	6 0 1
	15	1
	15	2
	15	3
	15	4
2	7A	2 2 2 1 1 11 1
	7B	

Stage	Card Type	Listing - Page 2											
	8	1	3			5.							
	8	9	11			5.							
	9A	2	3	3		.02340		683.		546.			
	9B		.79		5	7							
	10		1			0.364		4.69		2.752		3	3.685
	10		3			3.685						9	3.685
	10		9			3.685		45.31		2.752		11	0.364
	12A	1	1	1									
	13		1										
	13		2					1.410		0.898			
	13		3					0.336				1	1
	13		4					0.863		-0.142			
	13		5					0.300				1	1
	12A	2	0	0									
	12A	9	1	0									
	13		1										
	13		2					1.410		0.898			
	13		3					0.336				1	1
	13		4					0.863		-0.142			
	13		5					0.300				1	1
	12A	10	0	0									
3	7A	3	1	2	1	1	14				1		
	7B												
	8	1	2			10.							
	8	12	14			5.							
	9A	3	3	3		.02340		683.		546.			
	9B		.79		4	10							
	10		1			0.364		4.69		2.752		2	3.685
	10		2			3.685						12	3.685
	10		12			3.685		65.31		2.752		14	0.364
	12A	1	1	0									
	13		1										
	13		2					1.410		0.898			
	13		3					0.336				1	1
	13		4					0.788		-0.067			
	13		5					0.225				1	1
	12A	12	1	0									
	13		1										
	13		2					1.410		0.898			
	13		3					0.336				1	1
	13		4					0.788		-0.067			
	13		5					0.225				1	1
	12A	13	0	1									
4	7A	4	2	2	1	1	18						
	7B												
	8	1	3			5.							
	8	16	18			5.							
	9A	4	3	3		.01277		372.		298.			
	9B		1.208		4	14							
	10		1			.364		4.69		2.752		3	3.685
	10		3			3.685						16	3.685
	10		16			3.685		85.31		2.752		18	0.364

Stage	Type Card	Listing - Page 3											
	12A	1	1	0									
	13		1										
	13		2				1,410		0,898				
	13		3				0,336				1	1	
	13		4				0,788		-0,067				
	13		5				0,225				1	1	
	12A	2	0	0									
	12A	16	0	0									
	12A	17	0	0									
5	7A	5	1	2	1	1	21			1			
	7B												
	8	1	2			10,							
	8	19	21			5,							
	9A	5	3	3	,01277		372,		298,				
	9B		1,208		4	17							
	10		1		0,364		4,69		2,752		2		3,685
	10		2		3,685						19		3,685
	10		19		3,685		105,31		2,752		21		0,364
	12A	1	1	1									
	13		1										
	13		2				1,410		0,898				
	13		3				0,336				1	1	
	13		4				0,788		-0,067				
	13		5				0,225				1	1	
	12A	19	0	0									
	12A	20	0	1									
6	7A	6	2	2	1	1	25						
	7B												
	8	1	3			5,							
	8	23	25			5,							
	9A	6	3	3	,01277		372,		298,				
	9B		1,584		4	21							
	10		1		0,364		4,69		2,752		3		3,685
	10		3		3,685						23		3,685
	10		23		3,685		125,31		2,752		25		0,364
	12A	1	1	0									
	13		1										
	13		2				1,410		0,898				
	13		3				0,336				1	1	
	13		4				0,788		-0,067				
	13		5				0,225				1	1	
	12A	2	0	0									
	12A	23	0	0									
	12A	24	0	0									
7	7A	7	1	2	1	1	28						
	7B												
	8	1	2			10,							
	8	26	28			5,							
	9A	7	3	3	,00745		218,		174,				
	9B		1,584		4	24							
	10		1		0,364		4,69		2,752		2		3,685
	10		2		3,685						26		3,685
	10		26		3,685		145,31		2,752		28		0,364

Stage	Card Type	Listing - Page 4											
	12A	1	1	0									
	13		1										
	13		2				1.410		0.898				
	13		3				0.336					1	1
	13		4				0.788		-0.067				
	13		5				0.225					1	1
	12A	26	0	0									
	12A	27	0	1									
8	7A	8	1	2	1	1	31						
	7B												
	8	1	2			10.							
	8	29	31			5.							
	9A	8	3	3	.00638		186.		149.				
	9B		2.0		3	27							
	10		1		0.364		4.69		2.752		2		3.685
	10		2		3.685						29		3.685
	10		29		3.685		165.31		2.752		31		0.364
	12A	1	1	1									
	13		1										
	13		2				1.410		0.898				
	13		3				0.336					1	1
	13		4				0.788		-0.067				
	13		5				0.225					1	1
	12A	29	0	0									
	12A	30	0	0									
9	7A	9	1	1	1	1	33						
	7B	0	0	0	0	1							
	8	1	2			10.							
	8	32	33			10.							
	9A	9	3	3	.00638		186.		149.				
	9B		2.0		3	30							
	10		1		0.364		4.69		2.752		2		3.685
	10		2		3.685						32		3.685
	10		32		3.685		185.31		2.752		33		0.364
	12A	1	1	0									
	13		1										
	13		2				1.410		0.898				
	13		3				0.336					1	1
	13		4				0.788		-0.067				
	13		5				0.225					1	1
	12A	32	0	0									
10	7A	10	0	1	1	29	34						
	7B	1											
	8	33	34			5.							
	9A	10	2	3	.00638		186.		149.	-1			
	9B												
	10		29		3.795		172.81		.05		32		-.55
	10		32		-.55						34		-.55
	12B	1	1										
	12B	2	1										
	12B	3	1										
	12B	4	1										
	12B	5	1										

Stage	Card Type	Listing - Page 5													
	12B	6	1												
	12B	7	1												
	12B	8	1												
	12B	9	1												
	12B	10	1												
	12B	11	1												
	12B	12	1												
	12B	13	1												
	12B	14	2												
	13			1											
	13			2					1,41				1	0	1 0
	13			3					,336				1	0	1 0
	13			4					,938				1	0	1 0
	13			5					,375				1	0	1 0
	12B	15	0												
	12B	16	1												
	12B	17	1												
	12B	18	1												
	12B	19	1												
	12B	20	1												
	12B	21	1												
	12B	22	1												
	12B	23	1												
	12B	24	1												
	12B	25	1												
	12B	26	1												
	12B	27	1												
	12B	28	1												
	12B	29	1												
	12B	30	1												
	12B	31	1												
	12B	32	1												
	12A	33	0	0											
11	7A	11	1	0	1	1	14								
	7B														
	8	1	2			5,									
	9A	11	3	3	,00638				186,		149,				
	9B														
	10			1		-2,80			2,5		-3,24		2		-3,55
	10			2		-3,55							10		-3,55
	10			10		-3,55			75,		-2,98		14		3,795
	12A	1	1	0											
	13			1											
	13			2					1,410		0,898				
	13			3					0,336				1		1
	13			4					0,788		-0,067				
	13			5					0,225				1		1
12	7A	12	0	0	1	1	12					1			
	7B														
	9A	12	3	3	,00638				186,		149,				
	9B														
	10			1		-2,80			2,5		-3,24		2		-3,55
	10			2		-3,55							8		-3,55

Stage	Card Type	Listing - Page 6													
	10			8	-3.55			65.		-2.98			12		3.795
13	7A	13	0	0	1	1	9								
	7B														
	9A	13	3	3	.00638			186.		149.					
	9B														
	10			1	0.00			2.5		-0.416			2		-0.55
	10			2	-0.55								7		-0.55
	10			7	-0.55			52.19		.05			9		3.795
14	7A	14	0	0	1	1	6	0	0	0	1				
	7B	0	0	0	1	0									
	9A	14	3	3	.00638			186.		149.					
	9B														
	10			1	0.00			2.5		-0.416			2		-0.55
	10			2	-0.55								4		-0.55
	10			4	-0.55			32.19		.05			6		3.795
15	7A	15	0	1	1	18	36								
	7B	1	1	0	1	0									
	8	35	36			1.									
	9A	15	2	3	.00850			228.		198.		-1			
	9B														
	10			18	3.795			125.		-2.98			22		-3.55
	10			22	-3.55								36		-3.55
	11			1								0 0 0			
	11			2								0 0 0			
	11			3								0 1 0			
	11			4								0 0 0			
	12B	1	2												
	13			1											
	13			2										1	1
	13			3											
	13			4										1	1
	13			5											
	12B	2	0												
	12B	3	0												
	12B	4	0												
	12B	5	0												
	12B	6	0												
	12B	7	0												
	12B	8	0												
	12B	9	0												
	12B	10	0												
	12B	11	0												
	12B	12	0												
	12B	13	0												
	12B	14	0												
	12B	15	2												
	13			1											
	13			2										1 0	1 0
	13			3										1 0	1 0
	13			4										1 0	1 0
	13			5										1 0	1 0
	12B	16	0												
	12B	17	2												

Stage	Card Type	Listing - Page 7											
	13			1									
	13			2									
	13			3								1 0 1 0	
	13			4									
	13			5								1 0 1 0	
	12B	18	0										
	12B	19	0										
	12B	20	0										
	12B	21	0										
	12B	22	0										
	12B	23	0										
	12B	24	0										
	12B	25	0										
	12B	26	0										
	12B	27	0										
	12B	28	0										
	12B	29	0										
	12B	30	0										
	12B	31	0										
	12B	32	0										
	12B	33	0										
	12B	34	0										
	12A	35	0	0									
	15			1						1 1 1			
	15			2						1 1 1			
	15			3						1 0 1			
	15			4						1 1 1			
16	7A	16	0	0	1	20	36						
	7B	0	0	0	1	0							
	9A	16	2	3	.00850			228.	198.	-1			
	9B												
	10			20	3.795			135.	-2.98			24	-3.55
	10			24	-3.55							36	-3.55
17	7A	17	0	0	1	22	36						
	7B	0	0	0	1	0							
	9A	17	2	3	.00850			228.	198.	-1			
	9B												
	10			22	3.795			145.	-2.73			26	-3.30
	10			26	-3.30							36	-3.30
18	7A	18	0	0	1	24	36						
	7B	0	0	0	1	0							
	9A	18	2	3	.00850			228.	198.	-1			
	9B												
	10			24	3.795			155.	-2.73			28	-3.30
	10			28	-3.30							36	-3.30
19	7A	19	0	0	0								
	7B	0	1	1	1	0							
	11			1									
	11			2									
	11			3				-25.8					
	11			4									
	14	1	0	0	0								
	14	2	0	1	0								

Stage	Card Type	Listing - Page 8												
	14	3	0	1	0									
	14	4	0	1	0									
	15		1								1 1 1			
	15		2								1 1 1			
	15		3								1 0 1			
	15		4								1 1 1			
20	7A	20	0	0	1	26	36							
	7B	0	1	0	1	0								
	9A	19	2	3	.00638			288.		198.	-1			
	9B													
	10		26		3.795			165.		-2.615			30	-3.05
	10		30		-3.05								36	-3.05
	11		1											
	11		2											
	11		3					.1088			0 1 0			
	11		4											
	15		1								1 1 1			
	15		2								1 1 1			
	15		3								1 0 1			
	15		4								1 1 1			
21	7A	21	0	0	1	28	36							
	7B	0	0	0	1	0								
	9A	20	2	3	.00638			286.		198.	-1			
	9B													
	10		28		3.795			175.		-2.615			32	-3.05
	10		32		-3.05								36	-3.05
22	7A	22	0	0	0									
	7B	0	1	0	1	0								
	11		1											
	11		2											
	11		3					.13693754			1			
	11		4											
	15		1								1 1 1			
	15		2								1 1 1			
	15		3								1 0 1			
	15		4								1 1 1			
	BLANK CARD TERMINATES RUN													